Development of Mycobacterial Growth Inhibition Assays for the early evaluation and gating of novel TB vaccine candidates

A thesis submitted in fulfilment of the requirements
for the degree of Doctor of Philosophy in Clinical Medicine

Rachel Louise Tanner

St Cross College, Trinity Term 2015

Word Count ~48,000

Development of Mycobacterial Growth Inhibition Assays for the early evaluation and gating of novel TB vaccine candidates

Rachel Tanner, St Cross College, University of Oxford; Trinity Term 2015

Thesis submitted for the degree of Doctor of Philosophy in Clinical Medicine

Tuberculosis poses a serious global health threat, with an estimated 9 million new cases and 1.5 million deaths annually. The current vaccine, BCG, is inadequate but development of an effective alternative is severely hampered by the lack of an immune correlate of protection. Candidate vaccines are currently tested using preclinical animal models such as mice and non-human primates. Large numbers of animals are required and subjected to procedures classified as 'Moderate' in severity. Experiments are long and costly and it is unclear whether outcomes are predictive of efficacy or safety in humans. Work in this thesis describes the optimisation and evaluation of a functional *in vitro* Mycobacterial Growth Inhibition Assay, the MGIT, which takes into account a range of immune mechanisms and their interactions. Applying this assay, a BCG-induced reduction in mycobacterial growth was detected in humans, NHPs and mice. A correlation was observed between the *in vitro* MGIT response and *in vivo* protection from challenge in the mouse and NHP models. There was also concordance between the MGIT and epidemiological data or *in vivo* outcome in humans. Comparison of whole blood and PBMC compartments indicated that haemoglobin may act as a confounder and suggested a role for complement, but not antibodies, in determining mycobacterial growth. Classical monocytes and CD16- NK cells played a crucial role in PBMC MGIT. Cytokines correlating with mycobacterial growth represented a mixture of subsets, and the immunoregulatory cytokine IL-10 was highly influential. Genes correlating with mycobacterial growth were enriched for the immune response pathway, which included CD14 and HAMP, supporting the importance of monocytes and iron. Although further work is required, the MGIT assay represents a potential correlate of protection that may be applied in preclinical vaccine testing, reducing the number of animals used in challenge experiments and accelerating the development of an effective vaccine.

Acknowledgements

Thank you to my funders, UFAW, for awarding me their 3Rs Liaison studentship and making this DPhil possible.

I would like to express my sincerest gratitude to my supervisors, Helen McShane and Helen Fletcher. I could not have asked for a better PhD experience and your guidance and expertise were invaluable. You are both inspirational role models, and I am fortunate to count you as wonderful friends as well as advisors. You have supported me through all the ups and downs of the past 3 years (not least the broken neck incident!) and given me the confidence to be independent and follow my goals. From someone who used to pass out from standing up in front of the class, I can now present my work to a conference full of experts without even trembling (well, almost..!), and for that I will always be indebted.

My thanks also to the many other brilliant scientists I have been lucky enough to work with in the MGIA consortia who have encouraged and advised me; particularly Tom Scriba, Mike Brennan, Ann Rawkins and Sally Sharpe.

To Matt O'Shea, who has been an unwavering pillar of support. I can't thank you enough for all the hours you have spent selflessly helping me in Cat 3, for all the laughs (and occasional tears!) we have shared, and for always being there for me. To Elena Stylianou who came to the rescue on many occasions and patiently babysat me through the mouse work; I couldn't have done it without you. To Rachel K, who is always willing to lend a helping hand; it has been great to have someone to share the thesis writing experience with. There are so many people who have helped out when I needed it - Steve Smith, Andrew White, Julie, Iman, Steph, Vivek, Julius, Paulo, Janet, Zita, Drew, Marcus, George, Alex, Magali, Youlia and Leanne: Thank you. To my office mates Dan, RK and Sarah: you made it a pleasure to come into work even when everything was going badly - it has been thoroughly entertaining (if not

always productive)! Sean, Lynda, Carly, Iona, Danny, Pawan, Christos, Ahmed, Anita, Jenny and all the other friends I have made; you have all helped to make this a positive experience and I doubt there will ever be another department quite like the Jenner.

To Martin, who provided the escape of the countryside and horses, and a happy and loving home to come back to every day. Thank you for patiently enduring my terrible dinner conversation about the relative merits of rotating mycobacteria, for picking me up from the lab on late nights and keeping me sane through the thesis writing. To my polo buddies: Andreas, Nik, Jan, Mikey and Pinky. Polo provided a welcome release after long days in the lab, and playing with you guys were some of the best times of my life.

To the late Robin McCleery, whose decision to take me on as an undergraduate undoubtedly changed the course of my life. I never had the chance to thank you for believing in me, and in fairer access to Oxford for state school and unprivileged pupils. I hope this thesis proves that all those 'remedial' statistics tutorials were not entirely in vain!

To my grandmother, who was so proud of everything I achieved; I wish you could be here to share this next step of my journey. And finally, my parents, to whom I owe everything. Thank you for supporting me through 25 years of education. To my mum, for holding my hand every step of the way, for all the hours spent testing me for exams, and always encouraging me to do my best at everything. To my dad, for instilling in me a love of words and grammar; for wading through this thesis with a red pen, and for teaching me that "no one remembers second place"!

Contents

List of Figures

List of Tables

Acronyms and abbreviations

ACK	Ammonium Chloride Potassium
Ag	Antigen
AIDS	Acquired Immunodeficiency Syndrome
ALP	Alkaline Phosphatase
ANOVA	Analysis of Variance
APC	Antigen Presenting Cell
AUC	Area under the Curve
BMMφ	Bone Marrow Macrophage
BCG	Bacille Calmette-Guerin
BSA	Bovine Serum Albumin
CAF	Cationic Adjuvant Formulation
CCR	CC Chemokine Receptor
CD	Cluster of Differentiation
cDNA	Complementary DNA
CFU	Colony Forming Unit
CI	Confidence Interval
CL3	Containment Level 3
CR	Complement Receptor
CTL	Cytotoxic T Lymphocyte
CTLA	Cytotoxic T Lymphocyte-associated Molecule
CV	Coefficient of Variation
CV	Column Volume
DAVID	Database for Annotation, Visualisation and Integrated Discovery
DC	Dendritic Cell
DC-SIGN	Dendritic Cell-specific Intercellular Adhesion Molecule-3-Grabbing Non-Integrin
DFO	Deferoxamine
DMSO	Dimethyl Sulfoxide

DNA	Deoxyribonucleic Acid
DTH	Delayed-Type Hypersensitivity
EDTA	Ethylenediaminetetraacetic Acid
ELISA	Enzyme-Linked Immunosorbent Assay
ELISpot	Enzyme-Linked ImmunoSpot
ESAT	Early Secretory Antigen Target
FACS	Fluorescence-Activated Cell Sorting
FCS	Foetal Calf Serum
Fe	Iron
FGF	Fibroblast Growth Factor
FGF	Functional Genomics Facility
Foxp3	Forkhead Box P3
FSC	Forward Scatter
G+C	Guanine + Cytosine
GCP	Good Clinical Practice
G-CSF	Granulocyte Colony-Stimulating Factor
GDF	Growth Differentiation Factor
GFP	Green Fluorescent Protein
GM-CSF	Granulocyte-Macrophage Colony-Stimulating Factor
GTP	Guanosine Triphosphate
GWAS	Genome-Wide Association Study
HAMP	Hepcidin Antimicrobial Peptide
Hb	Haemoglobin
HEPES	4-(2-hydroxyethyl)-1-piperazineethanesulfonic Acid
HI	Heat Inactivated
HIV	Human Immunodeficiency Virus
HP	High Performance
Hr	Hour
Hsp	Heat Shock Protein
ICC	Intraclass Correlation Coefficient

ICS	Intracellular Cytokine Staining
ID	Intradermal
IFN	Interferon
IgA	Immunoglobulin A
IgG	Immunoglobulin G
IgM	Immunoglobulin M
IL	Interleukin
IM	Intramuscular
iNOS	Inducible Nitric Oxide Synthase
IP	Immune Protein
kDa	Kilodalton
KO	Knock-out
LAM	Lipoarabinomannan
LN	Lymph Node
MBL	Mannose Binding Lectin
MCHGB	Mean Corpuscular Haemoglobin
MCP	Monocyte Chemoattractant Protein
MDC	Human Macrophage-Derived Chemokine
MDLN	Mediastinal Lymph Node
MDR	Multi Drug-Resistant
MFI	Median Fluorescence Intensity
MGIA	Mycobacterial Growth Inhibition Assay
MGIT	Mycobacterial Growth Indicator Tube
MHC	Major Histocompatibility Complex
MIP	Macrophage Inflammatory Protein
ML	Monocyte to Lymphocyte
MN	Monocytes
MOI	Multiplicity of Infection
mRNA	Messenger Ribonucleic Acid
M.tb	*Mycobacterium tuberculosis*

MSMD	Mendelian Susceptibility to Mycobacterial Disease
MTBC	*Mycobacterium tuberculosis* Complex
MVA	Modified Vaccinia virus Ankara
NHP	Non-human Primate
NIBSC	National Institute for Biological Standards and Control
NK	Natural Killer
NO	Nitric Oxide
NOS	Nitric Oxide Synthase
NTM	Non-tuberculous Mycobacteria
OADC	Oleic acid, Albumin, Dextrose and Catalase
OD	Optical Density
PBL	Peripheral Blood Lymphocytes
PBMC	Peripheral Blood Mononuclear Cell
PBS	Phosphate-Buffered Solution
PCA	Principal Components Analysis
PCR	Polymerase Chain Reaction
PDGF	Platelet-Derived Growth Factor
pfu	Plaque-forming Units
PHA	Phytohaemagglutinin
PHE	Public Health England
PHS	Pooled Human AB Serum
PMA	Phorbol 12-myristate 13-acetate
PPAR	Peroxisome Proliferator Activated Receptor
PPD	Purified Protein Derivative
PV	Pre-vaccination
qPCR	Quantitative Polymerase Chain Reaction
rBCG	Recombinant BCG
rIFN	Recombinant Interferon
RANTES	Regulated on Activation, Normal T cell Expressed and Secreted
RLU	Relative Light Units

RNA	Ribonucleic Acid
RPM	Rotations per Minute
rRNA	Ribosomal Ribonucleic Acid
S1P	Sphingosine-1-phosphate
SA	South African
SC	Subcutaneous
SDS	Sodium Dodecyl-Sulphate
SEM	Standard Error of the Mean
SIV	Simian Immunodeficiency Virus
SEM	Scanning Electron Micrograph
SPF	Specific Pathogen Free
SSC	Side Scatter
SSI	Statens Serum Institute
TB	Tuberculosis
T_{CM}	Central Memory T cell
TCR	T Cell Receptor
TDR	Totally Drug-Resistant
T_{EM}	Effector Memory T cell
TGF	Transforming Growth Factor
TGN	Trans-Golgi Network
Th	T Helper
TLR	Toll-like Receptor
TNF	Tumour Necrosis Factor
T_{reg}	Regulatory T cell
TST	Tuberculin Skin Test
TTP	Time to Positivity
VEGF	Vascular Endothelial Growth Factor
W	Week
WHO	World Health Organisation
XDR	Extensively Drug-Resistant

Introduction

1 Introduction

1.1 Tuberculosis

Tuberculosis (TB) is an ancient scourge that has plagued humankind throughout known history and may have killed more people than any other pathogen[1]. However, until the late 19th century, very little was known about the disease; patients were simply advised to 'sleep and eat nutritious foods'[2]. In 1882, the history of TB was changed dramatically when Robert Koch discovered the causative agent to be the Tubercle bacillus, now known as *Mycobacterium tuberculosis* (*M.tb*)[3]. Though the following 60 years saw the development of both antibiotic treatment and the Bacille Calmette-Guerin (BCG) vaccine, the struggle was far from over[2].

Infection with *M.tb* remains a serious global health threat, with an estimated 9 million new cases and 1.5 million deaths annually[4]. Due to the nature of the disease, treatment is prolonged and complex. As TB incidence is concentrated in areas of low socioeconomic status with limited access to healthcare, implementing such strategies is challenging. Furthermore, current treatments do not ensure complete cure, and frequently result in adverse side-effects such as hearing impairment and hepatitis, leading to poor adherence[5]. The problem is now further confounded by the continuing rise of multi drug-resistant (MDR), extensively drug-resistant (XDR) and totally drug-resistant (TDR) TB. Drug resistance can occur in both patients treated for TB and in new cases, with an estimated 3.5% and 20.5% of all cases respectively being multi drug-resistant[6].

1.1.1 Epidemiology

TB is a disease of poverty that mainly affects the developing world. In 2013, the South-East Asia and Western Pacific regions accounted for 56% of the world's TB cases. The African region accounted for approximately 25%, with the highest rates of cases and deaths per

capita. India and China had the largest absolute number of cases (24% and 11% of the global total respectively)[6] (Figure 1-1). In these high burden settings, TB rates peak in early adulthood, affecting the most economically productive age-groups. TB incidence in developed countries such as Western Europe, the US and Japan is <20 cases per 10,000 population (compared with >1,000 per 10,000 population in South Africa and Swaziland). In these developed areas, TB is more common among the elderly, immigrant populations and those of low socioeconomic status[6].

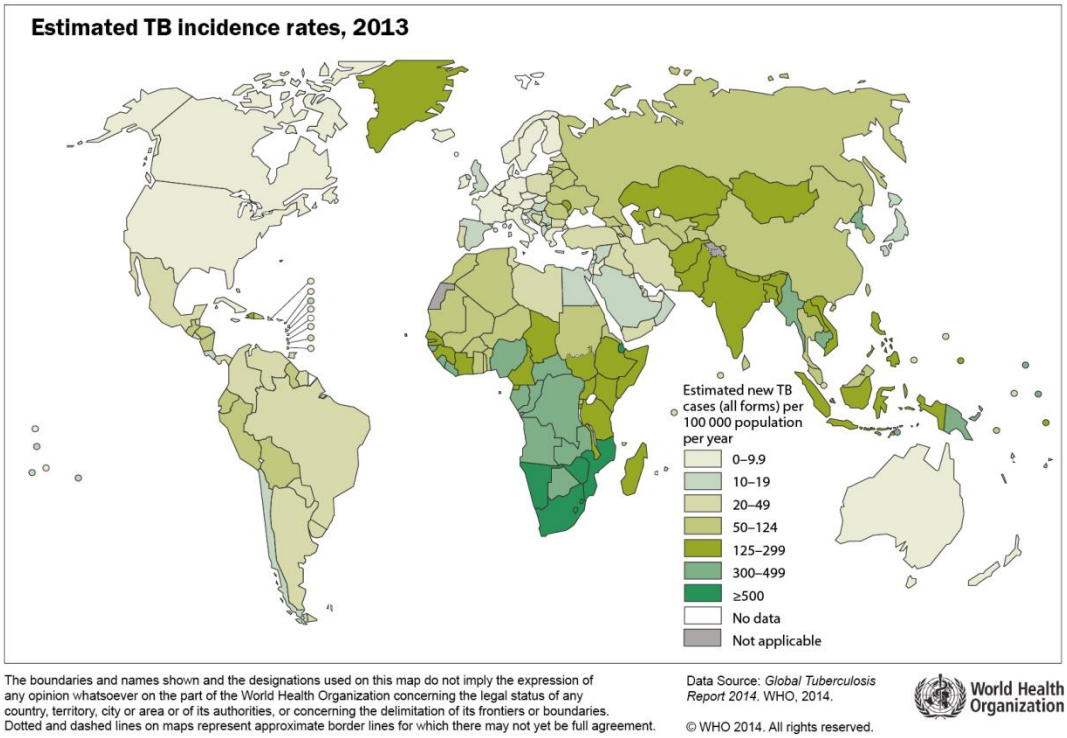

Figure 1-1 Global TB Incidence Rates 2013. Taken from the WHO Global Tuberculosis Report 2014[6].

Approximately twice as many TB cases are reported in men as women, which may be due to differences in smoking rates, occupational lung damage or immune function. However, there is also likely to be a detection bias in settings where women have greater difficulty accessing healthcare[7]. TB remains a leading non-obstetric cause of death in women from endemic

areas[8]. Due to poor reporting, the contribution of TB to child mortality is undetermined, though children between the ages of 5 and 15 years appear relatively immune from developing the disease. The basis for this 'golden age' is unclear, but protection may be related to endocrine regulation of immune responses[9,10].

Susceptibility to active TB is increased by malnutrition, chronic lung disease and other co-morbidities[11]. TB and HIV/AIDS have a fatal synergistic interaction, with major epidemiological overlap. Infection with HIV greatly increases the chances of developing active TB following exposure, reactivation of latent disease and mortality[12]. It has also been suggested that the chronic immune stimulation resulting from active TB accelerates HIV disease progression[13]. Of all TB cases identified in 2013, 1.1 million (12%) were co-infected with HIV, with TB the leading cause of death among patients who have progressed to AIDS[6]. In 2012, 75% of TB-HIV co-infection cases were in sub-Saharan Africa. Individuals living with diabetes have a 2 to 3 times higher risk of developing active TB; around 10% of TB cases globally are now linked to diabetes. It has been predicted that global diabetes prevalence will increase by 69% by 2030, with 80% of prevalent cases in the developing world[14].

The high burden of TB in developing countries is due to a combination of poor living conditions, lack of medical resources, high prevalence of HIV and other co-morbidities, and low efficacy of BCG[15]. The advent of drug-resistant TB has further exacerbated the problem. With increasing mobility due to job migration, drug-resistant TB poses a threat to the UK and wider European community as well as developing countries[16]. The need for an effective vaccine has never been greater.

1.1.2 Etiology

The causative agent of TB is *Mycobacterium tuberculosis* (*M.tb*); a pathogenic bacterial species belonging to the family *Mycobacteriaceae*, of the genus *Mycobacterium* and the

phylum Actinobacteria. The Greek prefix ‘myco’ meaning ‘fungus’ refers to the mould-like manner in which mycobacteria grow when cultured. All mycobacteria share a similar structure and distinct properties: they are straight or slightly curved rods of 2-4µm long (Figure 1-2), aerobic, non-motile and acid-fast[17]. The lipid-rich cell wall is hydrophobic, waxy and particularly thick; making the genus characteristically hardy and resistant to many disinfectants and antibiotics[18]. Mycobacteria replicate at a relatively slow rate; ‘rapid-growers’ form clearly visible colonies within 7 days of subculture, whereas ‘slow-growers’ take 2-4 weeks. *Mycobacterium leprae* may take more than 20 days for one division cycle[19].

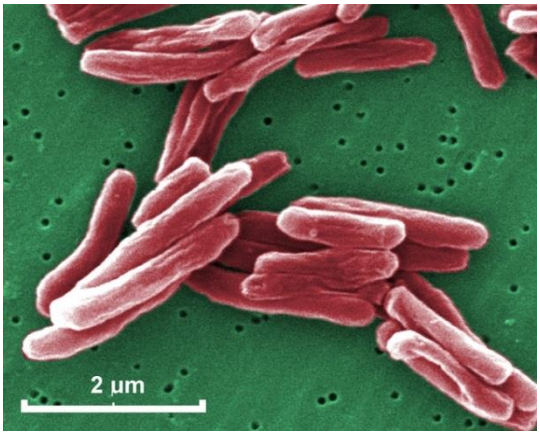

Figure 1-2 ***Mycobacterium tuberculosis (M.tb)***. Colourised scanning electron micrograph (SEM) of multiple *M.tb* bacilli under high magnification (15549x). Taken from www.microbiologyinpictures.com. (This image is in the public domain and free of any copyright restrictions).

Mycobacteria that do not cause TB or leprosy are known as ‘environmental’ or non-tuberculous mycobacteria (NTM). NTM are widely distributed in the environment, particularly in wet soil and marshland[20]. For reasons not fully understood, these species tend to cluster in specific geographical distributions; *M.Kansasii* is most commonly found in the southern and central regions of the US, while *M.abscessus* is found mainly in the south-

eastern states[21]. Other common NTM organisms include *M.avium* and *M.smegmatis*. NTM can cause human disease due to environmental exposure, but usually only in those with immunosuppression (such as AIDS or diabetes) or structural lung disease[22]. Although animals may serve as a reservoir, animal-to-human or human-to-human transmission has never been convincingly demonstrated[21].

The group of closely-related mycobacteria that are capable of causing tuberculosis in humans and animals are known as the *Mycobacterium tuberculosis* complex (MTBC). The MTBC includes the typical human-associated pathogens *M.tuberculosis* and *M.africanum*, as well as several lineages adapted to different mammal species including *M.bovis*, *M.microti*, *M.caprae*, *M.orygis* and *M.pinnipedii*[23]. *M.bovis*, the classical causative agent of bovine TB, is an important zoonotic species that can cause disease in humans. In developed countries, the introduction of pasteurisation and eradication of infected herds have considerably reduced prevalence of human disease, but it remains a problem in developing countries and immunosuppressed individuals[24]. In one study in San Diego, 34.9% of cases of TB infection in HIV-positive individuals were caused by *M.bovis*[25].

The characteristic features of *M.tb* include its slow growth, dormancy, intracellular pathogenesis and genetic homogeneity. Sequence analysis of multiple loci in a large number of isolates indicated that the genome of *M.tb* is either particularly inert or that the organism is relatively evolutionarily young[26]. It is a Gram-positive bacterium with a G+C-rich genome and a typical generation time of ~24 hours in infected animals or synthetic medium. The cell envelope contains an additional layer beyond the peptidoglycan that is rich in unique lipids, glycolipids and polysaccharides[27]. The cell wall contains mycolic acids, mycocerosic acid, phenolthiocerol, lipoarabinomannan and arabinogalactan which may contribute to mycobacterial longevity and pathogenesis[26] (Figure 1-3). *M.tb* is an obligate human pathogen with limited survival outside the human body and no other known reservoir[28]. Different strains of *M.tb* cause various spectrums of disease[29]; TB outbreaks are often caused by

hypervirulent strains such as HN878 (W-Beijing) which result in exacerbated immunopathology and increased mortality[30]. Such mutants often have deletions in cell wall-modifying enzymes or regulators that respond to environmental stimuli, and are rapid growers[31].

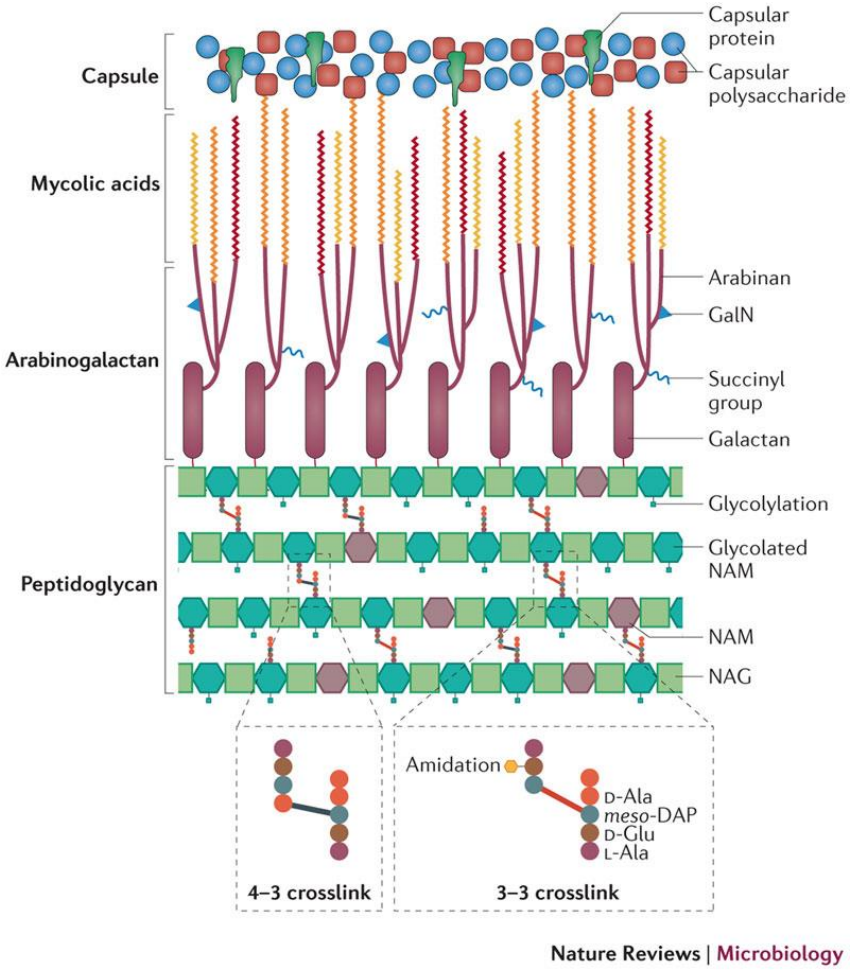

Figure 1-3 The mycobacterial cell wall. The cell wall is a complex structure composed of three distinct macromolecules: peptidoglycan, arabinogalactan and mycolic acids; surrounded by a non-covalently linked outer capsule of proteins and polysaccharides. Taken from Kieser & Rubin; Nature Reviews Microbiology 12, 550-562 (2014)[32].

1.1.3 Pathogenesis

The process of infection is initiated when one or more bacteria are delivered in water droplets into the alveolus of the lung, where they are ingested by alveolar macrophages[33]. The majority of individuals (90%) infected with *M.tb* do not develop disease. Following inhalation of infectious particles, there are four possible outcomes: 1) failure to register an infection, 2) infection occurs but is cleared, 3) infection is contained but bacilli continue to be harboured in the absence of symptomatic disease (latent infection), or 4) development of progressive active TB disease (Figure 1-3). If not initially cleared, mycobacteria multiply and eventually burst the host cells, leading to further infection and extracellular bacilli. The infected areas gradually transform into a granuloma, a complex formation of cells intended to contain the infection. Bacteria continue to grow and multiply, and over time the granuloma breaks down and ruptures necrotic lung tissue, releasing bacilli into the airways and reinitiating the infectious cycle[34].

In the majority of cases, the necrotised lesions heal with a degree of scarring and calcification. However, the pathogen can remain asymptomatic and latent for years or decades; less than 10% of such latent cases become reactivated infections[35]. Approximately one third of the world's population is estimated to be latently infected with TB[4]. If the host fails to contain the initial infection, or if it is reactivated in a latently infected individual, 'active' TB disease occurs. Active disease most commonly affects the lungs (>90% of cases), and symptoms include a persistent cough, coughing up blood or sputum, fever, night sweats and weight loss[2]. Untreated, the 10-year case fatality rate is between 53 and 86% in HIV-negative individuals[36].

In 15-20% of active cases, and usually in those with HIV or another form of immunosuppression, the infection spreads outside the lungs causing extrapulmonary TB[37]. The most common infection sites are the lymph nodes, pleura, gastrointestinal tract, bone and

central nervous system[38]. Widespread disease, usually spread through the bloodstream, is known as disseminated TB or miliary tuberculosis, and makes up about 20% of extrapulmonary cases. Disseminated TB is more commonly seen in infants[39].

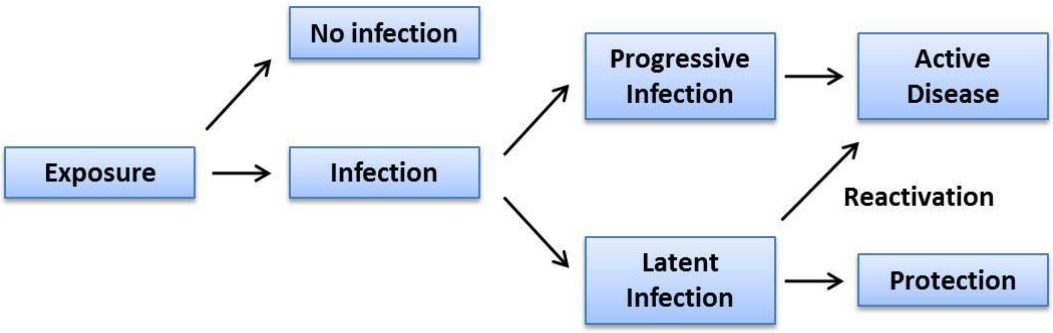

Figure 1-4 Outcomes of TB infection. Exposed individuals may develop an infection, which either progresses to become active disease or is controlled by the immune system and remains dormant as latent disease. Less than 10% of latent cases reactivate to become active disease.

1.2 The innate immune response to TB

The innate immune system is an evolutionarily ancient defence strategy that developed before the separation of vertebrates and invertebrates, and most multicellular organisms depend on it exclusively. The cells of the innate system recognise and respond to pathogens in a nonspecific way, and provide immediate but short-lived defence[40]. The major innate cell types involved in *M.tb* infection are macrophages, neutrophils, dendritic cells and natural killer cells.

1.2.1 Macrophages

Alveolar macrophages are one of the first cell types to encounter *M.tb* upon aerosol transmission[41]. While these cells function as the first line of defence against infection, they also provide the main reservoir for bacterial survival and replication[42]. Macrophages possess an array of receptors to recognise mycobacterial ligands including Collectins (eg. mannose-binding lectin), C-type lectins (eg. mannose receptor, DC-SIGN) and toll-like receptors (eg. TLR-2, TLR-4)[43]. The complement receptors CR1, CR3 and CR4, and receptors for CD14, also play a role in *M.tb* entry into macrophages[44]. As well as recognising ligands and mediating phagocytosis, macrophage receptors are involved in activating specific downstream pathways and influencing the ensuing inflammatory response. Mannose receptor, for example, ligates *M.tb* lipoarabinomannan and activates macrophage peroxisome proliferator activated receptor gamma (PPARγ) expression in a phospholipase A2 and TLR-2 dependent manner. PPARγ in turn induces the production of cyclooxygenase 2 and IL-8, which regulate inflammatory responses via arachidonic acid metabolites and the recruitment of neutrophils respectively[43].

Ordinarily, macrophages internalise bacteria into membrane-bound organelles known as phagosomes, which mature and fuse with lysosomes[45]. Phagolysosomal fusion results in an acidic environment rich in hydrolytic enzymes that degrade and kill bacteria. Furthermore,

proteolysis of bacteria in this compartment generates antigens that may elicit MHC- or CD1-restricted T cell responses[46]. *M.tb* employs a range of strategies to permit survival and uncontrolled replication in this hostile environment. Once inside the phagosome, acidification is inhibited[47]. The mycobacteria then prevent the phagosome from maturing[48] and trafficking to the lysosome[49], thus preventing phagolysosomal fusion[50]. It has been suggested that *M.tb* may in fact translocate to the cytosol[46,51], although the general consensus is that bacteria are retained within the phagosome until the host cell dies through necrosis or apoptosis[42].

1.2.2 Dendritic cells

Similar to macrophages, dendritic cells (DCs) express complement receptor 3 (CR3) and mannose receptors that mediate uptake of *M.tb* within the lung alveoli. In addition, they possess the DC-specific C-type lectin DC-SIGN that plays a key role in the dissemination of HIV-1 and has recently been proven an important receptor for viable mycobacteria[52]. Although *in vitro* studies indicate low levels of mycobacterial replication in DCs[53], it remains unclear whether these cells serve as a major cellular niche for *M.tb* replication *in vivo*. DCs are the primary antigen presenting cells (APCs) in *M.tb* infection, which are critical in bridging the innate and adaptive immune responses. Once infected, they migrate to the draining lymph nodes where they prime naïve T cells leading to expansion[54]. Work by Hanekom *et al*. suggests that *M.tb* is able to subvert DC function to impair T cell responses and evade adaptive immunity[55].

1.2.3 Neutrophils

Despite representing the most commonly infected phagocyte in human TB, neutrophils have been largely neglected - due in no small part to inherent difficulties working with these cells. Reports of their role are controversial and conflicting; they have been shown to contribute significantly to the control of *M.tb* in blood[56], yet neutrophilia at the time of TB diagnosis is associated with delayed clearance of sputum bacteria[57]. Depletion of granulocytes in mice

prior to *M.tb* challenge has been shown to increase the bacterial load in some studies[58,59] but not others[60]. Most reports indicate that early recruitment of neutrophils to the site of infection improves outcome, and risk of infection in TB contacts is inversely proportional to the peripheral blood neutrophil count[56]. However, the stage of infection appears to be crucial: higher neutrophil counts in established disease are associated with poorer outcome[61]. The mode of action of neutrophils is also subject to much debate. *In vitro* studies provide evidence both for[62-64] and against[65-67] the ability of neutrophils to kill internalised mycobacteria, and it may be that both outcomes are possible *in vivo*. Reports in the literature suggest that neutrophils influence the development of acquired immunity through the production of IL-12, MCP and other cytokines, which can attract T cells and direct their maturation[68]. However, they may also have suppressive functions, for example through IL-10 production[69]. It appears that the neutrophil response is highly complex and not yet fully understood.

1.2.4 Natural Killer cells

Natural killer (NK) cells are CD56+CD16+/-CD3- lymphocytes that have several effector functions including recognition and lysis of infected or stressed cells, as well as cytokine production[70]. Their role in TB is less well-defined than that of other cell types, though it has been demonstrated that NK cells are recruited to the lung following *M.tb* infection in mice, where they produce IFN-γ and perforin. However, depletion of NK cells does not affect lung bacterial load, suggesting that their functional role is redundant[71]. Human NK cells have been shown to directly lyse *M.tb*-infected macrophages *in vitro*[72,73], and to actively restrict mycobacterial growth in an apoptosis-dependent manner[74]. They also play an indirect role in restricting mycobacterial growth via promotion of CD8 and γδ T cell responses[75,76]. It is possible that the function of NK cells overlaps with that of other immune cells; indeed NK cells made a significant contribution to control of infection in the absence of T cell function[77].

1.3 The adaptive immune response to TB

The adaptive arm of the immune system is specific to the pathogen that induces it and involves the development of immunological memory. Compared with innate immunity, there is a delay in the mounting of an adaptive response as cells must process and present antigen, followed by activation and expansion of specific T and B cells.

1.3.1 CD4+ T cells and cytokines

Following infection, DCs in the lung phagocytose *M.tb* and traffic to the local lung-draining mediastinal lymph node (MDLN) where they present antigen in association with MHC class II, thus activating and inducing proliferation of antigen-specific CD4+ T cells[78-81]. Earlier CD4+ T cell activation in the MDLN is associated with superior control of *M.tb* in the lung[79], whilst delaying activation by DC depletion exacerbates disease outcome[82]. Many studies have indicated that CD4+ T cells are a requirement for the successful control of *M.tb* infection. Mice deficient in either CD4 molecules or MHC class II demonstrate increased susceptibility to *M.tb*[83,84]. Depletion of CD4+ T cells causes reactivation of latent *M.tb* infection in mice[85] and increased pathology and bacterial burden during the first 8 weeks of infection in NHPs[86]. The increased risk of TB disease due to decreased CD4+ T cell number and function associated with HIV infection in humans (and SIV in NHPs[87]) provides further evidence of a critical role for this cell type[88,89].

Following TCR activation in a particular cytokine milieu, naïve CD4+ T cells may differentiate into one of several lineages of T helper (Th) cells, including Th1, Th2, Th17 and regulatory T cells (T_{regs})[90]. The different lineages are defined by their pattern of cytokine production and function, and the dogma has long been that Th1 cells drive the type-1 ‘cellular immunity’ pathway to fight intracellular pathogens while Th2 cells drive the type-2 ‘humoral immunity’ pathway and upregulate antibody to fight extracellular organisms. Th1 cells produce IFN-γ, TNF-α and IL-2 as their ‘signature’ cytokines; Th2 cells produce IL-4, IL-5

and IL-13 among others[91]. Although this dichotomy may be helpful in breaking down complex responses, the utility of such a model has recently come into question due to considerable overlap and cross-talk between the two responses[92].

During the course of *M.tb* infection, naïve CD4+ T cells encounter *M.tb*-infected IL-12 secreting DCs in the MDLN and recognise antigen in the context of MHC class II. Under these conditions, CD4+ T cells are primed as Th1 cells and become a primary source of IFN-γ production during the acute phase of infection. In the murine model, peak production of IFN-γ occurs around 3-4 weeks after initial infection[93]. A central role for IFN-γ in TB disease was first suggested by observations of abundant IFN-γ mRNA in the lesions of self-healing leprosy[94]. When rIFN-γ was injected into leprosy lesions, there was an influx of large numbers of T cells and monocytes to the site of injection, and a corresponding decrease in bacilli[95,96]. Furthermore, T cells which adoptively transferred protection against *M.tb* challenge were shown to produce IFN-γ upon *in vitro* stimulation[97]. In the 1990s, murine experiments indicated that IFN-γ knock-out (KO) mice are extremely susceptible to *M.tb* infection[98,99], and genetic studies of Mendelian susceptibility to mycobacterial disease (MSMD) confirmed a role for IFN-γ in humans[100]. It was later shown that IFN-γ activates macrophages to kill intracellular mycobacteria by activating downstream antimicrobial effector pathways, including inducible nitric oxide synthase (iNOS)[101,102], GTPases[103], autophagy[104] and vitamin D receptor signalling[105]. Together with the work of North[106] and others on the importance of CD4+ T cells, these studies shaped the paradigm of TB immunity: that the production of IFN-γ by CD4+ T cells activates macrophages to kill intracellular mycobacteria.

Th1 CD4+ T cells are also potent producers of TNF-α and IL-2[107]. TNF-α, like IFN-γ, is involved in activation of bactericidal activity in infected macrophages[108]. Treatment of mice with anti-TNF antibody results in fatal reactivation of persistent *M.tb* infection with increased bacterial burden and severe pulmonic histopathological deterioration[109]. The importance of

this cytokine is highlighted by the increased incidence of TB in patients treated with anti-TNF agents for inflammatory conditions such as Crohn's disease[110]. IL-2 directly promotes T cell expansion and survival, while GM-CSF does so via the modification of DC function; increasing IL-12 production and expression of co-stimulatory molecules on the cell surface[111].

Antigen-specific T cells that gain the capacity to simultaneously produce two or more cytokines are known as polyfunctional T cells. While polyfunctional CD4+ T cells have been shown to be beneficial in other models of infection[112,113], their role in TB remains unclear. It has been reported that patients with active TB disease have higher frequencies of antigen-specific CD4+ T cells with a single or dual function (particularly TNF+ or TNF+IFN-γ+), compared with latent or cured TB patients who have higher frequencies of trifunctional IFN-γ+TNF+IL-2+ antigen-specific cells[114,115]. Conversely, it has also been suggested that active disease is associated with an increase in trifunctional CD4+ T cells compared with latent disease or those post-treatment[116,117]. The relevance of polyfunctional T cells as a correlate of protection in TB vaccine development will be discussed in section 1.6.

The Th2 response, characterised by the production of IL-4, IL-5, IL-10, IL-13 and antibodies, is associated with extracellular pathogens and may be detrimental in *M.tb* infection[118]. Reactivation of *M.tb* infection in mice is associated with a shift from a Th1 to Th2 type cytokine response, and control of infection with a return to the type 1 pattern[119]. In humans, active TB is associated with reduced Th1 and increased Th2 activity with upregulation of IL-4[120]. An increased Th2 response has been linked to the presence of cavitary lesions[121]. Furthermore, patients with a favourable outcome after treatment exhibit a higher Th1/Th2 ratio compared to those with a poor clinical outcome[120]. Helminth infection is associated with a strong Th2 response and significant suppression of Th1 response. There is evidence that intestinal helminth coinfection has a negative impact on both immunity to *M.tb* and clinical response to TB therapy[122,123], although this has recently been challenged[124]. The efficacy of

BCG is greatly reduced in areas endemic for helminth infection[125] and mice colonised with *S.mansoni* exhibit reduced protection from BCG following subsequent *M.tb* challenge, associated with production of IL-4 and IL-5[126]. More recently it has been suggested that the reduction in immunogenicity of BCG in helminth-infected individuals is linked to increased TGF-β production rather than an enhanced Th2 response[127].

The development of Th17 cells is initiated by IL-6 or IL-21 in the presence of low levels of TGF-β, and these cells produce the cytokines IL-17, TNF-α, IL-21 and IL-22[128]. IL-17 is primarily produced by γδ T cells[129,130], and its receptor is ubiquitously expressed in many cell types including DCs, macrophages and lymphocytes. IL-17 induces expression of proinflammatory genes such as G-CSF and IL-8, antimicrobial proteins such as defensins, neutrophil recruitment and inflammation[128]. Although IL-17 and other Th17 derived cytokines have a central role in the protective immune response to rapidly-growing extracellular bacterial pathogens[131], their role in intracellular bacterial infections is not well understood. IL-17 KO mice are unable to control infection by the hypervirulent *M.tb* strain HN878, although they do survive infection with less pathogenic strains[30]. After high-dose intratracheal infection, IL-17-deficient mice are unable to control *M.tb*[132]. During the chronic phase of infection, a balance must be achieved with Th1 and Th17 responses to control bacterial growth but limit immunopathology. Excessive IL-17 production can lead to extensive neutrophil recruitment and tissue damage[128].

A wide variety of cell types, cell surface molecules and cytokines contribute to regulation of the immune response to avoid excessive damaging inflammation. The most critical cellular subset is CD4+ T cells expressing the transcription factor Foxp3, or regulatory T cells (T_{regs}). However, such cells play a dual role: as well as benefiting the host by limiting immune-mediated pathology, they also facilitate chronic *M.tb* persistence by reducing effector immunity and clearance of infection[133]. Increased numbers or T_{regs} are observed in patients who develop active disease with a high bacterial burden[134]. The mechanisms by which T_{regs}

control the immune response are not well understood, but there is evidence for a central role of the inhibitory cytokines IL-10 and TGF-β, and the surface molecule CTLA-4[135]. IL-10 is an immunoregulatory cytokine that is a potent suppressor of macrophage activation and excess production of this cytokine impairs macrophage killing of phagocytosed *M.tb*, leading to reduced APC capacity, diminished production of cytokines and subsequent impairment of antigen-specific CD4+ and CD8+ T cell activation and proliferation[136].

1.3.2 CD8+ T cells

CD8+ T cells are activated by the presentation of antigen in association with MHC class I. It has been suggested that CD8+ T cells in *M.tb* infection are primed to be cytokine-producing or cytotoxic[137]. Similar to CD4+ T cells, cytokine-producing CD8+ T cells secrete IFN-γ, TNF-α and IL-2[138] which have critical functions during *M.tb* infection as described. Cytotoxic cells (CTLs) can kill *M.tb* infected cells via granule-mediated functions (perforin, granzymes and granulysin) or Fas-Fas ligand interaction to induce apoptosis[139-141]. The importance of CD8+ T cells in *M.tb* infection is unclear, but there is evidence that antigen-specific CD8+ T cells are induced during *M.tb* infection and that these cells are capable of recognising *M.tb* infected macrophages[142]. Some *in vivo* mouse studies support a role for CD8+ T cell immunity against TB[143-145], whereas others do not[146,147]; the involvement of this subset may depend of the phase of infection[148]. It has been suggested that mice may not be an appropriate model for evaluating the relevance of this cell type in humans as they lack some important immune features relating directly to CD8+ T cell function and specificity, such as expression of group 1 CD1 proteins capable of presenting *M.tb* lipid antigens and the cytotoxic protein granulysin[141,149]. In the more closely-related NHP, CD8+ T cells appear to be essential in controlling acute and chronic low-dose infection (Flynn, unpublished). CD8+ T cell depletion leads to a significant decrease in immunity against *M.tb* in both BCG-vaccinated and previously infected and treated monkeys upon re-infection[150]. In the absence

of a situation akin to HIV and CD4+ T cells, where CD8+ T cells are specifically deficient, it is difficult to determine the contribution of CD8+ T cells to protection against TB in humans.

1.3.3 B cells and antibodies

Due to the intracellular nature of *M.tb*, it is the cell-mediated rather than humoral response that is considered central to immunity against TB[151]. However, recent evidence suggests that the division of labour may not be so clear-cut, and B cells may modulate the T cell response, participating in T cell priming through antigen capture and presentation[152,153]. Such a role is somewhat inconsistently observed, and may depend on antigen types and prevailing immunological conditions. The cytokine milieu at the site of the APC to T cell interaction strongly influences CD4+ T cell development; B cells produce a variety of cytokines either constitutively or in the presence of antigens, and as such may influence T cell lineage outcome[154].

The role of antibodies in TB has been controversial since the serum therapy experiments of the late 19th and early 20th centuries. The inability of various investigators to consistently generate effective sera suggested that antibody-mediated immunity plays at best only a minor role in the outcome of *M.tb* infection[155]. However, more recently monoclonal antibodies specific for mycobacterial components such as arabinomannan and 16 kDa α-crystallin have been shown to protect mice against *M.tb*; albeit with varying efficacy[156-158]. Children with low serum IgG against mycobacterial antigens and LAM, or those who could not mount antibody responses to these antigens, were shown to be predisposed to disseminated TB[159]. Furthermore, the presence of high antibody titers to Ag85 complex antigens were observed in cured patients and those with non-cavitary TB, while patients with poor disease outcome lacked these antibodies[160]. Despite such evidence, a vaccine comprising an *M.tb* arabinomannan-protein conjugate that induced a superior antibody response to BCG failed to improve survival of challenged mice[161].

1.3.4 The granuloma

Following initial infection, cytokine and chemokine secretion by *M.tb*-infected macrophages results in the recruitment of a range of cells, including more macrophages, to the site of infection[162]. The controlled sequential recruitment of different cell populations leads to the formation of a highly ordered structure known as a granuloma. Infected macrophages in the centre are surrounded by uninfected macrophages, DCs, NK cells and neutrophils. Beyond this sits a layer of B and T cells, and finally epithelial cells (Figure 1-4)[163]. Granulomas are developed by the host to contain and eliminate bacteria, but they also provide a 'protected' environment for *M.tb*, where it can persist in a latent state for decades. For reasons which remain unclear (but include immunosuppression and genetic factors), bacilli will reactivate in 10% of latently infected individuals, escape the granuloma and spread; giving rise to clinical disease[164].

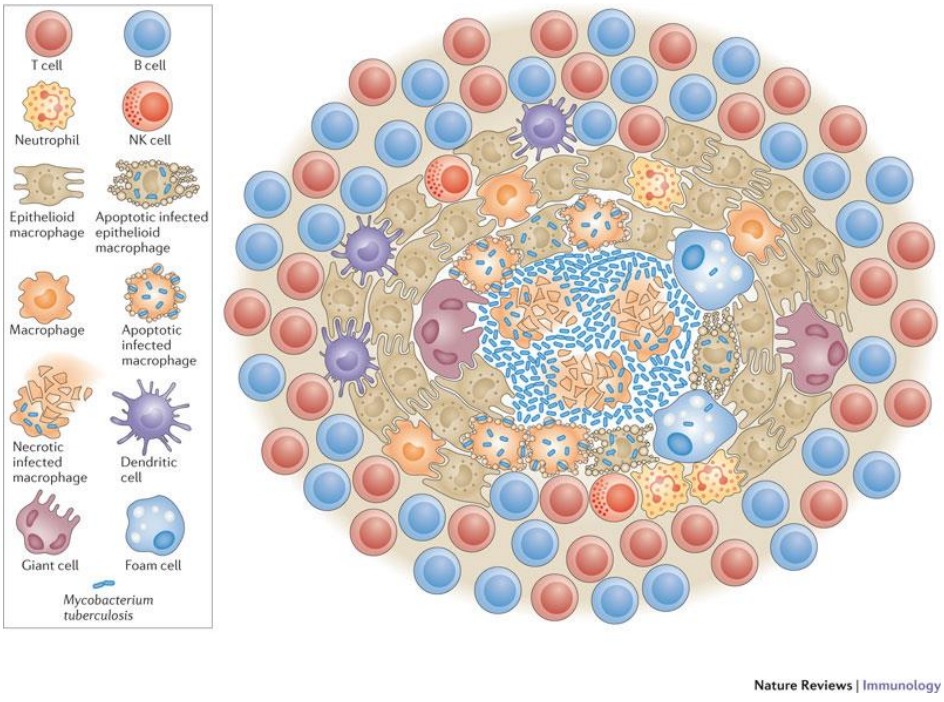

Figure 1-5 The TB granuloma. Infected macrophages in the centre are surrounded by uninfected macrophages, DCs, NK cells and neutrophils. Beyond this sits a layer of B and T cells. Taken from Ramakrishan; Nature Reviews Immunology 12, 352-366 (2012)[163].

1.3.5 Immunological memory

Following infection, antigen-specific T cells and/or B cells undergo clonal expansion. After clearance, approximately 90% of activated effector cells die off, leaving a small residual population of 'memory' cells with high sensitivity to the antigen. Re-exposure to the same pathogen will trigger responsive memory cells to become 'secondary effectors', mounting a more rapid and robust response[165]. This is the basis for most successful vaccines. Evidence indicates two populations of memory T cells, effector memory T cells (T_{EM}) and central memory T cells (T_{CM}). T_{EM} express homing receptors that facilitate migration to non-lymphoid sites of inflammation and rapidly produce microbicidal cytokines (including IFN-γ, IL-4 and IL-5) following stimulation[166]. T_{CM} do not produce any of the effector cell lineage cytokines following stimulation, but they do secrete IL-2 and proliferate extensively; acquiring effector functions later. T_{CM} express CD62L and CCR7, which are involved in migration through the LN and are also found on naïve T cells prior to activation[167]. Little is known about the memory response in TB; the majority of data on memory T cells derives from mouse models of acute viral infection. Early studies indicated that mice infected with *M.tb* generated long-lived memory immunity which provided a level of acquired resistance to secondary infection[168,169]. However, the discovery of two distinct cellular subsets has complicated this picture; more recent reports suggest that these cells predominantly express an effector phenotype and that effector-to-memory T cell transition may be minimal in persisting infections[170].

1.4 TB vaccines

1.4.1 BCG

Mycobacterium bovis Bacille Calmette-Guerin (BCG) is the only currently available vaccine against TB. BCG confers reliable protection against disseminated forms of TB, principally

miliary disease and meningitis[171,172]. Withdrawal of BCG vaccine from Sweden and the former Czechoslovakia resulted in a concomitant increase in cases of tuberculous meningitis and mycobacterial glandular disease[173-175]. BCG is also effective at preventing leprosy[176,177], and recent reports have suggested a role in reducing infant mortality from other non-mycobacterial causes[178,179]. However, although efficacy against infection with *M.tb* has been reported in observational studies in low-burden settings[180], there are reports that BCG provides little or no protection against initial infection with *M.tb*[181], and the incidence of infection in endemic countries is very high despite good BCG coverage[182,183]. The use of BCG is contraindicated in neonates where HIV is suspected due to the risk of disseminated BCG disease and associated complications, which is problematic due to the geographical overlap between HIV and TB epidemics[184]. Furthermore, protection against pulmonary TB (the most common form of TB disease) varies considerably, with the lowest efficacies found in the tropics where TB incidence is greatest[185]. Though in some populations efficacy is estimated at >80%[186], a complete lack of protection has been reported in other areas, such as Chingleput in India[187]. The reasons for varying protective efficacy with geography and population age are poorly understood.

Palmer and colleagues hypothesised that exposure to NTMs, considered to be more common closer to the equator, may play a role[188]. Individuals exposed to NTMs may develop sensitivity that may impart some protection against TB; BCG could then do little to improve upon this naturally acquired protection. This is known as 'masking'. Alternatively, pre-existing immunity may 'block' the ability of BCG to replicate and thus induce a protective immune response. Indeed in two trials where BCG did not perform well in Georgia, Alabama and the aforementioned Chingleput, India, >68% and 95% of individuals respectively were PPD positive by 15-20 years of age[189,190]. In a trial in Malawi where there is high NTM exposure and poor BCG efficacy, individuals with lower immune responses to NTM showed greater IFN-γ responses to BCG[191]. Furthermore, in mice sensitised with NTMs, the

protective effect of BCG (but not a TB subunit vaccine) was considerably reduced[192]. As the lowest levels of BCG protection and the highest rates of HIV are found in countries with the highest incidence of TB, it has been estimated that globally, BCG prevents only 5% of all potentially vaccine-preventable deaths due to TB[193].

It is important to understand why the current vaccination strategy is ineffective, though this remains unclear. There is evidence that large populations of circulating antigen-specific memory cells are induced by BCG[170,194,195], and it has been suggested that the issue lies with the kinetic of the response[196]. During an initial, un-primed response to *M.tb*, it takes 18-20 days for specific T cells to migrate to the lungs. In BCG vaccinated mice, this response is accelerated by only a few days. There is thus still sufficient time for bacteria to become established in the lung, and the memory cells must act in an environment that has been modulated by *M.tb*. Disseminated bacteria, on the other hand, would have less opportunity to modulate the environment, which may explain why BCG is more effective against disseminated than initial pulmonary infection[151]. A more recent study has looked at memory cell subsets in BCG vaccinated mice and shown that antigen-specific populations in the lungs predominantly express an effector or effector memory cell phenotype[170]. It is possible that the flaw in BCG is its poor ability to establish any degree of central memory. Orme proposes a model in which BCG vaccination in neonates induces strong effector memory which is slowly lost (due to a short half-life of effector memory cells or repeated exposure driving cell transition), so that by the age of 10-15 the children are once again susceptible. With no central memory population to back up the response, resistance is lost[196]. The poor ability of BCG to induce T_{CM} cells could be due to vaccine persistence, as BCG is often incompletely eradicated with bacilli persisting in the lymphoid tissues for long periods[197]. This hypothesis is supported by the finding that complete clearance of *M.tb* by chemotherapy does allow expansion of T_{CM} cells[198].

Despite its failings, BCG does confer protection against disseminated disease in childhood, protection against leprosy and possible non-specific protection from sepsis and other causes of infant mortality. As such most novel vaccine strategies are based on two approaches. The first is to improve on BCG itself and the second is a prime-boost strategy in which a new vaccine is given at a later stage as a booster to BCG.

1.4.2 Replacements for BCG

Potential replacements for BCG include recombinant strains of BCG (rBCG), attenuated strains of *M.tb* and inactivated strains of other mycobacteria. rBCG strains that have been evaluated in clinical trials include rBCG30 (engineered to over-express the 30kDa major secreted antigen from *M.tb*)[199], hly+rBCG (constructed to secrete listeriolysin)[200] and Aeras-422 (engineered to express perfringolysin O and over-express antigens 85A, 85B and Rv3407)[201]. Further development of Aeras-422 has been terminated due to the development of shingles in some phase I trial volunteers[202]. Despite intial safety concerns, two groups are currently evaluating attenuated strains of *M.tb* in preclinical models. The live *M.tb* phoP mutant strain (MTBVAC) has been shown to be more attenuated than BCG and confers protective immunity against TB challenge in mice and guinea pigs[203]. Phase I trials of this vaccine are nearing completion (clinicaltrials.gov ref. NCT02013245). The live *M.tb* double-deletion vaccine strains mc(2)6020 and mc(2)6030 were safe and well-tolerated in preclinical studies and afforded some protection in both mice and NHPs[204]. Finally, a trial of *M.vaccae* in BCG-vaccinated, HIV-infected patients in Tanzania demonstrated significant protection against definite TB, but not probable TB or disseminated disease[205].

1.4.3 Heterologous booster vaccines

There are two main strategies for developing a booster vaccine. The first is to use a protein vaccine, which requires co-administration of an adjuvant to induce high levels of cellular immunity. Examples include M72 (a polyprotein of the *M.tb*32 and *M.tb*39 antigens,

administered with the adjuvants AS01 or AS02)[206], and Hybrid I (a fusion protein of the secreted antigens ESAT 6 and antigen 85B delivered with the adjuvant IC31)[207]. Alternatively, a recombinant viral vector may be used, as the virus itself induces strong cellular immunity. Examples include Areas 402 (a replication-deficient Adenovirus serotype 35 expressing a fusion protein of Ag85A, Ag85B and TB10.4 from *M.tb*)[208] and MVA85A. All of these vaccines have been shown to be safe and induce a cellular immune response of varying magnitude. An overview of these and other TB vaccine candidates currently in the TB pipeline is provided in Table 1-1.

MVA85A is a recombinant strain of modified vaccinia virus Ankara (MVA) expressing Ag85A from *M.tb* developed in the host group in Oxford. In preclinical trials, MVA85A can improve on BCG-induced immunogenicity and protection in mice[209], guinea pigs[210], NHPs[211] and cattle[212]. Its safety has been demonstrated in a number of clinical trials in healthy[213], HIV-positive[214] and *M.tb* infected adults[215], infants[216], children and adolescents[217]. It has variously been shown that MVA85A induces IFN-γ producing polyfunctional antigen-specific CD4+ T cells[218], IFN-γ producing CD8+ T cells and expansion of long-lasting memory cell populations[216]. However, no efficacy was demonstrated in a large phase IIb trial in healthy, BCG vaccinated South African infants[219]. This may be due to the population, as immunogenicity was lower than that seen in UK trials, which may be associated with higher baseline indoleamine 2,3-dioxygenase (IDO) activity[220]. The route of vaccination may also be sub-optimum. It has been suggested that preferential circulation of memory lymphocytes back to the tissue in which they first encountered antigen may underlie the limited efficacy of BCG by ID administration[221], and the same may apply to MVA85A. In NHPs, nebulisation of BCG conferred improved protection against *M.tb* challenge compared with ID vaccination[222]. Recent work has focused on MVA85A delivery via aerosol, demonstrating that this route is safe and immunogenic in both NHPs[223] and humans[224].

Name	Type	Composition and attributes	Strategy	Phase
Hybrid1-IC31	Adjuvanted subunit	Recombinant fusion protein of Ag85B and ESAT-6 adjuvanted with IC31	Prime-boost	I
Hybrid1-CAF01	Adjuvanted subunit	Recombinant fusion protein of Ag85B and ESAT-6 adjuvanted with a two-component CAF01 liposomal adjuvant system	Prime-boost	I
M72+AS01E	Adjuvanted subunit	Immunogenic fusion protein (M72) derived from two *M.tb* antigens (*M.tb*32A and *M.tb*39A) and the adjuvant AS01E. *M.tb*32 is a putative 32-kDa serine protease found in culture supernatants and lysates of *M.tb*	Prime-boost	IIb
H4:IC31	Adjuvanted subunit	Fusion protein of *M.tb* antigens 85B and TB10.4 combined with adjuvant IC31	Prime-boost	II
H56:IC31	Adjuvanted subunit	Fusion protein of 3 *M.tb* antigens (85B, ESAT-6 and Rv2660c) formulated in the adjuvant IC31	Prime-boost	II
ID93+GLA-SE	Adjuvanted subunit	Recombinant fusion protein of 4 *M.tb* antigens (virulence-associated Rv2608, Rv3619, Rv3620, and latency-associated Rv1813). GLA-SE adjuvant is a TLR-4 agonist formulated in a squalene-based oil-in-water emulsion	Prime-boost	I
MVA85A	Viral vectored	Attenuated Vaccinia virus MVA vector combined with *M.tb* antigen 85A	Prime-boost	IIb
Crucell Ad35/Aeras 402	Viral vectored	Replication-deficient Adenovirus (Ad35) vector containing the *M.tb* antigens 85A, 85B and TB10.4	Prime-boost	IIb
AsAg85A	Viral vectored	Replication-deficient serotype 5 Adenovirus vector expressing *M.tb* antigen 85A	Prime-boost	I
DAR 901	Whole cell	Heat-inactivated whole cell *Mycobacterium obuense*	Prime-boost	I
VPM 1002(rBCG+Hly)	Recombinant	Recombinant BCG mutant expressing listeriolysin O. Perforation of the phagosomal membrane allows egress of recombinant BCG antigens into the cytosol, facilitating MHC I-mediated CD8+ T-cell priming	Prime	II
MTBVAC	Recombinant	Recombinant *M.tb* mutant lacking expression of genes for several virulence factors, including ESAT6, as well as mutations in genes required for synthesis of bacterial cell wall components that protect *M.tb* from host defences	Prime	I

Table 1-1 Candidate TB vaccines in clinical stage development. Adapted from de Costa *et al*. Int J Infect Dis. 2015 Mar; 32:5-12.

1.5 Preclinical animal models

New candidate TB vaccines are currently tested for safety, immunogenicity and efficacy using preclinical animal models such as mice, guinea pigs and non-human primates (NHPs). However, it is not clear how useful such models are in predicting outcomes in humans. 'Protection' in animal models, as determined by the outcome of *M.tb* challenge experiments, is defined in terms of an improvement in a disease-related readout such as bacterial load, pathology score or long-term survival[212,225,226]. A vaccine is considered to provide protection even if there is measurable bacteria or pathology in the organs or some animals do not survive. In humans, however, efficacy is defined as the prevention of TB disease using clinical endpoints, and any individual becoming infected is not protected. Clearly, an artificial aerosol challenge is very different from natural transmission in humans, and the laboratory strains of *M.tb* commonly used (such as H37Rv) are genetically dissimilar to clinical isolates[227], with much higher challenge doses employed[226]. In addition to these fundamental differences in the model itself, animals are genetically distinct from humans; importantly mice lack most CD1 subtypes and differ in the distribution of Toll-like receptors. The widely used Balb/c and C57BL/6 mouse strains do not exhibit caseating granuloma formation following TB infection[228].

There is yet to be an established link between a vaccine effect observed in animal models and human protection; recently the modest protection conferred by MVA85A in animal models did not translate to efficacy in humans[219,229]. These findings highlighted a gap in our understanding of what magnitude of improvement on BCG in an animal model translates to an acceptable level of clinical efficacy. Animal models can also fail to reliably predict safety in humans, as evidenced by trials of the anti-CD28 monoclonal antibody TGN1412[230] and Fialuridine for the treatment of Hepatitis B[231]. Other limitations include the large numbers required, and the nature and slow growth of mycobacteria making experiments long and

costly with the need for highly specialised Category 3 animal facilities. *M.tb* challenge is classified as a procedure of 'Moderate' severity by the Home Office, indicating that the animals are likely to experience "short term moderate pain, suffering or distress or long-lasting mild pain, suffering or distress… or moderate impairment of the well-being or general condition". Development of an *in vitro* alternative would be unlikely to replace such models, but may provide an opportunity for early 'gating' or down-selection of candidates such that only the most promising go forward to animal testing. Furthermore, such an assay could negate the need for *in vivo M.tb* challenge, measuring instead responses to an *in vitro* infection of cell samples from vaccinated animals.

1.6 Immune correlates of protection

One of the greatest challenges in developing an *in vitro* alternative to animal models in the TB vaccine field, or indeed in developing an effective vaccine itself, is the lack of a single immune parameter that robustly correlates with protection. A candidate biomarker for protective immunity can only be validated through a clinical trial of an effective vaccine. However, without a validated correlate of protection, it is not possible to identify the most promising candidates to take forward to clinical trials in the first place.

In the absence of a known correlate of protection from TB, IFN-γ has been widely used as the primary immunological read-out in human trials. However, in recent years the dogma of 'the more IFN-γ the better' has been challenged. In both TB patients and healthy vaccinated individuals, it transpired that having more IFN-γ secreting T cells, or greater levels of IFN-γ, does not correlate with protection. Rather, TB patients who produce more IFN-γ are more likely to progress to active disease[232], and IFN-γ production has been shown to correlate with *M.tb* bacterial burden in humans, NHPs and mice[233,234]. Although BCG vaccination induces protective T cells in animal studies, production of IFN-γ by these cells does not predict vaccine protection[225,235]. As described, strong induction of an antigen-specific CD4+ and

CD8+ T cell response in BCG-vaccinated individuals receiving an MVA85A boost[236] did not translate to an enhancement in protection[219].

It has recently been proposed that polyfunctional T cells provide a better correlate of protection than IFN-γ secreting monofunctional T cells in several disease models. Antigen-specific memory T cells capable of co-producing IFN-γ, TNF-α and IL-2 were protective against leishmania[112] and have been associated with non-progression in HIV[113]. In a preclinical study of the TB subunit vaccine Ag85B-ESAT-6/CAF01, the robust memory CD4+ T cell population consisted almost exclusively IFN-γ, TNF-α and IL-2 triple-positive cells, and this was associated with protection from challenge[237]. Furthermore, in a study of 5 different vaccine candidates, levels of vaccine-induced protection correlated with the frequency of these triple-positive cells[238]. However, in a 2 year follow-up study of BCG-immunised infants, there was no association between the polyfunctional cytokine profile of induced T cells and protective efficacy[239]. In addition to a strong antigen-specific response, MVA85A also induced a significantly higher frequency of polyfunctional T cells than BCG alone[218] (albeit at relatively modest levels), and this did not confer protection[219].

Other potential correlates include Th17 cells, NK cells, γδ cells and CD4-CD8- double negative T cells, which have all been shown to be long-lived and mediate protection in various disease models[240]. With the advent of improved technology, a promising direction is the study of large cohorts in which the natural immune response to *M.tb* can be followed using an "omics" approach[241]. Immune protection from TB is likely to be dependent on more than CD4+ T cells and IFN-γ, rather requiring the coordinated activity of multiple cell types and immune mechanisms.

1.7 Mycobacterial growth inhibition assays

The failure to identify a single robust correlate of protection from TB has led to a resurgence of interest in emerging 'functional' assays, which take into account a whole range of immune mechanisms. One such assay is the mycobacterial growth inhibition assay (MGIA), which represents an '*in vitro* challenge model' for assessing vaccine efficacy. Several MGIAs have been reported in the literature (summarised in Table 1-2), but have failed to be taken up by vaccine developers. This is likely due to concerns regarding reproducibility, as well as previous focus on the discovery of T-cell signatures.

1.7.1 Cellular MGIAs

The first MGIA was described by Crowle *et al*. in 1981, who cultured lymphocytes (with antigen) and monocytes separately. Macrophages were then infected with mycobacteria and cultured for 7 days with or without the addition of lymphokine produced by the lymphocyte stimulation. It was shown that cultures containing lymphokine from TST+ and BCG-vaccinated individuals were able to control intracellular replication of the bacilli, as measured by [3H]thymidine uptake, bacillary counts and morphological evidence of 'tuberculoimmunity'[242]. The same group went on to develop an MGIA using murine peritoneal macrophages and human alveolar lavage cells, assessing the anti-mycobacterial effects of lymphokine and rIFN-γ on these two cell types[243]. The authors noted numerous technical difficulties, highlighting early challenges in the field.

In 1988, Cheng *et al*. used a complex MGIA to assess anti-mycobacterial effects pre- and 8 weeks post-BCG vaccination in UK children. Monocytes were separated, infected with *M.microti* and allowed to form monolayers in microtitre wells over 24 hours. The lymphocytes were stimulated with whole dead tubercle bacilli and these were added to autologous monolayers for 2 hours per day over 3 consecutive days. The infected monolayers were rinsed daily and the number of live mycobacteria monitored by colony counts.

Interestingly, when monolayers received pulsed exposure to stimulated lymphocytes, growth of *M.microti* was increased. However, growth rates in pulsed monolayers were significantly lower at 8 weeks post-BCG compared with pre-vaccination[244]. When the same assay was applied to volunteers in Southern India, no effect of BCG vaccination was observed, consistent with a lack of *in vivo* efficacy in this population. The observed differences between groups in these studies were not reflected in levels of cytokines such as macrophage-activating factor or GM-CSF[245].

A similar system was later developed by Silver *et al*., who infected monocytes with *M.tb* in a 96-well plate for 1 hour. Infected monocytes were then incubated alone or with (unstimulated) autologous effector cells (PBL) for 1 hour, 4 days and 7 days. Cells were lysed and mycobacteria quantified by plating. Intracellular mycobacterial growth was reduced significantly at 4 and 7 days following addition of autologous PBL to monocytes from both PPD-positive and PPD-negative individuals. Emetine-treated PBL still retained the ability to partially reduce mycobacterial growth, suggesting cytokine-independent cell-to-cell contact-based mechanisms[246]. In a study of BCG vaccination and boost in a US population, PBL-mediated inhibitory responses showed a non-significant increase at 16 weeks post-BCG and remained elevated throughout the study[247].

In 2000, Worku *et al*. returned to a model of T cell stimulation and expansion followed by coculture with infected monocytes. Adherent monocytes were cultured for 6 days followed by overnight infection with BCG. In parallel, lymphocytes were cultured for 7 days alone or with the addition of antigen (*M.tb* Erdmann lysate, live BCG or purified mycobacterial antigens). Expanded effector cells were added to autologous monocyte targets for 72 hours, cells lysed and mycobacteria quantified by radiolabelling with tritiated uridine. Expanded lymphocytes significantly inhibited BCG growth compared with unexpanded, and there was an enhanced ability of T cells to inhibit mycobacterial growth following BCG vaccination in

3 out of 5 volunteers[248]. In the study of BCG vaccination and boost in US volunteers, there was a significant reduction in mycobacterial growth at 8 weeks post-boost only[247].

1.7.2 Whole blood MGIAS

Kampmann *et al*. described a whole blood assay using BCG transfected with luciferase (BCG-*lux*) as a reporter. Diluted whole blood was infected with BCG-*lux* for 96 hours followed by cell lysis. Mycobacterial growth was quantified by relative light units (RLU). Initial studies showed that mycobacterial growth was significantly lower in whole blood, but not plasma, from tuberculin-positive compared with tuberculin-negative individuals[249]. In the combined BCG study of US volunteers, the luciferase assay detected a significant reduction in BCG *lux* growth at 8 weeks post-BCG boost (8 months post primary BCG)[247]. An effect of BCG vaccination was also demonstrated in a study of 50 South African infants, where mycobacterial growth was significantly lower at 3 to 6 months post-vaccination[250].

Wallis *et al*. developed a similar whole blood MGIA to measure the bactericidal effects of drugs. Blood was collected before, and at intervals after, drug administration. Mycobacteria were washed, resuspended in RPMI and mixed with an equal volume of blood. The cultures were incubated for 72 hours with constant 360° mixing. Cells were then lysed with water, and bacteria sedimented and resuspended in BACTEC medium before adding to MGIT tubes. Mycobacterial survival was determined by comparing the time-to-positivity (TTP) on the BACTEC 960 machine of the control and experimental cultures. The authors demonstrated a model of intracellular infection in which microbial killing reflected the combined effects of therapeutic agents and immune mechanisms[251].

This assay was applied to a study of BCG vaccination and boost in 10 healthy adults from the US using both 72 and 96 hour cultures. Four subjects showed improved inhibition of mycobacterial growth following the first vaccination. Their responses waned at 6 months but recurred after boost. Three subjects responded only after the boost, and three subjects showed

no response after either primary or boost vaccination. When grouped together, there was an overall effect of boosting but not primary BCG vaccination. Depletion of CD4+ or CD8+ T cells alone had little or no effect on mycobacterial growth, but depletion of both subsets together resulted in significantly reduced control of mycobacterial growth in the blood of tuberculin-positive donors only[252].

1.7.3 Murine MGIAs

The murine *ex vivo* culture system developed by Cowley and Elkins is similar to the Hoft assay in that stimulated splenocytes were added to infected macrophages. Bone marrow macrophages (BMMφ) were cultured for 7 days and then infected with *M.tb* Erdman for 2 hours. Splenocytes were primed by *in vivo* infection with *M.tb* followed by chemotherapy to clear infection. They were then harvested and added to the bone marrow macrophages at various concentrations. Addition of primed splenocytes to the macrophage cultures resulted in a significant reduction in *M.tb* growth. This only occurred at an optimal splenocyte to BMMφ ratio; higher concentrations of splenocytes were found to be either detrimental to the culture system or to provide no further control of growth. Various experiments altering cellular and cytokine subsets both *in vivo* and *in vitro* suggested that CD4+ T cells possess an IFN-γ independent mechanism that can limit the growth of an intracellular pathogen and are dominant in secondary responses to *M.tb* in mice[253].

Parra and colleagues applied this assay to evaluate the protective efficacy of novel TB vaccines. They demonstrated enhanced inhibition of *M.tb* (both laboratory strains and clinical isolates) in cocultured BMMφ from BCG vaccinated mice compared with naïve controls. Immunisation with each of 5 different vaccines (BCG, an *M.tb* attenuated mutant, a TB DNA vaccine, a TB fusion protein and a viral-vectored vaccine expressing 4 TB antigens) enhanced mycobacterial growth inhibition at day 7 compared with naïve controls. Furthermore, there was a significant correlation between *in vitro* growth inhibition and *in*

vivo protective immunity at 28 days post-challenge, measured using a mouse model of pulmonary TB[254].

In the host group, we developed a murine splenocyte assay based on the methods of Wallis[251]; employing the Bactec MGIT system. Splenocytes were cultured for 96 hours at 37°C with rotation. The pellet was lysed with water and added to Bactec MGIT tubes for quantification. The authors note that this assay represents a simpler murine model compared to that of Morris, without the need for BMMφ harvesting. Splenocytes from BCG immunised mice were better able to inhibit growth of BCG in culture compared with those from naïve animals. This corresponded with protection from *in vivo* challenge with *M.tb*, where the same experimental conditions conferred protection in the immunised but not the naïve group. Microarrays of differential gene expression between groups were used to identify potential mechanisms for the growth inhibition observed. Genes that correlated negatively with mycobacterial growth included proinflammatory genes such as IFN-γ; expression of which was enhanced in BCG vaccinated mice. Positive correlations were predominantly observed with lysosome pathway genes[255].

This project focusses on the further development and application of the Wallis MGIA assay and the murine splenocyte adaptation. The assay will henceforth be referred to as the 'MGIT' (Mycobacterial Growth Indicator Tube) in reference to the Bactec system employed.

Group / reference	Species / sample	Method overview	Vaccine effect	Immune mechanisms
Lowrie, London [244,245]	Human PBMC	Monocytes infected with *M.microti* and stimulated lymphocytes added for 2 hours per day over 3 days	Mycobacterial growth inhibition in pulsed monolayers at 8 weeks post-BCG compared with pre-vaccination in UK but not South Indian children	Observed differences between groups were not reflected in levels of cytokines such as GM-CSF
Silver, Case Western Reserve University, OH[246,247]	Human PBMC	Monocytes infected with *M.tb* in 96 well plate; autologous lymphocytes (PBL) added	In US adults, PBL-mediated inhibition increased non-significantly at 4 months post-BCG and remained elevated	CD4+ (but not CD8+) T cells contributed to inhibition in PPD-positive (but not negative) subjects
Hoft, St Louis University, MO[247,248]	Human PBMC	Monocytes cultured for 6 days then overnight infection with BCG; lymphocytes cultured with antigen stimulation and added to monocytes for 72 hours	Enhanced ability of expanded T cells to inhibit growth following BCG in 3 out of 5 volunteers; significant reduction in growth at 2 months post-boost in US adults	Growth inhibition mediated by total BCG-expanded PBMC and γδ T cell enriched fractions; cell-to-cell contact required
Kampmann, Imperial College, London[249,250]	Human whole blood	Whole blood infected with BCG *lux* for 96 hours; cells lysed and mycobacteria quantified by RLU	In US adults, inhibition at 8 weeks post-BCG boost; in SA infants inhibition at 3 to 6 months post primary BCG	Blocking IFN-γ, IFN-α and IL-12 resulted in a partial increase in growth
Wallis, UMD-NJMS[251,252]	Human whole blood	Whole blood infected with *M.tb* for 72 hours with 360° mixing; cells lysed and mycobacteria quantified by Bactec MGIT TTP	Inhibition in 4 out of 10 US adults following primary BCG (waned by 6 months but recurred after boost); 3 subjects responded only after boost	Inhibition of TNF-α or removal of CD4+ & CD8+ T cells reduced growth inhibition in tuberculin-positive donors
Morris, FDA, US[254]	Mouse BMMφ and splenocytes	Bone marrow macrophages cultured for 7 days; 2 hour infection with *M.tb* then addition of splenocytes	Enhanced inhibition in BMMφ cocultured from BCG vaccinated mice compared with naïve controls; correlation between inhibition and *in vivo* protection of 5 vaccine candidates	Immune cocultures consistently showed upregulation of IFN-γ, GDF-15, IL-21, IL-27 and TNF-α
McShane, Oxford[255,256]	Human whole blood, PBMC and mouse splenocytes	Sample infected with BCG for 96 hours with 360° mixing; cells lysed and mycobacteria quantified by Bactec MGIT TTP	Significant inhibition at 8 weeks post-BCG in whole blood, 4 and 8 weeks post-BCG in PBMC; no effect of BCG revaccination. Significant difference between naïve and BCG vaccinated mice	In mice, proinflammatory genes (eg. IFN-γ) correlated inversely with growth; positive correlations with lysozyme pathways genes

Table 1-2 Published MGIAs. Summary of the published MGIAs that have been applied in detection of a TB vaccine effect including a summary of the methodology and main findings.

1.8 Study Aims

Broadly, the aims of this study are:

1) To adapt and optimise a PBMC-based adaptation of the whole blood MGIT assay and to evaluate both assays across different animal species to:
    a. Correlate with efficacy in preclinical challenge studies
    b. Evaluate in clinical vaccine trial samples from BCG and novel TB vaccine trials

2) To elucidate the mechanisms underlying vaccine-induced mycobacterial growth inhibition and mediating protection, and gain a better understanding of the immunological basis of protection from TB.

As described, TB remains a major global health and socioeconomic threat. With the emergence of multi-drug resistant strains and the spread of HIV, development of a new vaccine is paramount. A major challenge facing vaccine development is the lack of an immune correlate of protection. The ultimate goal of this project is to optimise an MGIA that could represent a functional correlate and is deployable for use in screening candidate vaccines, thus down-selecting or 'gating' them at an early preclinical stage. This would reduce the need for challenge experiments in animals and the number of candidates going forward to long and costly clinical efficacy trials. Determining the immune mechanisms mediating mycobacterial growth inhibition may aid in future vaccine development.

Materials and Methods

2 Materials and Methods

2.1 Materials

2.1.1 Reagents

The reagents used in this project are detailed in Table 2-1 and consumables in Table 2-2.

Reagent	Supplier	Catalogue No.
Anti-human CD14 PE/Cy7 antibody	Biolegend	325618
Anti-human CD3 Alexa Fluor 700 antibody	Biolegend	300324
Anti-human CD4 APC antibody	Biolegend	357408
Anti-human CD8 eFluor 605NC antibody	eBioscience	93-0088
Anti-mouse CD11b APC antibody	eBioscience	17-0112-82
Anti-mouse CD3 Pacific Blue antibody	Biolegend	100334
Anti-mouse CD4 eFluor 650NC antibody	eBioscience	95-0041
Anti-mouse CD8 APC-eFluor 780 antibody	eBioscience	47-0081-82
Anti-mouse Ig/κ compensation beads	Becton Dickinson	552843
Anti-rat/hamster Ig/κ compensation beads	Becton Dickinson	552845
Bactec Mycobacterial Growth Indicator Tubes	Becton Dickinson	245122
BCG Pasteur	In-house	n/a
BCG SSI	Statens Serum Inst.	n/a
BCIP/NBT (plus) solution (ELISpot developing)	Europa	M0711A
Benzonase nuclease	Sigma Aldrich	E1014
Bovine Serum Albumin (BSA)	Sigma Aldrich	A8531
Casein blocking buffer	ThermoFisher	37528
CASYTON solution	Roche Diagnostics	43001
Deferoxamine (DFO)	Sigma Aldrich	D9533
Deionised water	In-house	n/a
Dimethyl sulfoxide (DMSO)	Sigma Aldrich	D2650
DNase I stock solution	Stemcell Tech.	7900
EasySep™ Direct Human Neutrophil Isolation Kit	Stemcell Tech.	19666
ELISpot assay for human IFN-γ	Mabtech	3420-25A
Ethanol	Sigma Aldrich	32221
Ferrous iron (Fe)	Sigma Aldrich	F5879
Foetal Calf Serum (FCS)	Sigma Aldrich	F2442
Glycerol	Sigma Aldrich	G5516
Goat anti-human γ-chain whole IgG alkaline phosphatase conjugate	Sigma Aldrich	A3187
Goat anti-human-IgG pAb	Invitrogen	H17000
Haemoglobin (human)	Sigma Aldrich	H7379
HEPES	Sigma Aldrich	H3375
HiTrap Protein G HP 1ml columns	GE Healthcare	17-0404-01
Human CD14 MicroBeads	Miltenyi	130-050-201

Human CD4 MicroBeads	Miltenyi	130-045-101
Human CD8 MicroBeads	Miltenyi	130-045-201
L-glutamine (4mM)	Sigma Aldrich	G7513
Luminex assay buffer	Millipore	L-AB
Luminex bead diluent	Millipore	LBD
Lymphoprep	Stemcell Tech.	7801
M.tb H37Rv	BEI Resources	NR-15404
Middelbrook 7h10 agar	Becton Dickinson	295964
Middlebrook 7h9 broth	Becton Dickinson	271310
Mouse CD11b MicroBeads	Miltenyi	130-049-601
Mouse CD4 MicroBeads	Miltenyi	130-049-201
Mouse CD8 MicroBeads	Miltenyi	130-049-401
Multiplex Luminex MAP human cytokine kit	Millipore	MPXHCYTO60
Mycobacterium bovis BCG-GFP	In-house	n/a
OADC enrichment	Becton Dickinson	245116
PANTA antibiotics	Becton Dickinson	245114
Penicillin-streptomycin solution (100U/100µg)	Sigma Aldrich	P0781
Phorbol 12-Myristate 13-Acetate (PMA)	Sigma Aldrich	P8139
Phosphate-buffered Saline (PBS)	Sigma Aldrich	D8662
Phytohaemagglutinin (PHA)	Sigma Aldrich	L8902
Pooled Human AB Serum (PHS)	Sigma Aldrich	H4522
Taqman primers	Thermo Fisher	Various
Purified Protein Derivative (PPD)	Statens Serum Inst.	2390
Recombinant human interleukin-10 (rIL-10)	Biolegend	571006
Recombinant mouse interferon-gamma (rIFN-γ)	Biolegend	575306
RNase-free water	Sigma Aldrich	W4502
RNeasy Mini Kit	Qiagen	74106
RPMI-1640 media	Sigma Aldrich	R0883
Saponin	Sigma Aldrich	47036
Sodium dodecyl-sulphate (SDS)	Sigma Aldrich	862010
Trypan blue 0.4%	Sigma Aldrich	T8154
Tween 20	Sigma Aldrich	P9416
Tween 80	Becton Dickinson	231181
Tyloxapol	Sigma Aldrich	T8761

Table 2-1 Reagents. A list of reagents used in this project.

2.1.2 Solutions

- **ACK lysis buffer:** 0.15M NaCl, 1mM $KHCO_3$ and 0.1mM Na_2EDTA in dH_2O. pH adjusted to 7.2-7.4 with 1M HCl then made up to 1L with dH_2O
- **Agar (7H10):** 900ml dH_20 + 19.7g Middlebrook agar base + 5ml glycerol (+ 100ml OADC after autoclaving and cooling below 55°C)
- **Cryopreservation medium:** 90% foetal calf serum (FCS) with 10% DMSO
- **ELISpot coating buffer:** 1 packet of ELISpot coating buffer powder reconstituted in 1 litre of dH_20 and filtered using a 0.22µM filter
- **ELISpot developing buffer:** 1ml: 940µl sterile water, 40µl developing buffer stock, 10µl Solution A and 10µl Solution B
- **FACS buffer:** 1% FCS in PBS
- **MACS buffer:** PBS with 2mM EDTA and 0.5% BSA
- **Middlebrook 7H9:** 4.7g/l 7H9 powder made up with water and 0.05% Tween 80 and supplemented with 10% ADC after autoclaving and cooling below 55°C
- **PBS:** 0.01M: NaCl 0.138M, KCl 0.0027M, pH 7.4; made by dissolving tablets in dH_2O
- **R0:** RPMI 1640 supplemented with 2mM L-glutamine and 100U/ml penicillin and streptomycin sulphate (pen-strep)
- **R10:** RPMI 1640 supplemented with 10% serum, 2mM L-glutamine, 100U/ml penicillin and streptomycin sulphate (pen-strep) and 1.7mM sodium glutamate
- **RPMI-MGIT:** RPMI 1640 media with HEPES supplemented with 2mM L-glutamine and 10% FCS or PHS (as specified)
- **SDS lysis buffer:** 0.067% SDS in 7H9 media and filtered through a 0.2µM syringe filter

2.1.3 Consumables

Consumable	Supplier	Catalogue No.
Bijou (5ml)	Sigma Aldrich	Z645338
Casy cups	Roche Diagnostics	43003
Corning cell culture flasks	Sigma Aldrich	CLS3276
Cell strainers (70μm)	Corning Life Sciences	352350
Cling film	Sphere	SEL-360-020H
Collection tubes (2ml)	Qiagen	19201
Cryovials (2ml)	Sigma Aldrich	BR114832
Dispomix tubes (MACS)	Miltenyi Biotech	130-096-335
ELISpot plates (96 well)	Millipore	MAIP54510
Eppendorf tubes (2ml)	Sigma Aldrich	Z628034
Falcon tubes (15/50ml)	BD Falcon	352097/98
Flat-bottom microtiter plates (96 well)	Sigma Aldrich	M9410
Borosilicate glass beads (2mm)	Sigma Aldrich	Z273627
Leucosep tubes (50ml)	VWR	89048-936
Luminex 96-well filter plates	Merck Millipore	MX-PLATE
Microtubes (0.2ml)	Sigma Aldrich	Z374962
29G needles for vaccinations	Becton Dickinson	324892
MS magnetic separation columns	Miltenyi Biotech	130-042-201
Parafilm	Sigma Aldrich	P7543
Pasteur pipettes	Fisher Scientific	12827625
Petri dishes (60mm)	Sigma Aldrich	P5481
Pipette tips and filter tips (10, 20, 200 and 1000μl)	Starlab	Various
Plastipack syringes 1ml Luer slip	Nu-care Products	M0013
Polystyrene round-bottom tubes (5ml)	Fisher Scientific	14-959A
Precellys tubes with 2.8mm ceramic beads	Precellys	KT03961-1-002.2
QIA shredders	Qiagen	79656
Sarstedt screw-cap tubes (2ml)	Sarstedt	72.694.007
Silver foil	Sphere	AKL-300-040J
Plastic cell scrapers	Sigma Aldrich	CLS3010
Stripettes (2, 5, 10, 25, 50ml)	Corning	4487
Syringe filters (0.2μM)	Sigma Aldrich	CLS431229
Syringe plungers (5ml)	Becton Dickinson	302188
Syringes (1/5/10/50ml)	Becton Dickinson	Various
Tissue culture grade 100mm polystyrene petri dishes	Sigma Aldrich	Z707686
Tissue culture plates (6/12/24/96-well)	Costar	CLS35-16
Vaccutainers (green, heparin 6ml)	Becton Dickinson	368987
Vaccutainers (red, serum 6ml)	Becton Dickinson	368815
Erlenmeyer cell culture flasks with vent cap	Sigma Aldrich	CLS431145

Table 2-2 Consumables. A list of consumables used in this project.

2.2 Samples

2.2.1 Human samples

Samples used in optimisation and exploratory experiments were collected from healthy Jenner Institute personnel with full written consent. Where specified, samples were taken from clinical trials conducted in Oxford, UK and South Africa. All trials were registered on the clinical trials database and were fully approved by the relevant ethical and regulatory agencies (Oxfordshire Research Ethics Committee, the UK Medicines and Healthcare Products Regulatory Agency, the University of Cape Town Faculty of Health Sciences Human Research Ethics Committee, Oxford University Tropical Research Ethics Committee, and the Medicines Control Council of South Africa). Full written consent was obtained from each volunteer (or for infants, from their parent or legal guardian) prior to enrolment in the trials. Trials were conducted according to the principles of the Declaration of Helsinki and in accordance with Good Clinical Practice (GCP). Storage of samples for exploratory immunological analysis was fully ethically approved. Trial information is detailed in Table 2-3; associated primary papers contain methods used for cell separation and cryopreservation. Volunteer demographics for trial TB024 are detailed in Table 2-4.

Trial	Title	ClinicalTrials.gov ID	Reference
TB024	A clinical study to evaluate *in vitro* mycobacterial growth inhibition assays in BCG vaccinated and BCG re-vaccinated adults	n/a	Fletcher *et al*.[256]
TB014	A phase II study evaluating the safety and immunogenicity of a new TB vaccine, MVA85A, in healthy children and infants after BCG vaccination at birth	NCT00679159	Scriba *et al*.[216]
TB020	Safety and efficacy of MVA85A, a new tuberculosis vaccine in infants previously vaccinated with BCG: a randomised, placebo-controlled phase IIb trial	NCT00953927	Tameris *et al*.[219]

Table 2-3 Clinical trials from which samples were taken for this project.

Characteristic	BCG naïve (n = 15)	Historically BCG vaccinated (n = 15)
Gender	67% female 33% male	47% female 53% male
Median age [years (range)]	28 (18-55)	27.5 (19-53)
Time since BCG vaccination [years(range)]	n/a	17.8 (3-38)

Table 2-4 Volunteer demographics for trial TB024: A clinical study to evaluate *in vitro* mycobacterial growth inhibition assays in BCG vaccinated and BCG re-vaccinated adults.

2.2.2 Non-human primate (NHP) samples

The project licence for these studies was approved by the Ethical Review Process of Public Health England, UK and the Home Office, UK. Animals were housed in socially compatible groups and according to the Home Office Code of Practice for the Housing and Care of Animals used in Scientific Procedures (1989) (now updated to the Code of Practice for the Housing and Care of Animals Bred, Supplied or Used for Scientific Purposes, Dec. 2014), the NC3Rs, and the Guidelines on Primate Accommodation, Care and Use, August 2006 (NC3Rs). Studies used in this project are detailed in Table 2-5.

Study Ref.	Title	Species	*n*
4858	Evaluation of early events following vaccination with BCG	Rhesus macaques (Indian genetic background)	7
5102	Evaluation of a BCG challenge model as an approach for the assessment of anti-mycobacterial immunity induced by BCG vaccination	Cynomolgus macaques (Mauritian genetic background)	16
5354	Evaluation of the effect of haemoglobin on the MGIT MGIA	Cynomolgus macaques	7
4403	Evaluation of a BCG challenge model as a method of assessing anti-mycobacterial immunity induced by BCG vaccination	Rhesus macaques	12

Table 2-5 NHP studies from which samples were taken for this project.

2.3 Methods

2.3.1 The Mycobacteria Growth Indicator Tube (MGIT) assay

2.3.1.1 MGIT mycobacteria stock preparation

A 1:200 dilution of strain seed stock (at a 10^7 CFU/ml titre) was prepared in 4ml Middlebrook 7H9 broth in a 50ml falcon tube. The tube was vortexed thoroughly and left for 10 minutes at room temperature to allow the clumps to settle. The top 3ml was added to a new 50ml falcon without disturbing the sediment. 400µl of this diluted stock was added to each of 6 BACTEC MGIT tubes supplemented with PANTA antibiotics and OADC enrichment. Tubes were placed in the BACTEC 960 MGIT machine and harvested 24-48 hours after they flagged positive (harvesting time was selected such that all tubes fell within the 24-48 hour post-positivity range). Cultures not positive within the desired time frame of 6-16 days after inoculation were discarded and the process repeated with more or less dilute stock as appropriate. Positive MGIT tubes were mixed by inversion and left for 10 minutes at room temperature to allow the clumps to settle. 14ml of the solution was transferred to a 50ml falcon tube without disturbing the sediment. The solution was mixed thoroughly by vortexing, aliquoted into 2ml microtubes and cryopreserved at -80°C.

2.3.1.2 Mycobacteria stock titration

A 1.5ml aliquot of stock was thawed and vortexed. 5 serial 10-fold dilutions (of 120µl total volume) were prepared in supplemented Middlebrook 7H9 with vortexing between each dilution. 12 MGIT tubes were supplemented with 800µl of PANTA/OADC enrichment. 500µl of each dilution was added to MGIT tubes in duplicate, including 2 ‘neat’ tubes. A standard curve was created using the inoculum volume against time to positivity (TTP) values and an equation calculated in the form of $y = m (\ln x) + c$ where y = TTP, m = slope

and c = the y-intercept (logarithmic straight line). A sample standard curve is provided in the Appendix (section 8.1).

Two 7H10 agar plates were divided into 3 sectors and 10µl of each dilution was spotted 3 times into a section. Plates were incubated at 37°C with CO2 and colonies counted after 3-4 weeks. A standard curve was created using the inoculum volume against CFU and the stock CFU/ml was calculated.

2.3.1.3 Whole blood MGIT assay

An aliquot of BCG Pasteur or *M.tb* H37Rv (as specified) was thawed and added to duplicate 2ml microtubes for each sample. Mycobacteria were washed and resuspended in 300µl RPMI-MGIT. 300µl of whole blood was added to each tube and cultures were incubated at 37°C for 96 hours with 360° rotation. Cultures were centrifuged at 12000rpm for 5 minutes, supernatants removed and 1ml of sterile water added to the cell pellet. Tubes were vortexed for 30 seconds and incubated at room temperature for 5 minutes (x3). Following a further centrifugation at 12000rpm for 10 minutes, supernatants were removed and 500µl of supplemented Middlebrook 7h9 from a spare MGIT tube was added. Tubes were vortexed for 30 seconds and the solution transferred to a BACTEC MGIT tube supplemented with PANTA antibiotics and OADC enrichment broth. Tubes were placed on the BACTEC 960 machine and incubated at 37°C until the detection of positivity by fluorescence. On day 0, duplicate direct-to-MGIT viability control tubes were set up by directly inoculating supplemented BACTEC MGIT tubes with the same volume of mycobacteria as the samples.

2.3.1.4 PBMC/splenocyte MGIT assay

Cryopreserved PBMC were thawed in a water bath at 37°C, washed twice in RPMI-MGIT and incubated overnight (or for 2 hours following optimisation experiments) at 37°C with CO_2 at a concentration of $1x10^6$ cells/ml in MGIT medium + 2µl/ml benzonase. Cells or fresh

splenocytes were counted, washed and resuspended in MGIT medium at a concentration of $1x10^6$ PBMC per 300µl medium. 300µl of cell suspension was added to each of 2 duplicate 2ml microtubes per sample. A mastermix of BCG Pasteur was prepared in the same medium to give a final MOI of 0.003. 300µl of this mastermix was added to each tube, which was incubated at 37°C for 96 hours with 360° rotation. Cultures were centrifuged at 12000rpm for 10 minutes, supernatants removed and 1ml of sterile water added to the cell pellet. Tubes were vortexed for 30 seconds and incubated at room temperature for 5 minutes (x3). Following a further centrifugation at 12000rpm for 10 minutes, supernatants were removed and 500µl of supplemented Middlebrook 7h9 from a spare MGIT tube was added. Tubes were vortexed for 30 seconds and the solution transferred to a BACTEC MGIT tube supplemented with PANTA antibiotics and OADC enrichment broth. Tubes were placed on the BACTEC 960 machine and incubated at 37°C until the detection of positivity by fluorescence. On day 0, duplicate direct-to-MGIT viability control tubes were set up by directly inoculating supplemented BACTEC MGIT tubes with the same volume of mycobacteria as the samples.

Based on the findings of optimisation experiments, the following changes were made to the protocol: aliquots of mycobacteria were thawed directly before addition to all culture tubes. After thawing, approximately 10 borosilicate glass beads of 2mm diameter were added to the mycobacteria and vortexed for 2 minutes. The mycobacteria wash step was removed and a mastermix was prepared containing the correct volume of mycobacteria per 300µl of MGIT medium, with enough volume for the number of tubes to be inoculated. PBS Tween 20 was used for cell lysis rather than sterile water and the supernatant was only partially removed following centrifugation steps (100µl left). Heat inactivated pooled human serum rather than FCS was used in the MGIT medium.

Variations on the PBMC/splenocyte MGIT assay:

- For experiments where cultures were supplemented with haemoglobin (Hb), lyophilised human Hb was dissolved in RPMI-MGIT and vortexed until a homogeneous solution was obtained, which was diluted to the concentration specified.
- For experiments where cultures were supplemented with iron (Fe), Ferrous iron was filtered using a 0.2µM syringe filter and diluted in RPMI-MGIT to the concentration specified.
- For experiments involving heat inactivated serum, serum was heated in a water bath at 56°C for 45 minutes before cooling to room temperature and adding to the culture.
- For experiments involving the addition of rIFN-γ or rIL-10, cytokines were added to cultures at approximately physiological concentrations, or as specified.

2.3.1.5 Calculation of 'Net Growth' value

To calculate the net growth read-out, the mean time to positivity (TTP) for matched duplicates of both the samples and controls was converted to an apparent inoculum volume based on the stock titration curve (described above). The value of x (inoculum volume) was determined by rearranging the equation of the standard curve to $x = (y - c) / m$ where y = TTP, m = slope and c = y-intercept. This value was then converted to a CFU count by multiplying it by the CFU/µl value of the stock (determined by agar plating as described above), and $\log_{10}$ transformed. Finally, the net growth (or $\Delta\log_{10}$ CFU) in viable bacilli was calculated as (sample $\log_{10}$ CFU - control $\log_{10}$ CFU). An example calculation is provided in the Appendix (section 8.1).

2.3.2 Mouse procedures

All mouse procedures were performed in accordance with the terms of the UK Animals (Scientific Procedures) Act Project Licence (PPL 30/2414) and were approved by the University of Oxford Animal Use Ethical Review Committee. 6 week old female mice of strain Balb/c or C57BL/6 (as specified) were obtained from Harlan Laboratories (UK). Mice were housed in the Wellcome Trust Centre for Human Genetics Functional Genomics Facility (FGF, Oxford) under specific pathogen free (SPF) conditions, and rested for 1-2 weeks prior to commencing procedures.

2.3.2.1 BCG vaccinations

Mice were vaccinated with $1x10^6$ CFU of BCG Pasteur in 100µl of PBS subcutaneously in the base of the tail. Where specified, intradermal vaccinations were performed in the ear with the kind assistance of Elena Stylianou. Mice were rested for 6 weeks before sacrifice for use in the MGIT assay or aerosol challenge with *M.tb*.

2.3.2.2 *M.tb* challenge

The *M.tb* challenge was conducted with the invaluable assistance of Elena Stylianou and Rachel Kandt. An aliquot of *M.tb* Erdmann was thawed and sonicated for 1 minute followed by resting on ice for 1 minute (x3). A sample of *M.tb* was plated on 7H10 agar and incubated at 37°C for 3 weeks to allow estimation of CFU/ml. Mice were challenged using a Biaera aeroMP in a CL3 facility by restraint in individual nose-only chambers fitted to the exposure apparatus. A collision nebuliser was used to create mono-dispersed bacteria in particles which were delivered to the mice. A 10 minute challenge cycle was followed by a 5 minute purge cycle, after which mice were removed from the apparatus and housed in a CL3 unit until sacrifice. 2 naïve mice were sacrificed the following day for calculation of the mean challenge dose; all other animals were sacrificed 4 weeks post-challenge by cervical

dislocation. Lungs and spleen were dissected aseptically and homogenised in 1ml of PBS using a Precellys24 with 2.8mm ceramic beads for 15 seconds at 5500rpm. 5 x 10-fold serial dilutions were prepared from the homogenates and plated onto 7H10 agar. Plates were incubated at 37°C for 2-3 weeks before colony counting.

2.3.2.3 Splenocyte processing for MGIT

Spleens were dissected aseptically from mice and placed in 5ml of PBS. The spleens were poured into a 70µm cell strainer in a 6-well plate and mashed through the strainer using the rubber end of a 5ml syringe plunger. Cells were then transferred to a 50ml falcon using a disposable pipette, and centrifuged at 450g for 5 minutes at 4°C followed by removal of the supernatant. 5ml of ACK lysis buffer was added per tube and cells were incubated for 2 minutes at room temperature. 25ml of RPMI-MGIT was added and cells were centrifuged as above followed by removal of the supernatant. Cells were resuspended in 10ml RPMI-MGIT and counted.

2.3.3 NHP procedures

The NHP samples used in this project were provided by Public Health England. Rhesus macaques were 6 females and 1 male of Indian genetic background aged between 9 and 12 years at the time of the study. Cynomolgus macaques were 8 females of Mauritian genetic background aged between 14.3 and 15.6 years at the time of the study. All animals were bred in the UK (PHE colony, Beck Farm, dstl site, Porton Down). Prior exposure to *M.tb* was assessed before study entry as part of the health screening performed in the breeding facility, where animals were demonstrated to be free of TB using the interpalprebal eyelid test. For procedures requiring removal from their housing, animals were sedated by intramuscular (IM) injection with ketamine hydrochloride (10mg/kg body weight) (Ketaset, Fort Dodge Animal Health Ltd. UK). None of the animals had been used previously for experimental procedures. Animals were monitored daily for behavioural or clinical changes, and

throughout the duration of the studies for weight, temperature, lymph node size and haemoglobin levels. All procedures carried out on NHPs were performed by Andrew White and colleagues at PHE.

2.3.3.1 BCG vaccination and challenge

Animals were vaccinated using an adult human dose of BCG Danish strain 1331 (SSI, Copenhagen) 100µl of 2-8x10^6 CFU/ml intradermally (ID) into the upper left arm using a limited volume insulin syringe. For BCG 'challenge', animals were vaccinated with 1-4x10^6 CFU of BCG Danish ID in 100µl into the upper right arm. The BCG vaccine was prepared and administered according to the manufacturer's instructions for preparation of vaccine for administration to human adults, by addition of 1ml Sauton's diluent to a lyophilised vial.

2.3.3.2 Necropsy

Animals were bled 20ml at the time-points indicated with blood collected into heparin as an anti-coagulant. On day of necropsy, animals were sedated and the level of anaesthesia deepened prior to termination by intra-cardiac injection of a lethal dose of pentobarbitone sodium at 140mg/mg of body weight (Dolelethal, Vetoquinol, UK). A full necropsy was performed immediately, gross pathology assessed and the left and right axillary lymph nodes were collected.

2.3.3.3 Lymph node homogenisation and culture

Axillary lymph nodes were snap-frozen in liquid nitrogen at time of necropsy. They were later thawed in a 37°C water bath and transferred to a Dispomix tube (MACS) containing 1ml of sterile PBS. Tubes were loaded onto a Dispomix machine (Thistle Scientific) and homogenised using a two-step program of a degradation spin-cut cycle (20 seconds) followed by homogenisation specific for fibrous tissue (90 seconds). The homogenate was sonicated at half-power for 15 seconds. 100µl of homogenate was plated in triplicate at neat and 1:10

dilutions in PBS onto Middlebrook 7H10 agar. A BCG SSI vaccine vial was plated as a positive control. Plates were incubated at 37°C for 4 weeks before colony counting.

2.3.4 Immunology

2.3.4.1 PBMC isolation, counting, cryopreservation and thawing

PBMC were separated from fresh heparinised whole blood obtained from healthy human volunteers/NHP or from cone cells (National Blood Service). 10ml of Lymphoprep was loaded onto 50ml Leucosep tubes and centrifuged at 1800rpm for 1 minute. Whole blood (or blood diluted 1:2 with RPMI for cone cells) was layered onto the Lymphoprep and centrifuged at 600g for 20 minutes without a brake. PBMC were collected from the interface using a Pasteur pipette and retained. Tubes were topped up to 45ml with RPMI, and centrifuged at 1800rpm for 5 minutes with a brake. The supernatants were removed, and pellets flicked and resuspended in 45ml of RPMI for a second wash as above. Cells were resuspended in 10ml RPMI and counted using a CASY counter. Briefly, 10µl of cell suspension was added to 10ml of CASYTON solution and the mean cell count from 2 runs determined.

For cryopreservation, cells were centrifuged at 1800rpm for 5 minutes and resuspended in FCS to a concentration of $12x10^6$ cells per ml. An equal volume of ice-cold 20% DMSO in FCS was added to the cell solution and mixed by inversion. Cells were immediately aliquoted into cryovials at 1ml ($6x10^6$ cells) per vial and placed in a Mr Frosty container which was stored at -80°C. After 1-2 days, vials were transferred to liquid nitrogen.

Vials removed from liquid nitrogen were placed on dry ice. Cells were thawed in a water bath at 37°C until a small amount of ice remained. Using a Pasteur pipette, the solution was gently pipetted up and down to encourage thawing. It was then transferred to a 15ml falcon tube containing 10ml RPMI-MGIT and centrifuged at 1400rpm for 7 minutes. The supernatant

was removed and cells were resuspended in 10ml of RPMI-MGIT containing 2µl/ml of benzonase and rested at 37°C for 2 hours before counting.

2.3.4.2 *Ex vivo* ELISpot

Coating solution was prepared by adding anti-IFN-γ primary antibody to coating buffer to a final concentration of 15µg/ml. 50µl of this solution was added to each well of an ELISpot plate which was tapped until the base of each well was covered. Plates were incubated overnight at 4°C. The following day, plates were washed 5 times with sterile PBS, with flicking and blotting between each wash. Plates were blocked by adding 100µl R10 per well and incubating for 2-5 hours at 37°C. Blocking solution was flicked out and 100µl of cell suspension added ($0.3x10^6$ cells per well). PPD antigen was added to give a final concentration of 10µg/ml and PHA as a positive control to a final concentration of 20µg/ml. 2 negative control wells contained cells in R10 alone with no antigen. Plates were incubated overnight at 37°C. The following day, they were washed 5 times with PBS 0.05% Tween 20. Biotin anti-IFN-γ secondary antibody was diluted 1/1000 in PBS and 50µl added per well, followed by 2 hours incubation at room temperature. Plates were then washed 5 times with PBS 0.05% Tween 20. Streptavidin-ALP was diluted 1/1000 in PBS and 50µl added per well, followed by 1 hour incubation at room temperature. Plates were washed 5 times with PBS 0.05% Tween 20. Finally, 50µl of developing buffer was added to each well and incubated for 5-10 minutes at room temperature until colour developed. Spots were counted on an ELISpot reader (AID Germany, software version 5.0). Results are reported as spot-forming cells (SFU) per $1x10^6$ PBMC, calculated by subtracting the mean count of the unstimulated PBMC from the mean count of duplicate antigen wells and correcting for number of PBMC in the well. Responses were considered positive if the count was twice (and at least 5 spots greater) than that of the unstimulated wells.

2.3.4.3 ELISA

96 well flat-bottom microtiter plates were coated overnight with 50µl per well of BCG SSI ($1x10^4$ CFU/well) (or 50µl goat anti-human-IgG pAb for IgG capture ELISA). Samples were prepared by diluting test serum and positive/negative control serum 1:10, 1:100 and 1:000 in Casein blocking buffer. A sample of pooled serum from active TB patients was used as a positive control. The plates were flicked off and washed 6 times with PBS 0.05% Tween 20, followed by blocking with 200µl Casein per well for 1 hour at room temperature. The blocking solution was flicked off and blotted. 50µl of sample was added per well (50µl Casein to the negative control wells), and the plates were incubated for 2 hours at room temperature. The contents were then discarded and the plates washed 6 times with PBS 0.05% Tween 20. Secondary antibody (goat anti-human γ-chain whole IgG alkaline phosphatase conjugate) was diluted 1:1000 in Casein, vortexed and 50µl added per well. The plates were then incubated for 1 hour at room temperature, flicked out and washed 6 times with PBS Tween 20. 100µl of development buffer was added to each well and the plates covered in foil and incubated at room temperature for 30 minutes. OD_{405} was read using a Model 550 Microplate Reader (Bio-Rad, UK).

2.3.4.4 Cell sorting and depletions

A) Monocyte sorting by adherence

Tissue culture grade 100mm polystyrene petri dishes were pre-coated with 2ml of pooled human serum and pre-warmed to 37°C. PBMC were added to the petri dish and incubated for 1 hour at 37°C. Non-adherent cells were removed by gently rinsing with warmed RPMI-MGIT and retained. Cold PBS was added to the petri dish and cooled to 4°C for 30 minutes. A sterile plastic scraper was used to remove adherent monocytes from the plate which were washed with RPMI-MGIT and retained.

B) Monocyte/CD4+/CD8+ T cell depletion by magnetic beads

Human PBMC or mouse splenocytes were counted and placed in Eppendorf tubes at a concentration of up to 10^7 cells in 1ml. Cells were centrifuged at 300g for 10 minutes, and the supernatant aspirated. The cell pellet was resuspended in 80µl (or 90µl for mouse monocytes) of MACS buffer per 10^7 cells. 20µl (or 10µl for mouse monocytes) of Miltenyi MicroBeads were added per 10^7 cells. The solutions were mixed well and incubated for 15 minutes at 4°C (increased to 30 minutes in darkness on a rocking platform following optimisation experiments). 1.5ml of MACS buffer was added per tube, followed by centrifugation at 300g for 10 minutes and removal of supernatant. The cell pellet was resuspended in 500µl of MACS buffer and placed on ice. MS magnetic separation columns were placed in a magnetic field and rinsed with 500µl of MACS buffer. The cell suspension was added to the column and the effluent collected. The column was washed through 3 times with 500µl of MACS buffer. Cell solutions were centrifuged at 1800rpm for 5 minutes, supernatant removed, and resuspended in 10ml of RPMI-MGIT for counting. Undepleted fractions were subjected to the same process without the addition of MicroBeads.

C) Neutrophil depletion by magnetic beads

2.4ml of blood per volunteer was added to a 5ml polystyrene round-bottom tube and diluted with 1.6ml RPMI-MGIT. 200µl of EasySep Positive Selection Cocktail was added to each tube (50µl/ml whole blood/media). Samples were mixed well by pipetting and incubated for 15 minutes at room temperature, with mixing halfway through the incubation period. EasySep Whole Blood Magnetic Nanoparticles were mixed by vigorous pipetting to ensure a uniform suspension. 200µl of nanoparticles were added per tube (50µl/ml whole blood/media) followed by a 15 minute incubation at room temperature. The cells were mixed by gentle pipetting and the tube (without cap) placed in the EasySep magnet for 5 minutes. With the tube still in place, the magnet was inverted in one continuous motion and the

depleted fraction poured into a new tube. A second round of depletion was conducted to ensure efficiency. The positive fraction was retained by removing the tube from the magnet and resuspending the remaining cells in RPMI-MGIT. Both the depleted and positive fractions were washed and resuspended in 10ml of RPMI-MGIT for counting. Undepleted blood was subjected to the same process with the addition of nanoparticles but not antibody to control for the effect of the depletion process on cell activity and functionality.

D) IgG depletion by Protein G

HiTrap Protein G HP 1ml columns prepacked with Protein G Sepharose (GE Healthcare Life Sciences) were equilibrated with 10 column volumes (CV) of PBS. 1ml of undiluted serum per volunteer was passed over the column at a flow rate of 0.5ml/min and flow-through (depleted serum) was collected. Columns were washed with 10 CV of PBS, after which the bound IgG was eluted using 5 CV of elution buffer. The columns were re-equilibrated with 10 CV of PBS between samples. Depletions were confirmed by human IgG capture ELISA.

2.3.4.5 Flow cytometry

Efficiency of cell depletion experiments was determined using flow cytometry to quantify the cell type of interest in the undepleted and depleted fractions. Antibodies were titrated to determine the optimum volume. $1x10^6$ cells per well were added to a 96-well plate and washed twice with PBS. They were then resuspended in 50µl per well of surface stain mix containing the antibody cocktail of CD3, CD4, CD8 and CD14 (CD11b for mice). Flow panels are detailed in the Appendix section 8.2. The plate was incubated at 4°C for 30 minutes in the dark. Wells were washed twice with FACS buffer and transferred to cluster tubes. Compensation was performed using unstained cells and single-stained anti-mouse Ig/κ compensation beads for human PBMC or anti-rat/hamster Ig/κ compensation beads for mouse splenocytes. Samples were acquired on the LSR-II flow cytometer and analysed using FlowJo version 8.3 (Tree Star inc.).

2.3.4.6 BCG-GFP monocyte infections

Mycobacterium bovis BCG-GFP was cultured in OADC supplemented Middlebrook 7H9 broth (plus 0.5% glycerol and 0.05% Tyloxapol) at 37°C on a shaker at 200rpm. Bacteria were sub-cultured every week in fresh medium before use. The human acute monocytotic leukaemia cell line THP-1 (ATCC TIB202) was maintained in suspension in R10 medium. Differentiation into macrophage-like cells was induced with 20nM phorbol 12-myristate 13-acetate (PMA) overnight. Differentiated cells were maintained adherent in 24-well plates in R10 medium.

Bacterial cultures in exponential growth phase were centrifuged at 3500rpm for 10 minutes, washed in PBS and suspended in RPMI-MGIT. Bacterial clumps were removed by low-speed centrifugation for 2 minutes. Adherent macrophages in 24-well tissue culture plates ($5x10^4$ cells per well) were infected with a suspension of mycobacteria at a multiplicity of infection (MOI) of 1:1. Cultures were incubated at 37°C with 5% CO_2 for 1 hour in medium containing heat inactivated or non-heat inactivated serum as specified. Cells were then washed with PBS and internalised BCG-GFP was quantified by flow cytometry.

2.3.4.7 Luminex

200µl per well of wash buffer was added to the luminex plate, which was then sealed and mixed on a plate shaker for 10 minutes at room temperature. Wash buffer was decanted by inverting and blotting. Working standards were prepared by preparing serial 7 x 5-fold dilutions of Human Cytokine Standard in Assay Buffer and adding 25µl of each standard to the appropriate wells. 2 quality controls were prepared by reconstituting in 250µl deionised water, vortexing, and incubating for 10 minutes at room temperature. 2 wells of assay buffer alone were used to determine background. 25µl of Serum Matrix was added to the background, standard, and control wells. 25µl of serum sample was added per well, followed

by 25µl of cytokine bead mix. The plate was sealed, wrapped in foil and incubated on a plate shaker for 2 hours at room temperature.

The well contents were then aspirated and the plate rested on the magnet for 60 seconds before gently decanting and blotting. The plate was removed from the magnet, 200µl of wash buffer was added and the plate was placed on a shaker for 30 seconds before reattaching to the magnet and repeating twice. 25µl of detection antibody was added to each well, and the plate was sealed, covered with foil and incubated on a plate shaker for 1 hour at room temperature. 25µl of Streptavidin-Phycoerythrin was added to each well, and the plate was sealed, covered with foil and incubated on a plate shaker for 30 minutes at room temperature. The well contents were carefully aspirated and the plate washed twice using the magnet as described above. 150µl of Sheath Fluid was added to each well, and the beads resuspended on a plate shaker for 5 minutes. The plate was then run on the Luminex^{200} machine and analysed using xPONENT software with the kind assistance of Steve Smith.

2.3.5 Gene Expression

2.3.5.1 RNA extractions

$1x10^6$ PBMC were thawed and rested overnight with and without BCG stimulation at an MOI of 1:1. Cells were pelleted, lysed in 350µl RLT buffer containing 10µl/ml β-mercaptoethanol and the RNA was extracted using the Qiagen RNeasy mini kit according to the manufacturer's instructions. RNA was quantified using a Nanodrop.

2.3.5.2 qPCR

RNA was reverse transcribed to cDNA using a thermal cycler machine with a reaction volume of 20µl and a program of 37°C for 60 minutes, 95°C for 5 minutes and 10°C for 20 minutes. cDNA dilutions were calculated using the nanodrop readings, and the required volume added to H_20 in eppendorfs. The target gene mix and the reference gene mix (primers

+ probes + mastermix) were prepared. The mastermix was added to each well, the plate sealed and optical film and centrifuged at 500rpm for 2 minutes. Plates were run on the LightCycler with the program ABI Prism 770 50°C for 2 minutes, 95°C for 10 minutes, 40 cycles of 95°C for 50 seconds and 60°C for 1 minute.

2.3.5.3 Microarrays

Microarrays were performed by Magali Matsumiya. Briefly, RNA was amplified using the Illumina Totalprep RNA Amplification Kit according to the manufacturer's instructions. The quality of the RNA was checked using an Agilent bioanalyser following extraction and again following amplification using the RNA Pico or Nano kits. Amplified RNA (750ng per array) was hybridised to the Illumina HumanHT-12 version 4 expression beadchip according to the manufacturer's instructions. Arrays were scanned with an Illumina bead array reader confocal scanner.

2.3.6 Statistical analysis

Statistical analysis was performed using Prism version 5.04 and SPSS version 22. Variability between data sets was compared using the coefficient of variation (CV) and intra-class correlation (ICC) with a two-way mixed model and groupings by Fleiss Category. For experiments comparing two groups, a Shapiro-Wilk normality test was used to determine normality. Parametric data sets were analysed using a paired t-test (where there were matched pairs) or an unpaired t-test. Small or nonparametric data sets were analysed using a Wilcoxon matched-pairs signed rank test (where there were matched pairs) or a Mann-Whitney test. For experiments comparing more than two groups, a Shapiro-Wilk normality test was performed followed by a repeated measures ANOVA (where the same individuals/animals were tested over time or conditions) or one-way ANOVA (where different individuals/animals were tested over time or conditions, or where values were missing) for parametric data. Where there were two or more groups tested at two or more time-points or conditions, a two-way

ANOVA was used. ANOVAs were followed by a Bonferroni post-test to compare all groups with one another, or a Dunnett's post-test if groups were compared with the control (or pre-vaccination) group only. Kruskal-Wallis tests were followed by a Dunn's post-test to compare all groups with one another or selected pairs of groups, as specified. When exploring correlations, data was tested for normality followed by a Pearson's correlation for two parametric data sets or a Spearman's correlation for one or more non-parametric data sets. A Bonferroni test was used to correct for multiple comparisons. Data from the correlates study were analysed using multiple linear regression analysis in SPSS. Heat maps were created by Magali Matsumiya and Julius Muller using 'R' statistical software.

Results

3 Optimisation of the PBMC MGIT Assay

3.1 Introduction

3.1.1 Scope of the problem

As described, a number of groups have developed MGIAs and reported discriminant validity (ability to successfully distinguish volunteers pre- and post-BCG vaccination)[247,248,250,252,254]. With such a pressing need for a surrogate of protective efficacy to facilitate vaccine development, one must question why such assays have not been adopted by the field despite more than a decade of use. This is largely due to concerns regarding reproducibility. It has been clear from discussions within biomarker consortia that attempts have been made to transfer such assays and replicate findings with very limited success. The thesis of Marsay, 2011, assessed an established cultured and novel MGIA but encountered significant problems with both inter- and intra-assay variability. Despite the numerous optimisation experiments performed, Marsay was unable to detect differences in mycobacterial growth inhibition between naïve and BCG vaccinated animals. Other attempts within the group to apply the whole blood BCG *lux* assay, the primary PBMC assay and a mouse splenocyte model with bone marrow derived macrophages have all been hampered by reproducibility issues (unpublished data).

3.1.2 Why the PBMC MGIT Assay?

Preliminary work suggested that the MGIT assay, though still subject to variability associated with functional assays, was less prone to the wildly disparate read-outs produced by some of the other MGIAs (data not shown). This may be due to the relative simplicity of the assay, which does not involve complex pre-culture and stimulation steps or manipulation of the cells involved. Furthermore, use of the Bactec MGIT system to quantify mycobacteria is considerably more accurate than traditional methods of CFU counting which have many

limitations[257]. Serial dilutions on agar are susceptible to pipetting error, clumping, adherence to plastic-ware and subjectivity in counting. Any colony is counted as 1, regardless of size, fitness or growth kinetic. The MGIT system utilises oxygen depletion as a detection method, and as such is sensitive not only to the number of viable bacteria, but also to their rate of metabolism and growth. It is unaffected by clumping and does not require serial dilutions, providing an accurate computer-generated read-out based on validated technology.

I have chosen to develop a novel PBMC-based adaptation of the Wallis MGIT assay[251] for a number of reasons. Importantly, the primary purpose of this project is to develop an assay that may be used in the selection of vaccine candidates, and as such must measure a biologically meaningful vaccine effect. It is widely accepted that the cellular immune response is central to protection against *M.tb*[99,143,258,259]. Though innate whole blood components such as neutrophils are known to play a role in the host response[260], they are less relevant when considering a vaccine-induced effect on adaptive immunity. It is possible that innate responses may even mask the adaptive response in this context.

In addition, the ability to use cryopreserved cells would enable the retrospective study of samples from clinical trials of novel vaccine candidates. Notably, the host group had available cryopreserved PBMC from 2797 South African infants enrolled in a Phase IIb efficacy trial of the candidate vaccine MVA85A[219]. Using cryopreserved PBMC could aid in transferability of the assay to different trial sites, as it would eliminate the need to run samples in real time at every post-vaccination time-point on fresh material. Rather, cells could be frozen down and run at a later time. This is not only logistically simpler, but would also negate the need for an expensive MGIT machine at every site. It was hypothesised that the PBMC assay would address some of the issues with variability over time due to the possibility of running a complete time-course in a single batch.

Finally, the establishment of a PBMC-based MGIT assay would also enable adaptation for use with murine cells. Applying this assay to preclinical studies is critical in the early stages of development, where the read-out must be correlated with measures of *in vivo* protection to permit biological validation. A whole blood assay would not be feasible in mice, where total blood volume is limiting.

3.1.3 Approaches to optimising the PBMC MGIT Assay

The main aims of optimising this assay are to minimise variability and maximise discriminant validity. The latter will be considered in the subsequent chapter; the current chapter will focus on identifying and addressing sources of variability. In their paper 'Validation overview of bio-analytical methods', Tuomela *et al*. emphasise the importance of 'precision' in any meaningful biological assay[261]. They define precision as "the closeness of agreement (degree of scatter) between a series of measurements obtained from multiple sampling of a homogeneous sample under prescribed conditions". This parameter may be partitioned into intra-assay variability (variation between multiple runs of a single sample in a single test batch) and inter-assay variability (variation of multiple runs of a single sample across different assay batches). Initial work tested the hypothesis that inter-assay variability would be reduced in the PBMC MGIT compared with whole blood MGIT. Aspects of the assay where variability may be introduced were then identified, and alternative methods for reducing it compared. Variables investigated include cell culture medium, cell number, mycobacterial stock preparation and inoculum, and cell lysis and processing.

3.2 Aims

The aims of the experiments detailed in this chapter were to:

- Compare the variability associated with the whole blood and PBMC-based MGIT assays

- Reduce the intra-assay variability in the PBMC MGIT assay by optimising the assay conditions
- Demonstrate improved precision using the newly-optimised protocol

3.3 Results

3.3.1 Comparison of whole blood and PBMC MGIT

A study was conducted of BCG vaccination in 30 healthy UK volunteers[256]. 15 had no prior history of BCG vaccination and the remaining 15 had been historically vaccinated with BCG (median time since vaccination 17.8 years). All volunteers received a single intradermal immunisation with BCG-SSI with follow-up bleeds at weeks 4, 8 and 24 post-vaccination. Prior to vaccination, all volunteers had 3 repeated baseline bleeds (taken over a 1 month period) for the assessment of inter-assay variability. Whole blood MGIT cultures were set up within 4 hours of volunteer bleed, and the rest of the blood was used to separate PBMC. Fresh PBMC were used for IFN-γ ELISpot, with the remainder cryopreserved for PBMC MGIT at a later date.

3.3.1.1 Intra-assay variability

Each sample at each time-point was run in duplicate to assess intra-assay variability. Such duplicates represent more than technical repeats, with each cultured independently over the 96 hour period prior to addition to the MGIT tube. The mean coefficient of variation (CV) and 95% confidence interval for whole blood and PBMC were 2.2 (1.8 to 2.6) and 8.0 (6.6 to 9.5) respectively. Using intraclass correlation (ICC) with a two-way mixed model (where 1 indicates perfect agreement and 0 indicates no agreement), there was ‘good’ agreement between duplicates using both the whole blood (0.74) and the PBMC assay (0.60), based on groupings defined by Cicchetti & Sparrow[262,263]. There was no difference in intra-assay

variability between different time-points or vaccine groups within each assay (data not shown).

3.3.1.2 Inter-assay variability

Over 3 consecutive baseline bleeds, the mean CV and 95% confidence intervals for whole blood and PBMC were 24.5 (15.3 to 33.7) and 7.7 (6 to 9.4) respectively (Figure 3-1). Using ICC with a two-way mixed model, there was 'fair' agreement between the 3 measures in whole blood (0.466) and 'good' agreement between the 3 measures in PBMC (0.625). There was no difference in inter-assay variability between BCG naïve and historically vaccinated volunteers using either compartment.

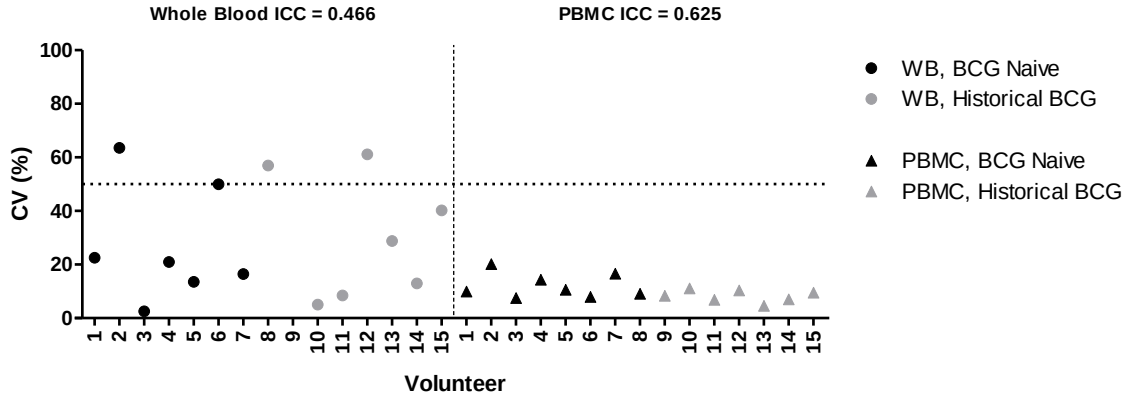

Figure 3-1 Inter-assay variability is greater in whole blood than PBMC MGIT assay. Coefficient of variation (CV) for 3 repeated baseline visits of 15 healthy UK volunteers either BCG naïve or historically vaccinated. The dotted line indicates the maximum CV (50%) considered to be acceptable for the measurement of a bacterial target of a cell-based assay[17]. Intra-class correlation (ICC) values for each assay are shown at the top.

3.3.2 Pre-culture conditions

In the study described above, cryopreserved PBMC were rested overnight to allow apoptotic cells to die and leave a higher frequency of viable, functional cells for the assay. However, this increases the labour and time required for the protocol, and a comprehensive comparison indicated that it may not be advantageous or accurate in monitoring immune responses among healthy subjects[20]. Cells were rested in standard R10 medium (RPMI containing 10% FCS, L-glutamine and Pen-Strep) both pre-freezing and post-thawing, before washing and resuspending in culture medium (RPMI containing 10% FCS, L-glutamine and HEPES buffer). Net growth values generated using the PBMC assay were predominantly negative, even at baseline, indicating more growth inhibition than would be expected. It was hypothesised that the antibiotics in the cell rest medium may be taken up by cells and thus continue to mediate an inhibitory effect, despite the wash step prior to culture.

To investigate these issues, mycobacterial net growth was compared under all permutations of antibiotics present in the pre-freezing and post-thawing cell culture medium, with either an overnight or 2 hour cell rest. Cryopreserved PBMC were used from 3 healthy UK volunteers. Antibiotics had a pronounced inhibitory effect when present in the cell rest medium post-thawing, and removing antibiotics from this medium solved the issue of negative growth values (Figure 3-2). There was little effect of Pen-Strep when present in pre-freezing medium alone. No difference was observed between the overnight and 2 hour cell rest conditions other than in the YY condition (P/S in pre-freeze and post-thaw medium). The variability was consistent between groups, but for conditions where no antibiotics were present post-thawing, YN (P/S in pre-freeze medium only) with a 2 hour cell rest had a slightly lower mean CV.

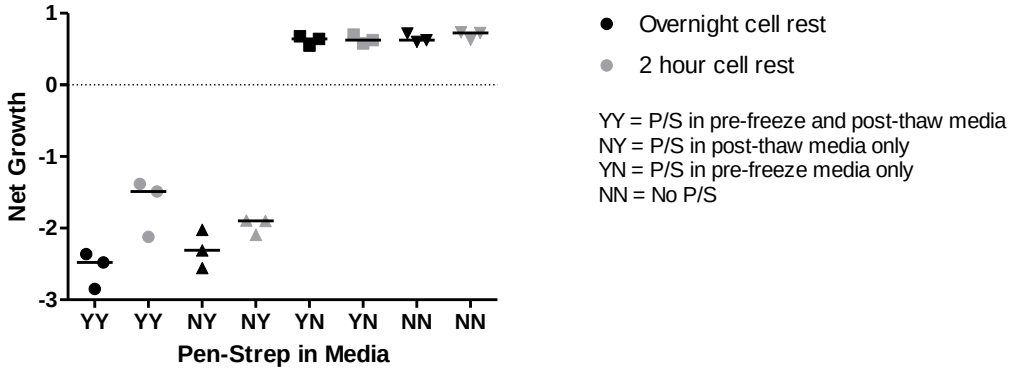

Figure 3-2 Pen-Strep antibiotics in the pre-culture cell rest medium and length of cell rest affect MGIT mycobacterial growth. PBMC MGIT data from 3 healthy UK volunteers. Cells were rested either overnight or for 2 hours prior to addition to the culture. Pen-strep antibiotics were present in the cell rest medium either post-freezing or post-thawing and all permutations of these conditions. The bars represent the median values. Net growth = (Log_{10} CFU of sample - Log_{10} CFU of control).

3.3.3 Mycobacterial inoculum and stock preparation

3.3.3.1 Inoculum

It is clear from the experiments described above that antibiotics in the post-thaw cell rest medium were acting to artificially knock down the mycobacterial inoculum, resulting in negative growth values. Removing them to avoid this potentially confounding factor had the result of altering the multiplicity of infection (MOI) such that the previously used inoculum was overwhelming the vaccine effect (discussed in the following chapter). A smaller inoculum was required, and the effect this might have on the intra-assay variability was determined. Variability, expressed as the coefficient of variation and intraclass correlation coefficient, was calculated at different inoculum inputs using cells from both humans and mice. In all cases, reducing the inoculum (increasing the target TTP) resulted in increased variability between sample replicates. Based on non-overlapping confidence intervals, one

may estimate that there was a significant increase in variability between a TTP of 6.5/7.5 and 9.5, and 9.5 and 11.5 days using human PBMC (Table 3-1).

Species	*n*	Target TTP (days)	Mean CV (95% CI)	ICC	Fleiss Category
Human	6	6.5	1.7 (-0.6 to 4.0)	0.87	Excellent
	9	7.5	2.0 (0.5 to 3.5)	0.82	Excellent
	6	8.5	6.0 (3.1 to 9.0)	0.83	Excellent
	11	9.5	8.7 (4.9 to 12.4)	0.60	Good
	6	10.5	14.7 (8.2 to 21.1)	0.48	Fair
	30	11.5	16.3 (11.2 to 21.4)	0.33	Poor
Mouse	10	5.5	1.8 (0.6 to 3.0)	0.91	Excellent
	14	6.5	2.5 (1.5 to 3.5)	0.88	Excellent
	16	7.5	3.0 (1.4 to 4.6)	0.70	Good
	14	8.5	3.6 (0.9 to 6.3)	0.43	Fair

Table 3-1 Increased TTP results in increased MGIT intra-assay variability. Intra-assay variability is presented as the mean coefficient of variation between duplicates at different mycobacterial inoculum volumes. The intra-class correlation coefficient provides a summary measure of the absolute agreement between duplicates within a group, performed using a two-way mixed model and grouped by Fleiss category (1981).

Notably, even within a single study with one inoculum, there is a significant correlation between time to positivity and variability between replicates for both human and macaque PBMC (Figure 3-3A-B, $p<0.005$), and a trend in mouse splenocytes (Figure 3-3C).

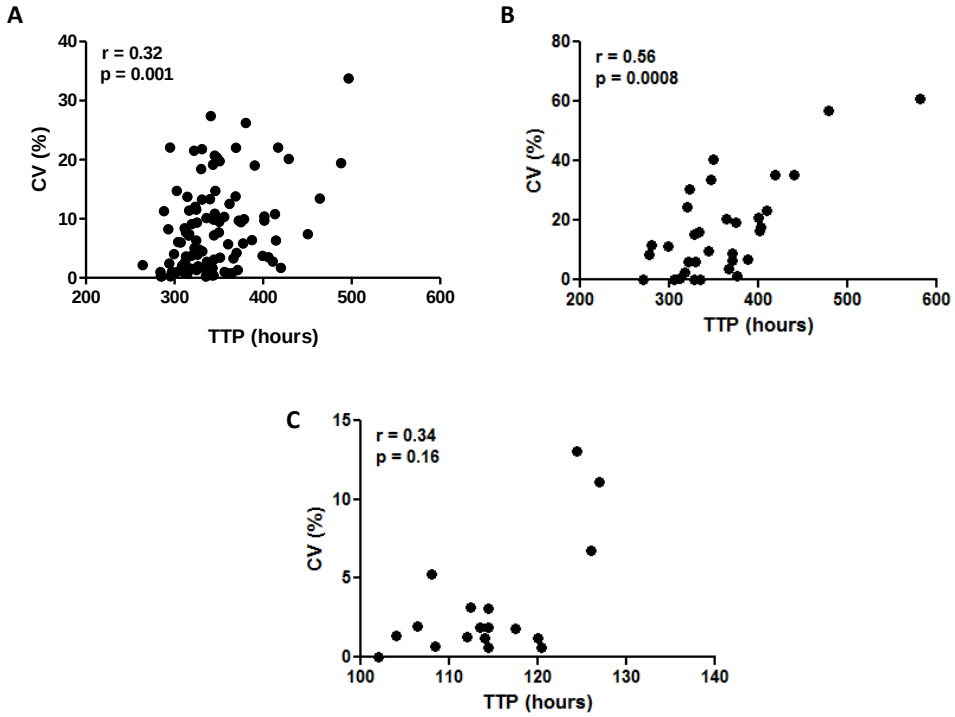

Figure 3-3 Increased TTP results in increased MGIT intra-assay variability. Spearman's rho correlation between mean time to positivity and coefficient of variation of duplicate MGIT cultures of A) human PBMC, B) macaque PBMC and C) mouse splenocytes.

3.3.3.2 Stock preparation

In an attempt to reduce the variability associated with a smaller inoculum volume, two features of the mycobacteria were investigated that were considered possible contributors: time from thawing to inoculation and mycobacterial clumping.

Mycobacteria were thawed and added to duplicate PBMC culture tubes after sitting on the bench at room temperature for between 1 and 5 hours. This was to replicate conditions during large experiments, where considerable time elapsed between inoculation of different batches of tubes from the same thawed vial of mycobacteria. Mycobacterial viability was shown to

progressively decrease between 1 and 4 hours, before beginning to recover at 5 hours (Figure 3-4).

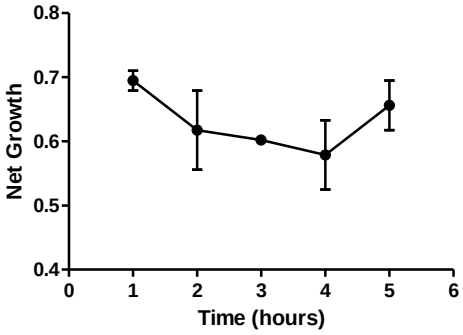

Figure 3-4 Viability of thawed mycobacteria over time. PBMC MGIT data using a vial of thawed BCG Pasteur, inoculated into the culture after standing on the bench at room temperature for between 1 and 5 hours. The points represent the mean of duplicates with the SEM. Net growth = (Log_{10} CFU of sample - Log_{10} CFU of control).

Six different methods of de-clumping mycobacteria were compared using six replicate cultures of the same sample for each method. These were: 1) vortexing for 5 minutes on the highest speed, 2) leaving to stand for 5 minutes to allow clumps to settle to the bottom and then removing only the top fraction, 3) centrifuging at a slow speed to bring the clumps down and then removing only the top fraction, 4) sonicating for 2 minutes, 5) vortexing with glass beads for 2 minutes, and 6) syringing through a 5 micron filter. Mycobacterial recovery, as measured by net growth, was highest using the glass beads method (median 1.606); other methods appeared to result in some loss of mycobacteria - particularly centrifuging and filtering (median 0.2007 and 0.3397 respectively) (Figure 3-5). Variability between the six replicates was greatest for vortexing (CV = 13.0%) and smallest for glass beads and filtering (CV = 2.2 and 1.2% respectively).

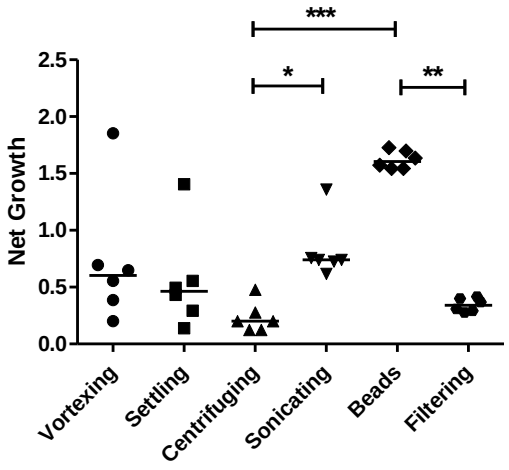

Figure 3-5 Different methods of de-clumping mycobacteria affect MGIT mycobacterial growth and intra-assay variability. PBMC MGIT data using six different methods of de-clumping BCG Pasteur prior to inoculation into the culture. Points represent 6 replicates from one volunteer; bars represent the median value. As the data was non-parametric, a Kruskal-Wallis test was performed followed by a Dunn's post-test where * represents a p-value of <0.05, ** represents a p-value of <0.005 and *** represents a p-value of <0.0005. Net growth = (Log_{10} CFU of sample - Log_{10} CFU of control).

3.3.3.3 Direct-to-MGIT control

As described, duplicate MGIT tubes are inoculated on day 0 with the same volume of mycobacteria as added to the sample cultures. This allows control between different assay runs using the same mycobacterial stock, as sample net growth values are normalised to the growth of their corresponding control. The original protocol involved adding the calculated volume of mycobacteria to each sample tube, pelleting by high-speed microcentrifugation, removing supernatant and resuspending in MGIT tube media[251]. This wash step seemed unnecessary (as the stock is grown up and frozen in MGIT tube media) and likely to introduce variability.

An alternative process was thus tested whereby a large mastermix is prepared in culture medium, with the calculated volume of mycobacteria contained in every 300µl of mastermix;

the total volume of which is dependent on the number of cultures being set up. The cells are then prepared such that $1x10^6$ PBMC are contained in every 300µl of culture medium, and the cells and mycobacteria mastermix are combined to make the 600µl culture. This would mean that rather than adding the calculated volume of mycobacteria directly to the control tubes and making the volume up to 500µl using MGIT tube medium, 300µl of mastermix plus 200µl of MGIT tube medium would be added. It was hoped that this would better standardise the amount of mycobacteria being inoculated into both the samples and controls. To check that adding culture medium to the control MGIT tubes did not affect mycobacterial growth, the net growth of control tubes inoculated using either the original or revised mastermix method was compared. There was no difference in net growth between the two conditions (Figure 3-6). There was slightly reduced variability between 13 replicate tubes using the revised compared with original method (CV = 25% and 33% respectively).

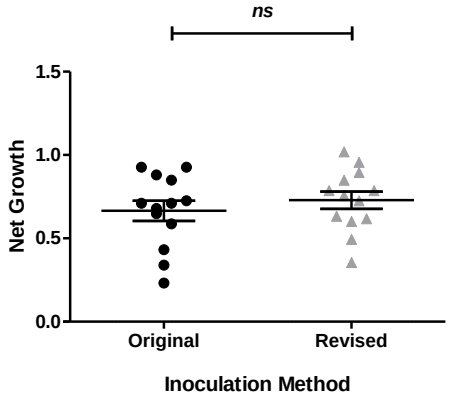

Figure 3-6 A revised method for inoculating the direct-to-MGIT control does not affect mycobacterial growth. MGIT control tubes were inoculated with mycobacteria that had either been washed and resuspended in MGIT tube medium (original method), or added directly to a mastermix in culture medium (revised method). Bars represent the mean values with SEM. Having passed a normality test, an unpaired t-test was performed where there was no significant difference. Net growth = (Log_{10} CFU of sample - Log_{10} CFU of control).

3.3.4 Culture conditions

3.3.4.1 Cell input

It was postulated that an alternative to using small mycobacterial inocula associated with high variability was to increase the cell input. This would permit a low MOI while still having a feasibly measurable mycobacterial input. It was considered what effect increased cell number may have on intra-assay variability. Variability, expressed as CV and ICC, was calculated at different PBMC concentrations using cells from 5 volunteers. Increasing the cell number resulted in reduced variability between sample replicates (Table 3-2).

N	**No. of PBMC**	**Mean CV (95% CI)**	**ICC**	**Fleiss Category**
5	1×10^6	6.72 (3.1 to 8.9)	0.27	Poor
5	3×10^6	6.74 (0.6 to 12.8)	0.40	Fair
5	5×10^6	3.15 (-0.4 to 6.7)	0.95	Excellent

Table 3-2 Increased cell number results in reduced intra-assay variability. Intra-assay variability is presented as the mean coefficient of variation between duplicates at different cell inputs. The intra-class correlation coefficient provides a summary measure of the absolute agreement between duplicates within a group, performed using a two-way mixed model and grouped by Fleiss category (1981).

3.3.4.2 Serum in the cell culture medium

As the assay was predominantly being developed using human PBMC, it was felt that Pooled Human AB Serum (PHS) rather than Foetal Calf Serum (FCS) in the culture medium would represent a more natural environment for the cells. To determine the effect on mycobacterial growth or variability, the MGIT assay was performed using cells from 9 healthy volunteers with either PHS or FCS in the medium. Mycobacterial growth was significantly higher using PHS compared with FCS (median net growth 1.63 and 0.25 respectively, $p<0.0005$) (Figure

3-7A), though cell viability was unaffected (data not shown). There was no difference in variability between duplicates (Figure 3-7B).

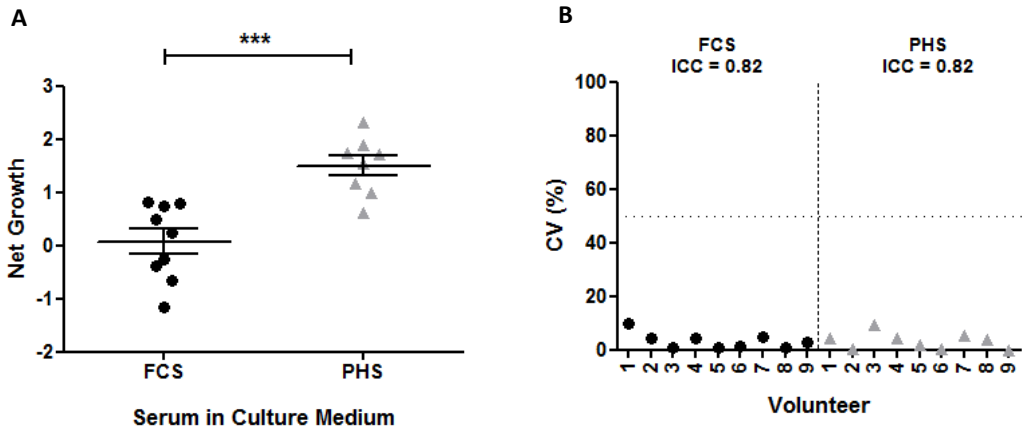

Figure 3-7 PHS in culture medium results in greater MGIT mycobacterial growth than FCS, but does not affect intra-assay variability. PBMC cultured with FCS or PHS in the culture medium. A) MGIT net growth (Log_{10} CFU of sample - Log_{10} CFU of control). Bars represent the mean values with SEM. Having passed a normality test, a paired t-test was performed where *** represents a p-value of <0.0005. B) Intra-assay variability plotted as CV between duplicates. The intra-class correlation coefficient at the top of the graph provides a summary measure of the absolute agreement between duplicates within a group, performed using a two-way mixed model.

The effect of heat inactivating the PHS was explored, using cells from 6 healthy volunteers. Mycobacterial growth was significantly lower using heat-inactivated serum compared with normal serum (median net growth 1.0 and 1.6 respectively, $p<0.005$) (Figure 3-8A). Using heat-inactivated serum also resulted in lower variability between duplicates (Mean CV = 6.2% compared with 30.4% for normal serum) (Figure 3-8B).

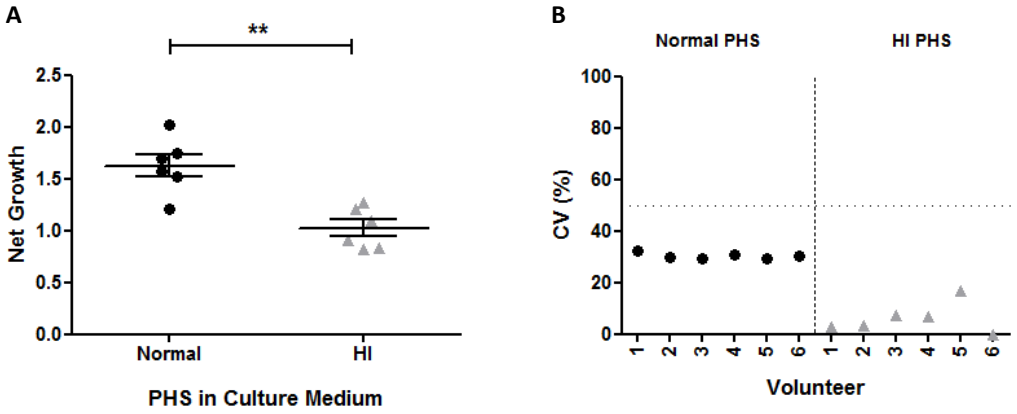

Figure 3-8 Heat inactivation of culture PHS results in decreased MGIT mycobacterial growth and decreased intra-assay variability. PBMC cultured with normal or heat-inactivated PHS in the culture medium. A) MGIT net growth (Log_{10} CFU of sample - Log_{10} CFU of control). Bars represent the mean values with SEM. Having passed a normality test, a paired t-test was performed where ** represents a p-value of <0.005. B) Intra-assay variability is plotted as coefficient of variation between duplicates.

3.3.4.3 Culture period

The culture period originally selected was 96 hours due to the slow-growing nature of mycobacteria and to allow antigen-specific T cells sufficient time to expand and mediate an effect. However, different culture periods were also considered to determine the effect on intra-assay variability and cell viability. Cells from 9 BCG vaccinated volunteers (at 4 weeks post-vaccination) were cultured in duplicate. Net growth of mycobacteria increased with increasing culture period (median net growth at 24, 48, 72 and 96 hours was 0.42, 0.55, 0.59 and 0.63 respectively) (Figure 3-9). There was a significant increase between 24 and 72 hours ($p<0.0005$), between 24 and 96 hours ($p<0.0005$) and between 48 and 96 hours ($p<0.05$). There was little effect of culture period on reproducibility between replicates, which showed 'good' agreement at 24 hours and 'excellent' agreement at 48, 72 and 96 hours (ICC = 0.65, 0.81, 0.80 and 0.82 respectively) (Table 3-3).

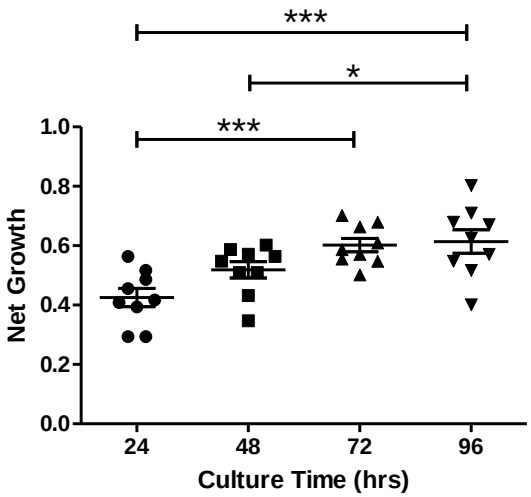

Figure 3-9 MGIT mycobacterial growth increases with increased culture period. PBMC MGIT data from 9 BCG vaccinated volunteers with cultures of different periods. Bars represent the mean values with the SEM. Having passed a KS normality test, a repeated measures ANOVA was performed followed by a Bonferroni post-test where * represents a p-value of <0.05 and *** represents a p-value of <0.0005. Net growth = (Log_{10} CFU of sample - Log_{10} CFU of control).

N	Culture Period	Mean CV (95% CI)	ICC	Fleiss Category
9	24	2.26 (0.4 to 4.1)	0.65	Good
9	48	1.61 (0.7 to 2.4)	0.81	Excellent
9	72	1.87 (0.0 to 3.7)	0.80	Excellent
9	96	2.01 (0.5 to 3.5)	0.82	Excellent

Table 3-3 Culture period does not affect intra-assay variability. Intra-assay variability is presented as the mean coefficient of variation between duplicates at different culture periods. The intra-class correlation coefficient provides a summary measure of the absolute agreement between duplicates within a group, performed using a two-way mixed model and grouped by Fleiss category (1981).

3.3.4.4 Culture mixing

Although optimisation work with this assay was conducted using BCG, there were plans to use *M.tb* and safety concerns were raised over 360° rotation of the cultures. The effect of rotating was investigated in 2 separate experiments using PBMC from South African (SA) infants participating in the MVA85A efficacy trial. In both cases, there was significantly more mycobacterial growth inhibition when cultures were rotating compared to standing stationary (Figure 3-10A and B).

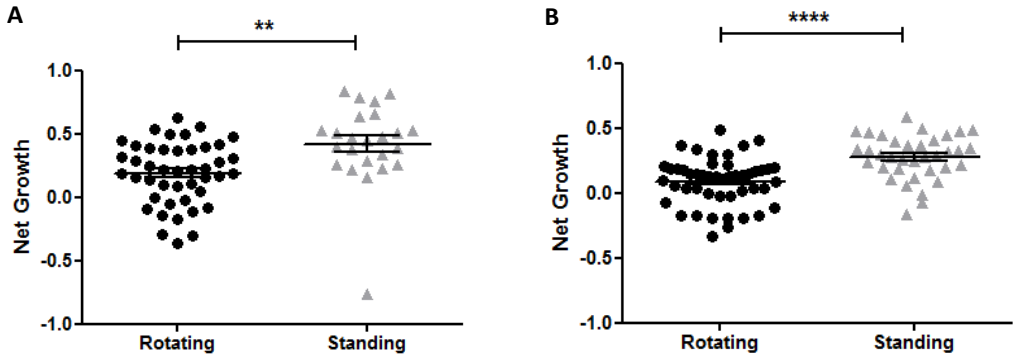

Figure 3-10 Rotating MGIT cultures decreases mycobacterial growth. PBMC MGIT was performed using cells from healthy BCG-vaccinated SA infants, with cultures that were either rotating or standing stationary. Two separate batches of samples were compared. Bars represent mean values with SEM. Having passed a normality test, an unpaired t-test was performed where ** represents a p-value of <0.005 and **** represents a p-value of <0.0001. Net growth = (Log_{10} CFU of sample - Log_{10} CFU of control).

Using a Pearson's test, there was no correlation between results for the same samples under the two conditions (r = 0.2, p = 0.4 for experiment 1; r = -0.3, p = 0.1 for experiment 2) (data not shown). Variability between duplicates did not differ between rotating and standing cultures (CV = 13% and 13% respectively for experiment 1; 12% and 10% respectively for experiment 2).

3.3.5 96 hour processing

Following the 96 hour culture period, cells are centrifuged at high speed to pellet cells and mycobacteria, and the supernatant is removed. The cells are then lysed to release intracellularised mycobacteria by addition of tissue-culture grade water and vortexing three times at 5 minute intervals. This is followed by a further centrifugation step, removal of supernatant and addition of MGIT tube medium. Incomplete or inconsistent lysis and the centrifugation/supernatant removal steps were identified as potential sources of variability.

3.3.5.1 Cell lysis

Host cells must be lysed at 96 hours to release intracellularised mycobacteria. Due to the need to retain live mycobacteria for quantification, the lysing process must damage animal but not bacterial cells. For this reason detergents are favoured over mechanical methods. Using cells from 9 healthy UK volunteers, lysing with either water or PBS Tween 20 was compared. There was no significant difference in mycobacterial recovery between the two agents, as measured by final net growth, although there was a trend towards increased recovery using PBS Tween (Figure 3-11A). There was also reduced variability between duplicates using PBS Tween compared with water, as shown by CV values (Figure 3-11B). Using intraclass correlation with a two-way mixed model, there was ‘good’ agreement between duplicates using water (ICC = 0.65) and ‘excellent’ agreement using PBS Tween (ICC = 0.90).

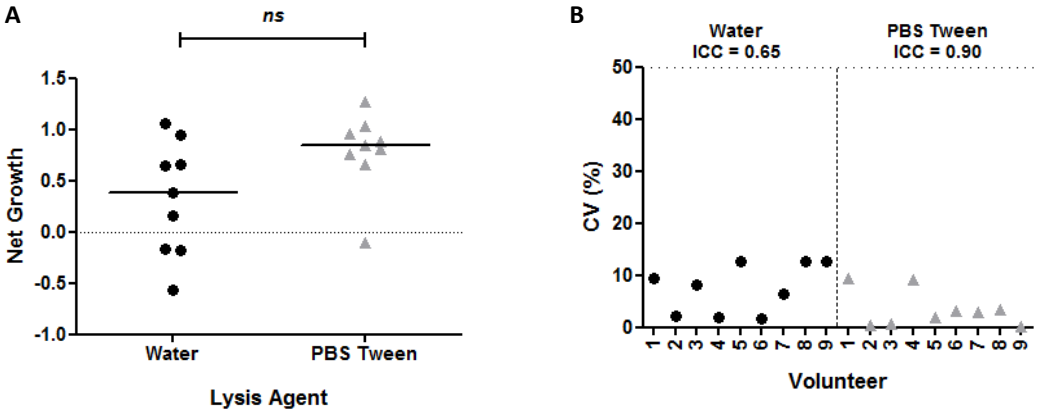

Figure 3-11 Lysing cells with PBS Tween results in increased MGIT mycobacterial growth and decreased intra-assay variability compared with water. A) MGIT PBMC data from 9 healthy UK volunteers when cells were lysed at the end of the 96 hour culture using either water or PBS Tween. Bars represent the median values. As the data were non-parametric, a Wilcoxon matched-pairs test was performed where there was no difference between groups. Net growth = (Log_{10} CFU of sample - Log_{10} CFU of control). B) Coefficient of variation (CV) of 2 duplicates from each volunteer. Intra-class correlation (ICC) values for each condition are shown at the top.

Other lysis agents that have been described in the literature were also tested for their effect on intra-assay variability. In this experiment water and PBS Tween 20 were included again, as well as 0.2% Saponin in water and 0.067% SDS in Middlebrook 7H9 (filtered through a 0.2 micron filter). There was also a 'no lysis' condition to determine whether lysis is necessary at all. There was little difference in the net growth between conditions, and it was surprising to see that removing the lysis step completely did not result in decreased recovery of mycobacteria (Figure 3-12). Variability between duplicates was greatest when there was no lysis step (CV = 5.7%) and lowest using PBS Tween (CV = 2.6%).

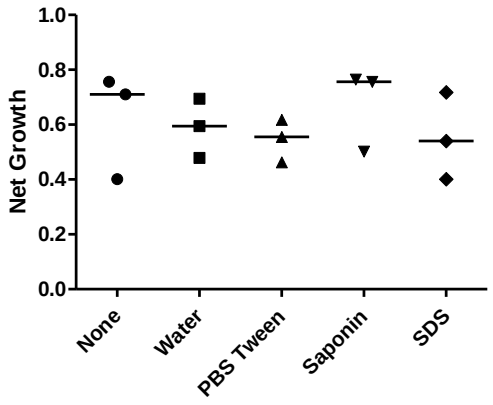

Figure 3-12 Different cell lysis agents do not affect MGIT mycobacterial growth. PBMC MGIT data from 3 healthy UK volunteers; cells were lysed at the end of the culture period using 4 different agents, or no lysis. Bars represent the median values. Net growth = (Log_{10} CFU of sample - Log_{10} CFU of control).

PBS Tween was selected as the most promising lysis agent, and the time-sensitivity of the lysis step was then investigated. Following the vortexing steps, cells were left in PBS Tween for between 0.5 and 4 hours to compare the effect on mycobacterial recovery. Mycobacterial recovery, as measured by net growth, increased with increasing lysis period (Figure 3-13). The CV between 3 replicates was greatest at 0.5 hours (81%) and smallest at 4 hours (13%).

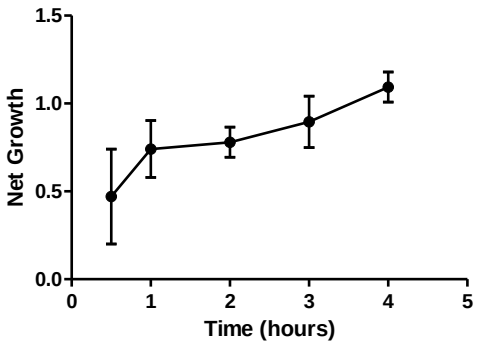

Figure 3-13 MGIT mycobacterial growth increases with increased lysis time. PBMC MGIT data using cells lysed for between 0.5 and 4 hrs following the 96 hr culture. The points represent the mean of 3 replicates with the SEM. Net growth = (Log_{10} CFU of sample - Log_{10} CFU of control).

3.3.5.2 Supernatant removal

As described, cells and mycobacteria are pelleted both before and after lysis using high-speed microcentrifugation (12,000rpm). It was noted that the pellets were easily disturbed, and supernatant had to be very carefully removed to avoid potential loss of mycobacteria. In an attempt to remedy this, an alternative method was considered, removing only 500µl of lysis agent and leaving 100µl behind. 400µl of MGIT tube media would then be added rather than 500µl at the end. To determine whether this process would reduce intra-assay variability and/or impact on mycobacterial growth in the MGIT tube, the two methods were compared using cells from 9 healthy volunteers. Leaving 100µl of supernatant in the tube resulted in a non-significant increase in mycobacterial recovery (Figure 3-14A) and a reduction in variability between duplicates (Figure 3-14B) compared with removing the entire supernatant. Using intraclass correlation with a two-way mixed model, there was 'good' agreement between duplicates when the whole supernatant was removed (ICC = 0.65) and 'excellent' agreement when 100µl was left (ICC = 0.90).

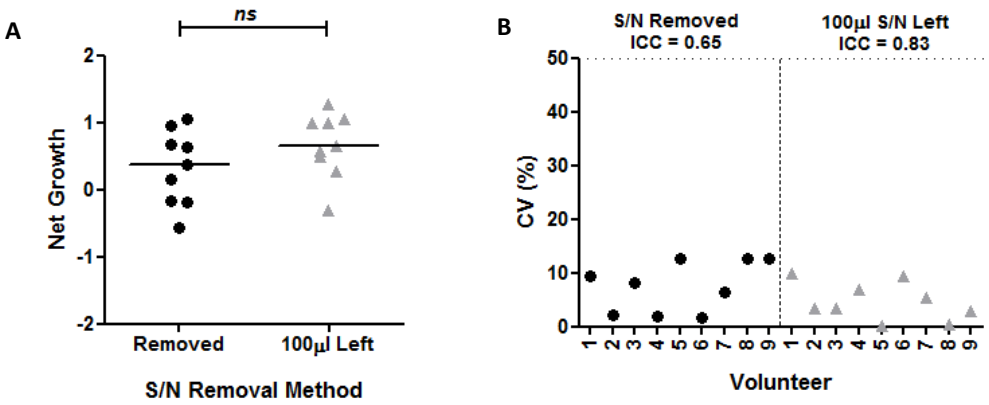

Figure 3-14 A revised method for removing supernatant reduces intra-assay variability. A) MGIT PBMC data from 9 healthy UK volunteers; following centrifugation, supernatant was either removed completely or 100µl was left in the tube. Bars represent the median values. Having passed a normality test,

a paired t-test was performed where there was no difference between groups. B) Coefficient of variation of 2 duplicates from each volunteer. Intra-class correlation (ICC) values for each condition are shown at the top. Net growth = (Log_{10} CFU of sample - Log_{10} CFU of control).

3.3.5.3 Centrifugation

The effect of the post-lysis centrifugation step was investigated by comparing 10 replicates of the same sample either with or without the second centrifugation step. There was no difference in mycobacterial net growth between the two conditions, although removing the centrifugation step did result in increased variability between duplicates compared with retaining this step (CV 22.3% and 14.3% respectively) (Figure 3-15).

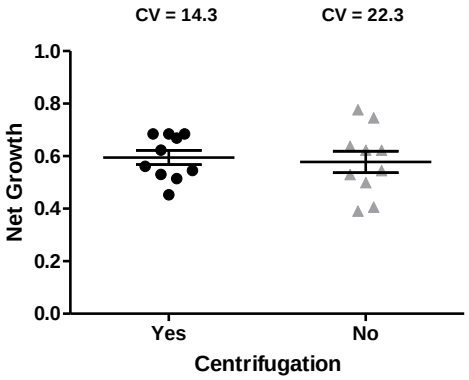

Figure 3-15 Removing the second centrifugation step does not affect MGIT mycobacterial growth but increases intra-assay variability. PBMC MGIT using 10 replicates of the same sample either with or without the second centrifugation step at 96 hours. Bars represent the mean values with the SEM. Having passed a normality test, an unpaired t-test was performed where there was no difference between groups. Net growth = (Log_{10} CFU of sample - Log_{10} CFU of control).

3.3.6 BCG as a surrogate for *M.tb*

For most of the experiments described in this project, BCG is used as a surrogate for *M.tb* for *in vitro* infections. This is due to the relative logistical ease of working with BCG, and the problems encountered attempting to culture *M.tb* Erdmann. Furthermore, for the first 12 months, samples had to be transported to the local hospital for access to a MGIT machine, which precluded the use of *M.tb*. To test the hypothesis that inhibition of BCG provides a satisfactory estimate of inhibition of *M.tb*, experiments were run in each of the three species studied directly comparing the assay read-out for BCG Pasteur and *M.tb* H37Rv. In all cases, there was a significant correlation between growth inhibition of the two strains (Figure 3-16A-C).

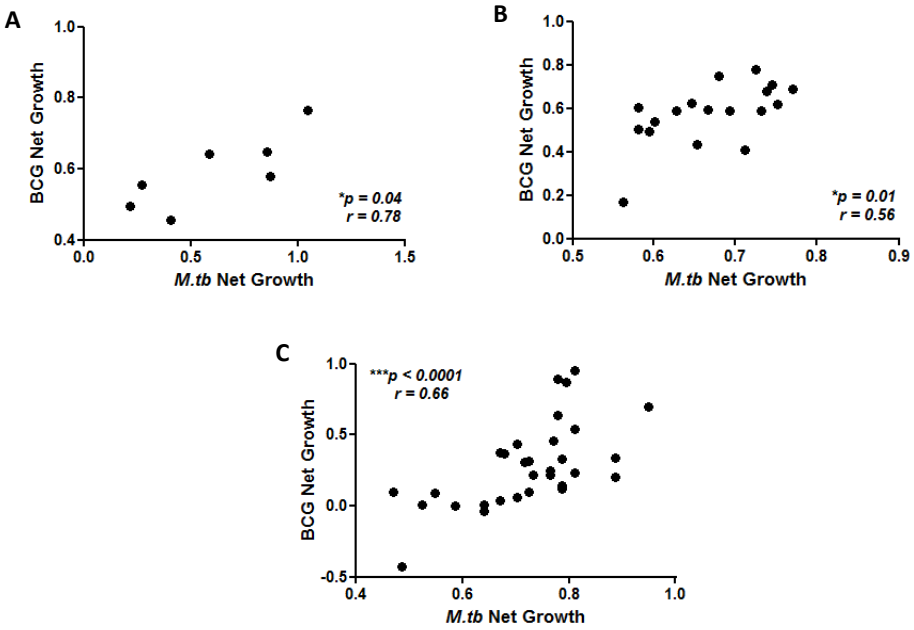

Figure 3-16 Positive correlation between BCG and *M.tb* growth in the MGIT assay. Spearman's rho correlation between net growth of BCG Pasteur and *M.tb* H37Rv in MGIT cultures of A) Human PBMC, B) Mouse splenocytes and C) Cynomolgus macaque whole blood.

3.3.7 Applying the optimised protocol

Using cells from 9 healthy volunteers at baseline, the PBMC MGIT was run using the original conditions and the optimised conditions identified through the course of this chapter. There was a reduction in intra-assay variability between replicates for each sample when the optimised protocol was applied compared with the original (Mean CV = 2.0% and 13.4% respectively). Using intraclass correlation (ICC) with a two-way mixed model, there was 'fair' agreement between duplicates using the original protocol (0.42) and 'excellent' agreement using the optimised protocol (0.82) (Figure 3-17).

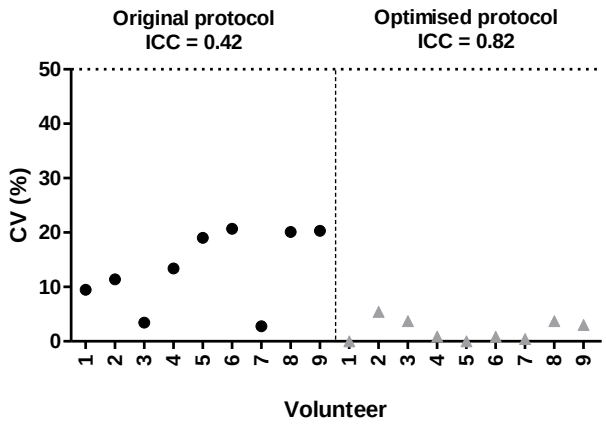

Figure 3-17 Intra-assay variability is reduced using the optimised protocol. Coefficient of variation (CV) of duplicates from baseline visits of each of 9 healthy volunteers. Intra-class correlation (ICC) values for each protocol are shown at the top.

3.4 Discussion

Inter-assay variability was compared between the whole blood and PBMC MGIT assay using repeated baseline sampling. Both assays had a CV of less than 50%, which is considered acceptable variation for the measurement of a bacterial target of a cell-based assay[261]. However, there was higher overall variability in the whole blood assay. This is likely due to the necessity for running the fresh blood assay in real time, with a separate batch of cultures set up at each bleed. Variations in mycobacterial stock (as a different aliquot is used for each batch) and week-to-week performance of the assay may have an effect, despite correcting to the direct-to-MGIT control. Volunteers were recruited and the assay set up many times over a 12-month period, whereas the PBMC assay was run in just two batches. Furthermore, cell number is more standardised in the PBMC assay, where $1x10^6$ cells are added per culture, as opposed to 300µl of blood which will contain different numbers of cells depending on the volunteer. There may also be variables between sample draws which are present in blood but not the PBMC compartment and impact mycobacterial growth, such as neutrophil frequency and function[260], iron content[264] or serum glucose[265]. This finding supports the decision to pursue development of the PBMC MGIT assay in addition to the reasons outlined in section 3.1.2.

The intra-assay variability, though described as 'good' (Fleiss ICC categories[262]) for both assays, was higher for the PBMC than whole blood assay. This is consistent with reports of other MGIAs using these compartments[247]. It is possible that when PBMC are added to replicate cultures, each contains a slightly different proportion of specific T cells depending on which $1x10^6$ cells happen to be taken up by the pipette. When the culture is infected with mycobacteria, these cells will proliferate exponentially such that a negligible difference at day 0 could potentially translate into a significant difference over 96 hours. There may also be some effects of cryopreservation on cell viability and functionality, and cells in RPMI

medium are in a less natural environment than those cultured in whole blood. However, there was no evidence from the time-course experiment to suggest a loss of cell viability in either assay. Some measures of cell proliferation and functionality during the course of the culture are investigated in subsequent chapters, including flow cytometry and luminex.

To address the issue of intra-assay variability in the PBMC MGIT assay, several aspects of assay preparation, the culture period and 96-hour processing were identified as potential sources of variability. Different conditions were compared for each with the goal of developing an optimised protocol. It was first determined that the standard antibiotic supplement (penicillin and streptomycin) used in R10 cell rest medium had a pronounced effect on mycobacterial growth in the assay, despite the wash step prior to culture. Although penicillin has no reported activity against mycobacteria, streptomycin is a broad-spectrum bactericidal drug used as a first-line treatment for Tuberculosis[266,267]. Its mode of action involves binding to the small 16S rRNA of the 30S subunit of the bacterial ribosome, inhibiting protein synthesis and leading to cell death[268]. Streptomycin does not affect human cells due to the structural difference of ribosomes. However, uptake of streptomycin into human cells does occur (despite high water solubility), where it is sequestered in lysosomes and subsequently redistributed into the cytosol and concentrated[269,270]. It is likely that streptomycin was absorbed by cells during the rest period and retained, mediating an inhibitory effect when mycobacteria was added. This may represent a confounding factor in the assay, as different cells (or the same cells under different conditions) may possess differing abilities to uptake or retain the antibiotic. The effect may also be due in part to inadequate wash steps following the cell rest, as only a single wash was performed to prevent loss of cells. There was little effect of Pen-Strep being present in the pre-freezing medium on mycobacterial growth, and all cryopreserved cells from clinical trials available for retrospective study are routinely processed in such medium. There is also a higher risk of contamination at this stage, as many of the samples are taken and processed in resource-poor

settings in the field. Thus the conditions selected moving forward were to retain Pen-Strep in the pre-freezing medium, but remove from all steps post-thawing.

For this condition, there was no difference in net growth between a 2 hour and overnight cell rest, though with a 2 hour rest there was slightly lower variability between sample replicates. In a study performed by the host group, an overnight cell rest resulted in lower cell counts, lower IFN-γ ELISpot responses and a significant loss of T cell populations including monocytes in adults[271]. Furthermore, it has been suggested that an overnight cell rest is neither advantageous nor accurate in monitoring immune responses among healthy subjects[272]. Taking these factors into account, a 2 hour rather than overnight cell rest was selected.

It was clear from the first experiment that Pen-Strep in the cell rest medium acted to artificially reduce the mycobacterial inoculum, resulting in negative net growth values. However, removing it had the effect of altering the multiplicity of infection such that the previously used inoculum was overwhelming the vaccine effect (discussed in the following chapter). A smaller inoculum was therefore required, but it was found that intra-assay variability increased with decreasing inoculum for both the human PBMC and mouse splenocyte assays. This is likely due to pipetting error associated with working with such small volumes. Furthermore, when dealing with very small numbers of CFUs, the discrepancy between the absolute CFUs added to replicate cultures will be relatively larger.

Variability in the inoculum itself was addressed by considering the effects of time to inoculation and clumping. The reduction in mycobacterial growth for the first 4 hours followed by recovery was consistent with data from a separate experiment of viability of clinical BCG vaccine conducted by others in the group using CFU plating (Harris, unpublished data). It was decided that for future experiments all cultures must be fully prepared for inoculation before stock is thawed, and cultures should all be inoculated together

immediately following thawing. The comparison of different de-clumping methods indicated that filtering resulted in the lowest variability between replicates. However, there was also a substantial loss of mycobacteria in the process. Vortexing with glass beads resulted in similarly low intra-assay variability, and also the highest recovery of viable mycobacteria. This method is routinely used in drug susceptibility testing of *M.tb* to prepare a standardised inoculum[273]. Removing the mycobacterial wash step and preparing the inoculum as a large mastermix also resulted in a reduction in variability between duplicates. Pipetting larger volumes is associated with proportionately less error, and it is accepted as good practice to dilute small volumes and use a larger volume of the diluted mix. Thus moving forward, stock will be thawed, vortexed with glass beads and then a mastermix prepared and added directly to cell culture tubes.

It was postulated that an alternative to using small mycobacterial inocula associated with high variability was to increase the cell concentration. This would permit a low MOI while still having a reasonable mycobacterial input. Intra-assay variability decreased with increasing cell concentration in the culture, though the confidence intervals were too wide to draw any significant conclusions - likely due to the small sample size. The relative merits of different conditions must always be weighed up, and one major concern with such a high cell requirement is that for many trials cell number is the limiting factor in assay selection. This is particularly true for trials conducted in infants where blood volume is restricted. At $5x10^6$ cells per culture, $10x10^6$ would be required to run the necessary duplicates, and in many cases this number of cells will not be available. With this in mind, much of this project was conducted using $1x10^6$ cells per culture, with higher concentrations explored where available or necessary.

When cell culture conditions were investigated, it was found that using pooled human AB serum (PHS) rather than foetal calf serum (FCS) in the culture medium resulted in increased mycobacterial growth. No difference was observed in cell viability between the two

conditions, suggesting that the FCS may mediate a direct inhibitory effect on mycobacteria. BCG was used as the *in vitro* challenge strain in these experiments, and it is possible that FCS, being from the target host of *M.bovis*, has some innate immune activity against BCG. An experiment titrating the concentration of FCS in the absence of cells demonstrated decreased mycobacterial growth with increased FCS concentration, supporting this hypothesis (data not shown). Heat inactivating PHS resulted in reduced mycobacterial growth but also reduced intra-assay variability. It has been reported that heat inactivation of serum decreases uptake of mycobacteria into monocytes due to the destruction of complement[274]. As monocytes provide the target host cell for mycobacterial survival and replication, it follows that a decrease in monocyte invasion would lead to decreased net growth. To remove the potentially confounding effects of different PHS batches aiding monocyte uptake to varying extents and given the reduced intra-assay variability, heat-inactivated PHS was selected for the culture medium.

Net growth of mycobacteria was found to increase significantly with increasing culture period up to 72 hours. This may be due to mycobacteria replicating faster than the cellular arm of the adaptive immune response is able to respond during the first few days. There is no increase in mycobacterial growth between 72 and 96 hours, which is in keeping with evidence in the literature that significant T cell proliferation in response to specific antigens and APCs is evident after 3 days of culture[115]. Due to the slow-growing nature of mycobacteria (12-24 hours doubling time) and the importance of assessing the specific T cell response in this assay, a relatively long culture period is required. Any longer would not be feasible in a closed system such as that described, but with cell viability and reproducibility still good at 96 hours, this period was selected moving forward. Other closed system mycobacterial growth inhibition assays reported in the literature use culture periods of 72 hours[251] or 96 hours[249,252]. Systems permitting gas exchange use longer periods such as 7 days[246,254].

With regards to rotation of the culture, there was no effect of rotating on intra-assay variability compared with standing. However, rotating cultures showed significantly greater inhibition of mycobacterial growth. The thesis of Marsay demonstrated that culture mixing or standing has no effect on T cell viability or functionality (Marsay, unpublished data). It is possible that the observed inhibition is due to an increase in the number of effector T cells coming into contact with mycobacteria or infected monocytes and thus mediating a more effective immune response. In a stationary culture, cells tend to sink to the bottom and cell-mycobacterial contact may be reduced. Agitation may also increase oxygen content, and is recommended for optimal mycobacterial growth[275,276]. It was decided that cultures would continue to be rotated 360°, with those containing *M.tb* double-contained and sealed with parafilm. For previously described MGIAs, whole blood cultures are routinely rotated or shaken to prevent separation of the blood[250,251], whereas cell-based assays employ stationary plated cultures[246,248,254]. It would be interesting to explore the relative merits of mixing in such assays.

Surprisingly, there was little difference in mycobacterial recovery between the different lysis agents tested, even with the no lysis condition. This may be due in part to the small sample size. However, intra-assay variability was lower using PBS Tween 20 compared with water. PBS Tween 20 is a non-ionic detergent and as such milder and less denaturing than ionic detergents such as SDS. It is able to solubilise membrane proteins while maintaining protein function so does not impact mycobacterial cell integrity[277]. Mycobacterial recovery increased over time during a 4 hour period in PBS Tween 20, indicating that this step is time-sensitive. Reproducibility was also improved at 4 hours compared with 30 minutes. Unfortunately, it is not logistically feasible to have a 4 hour rest during an already time-consuming and complex assay, and thus it was decided to change to PBS Tween 20 but continue with a short lysis rest.

Leaving 100µl of supernatant following lysis did not adversely affect mycobacterial growth in the MGIT tube, and did reduce intra-assay variability. This is to be expected, as potential

to disturb the cell pellet was reduced, and 100µl of residual PBS Tween (which is not harmful to mycobacteria) in 7ml of media in the MGIT tube is unlikely to have any impact. Removing the second centrifugation step actually increased variability between replicates, which was surprising as one might expect minimal processing steps to support greater reproducibility. Based on these observations, it was decided to use the revised method of supernatant removal but to retain the second centrifugation step.

It was observed that measures of growth inhibition of BCG correlated with those of *M.tb* H37Rv in sample cultures from 3 different species. This validates the use of BCG as a surrogate *in vitro* challenge strain. Different mycobacterial species such as *M.smegmatis*, *M.fortuitum* and *M.bovis* are routinely used in exploratory research to avoid the use of highly pathogenic and slow-growing *M.tb*. Other reports of mycobacterial growth inhibition also employ BCG[248,250], and Kolibab *et al*. demonstrated a significant correlation between the murine BMMφ assay read-out using *M.tb* and isoniazid-resistant (INHr) BCG[278]. Recently, a human challenge model for TB has been developed using BCG vaccination as a surrogate for *M.tb* infection[279]. Indeed, *M.bovis* is similar in structure and metabolism to *M.tb*; the genomes being >99.52% identical at the nucleotide level[280]. The potential to use BCG as a surrogate is useful in this setting, increasing transferability to different laboratories - many of which will not have Category 3 facilities or capacity to contain a MGIT machine at this level.

To conclude the optimisation phase of this project, samples from the same volunteers were run using both the original and optimised assay conditions. The optimised protocol demonstrated lower intra-assay variability between replicates, suggesting that the assay has been improved.

3.5 Conclusions

- Inter-assay variability was reduced in the PBMC compared with whole blood MGIT assay, but intra-assay variability was increased.

- The following optimised conditions were selected to reduce this variability:
  - No Pen-Strep in any medium following cell thawing
  - A 2 hour rather than overnight cell rest
  - De-clumping of mycobacteria using glass beads and inoculation immediately after thawing
  - Generation of a mycobacterial mastermix with no pre-washing
  - Use of heat-inactivated Pooled Human Serum in the culture medium
  - A 96 hour culture period with rotation
  - Lysis using PBS Tween 20 with two centrifugation steps and partial removal of supernatant to preserve the cell pellet

- Applying this protocol reduced intra-assay variability.

4 Detecting a vaccine response

4.1 Statement of authorship

Human blood samples in the BCG vaccination trial were taken by Joel Meyer in Oxford. Samples from South African infants in the MVA85A efficacy trial and Pilot studies were taken and processed by the MVA85A 020 Trial Study Team. Non-human primate samples were provided by Sally Sharpe at Public Health England (PHE); animals were vaccinated and bled by Andrew White. The mouse work was performed by the author with help from Elena Stylianou during the *M.tb* challenge. Spleens from the novel vaccine candidate work were provided by James Keeble at the National Institute for Biological Standards and Control (NIBSC). All assays described were performed by the author, with help in the large MVA85A efficacy trial from Matthew O'Shea, Leanne Marsay and Vivek Naranbhai.

4.2 Introduction

4.2.1 Testing across species

It was decided that the MGIT assay would be tested across different species for a number of reasons; not least that an effect consistently observed in different models would strengthen its case. Mice and non-human primates are the most widely-used animal models in TB research; mice for ethical and financial reasons, and macaques for their close resemblance to the human response. Considering the MGIT assay in these species, importantly, provides potential to 'biologically validate' the read-out i.e. test that it is a biologically meaningful measure by correlating with *in vivo* measures of protection. However, one of the advantages of an *in vitro* model of protection such as the MGIT is that human samples may be used, thus modelling the target species. Though animal models have greatly progressed our understanding of TB disease, it is unclear how readily results may be translated to humans.

Indeed, it is well known that the physiology of TB differs considerably between mice and humans, as well as many relevant aspects of the immune system. The potential to apply the MGIT to clinical vaccine trial samples is an exciting prospect, and underpinned the decision to begin with human work.

4.2.2 BCG as a 'gold standard'

BCG vaccination was selected for study during the initial stages setting up and biologically validating the assay, as it is known to be effective in the populations and species tested. Although the efficacy of BCG in humans is highly variable depending on geographic location, it is known to be effective in the UK[190]. A controlled clinical trial of over 50,000 participants found a 78% reduction in TB incidence in BCG vaccinated compared with naïve adolescents[281]. In a cohort study of adults in Birmingham BCG showed 88% efficacy[282], and in various studies in the UK general population the efficacy has been estimated at >70%[283]. BCG has been shown to be highly protective against *M.tb* challenge in Cynomolgus macaques[204,284], and to a lesser extent in Rhesus species[211,285-287]. In the mouse model, BCG reliably confers a 1 to 3 log reduction in CFU counts or significant improvement in survival or pathology score[209,288,289]. If the MGIT assay is to be used to select novel vaccine candidates, it must be able to discriminate naïve and BCG-vaccinated individuals or animals in the first instance. A candidate vaccine, whether designed to boost or replace BCG, must then confer an improvement in mycobacterial growth inhibition compared with BCG alone. Thus detection of a BCG vaccine response is central to the development of this assay.

4.3 Aims

The aims of the experiments detailed in this chapter were to:

- Assess the ability of the whole blood and PBMC MGIT assays to detect a BCG vaccine-induced response across different species where BCG is known to be effective:
  - UK adults
  - Non-human primates
  - Mice (splenocytes)
- Optimise assay conditions to ensure maximum and consistent discriminatory validity
- Apply the MGIT assay to the testing of novel TB vaccine candidates
- Determine whether the MGIT assay correlates with measures of protection from *in vivo* mycobacterial challenge.

4.4 Results

4.4.1 BCG vaccination and revaccination in UK adults

As described in the previous chapter (3.3.1), a study was conducted of BCG vaccination in 30 healthy UK volunteers[256]. 15 had no history of BCG vaccination and the remaining 15 had been historically vaccinated with BCG (median time since vaccination 17.8 years). All volunteers had 3 pre-vaccination bleeds which were averaged to a single pre-vaccination value in the data presented in this chapter. Volunteers received a single intradermal immunisation with BCG-SSI with follow-up bleeds at weeks 4, 8 and 24 post-vaccination (Figure 4-1). The MGIT assay was initially conducted using BCG *lux* but due to problems with the strain, this data was discarded and standard BCG Pasteur was used. Therefore data is not available from all volunteers; particularly at early time-points.

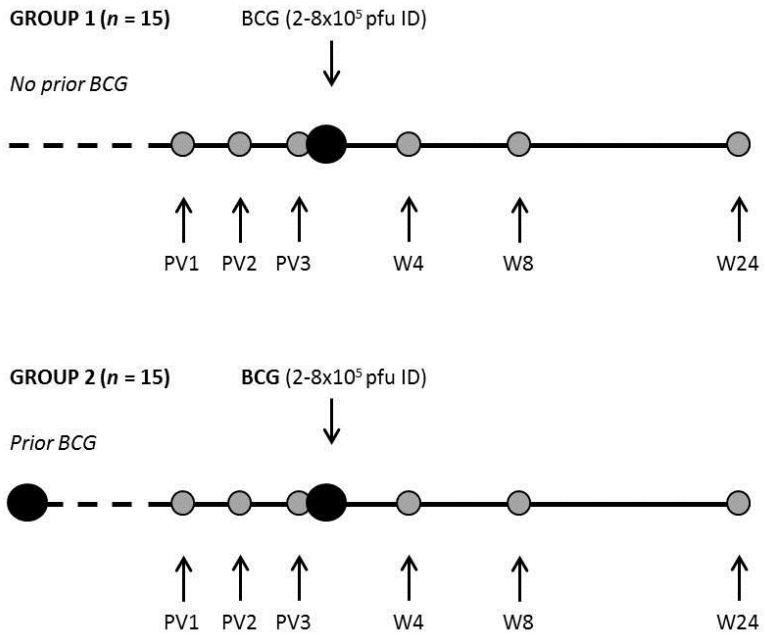

Figure 4-1 Schematic of human BCG vaccination and revaccination study design. 30 healthy UK adults, half of which were BCG naïve and half historically vaccinated. Following 3 pre-vaccination (PV) bleeds, all volunteers received 2-8x10^5 pfu of BCG SSI intradermally. Follow-up bleeds were taken at 4, 8 and 24 weeks post-vaccination.

4.4.1.1 Naïve vs. historically BCG vaccinated individuals

Using the mean of 3 pre-vaccination bleeds, the whole blood MGIT assay did not discriminate between naïve and historically vaccinated volunteers (median net growth = 0.13 and 0.12 respectively; p = 0.35) (Figure 4-2A). The PBMC MGIT assay detected a significant difference in mycobacterial growth inhibition between naïve and historically vaccinated volunteers (median net growth = 0.05 and -0.04 respectively; $p<0.05$) (Figure 4-2B).

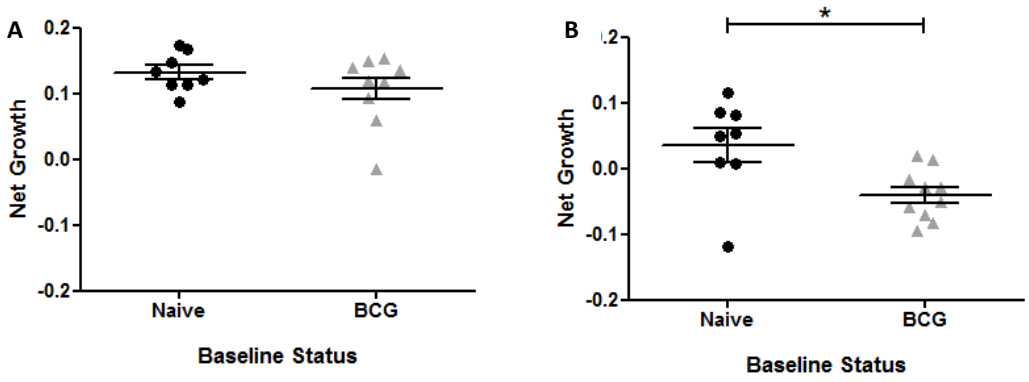

Figure 4-2 The MGIT assay using PBMC, but not whole blood, is able to discriminate naïve from historically BCG vaccinated volunteers. The MGIT assay was performed using A) whole blood and B) PBMC from volunteers that were BCG naïve or vaccinated at some time in the past. Bars represent the mean values with SEM. Having passed a normality test, a paired t-test was performed where * represents a p-value of <0.05. Net growth = (Log_{10} CFU of sample - Log_{10} CFU of control).

4.4.1.2 Primary BCG vaccination and revaccination

The whole blood MGIT assay detected a reduction in mycobacterial growth (enhancement in growth inhibition) at 8 weeks following primary vaccination (median PV = 0.13 and median W8 = 0.10; $p<0.05$) (Figure 4-3A). The PBMC MGIT detected an effect at both 4 and 8 weeks following primary vaccination, returning to baseline by week 24 (median PV = 0.05, W4 = 0.006, W8 = -0.05, W24 = 0.06; $p<0.05$) (Figure 4-3C). There was little effect of revaccination using either assay (Figure 4-3B and D), although an increase in mycobacterial growth was observed at week 24 using the PBMC MGIT, albeit non-significant following correction for multiple comparisons.

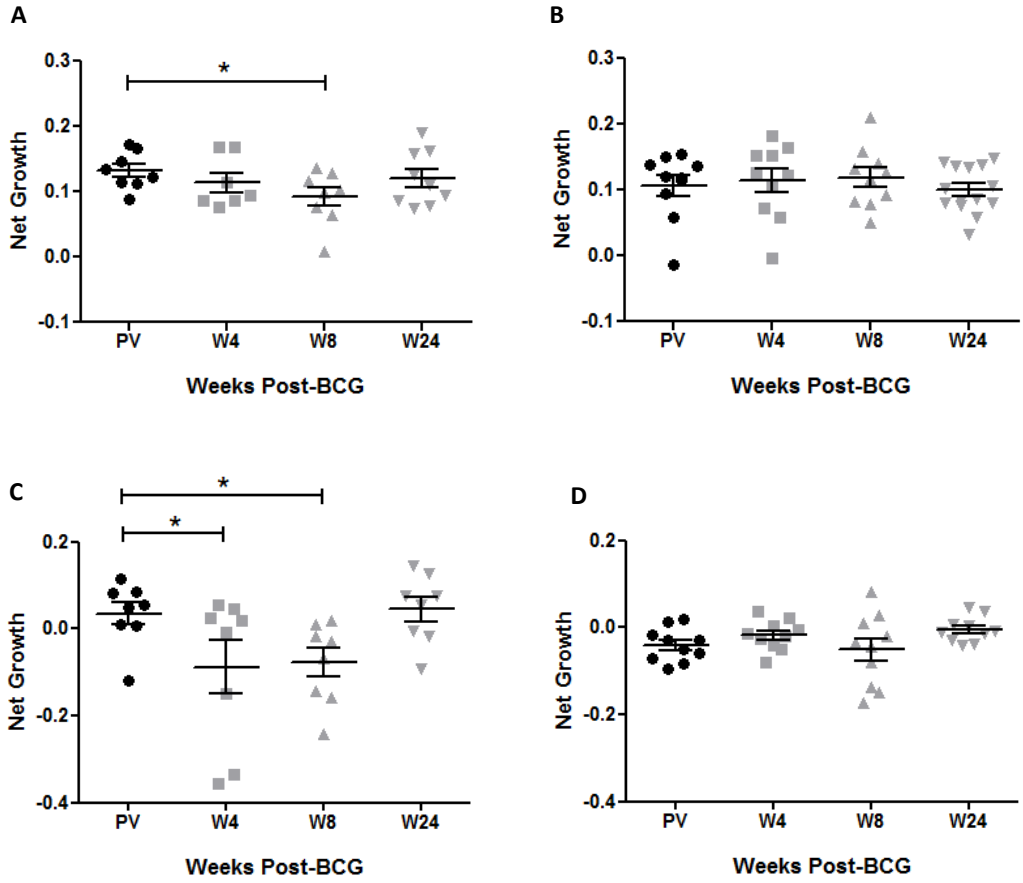

Figure 4-3 MGIT Mycobacterial growth decreases following primary BCG vaccination but not revaccination. The MGIT assay was performed pre- and post-BCG vaccination using A) whole blood from BCG naïve volunteers, B) whole blood from historically vaccinated volunteers, C) PBMC from BCG naïve volunteers and D) PBMC from historically vaccinated volunteers. Bars represent the mean values with SEM. Having passed a normality test, a one-way ANOVA was performed followed by a Dunnett's post-test where * represents a p-value of <0.05. Net growth = (Log_{10} CFU of sample - Log_{10} CFU of control).

4.4.1.3 Removal of Pen-Strep from the cell rest

As described in the previous chapter, the decision was taken to remove Pen-Strep from the standard cell rest medium. This increased the effective inoculum of mycobacteria as it was no longer artificially inhibited by the antibiotics. The same inoculum volume (6.5 day control

TTP) was tested in the presence and absence of Pen-Strep in the cell rest. When antibiotics were used, there was a significant difference between pre-vaccination and 8 weeks post-BCG (median net growth = 0.07 and -0.23 respectively; $p<0.05$). Removing Pen-Strep resulted in increased net growth and loss of discriminant ability of the assay between pre-vaccination and week 8 samples (median net growth = 2.23 and 2.20 respectively) (Figure 4-4).

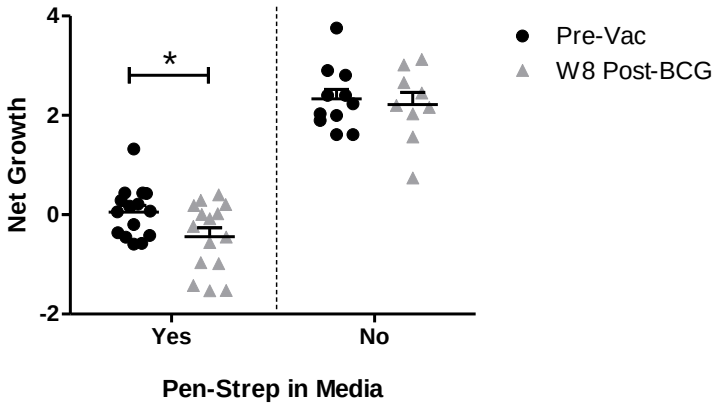

Figure 4-4 Removal of pen-strep from the pre-culture cell rest medium reduces ability to detect a BCG-mediated effect. The MGIT assay was performed pre- and post-BCG vaccination using PBMC from healthy volunteers. An inoculum of 6.5 days TTP was used; with and without Pen-Strep in the cell rest medium. Bars represent the mean values with the SEM. A two-way ANOVA was performed where * represents a p-value of <0.05. Net growth = (Log_{10} CFU of sample - Log_{10} CFU of control).

In the study described above where a vaccine effect could be detected, the average TTP of the samples was 12.5 days. Therefore mycobacterial inoculum was titrated in PBMC to identify the volume corresponding to a 12.5 day TTP in the absence of antibiotics. Firstly, a titration in two volunteers from 0.2 to 6µl demonstrated that a 12.5 day (300 hour) TTP was at the lower end of the curve (Figure 4-5A). Therefore a second experiment was conducted in 4 volunteers from 0.2 to 1µl (Figure 4-5B). In both cases, increasing the inoculum volume

decreased the TTP. Based on these observations, a 0.25µl inoculum was selected for future studies.

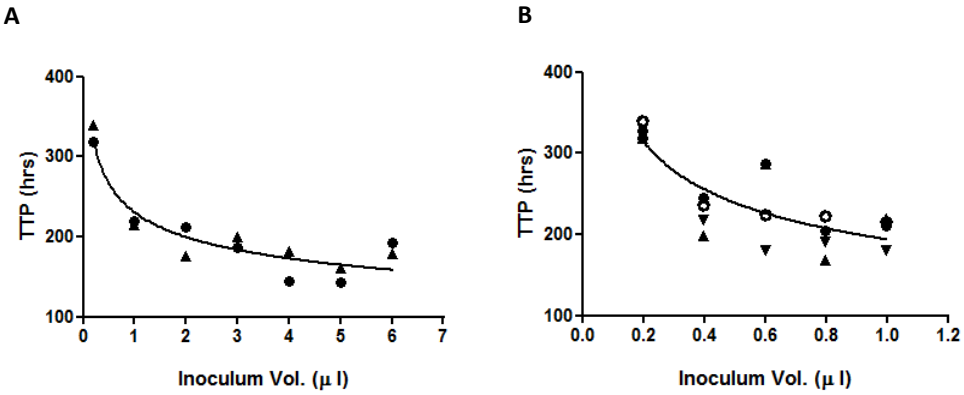

Figure 4-5 Titrating inoculum volume in PBMC to determine target volume. The MGIT assay was performed using PBMC from healthy volunteers, titrating the dose of mycobacteria to determine the volume required for a ~300 hour TTP from A) 0.2 to 6µl and B) 0.2 to 1µl. (TTP = time to positivity for MGIT cultures, where TTP is inversely proportional to mycobacterial growth).

To determine whether this reduction in mycobacterial inoculum would allow discrimination of samples pre- and post-vaccination (despite the absence of Pen-Strep in the cell rest), PBMC MGITs were run using 3 different TTPs: 6.5, 9.5 and 12.5 days. There was no difference between pre- and 8 weeks post-vaccination with the 6.5 day TTP (median net growth = 0.92 and 0.90 respectively) or 9.5 day TTP (median net growth = 0.65 and 0.69 respectively). A significant difference was observed between pre- and post-vaccination mycobacterial growth inhibition using the newly-selected 12.5 TTP (median net growth = 0.51 and 0.32 respectively; $p<0.05$) (Figure 4-6). To validate this inoculum, a larger experiment was performed, using samples from 15 volunteers at the same time-points. A significant effect of the vaccine on mycobacterial growth was detected (median PV net growth = 0.21 and median W8 net growth = -0.015; $p<0.05$) (Figure 4-7).

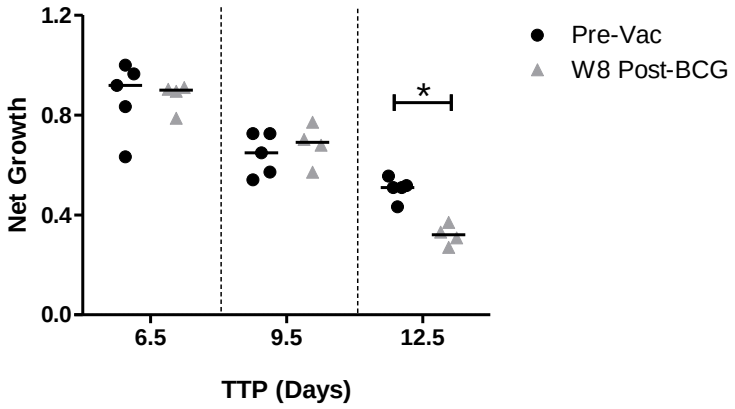

Figure 4-6 Increasing sample TTP improves ability to detect a BCG-mediated effect. The MGIT assay was performed pre- and post-BCG vaccination using PBMC from healthy volunteers. Pen-Strep was removed from the pre-culture cell rest medium. TTPs of mycobacterial inocula were 6.5, 9.5 and 12.5 days. Bars represent the median values. A two-way ANOVA performed, with a Bonferroni post-test where * represents a p-value of <0.05. Net growth = (Log_{10} CFU of sample - Log_{10} CFU of control).

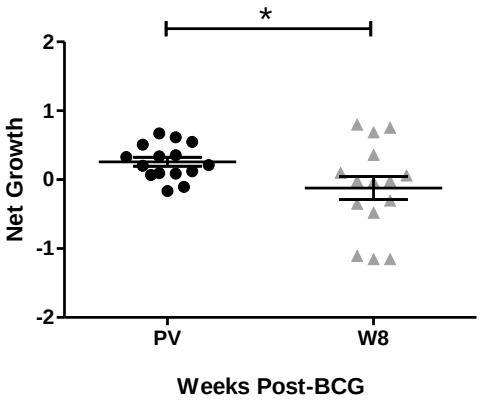

Figure 4-7 A BCG-mediated effect can be detected using low dose inoculum and no Pen-Strep. The MGIT assay was performed pre- and post-BCG vaccination using PBMC from healthy, BCG-naïve volunteers. Pen-Strep was removed from the pre-culture cell rest medium and a low-dose (12.5 day TTP) mycobacterial inoculum was used. Bars represent the mean values with SEM. Having passed a normality test, a paired t-test was performed where * represents a p-value of <0.05. Net growth = (Log_{10} CFU of sample - Log_{10} CFU of control).

4.4.2 MVA85A vaccination in SA infants

Due to the limited sample availability from the Phase IIb efficacy trial of MVA85A, two pilot studies were first conducted in samples from a prior Phase IIa study in the same population[216] to aid assay selection and optimisation. These were followed by analysis of 258 samples from the efficacy trial, including 53 cases (infants who met the primary definition of TB disease as summarised in the Appendix section 8.3) and 205 matched controls. The laboratory staff performing these studies were blinded to both vaccine/placebo and case/control.

4.4.2.1 Pilot study I

The first pilot experiment utilised samples from a dose-finding phase IIa study of MVA85A, the specifics of which are detailed elsewhere[216]. In brief, cryopreserved PBMC from 42 BCG-vaccinated South African infants (aged 5-12 months) were used, 36 of whom received a single intradermal dose MVA85A and 6 of whom received a Candin placebo (Figure 4-8). Half of these samples were used in the MGIT analysis (18 vaccinated and 3 placebo). Mycobacterial growth was reduced at 12 weeks post-MVA85A in the vaccinated infants; however this was not statistically significant after a two-way ANOVA with correction for multiple comparisons. However, growth was also reduced in the placebo group which was too small to determine statistical significance (PV median = 0.12, W12 median = -0.003) (Figure 4-9).

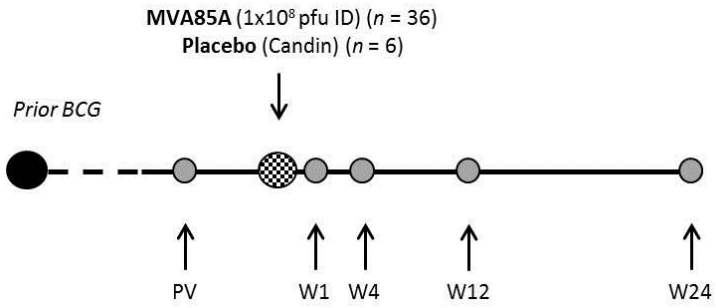

Figure 4-8 Schematic of human MVA85A pilot study I design. 42 healthy BCG-vaccinated South African infants, 36 of whom received 1x108 pfu of MVA85A intradermally and 6 of whom received a Candin placebo. Follow-up bleeds were taken at 1, 4, 12 and 24 weeks post-vaccination.

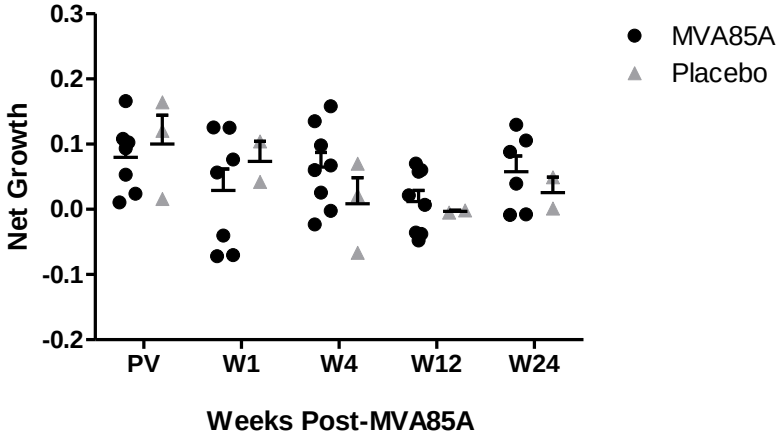

Figure 4-9 Pilot study I: MGIT mycobacterial growth in unchanged following MVA85A vaccination or Candin placebo. The PBMC MGIT assay was performed pre- and post-MVA85A vaccination in South African infants. Bars represent the mean values with SEM. A two-way ANOVA was performed where there were no statistically significant differences between groups. Net growth = (Log_{10} CFU of sample - Log_{10} CFU of control).

4.4.2.2 Pilot study II

For the second pilot experiment, a subset of samples from 60 infants (non-cases and non-controls) from the efficacy trial[219] was analysed. 30 of these received a single intradermal dose of MVA85A and 30 a Candin placebo. Bleeds were taken at 7 days before vaccination (PV) and 4 weeks post-vaccination (Figure 4-10). There were no differences in mycobacterial growth between the placebo and vaccinated infants or between either group pre- and post-vaccination (Figure 4-11).

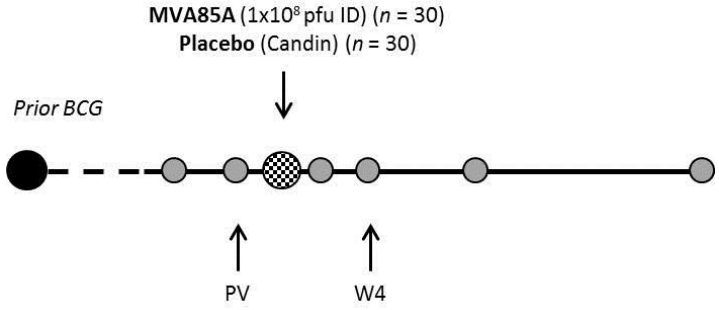

Figure 4-10 Schematic of human MVA85A pilot study II design. 60 healthy BCG-vaccinated South African infants, 30 of whom received $1x10^8$ pfu of MVA85A intradermally and 30 of whom received a Candin placebo. A follow-up bleed was taken at 4 weeks post-vaccination.

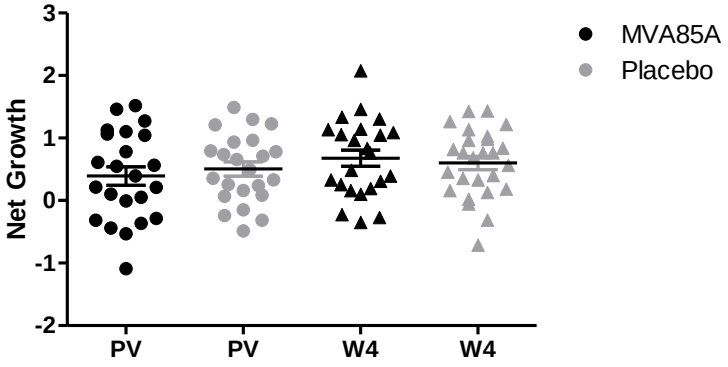

Figure 4-11 Pilot study II: Mycobacterial growth is unchanged following MVA85A vaccination or Candin placebo. The PBMC MGIT assay was performed pre- and post-MVA85A vaccination in South African infants. Bars represent the mean values with SEM. A two-way ANOVA was performed where there were no differences between groups. Net growth = (Log_{10} CFU of sample - Log_{10} CFU of control).

4.4.2.3 Phase IIb efficacy trial

The details of this trial (South African National Clinical Trials Register DOH-27-0109-2654 and ClinicalTrials.gov NCT00953927) are described elsewhere[219]. In brief, this was a double-blind, randomised, placebo-controlled phase IIb trial. 2797 healthy South African infants were enrolled (aged 4-6 months) who had previously been BCG vaccinated. Infants were randomised to receive either MVA85A vaccination (n = 1399) or an equal volume of Candida skin test antigen (n = 1398), and actively followed up every 3 months for up to 37 months. The primary study outcome was safety; the primary efficacy endpoint was incident tuberculosis. MVA85A did not confer additional protection against TB disease in this trial beyond that conferred by BCG alone (VE 17.3%; 95% CI -31.9 to 48.2).

In the correlates of risk cohort, infants who met the case definition for the stringent primary efficacy analysis (endpoint 1; see Appendix section 8.3) were included as TB cases. 3 control infants were matched to each TB case infant based on gender, race, weight and time on study. Samples from 53 TB case infants and 205 matched control infants taken from 7 days pre-vaccination and 4 weeks post-vaccination were analysed in this study. Multiple assays were run with a priority listing; the MGIT was run only when a sufficient number of cells were available, and samples were excluded if the standard deviation between duplicates was greater than 40 hours. This resulted in a mean *n* of 78 per group for the final analysis.

There were no differences in mycobacterial growth inhibition between the placebos and vaccinees or between either group pre- and post-vaccination (Figure 4-12).

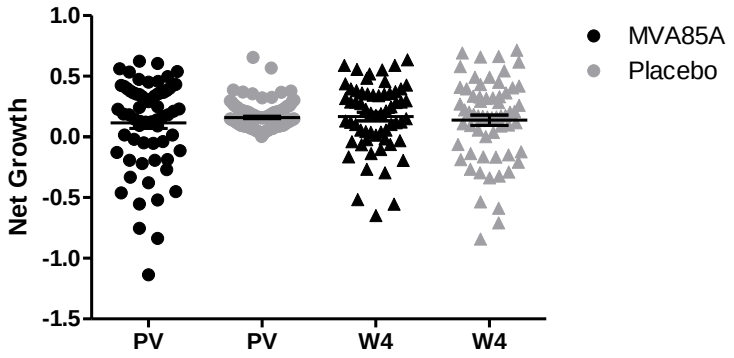

Figure 4-12 Mycobacterial growth is unchanged following MVA85A vaccination or Candin placebo. The PBMC MGIT assay performed pre- and post-MVA85A vaccination in SA infants. Bars represent the mean values with the SEM. A two-way ANOVA was performed (no differences between groups).

Following un-blinded analysis of cases and controls, there was no difference in mycobacterial growth inhibition between infants who went on to develop TB disease and those who did not; either at baseline (Figure 4-13A) or week 4 post-MVA85A or placebo (Figure 4-13B).

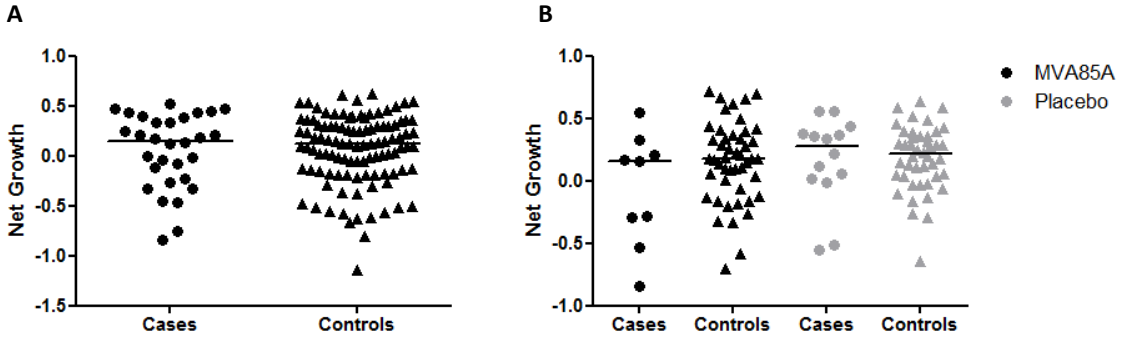

Figure 4-13 No difference in mycobacterial growth using PBMC from 'case' and 'control' infants. The PBMC MGIT assay performed in SA infants from the Phase IIb MVA85A efficacy trial. MGIT mycobacterial growth at A) baseline and B) 4 weeks post-MVA85A vaccination or Candin placebo for infants who went on to develop TB disease (cases) and those who did not (controls). Bars represent the median values. A two-way ANOVA was performed where there were no differences between groups. Net growth = (Log_{10} CFU of sample - Log_{10} CFU of control).

4.4.3 BCG vaccination in non-human primates (NHPs)

4.4.3.1 BCG vaccination in Rhesus macaques

A study was conducted in 7 Rhesus macaques of Indian genetic background (6 female, 1 male) which were vaccinated intradermally with the standard adult human dose of BCG Danish (2-8x10^5 CFU). Blood samples were collected on two occasions prior to BCG vaccination and at 2, 4 and 8 weeks post-vaccination. Animals were euthanised at the final time-point (Figure 4-14). Whole blood MGIT cultures were set up within 4 hours of volunteer bleed, and the remaining blood was used to separate and cryopreserve PBMC. Unfortunately the PBMC did not separate or freeze/thaw well and cell viability upon thawing was too low to perform PBMC MGIT assays. Using the whole blood MGIT assay, there was a significant reduction in mycobacterial growth between pre-vaccination and weeks 4 and 8 post-BCG (median net growth = 0.93, 0.32 and 0.32 respectively; $p<0.0001$). There was also a significant reduction in net growth between weeks 2 and 4 which remained at week 8 ($p<0.0001$) (Figure 4-15).

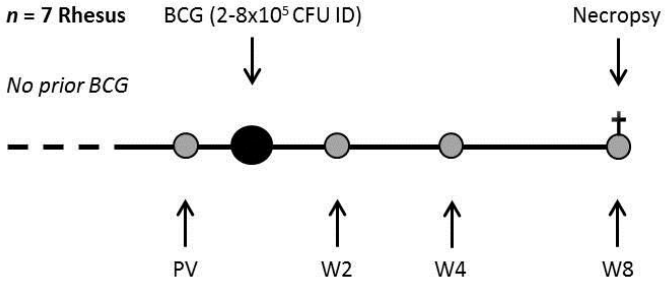

Figure 4-14 Schematic of Rhesus macaque BCG vaccination study design. 7 healthy Rhesus macaques were studied. Following 2 pre-vaccination (PV) bleeds, all animals received 2-8x10^5 pfu of BCG SSI intradermally. Follow-up bleeds were taken at 2, 4 and 8 weeks post-vaccination.

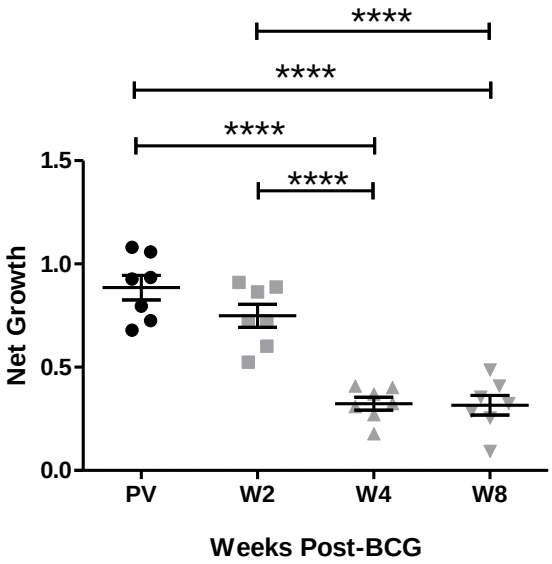

Figure 4-15 Reduction in MGIT mycobacterial growth following BCG vaccination in Rhesus macaques. The MGIT assay was performed pre- and post-BCG vaccination using whole blood from 7 Rhesus macaques. Bars represent the mean values with SEM. Having passed a normality test, a repeated measures ANOVA was performed followed by a Bonferroni post-test where **** represents a p-value of <0.0001. Net growth = (Log_{10} CFU of sample - Log_{10} CFU of control).

4.4.3.2 BCG vaccination and challenge in Cynomolgus macaques

A second study was conducted in 16 Cynomolgus macaques, 8 of which were vaccinated ID with the standard adult human dose of BCG Danish (2-8x10^5 CFU), and 8 of which were naïve controls for the challenge. Blood samples were collected from the vaccinated group prior to BCG vaccination and at 4, 8 and 20 weeks post-vaccination. The naïve group had 2 control bleeds prior to challenge. At week 21, all animals were challenged ID with 1-4x10^6 CFU BCG Danish. Animals were euthanised 2 to 3 weeks after challenge and axillary lymph nodes from the draining site of vaccination were snap frozen (Figure 4-16). Whole blood MGIT was performed using both BCG Pasteur and *M.tb* H37Rv as the *in vitro* challenge

strains. Once again, problems with separating and freeze/thawing the PBMC precluded application of the PBMC MGIT assay.

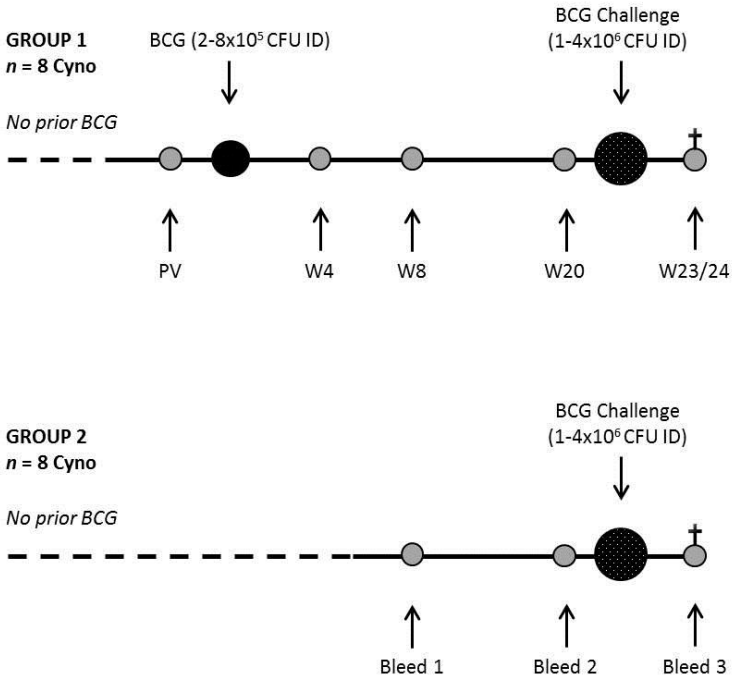

Figure 4-16 Schematic of Cynomolgus macaque BCG vaccination and challenge study design. 16 Cynomolgus macaques were used, 8 of which received 2-8x10^5 CFU of BCG Danish ID following a pre-vaccination bleed. Follow-up bleeds were taken at 4, 8 and 20 weeks post-vaccination. The remaining 8 animals served as naïve controls for the BCG challenge and had two pre-challenge bleeds. All animals were challenged at week 21 with 1-4x10^6 CFU of BCG Danish ID. 2-3 weeks after challenge, animals were euthanised and blood and axillary lymph nodes were taken.

Using the whole blood MGIT assay with BCG Pasteur as the *in vitro* challenge strain, there was a significant reduction in mycobacterial growth between pre-vaccination and week 8 post-BCG (median net growth = 0.62 and 0.008 respectively; p<0.0001) (Figure 4-17A). The magnitude of effect at week 8 was the same as that observed in Rhesus macaques ($\Delta\log_{10}$ CFU = 0.61 in both cases). Using *M.tb* H37Rv for the MGIT, there was also a significant reduction in mycobacterial growth between pre-vaccination and 8 weeks post-BCG (median net growth = 0.81 and 0.57 respectively; p<0.0001). There was an increase in *M.tb* growth between week 8 and week 20 (median net growth = 0.57 and 0.75 respectively; p<0.0001) (Figure 4-17B). For the control group, MGITs were run for the two pre-challenge bleeds using BCG Pasteur only. There was no difference in mycobacterial growth inhibition between the bleeds (data not shown).

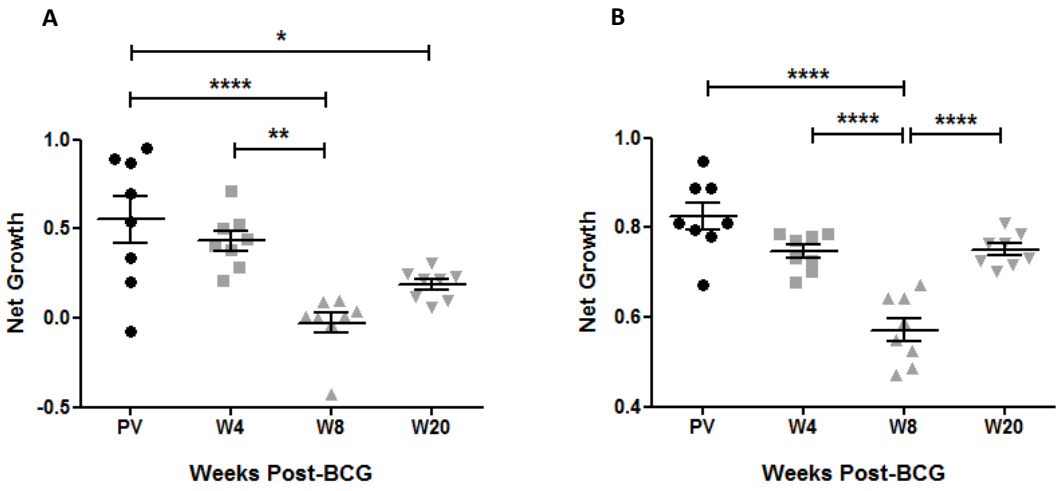

Figure 4-17 Reduction in MGIT mycobacterial growth following BCG vaccination in Cynomolgus macaques. The whole blood MGIT assay was performed pre- and post-BCG vaccination using A) BCG Pasteur and B) *M.tb* H37Rv as the *in vitro* challenge strain. Bars represent the mean values with SEM. Having passed a normality test, a repeated measures ANOVA was performed followed by a Bonferroni post-test where * represents a p-value of <0.05, ** represents a p-value of <0.005, *** represents a p-value of <0.0005 and **** represents a p-value of <0.0001). Net growth = (Log_{10} CFU of sample - Log_{10} CFU of control).

Post-challenge lymph node bacterial load was used as a measure of *in vivo* protection against BCG challenge. Lymph nodes were homogenised and plated onto Middlebrook 7H11 agar (neat and 10^{-1} dilution in PBS) for quantification. A BCG SSI vaccine vial was reconstituted and plated in serial dilutions as a positive control. Plates were incubated at 37°C for 4 weeks before colony counting. A significantly lower bacterial load was observed in the BCG vaccinated compared with control animals (median Log_{10} CFU = 1.66 and 2.52 respectively; $p<0.05$) (Figure 4-18A). Importantly, there was a significant positive correlation between lymph node bacterial load and mycobacterial net growth in the *M.tb* MGIT at the peak of response (8 weeks) ($r = 0.75$, $p<0.05$) (Figure 4-18B). There was also a trend toward a correlation with the BCG MGIT at week 8 but this was not significant (data not shown).

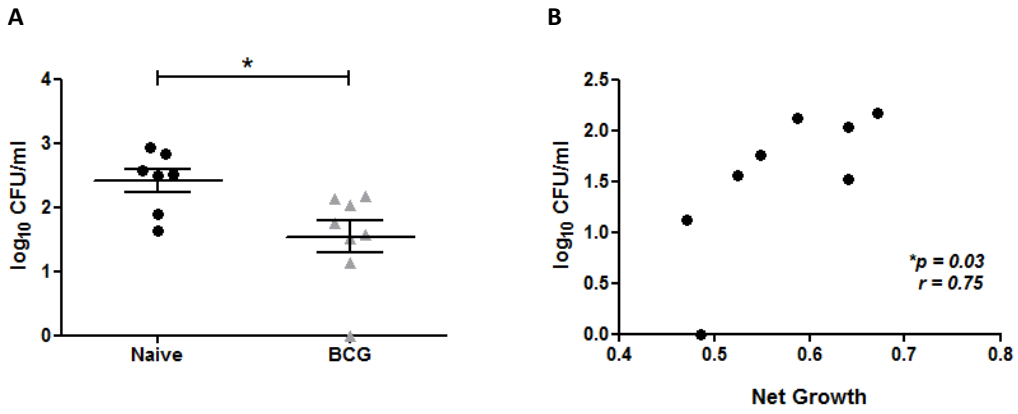

Figure 4-18 Lymph node CFU is reduced in BCG vaccinated Cynomolgus macaques following BCG challenge, and correlates with MGIT mycobacterial growth. A) Bacterial load was quantified (by plating) from axillary lymph nodes of naïve and BCG vaccinated Cynomolgus macaques, 2-3 weeks after BCG challenge. A Mann Whitney test was performed where * represents a p-value of <0.05. B) Spearman's correlation between bacterial load and *M.tb* net growth in the whole blood MGIT assay at 8 weeks post-vaccination in the BCG vaccinated group, where * represents a p-value of <0.05. Net growth = (Log_{10} CFU of sample - Log_{10} CFU of control).

4.4.3.3 PBMC MGIT in Rhesus macaques

As mentioned, problems were encountered in separating and freeze-thawing macaque PBMC. Cell recovery was too low for PBMC MGIT assays to be performed. Thus cryopreserved PBMC were obtained from an alternative historical BCG vaccination study at Public Health England. This study involved 12 Rhesus macaques, 6 of which were BCG vaccinated and 6 naïve. PBMC were provided from 3 weeks pre-vaccination and 8 weeks post-vaccination. The MGIT assay was initially run using $1x10^6$ PBMC per culture and no differences in mycobacterial growth inhibition were detected between groups (Figure 4-19A). It was repeated using $5x10^6$ PBMC per culture to determine whether this would aid detection of a vaccine effect. Under these conditions, a reduction in mycobacterial growth was observed between pre-vaccination and 8 weeks post-vaccination in the BCG vaccinated group (median net growth = 0.97 and 0.83 respectively), though this was not statistically significant after a correction for multiple comparisons (Figure 4-19B).

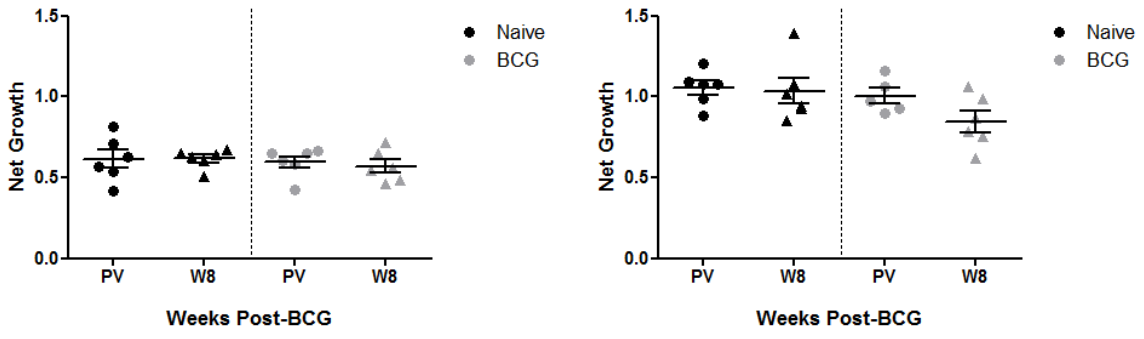

Figure 4-19 Increased cell number enhances ability to detect a BCG vaccine-mediated effect using PBMC from Rhesus macaques. The PBMC MGIT assay was performed pre- and 8 weeks post-BCG vaccination using A) $1x10^6$ PBMC and B) $5x10^6$ PBMC in the cell culture. Bars represent the mean values with SEM. A two-way ANOVA was performed followed by a Bonferroni post-test where there were no significant differences between groups. Net growth = (Log_{10} CFU of sample - Log_{10} CFU of control).

4.4.4 The mouse splenocyte MGIT

4.4.4.1 BCG vaccination in mice

A study was conducted using 32 Balb/c mice aged 6-8 weeks, half of which were naïve controls and half vaccinated subcutaneously with $1x10^6$ CFU of BCG Pasteur. 6 mice from each group were sacrificed at week 6 for MGIT assays, and the remaining 10 mice from each group were challenged with *M.tb* by aerosol. 4 weeks after challenge, all mice were sacrificed for lung and spleen CFU counts (Table 4-1).

Group	n	Vaccination Week 0	Sacrifice (MGIT) Week 6	*M.tb* Challenge Week 6	Sacrifice (CFU) Week 10
1	16	Naïve	6	10	10
2	16	BCG Pasteur	6	10	10

Table 4-1 Design and schedule for study of BCG vaccination in mice. 32 mice were used, half of which were naïve controls and half BCG vaccinated. 6 mice from each group were sacrificed at week 6 for MGIT assays, and the remaining 10 mice were challenged with *M.tb*. 4 weeks after challenge, mice were sacrificed for CFU counts.

Using the mouse splenocyte MGIT, there was a significant reduction in mycobacterial growth between naïve and BCG vaccinated mice (median net growth = 0.57 and 0.47 respectively; $p<0.05$) (Figure 4-20). In the *M.tb* challenged animals, there were significantly more CFU in the spleens of the naïve compared with vaccinated mice (median CFU = $2.7x10^5$ and $0.10x10^5$ respectively; $p<0.0001$) (Figure 4-21A). Similarly, there were significantly higher CFU counts in the lungs of naïve compared with vaccinated mice (median CFU = $37.7x10^5$ and $1.9x10^5$ respectively; $p<0.0001$) (Figure 4-21B).

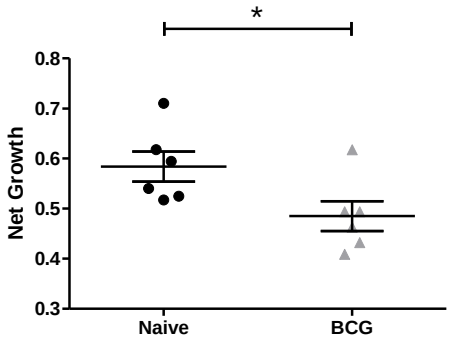

Figure 4-20 Reduction in MGIT mycobacterial growth using splenocytes from BCG vaccinated compared with naïve mice. The splenocyte MGIT assay was performed using splenocytes from naïve and BCG vaccinated Balb/c mice at 6 weeks post-vaccination. Bars represent the mean values with SEM. Having passed a normality test, a paired t-test was performed where * represents a p-value of <0.05. Net growth = (Log_{10} CFU of sample - Log_{10} CFU of control).

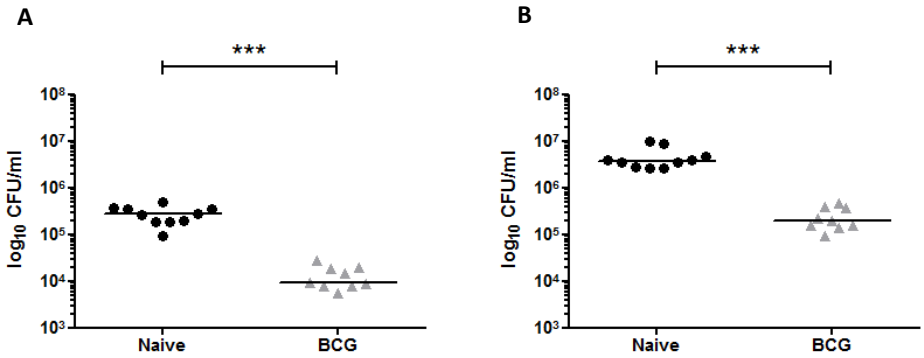

Figure 4-21 Reduction in spleen and lung CFU in BCG vaccinated compared with naïve mice following *M.tb* challenge. CFU counts from A) spleen and B) lungs from mice challenged with *M.tb* by aerosol at week 6 post-vaccination and sacrificed 4 weeks later. Bars represent the median values. A Mann Whitney test was performed, where *** represents a p value of <0.0005.

4.4.4.2 Testing a novel TB vaccine candidate

A novel TB vaccine candidate was tested in collaboration with the National Institute for Biological Standards and Control (NIBSC). As this vaccine is in the early stages of development, it will be referred to as 'Candidate X' and all data must remain confidential. The study involved 7 groups of 10 mice per group. Group 1 were naïve control animals which received no intervention. Groups 2-7 received a BCG prime at week 0 (BCG TICE). Group 2 received no further intervention, and group 7 received a homologous boost of BCG at week 8. Groups 3 to 6 each received 3 boosts at weeks 8, 10 and 12 of Candidate X at different concentrations (as specified). At week 14, half of each group was sacrificed for the MGIT assay. The remaining mice were challenged with *M.tb* at week 16 and sacrificed for CFU counting of spleen and lungs at week 28 (Table 4-2).

Group	N	Prime Week 0	Boost Week 8	Boost Week 10	Boost Week 12	Sacrifice (MGIT) Week 14	Challenge Week 16	Sacrifice (CFU) Week 28
1	10	Naïve				5	5	5
2	10	BCG TICE				5	5	5
3	10	BCG TICE	Candidate X 0.1mg	Candidate X 0.1mg	Candidate X 0.1mg	5	5	5
4	10	BCG TICE	Candidate X 0.3mg	Candidate X 0.3mg	Candidate X 0.3mg	5	5	5
5	10	BCG TICE	Candidate X 1mg	Candidate X 1mg	Candidate X 1mg	5	5	5
6	10	BCG TICE	Candidate X 2.5mg	Candidate X 2.5mg	Candidate X 2.5mg	5	5	5
7	10	BCG TICE	BCG TICE			5	5	5

Table 4-2 Design and schedule for study of novel TB vaccine 'Candidate X'. 7 groups of 10 mice were used, with 1 group of naïve controls. The remaining 6 groups received a BCG prime followed by a boost of BCG or 'Candidate X' at varying concentrations. Half of each group was sacrificed for MGIT and half challenged with *M.tb* and sacrificed for spleen and lung CFU quantification.

The MGIT assay was performed using $1x10^6$ splenocytes per culture in duplicate and BCG Pasteur as the *in vitro* challenge strain. A reduction in mycobacterial growth was observed between the naïve and BCG-TICE vaccinated animals (median net growth = 0.63 and 0.40 respectively), although this was not statistically significant after correction for multiple comparisons (Figure 4-22A). None of the groups receiving a boost of Candidate X showed an improvement on BCG vaccination.

A similar pattern between groups was observed using the *in vivo* challenge CFU counts from spleen (Figure 4-22B) and lung (Figure 4-22C). Spleen and lung CFU were significantly lower in the group receiving a boost of 1mg Candidate X compared with the naïve controls ($p<0.05$). Consistent with the MGIT data, none of the groups showed an improvement on BCG vaccination alone, and an increasing concentration of Candidate X showed a trend toward increased protection up to 1mg. The 2.5mg group showed increased MGIT net growth and increased spleen and lung CFU, though again this was not statistically significant. Due to the need to sacrifice mice for the MGIT assay, different animals were used for the *in vitro* and *in vivo* challenges, so a correlation could only be considered between the median values of corresponding groups. Using this method, there was a trend toward a positive correlation but it was not statistically significant (Figure 4-22D). The main discrepancy was the group that received a prime and homologous boost with BCG TICE. This group showed lower mycobacterial net growth in the MGIT but higher spleen and lung CFU than the Candidate X groups.

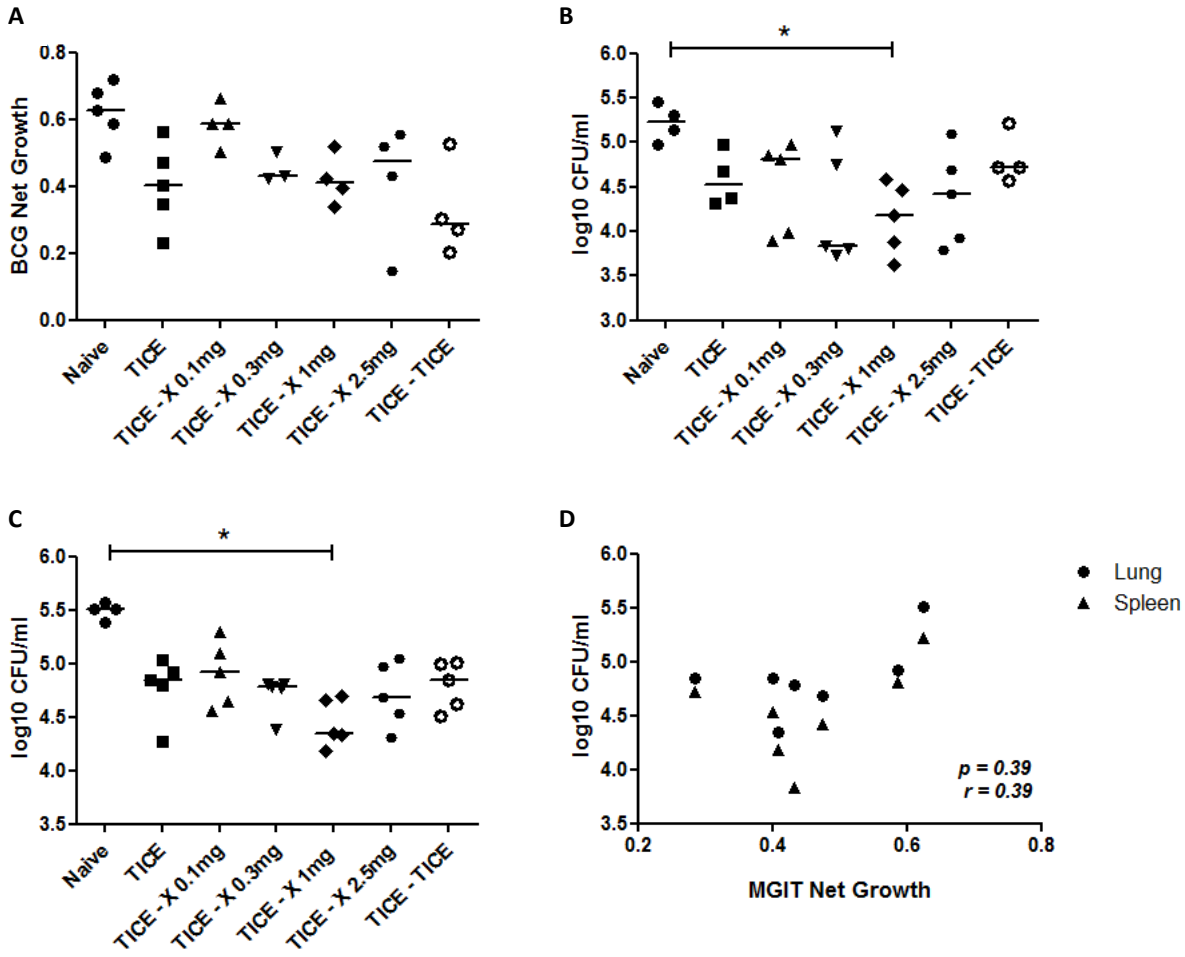

Figure 4-22 MGIT mycobacterial growth, spleen and lung CFU from mice vaccinated with BCG or a novel TB vaccine candidate. A) The splenocyte MGIT assay performed at week 14 following a BCG TICE prime. Net growth = (Log_{10} CFU of sample - Log_{10} CFU of control). CFU counts from B) spleen and C) lungs from mice challenged with *M.tb* at week 16 and sacrificed 12 weeks later. Bars represent the median values. A Kruskal-Wallis test followed by a Dunn's post-test was performed, where * represents a p value of <0.05. D) Spearman's correlation between MGIT net growth and spleen/lung CFU counts (group medians).

4.4.4.3 Optimising assay conditions

In the experiments described above, the mouse splenocyte MGIT detected a 0.1-0.2 log difference in CFU between naïve and BCG vaccinated mice, compared to *in vivo* challenge

which shows a 0.5-1 log difference. It would be desirable to improve the window of difference observed in the MGIT such that it matches that obtained using *in vivo* studies. The greater the discriminatory ability of the assay, the greater the chance of detecting improved protection conferred by novel vaccine candidates.

Previous experiments indicated that Pen-Strep antibiotics in the pre-culture medium conferred an effect on mycobacterial growth in the MGIT culture (see section 3.3.2). In the absence of Pen-Strep the mycobacterial inoculum had to be reduced to detect a vaccine effect (see section 4.4.1.3). Pen-Strep is routinely added to R10 medium used in mouse spleen processing due to the risk of contamination during dissection. Therefore the effect of Pen-Strep and mycobacterial inoculum were investigated in parallel using splenocytes from 6 naïve and 6 BCG vaccinated Balb/c mice of 6-8 weeks of age. A significant reduction in mycobacterial growth was observed in the BCG vaccinated compared with naïve group only under the conditions of no Pen-Strep and a low inoculum volume (longer TTP) ($p<0.05$) (Figure 4-23).

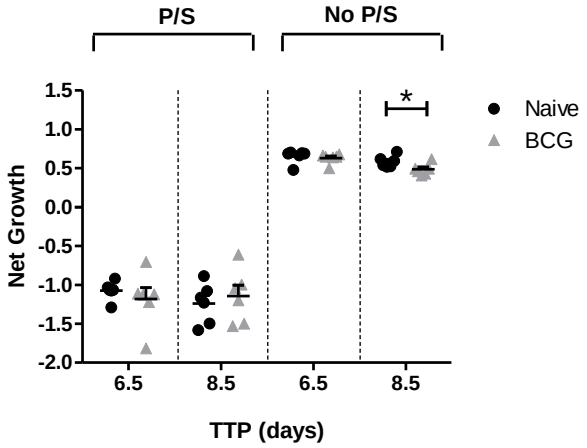

Figure 4-23 Effect of pen-strep and inoculum volume on ability to discriminate between naïve and BCG vaccinated mice using the splenocyte MGIT assay. The MGIT assay was performed using splenocytes from naïve and BCG vaccinated Balb/c mice at 6 weeks post-vaccination with and without Pen-Strep antibiotics in the splenocyte processing medium. 2 different mycobacterial inocula were tested

(where a longer TTP indicates a smaller inoculum volume). Bars represent the means with SEM. The P/S and no P/S conditions were separated for analysis. Within each condition, a two-way ANOVA was performed with a Bonferroni post-test where * represents a p value of <0.05. Net growth = (Log_{10} CFU of sample - Log_{10} CFU of control).

Given previous observations that decreasing mycobacterial inoculum and increasing cell number increases ability to discriminate between groups, an experiment was performed using 3 different inocula (6.5, 7.5 and 8.5 day TTP) and 3 different cell concentrations (1, 3 and $5x10^6$ splenocytes) using all possible permutations. 18 Balb/c mice (8 weeks of age) were used, 9 of which were naïve controls and 9 vaccinated subcutaneously with $4x10^5$ CFU BCG Pasteur in 100µl saline per animal. 6 weeks after vaccination, all animals were sacrificed and spleens were removed and processed for the MGIT assay. As expected, there was a decrease in TTP with increased inoculum and increased cell number. However, no difference in mycobacterial growth inhibition was observed between naïve and BCG vaccinated groups under any of the conditions (Figure 4-24).

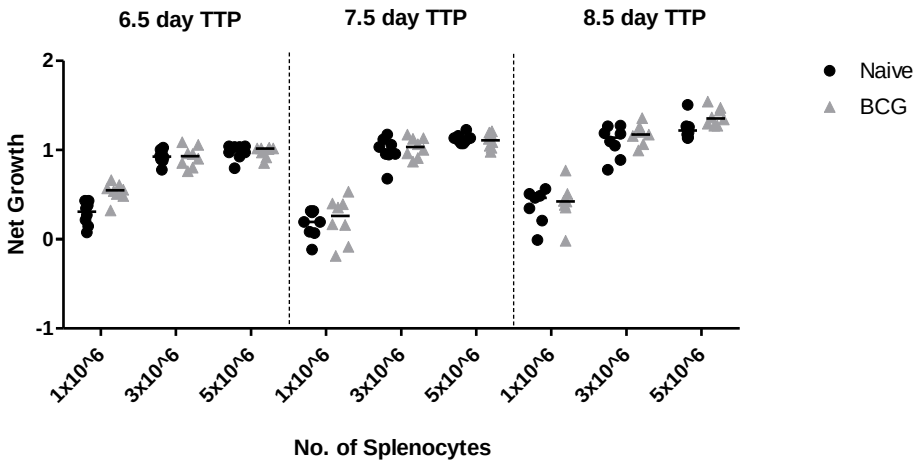

Figure 4-24 Increasing cell number and sample TTP does not improve ability to discriminate between naïve and BCG vaccinated Balb/c mice using the splenocyte MGIT assay. The MGIT assay

was performed using splenocytes from naïve and BCG vaccinated mice at 6 weeks post-vaccination using different cell concentrations and mycobacterial inocula (where a longer TTP indicates a smaller inoculum volume). Bars represent the median values. The inoculum volumes were separated for analysis. Within each inoculum, a two-way ANOVA was performed with a Bonferroni post-test where no differences were significant. Net growth = (Log_{10} CFU of sample - Log_{10} CFU of control).

As Balb/c and C57BL/6 mice differ in kinetics of immunogenicity following BCG vaccination, the $5x10^6$ splenocyte condition was repeated in C57BL/6 mice to rule out strain as the cause of the problem. 16 C57BL/6 mice were used (8 per group); all other conditions were the same as described above. Again, no difference was detected in mycobacterial growth between naïve and BCG vaccinated animals at any of the inoculum volumes tested, though there was a trend toward a vaccine effect using the 8.5 day inoculum (Figure 4-25).

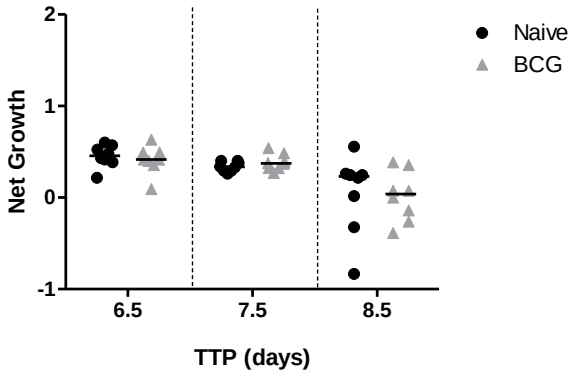

Figure 4-25 Increasing inoculum volume does not improve ability to discriminate between naïve and BCG vaccinated C57BL/6 mice using the splenocyte MGIT assay. The MGIT assay was performed using $5x10^6$ splenocytes from naïve and BCG vaccinated mice at 6 weeks post-vaccination using different mycobacterial inocula (where a longer TTP indicates a smaller inoculum volume). Bars represent the median values. Having passed a normality test, a two-way ANOVA was performed followed by a Bonferroni post-test where no differences were significant. Net growth = (Log_{10} CFU of sample - Log_{10} CFU of control).

Another potential confounder that was considered was the route of vaccination. 16 C57BL/6 mice (8 weeks of age) were vaccinated with $4x10^5$ CFU BCG Pasteur in 100µl saline. Half received the immunisation subcutaneously into the tail, and half intradermally into the ear pinnae. There was no significant difference in MGIT mycobacterial growth inhibition between the two vaccination routes, although there was a trend towards better control by the subcutaneous group (median net growth SC = 0.37, ID = 0.45) (Figure 4-26).

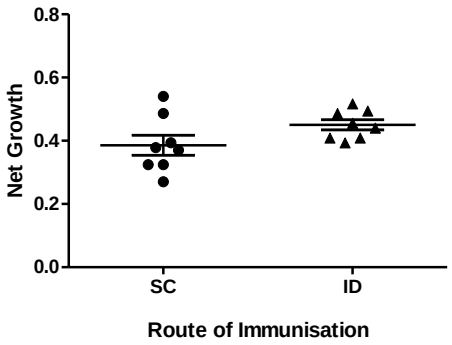

Figure 4-26 Route of vaccination in mice does not alter MGIT mycobacterial growth. The MGIT assay was performed using $5x10^6$ splenocytes from naïve and BCG vaccinated mice at 6 weeks post-vaccination using either subcutaneous or intradermal vaccination. Bars represent the mean and SEM. Having passed a normality test, an unpaired t-test was performed where p = 0.08. Net growth = (Log_{10} CFU of sample - Log_{10} CFU of control).

One potential cause of these issues is the persistence of residual BCG in the spleen following vaccination. Such BCG would grow in the culture and MGIT tube in addition to the *in vitro* inoculum of mycobacteria, and the two would be indistinguishable in determining the read-out. Therefore any mycobacterial growth inhibition mediated by the vaccinated animals may be masked by growth of the vaccine itself. To investigate this further, $5x10^6$ splenocytes from each animal were added directly to MGIT tubes. Mycobacterial growth was observed in 7 out of 8 (88%) mice vaccinated subcutaneously and 3 out of 8 (38%) mice vaccinated

intradermally. No residual BCG was detected in any of the naïve animals (Figure 4-27A). To confirm that this was not an issue in the human and macaque samples, PBMC were added from 6 human volunteers and 6 Rhesus macaque volunteers at 4 weeks post-BCG vaccination. As expected, there was no residual BCG present in these samples (Figure 4-27B).

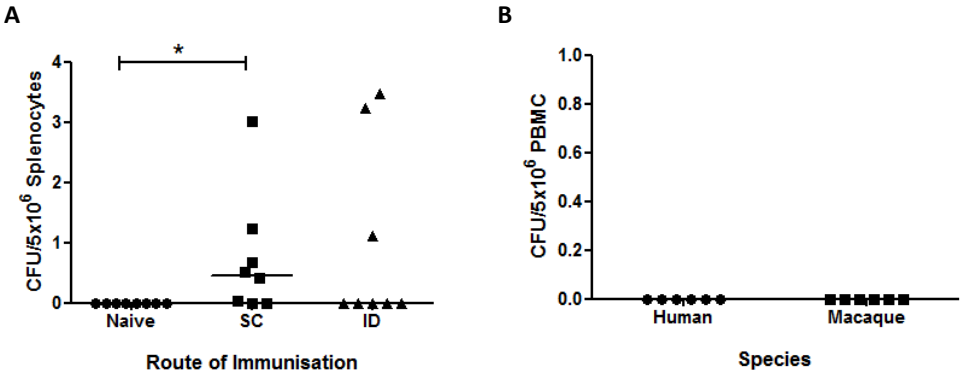

Figure 4-27 Residual BCG is detectable in splenocytes from vaccinated mice, but not PBMC from vaccinated humans or macaques. A) $5x10^6$ splenocytes from naïve and BCG vaccinated mice at 6 weeks post-vaccination using either subcutaneous or intradermal immunisation, added directly to MGIT tubes with no culture. Bars represent the median values. A one-way ANOVA was performed followed by a Dunnett's post-test (all groups vs. naïve) where * represents a p value of <0.05. B) $5x10^6$ PBMC from humans and macaques at 4 weeks post-BCG vaccination, added directly to MGIT tubes with no culture.

4.5 Discussion

The abilities of the whole blood and PBMC MGIT assays to detect a vaccine response were assessed in a human trial of BCG vaccination and revaccination. The PBMC assay performed better in that it was able to distinguish naïve from historically vaccinated individuals at baseline whereas the whole blood assay was not. The PBMC assay also detected a reduction in mycobacterial growth at 4 and 8 weeks following primary BCG vaccination, where the whole blood assay picked up a more modest reduction at week 8 only. The explanation for these differences may lie in the reliability of the assays; although the PBMC assay was shown to have greater intra-assay variability, this was improved using the optimisation results detailed in the previous chapter. Furthermore, the PBMC assay had superior inter-assay reproducibility: in the time-courses described above, the 3 pre-vaccination bleeds are averaged to give a single measure. Given the variability in these repeats using whole blood, the single pre-vaccination measure may be less accurate, reducing ability to detect relative differences. PBMC may also represent a 'cleaner' compartment for assessing vaccine efficacy, as the cellular immune response is widely considered central to protection against *M.tb*. Other factors present in whole blood may confound the true effect; this will be investigated in the following chapter.

That a vaccine effect was observed following primary but not secondary vaccination with BCG is consistent with reports in the literature. As described, primary BCG vaccination is known to have relatively high efficacy in the UK population[190,281-283]. Cheng *et al*. showed enhanced mycobacterial growth inhibition *in vitro* following primary vaccination in UK children[244]. Although no clinical trials of BCG revaccination have been performed in the UK, there is evidence in the literature that BCG revaccination does not improve on protection from TB in Finland[290], Hong Kong[291], Chile[292] or Brazil[293]. Using the PBMC assay, a slight worsening in mycobacterial control was actually observed at week 24 compared with

baseline. It is possible that boosting cellular responses by revaccination actually reduces long-term ability to control mycobacterial growth; either due to exhaustion or regulation of T cells. It would be interesting to investigate this possibility using cellular phenotyping.

Consistent with findings in the previous chapter, removing antibiotics from the cell rest medium reduced the inoculum TTP (effectively increasing the inoculum). This resulted in a loss of discrimination between pre- and post-vaccination samples in the MGIT assay. A similar effect is observed *in vivo* in mice if the *M.tb* challenge dose is too high, overcoming the protection of BCG. Lowering the inoculum did resolve this problem, but as described in the previous chapter it is associated with increased variability. It is clear that a delicate balance must be drawn between the mycobacterial inoculum being low enough not to override the vaccine effect, but not so low as to introduce detrimental variability into the assay.

In the first pilot study of MVA85A vaccination in BCG vaccinated South African infants, a significant reduction in mycobacterial growth was observed at 12 weeks post-MVA85A. This was surprising, as it was not consistent with the results of the efficacy trial showing that MVA85A did not confer protection against *M.tb* in this population[219]. However, it is clear from the data presented that the placebo group also declined during this time period, with a similarly reduced median net growth at week 12. Unfortunately due to a lack of sample availability, only 3 matched controls were available for this study. With poor cell recovery, this was reduced to 2 at some time-points. Therefore it was not possible to undertake statistical analysis on this group. However, a trend is clearly discernible and raises the possibility that the observations reflect the beginnings of an effect of BCG vaccination at birth rather than the MVA85A boost. Indeed an almost 2 log difference in mycobacterial growth has been observed in 10 week old BCG vaccinated compared with naïve infants using the PBMC MGIT assay (Steve Smith, private communication). The response may also be affected by age-related maturation of the immune system. It is well-documented that the

immune system is still developing up to 3 years of age, especially during the first 6 months of life[294,295]. There is evidence that young infants are particularly vulnerable to TB disease, being at greater risk of progression to active TB[296] and more likely to develop severe disseminated forms, with a higher death rate than other age groups[39,297,298]. This may be associated with a dampening of inflammatory responses to accommodate colonisation with beneficial commensal bacteria as well as an immature immune system[299]. It would be interesting to further explore the mycobacterial growth inhibition capacity of naïve infants.

The results of the second pilot study and the correlates of risk analysis were more consistent with the outcome of the efficacy trial. No differences in mycobacterial growth were observed between placebo and MVA85A vaccinated infants, or between pre- and 4 weeks post-vaccination for either group. Disappointingly, there was no difference in mycobacterial growth between infants who went on to develop TB disease and those who did not. However, of the 21 other immune response variables evaluated, only 2 cell types and Antigen 85A-specific IgG at week 4 were associated with reduced risk of TB disease (Fletcher *et al.* manuscript submitted). This suggests a previously unrecognised role for antibodies in protection against TB in infants, and may explain the lack of predictive power of the MGIT assay. As antibodies have widely been considered unimportant in mycobacterial control due to its intracellular nature[300], pooled human serum rather than autologous serum was used in the assay. Furthermore, using autologous serum from every individual (particularly in a study of these proportions) would be logistically unmanageable. However, if IgG is in fact important for protection, this may explain why the MGIT results did not differ between cases and controls. Alternatively, sample size and assay sensitivity may play a role.

The whole blood MGIT assay performed well in non-human primates, where a large effect of BCG vaccination was detected in both Rhesus and Cynomolgus macaques. It is well-documented that BCG is highly protective in Cynomolgus macaques[204,284], in keeping with the MGIT observations. However, it was surprising that an equally strong effect was

observed in Rhesus macaques, in which BCG is thought to confer a more modest protection *in vivo*[286]. This may be due the fact that this study used macaques of a Mauritian genetic background compared with the reported studies, which used animals of an Indonesian background. Cynomolgus macaques with a Mauritian background are known to have a remarkably restricted degree of MHC diversity[301,302], and it has been shown that the MHC alleles expressed by macaques can dramatically influence cellular immune responses and infection dynamics[303]. The age of the macaques may also contribute, as the Cynomolgus macaques were older and may thus have reduced vaccine efficacy due to immunosenescence[304]. It was interesting that mycobacterial growth had returned to baseline by week 20, which is consistent with the pattern observed in human volunteers and with the IFN-γ ELISpot response to PPD, which increased at week 8 and returned to baseline at week 20. The waning of response by 6 months in the MGIT assay is similar to the pattern observed for BCG responders in the Cheon study[252].

A BCG rather than *M.tb* challenge was used in the Cynomolgus macaque study due to efforts within the group to develop a human BCG challenge model. Human challenge models have greatly benefitted the development of vaccines for other infectious diseases[305-307], but challenging humans with *M.tb* is not ethically possible. Applying BCG as a surrogate has shown promise in previous studies[279,308]. A BCG challenge model in NHPs would provide biological validation for the human model and represent a more cost-effective and less severe method of testing vaccines in NHPs. Following BCG challenge, a significantly lower bacterial load was observed in the lymph nodes of vaccinated compared to naïve animals. Importantly, there was a significant correlation between the *M.tb* MGIT at peak of response (week 8) and lymph node CFU. This represents crucial progress toward biological validation of the MGIT assay, indicating that the results are meaningful in terms of predicting *in vivo* protection. Furthermore, correlation at an individual level within a group is a far more rigorous measure of association than correlation at the between-group level. Mouse studies

are limited to the latter due to the necessity to sacrifice animals for the splenocyte MGIT. Although the correlation with BCG MGIT was not significant, there was a trend and, as a correlation was demonstrated between outcomes of the BCG and *M.tb* MGIT in chapter 1, this is likely to be due to small numbers with only 8 animals per group.

Although PBMC were separated and cryopreserved during the NHP studies, cell recovery was extremely low making PBMC MGIT assays unfeasible. When alternative cells cryopreserved at PHE were thawed in Oxford, recovery was substantially improved, suggesting the issues were in the pre-freezing stages. Having no previous experience in NHP samples, human reagents were used which with retrospect were not best-suited. Furthermore, problems with red blood cell contamination led to repeated lysis steps which may have been influential. Using cells from a different BCG study conducted at PHE, a vaccine effect was observed only when a higher cell concentration ($5x10^6$ PBMC per culture) was used. This may be due to the increased presence of specific T cells mediating a greater overall effect, and reduced variability associated with higher cell number (see section 3.3.4.1) may also play a role. These studies represent exciting novel work, as there are no known reports in the literature of MGIAs using NHP samples. However, there were several limitations including the lack of a full sample time-course from the control group. As the assay is run in real-time on fresh samples, and given the inter-assay variability observed in the previous chapter, it will be important in future studies to include a control group throughout. It may also be interesting to include a group from a population in which BCG is known to be ineffective, or a group vaccinated with a non-protective vaccine as further controls.

Early work using the mouse splenocyte assay demonstrated a significant difference in mycobacterial growth inhibition between naïve and BCG vaccinated mice. This is consistent with previous work by Marsay *et al.*[255] and other unpublished data in the group. Concordantly, a significant difference in spleen and lung CFU was observed in experimentally-matched animals challenged with *M.tb in vivo*. The assay was thus applied to

the pre-clinical testing of a novel TB vaccine candidate. A significant improvement in mycobacterial growth inhibition was again observed in the BCG vaccinated compared with naïve animals, using a different strain of BCG vaccine (TICE rather than Pasteur). Although the correlation between group medians was not statistically significant, there were distinct similarities between the *in vitro* MGIT and *in vivo* challenge results. Firstly, none of the groups receiving a Candidate X boost improved on the protection conferred by BCG alone. A boost of 0.1mg of Candidate X appeared to do worse than BCG alone. However, increasing concentrations of Candidate X resulted in increased protection up to 1mg; at 2.5mg, there was a worsening of protection. The main discrepancy between the MGIT and challenge results was the group receiving a homologous prime-boost regime of BCG TICE. In the MGIT these animals performed the worst, whereas *in vivo* they appeared to be protected as well as those receiving one shot of TICE. These data indicate that the MGIT assay is less sensitive than *in vivo* challenge, as it failed to detect a significant reduction in mycobacterial growth in the mice receiving TICE-X 1mg, despite better *in vivo* protection in this group. Furthermore, the difference between naïve and BCG vaccinated in the MGIT was ~0.2 $\Delta\log_{10}$ CFU, compared with ~0.7 $\Delta\log_{10}$ CFU *in vivo*. However, the observation of similar patterns between groups is promising; particularly given the limitation of very small group size (determined by the organisations directing the study).

In an effort to address the low sensitivity of the mouse splenocyte assay, some optimisation work was conducted comparing different permutations of Pen-Strep (in cell processing medium), mycobacterial inoculum and cell number. Removal of Pen-Strep and a lowering of inoculum allowed better discrimination between groups, consistent with the human and NHP data. However, this effect was lost in the subsequent work despite identical conditions. Mouse strain and route of inoculum were both explored as confounding factors but did not appear to be the cause. One altered variable coinciding with these issues was the BCG vaccination strain. Though the same number of CFU were immunised in the same overall

volume, it was a higher titre stock of BCG Pasteur. When plated, this stock grew remarkably fast. It was postulated that the strain may be growing differently in the mice, with concern about the potential for residual BCG in the spleens of vaccinated animals. Indeed, there is evidence in the literature that even a low dose of BCG results in persistent 'infection', with viable vaccine bacilli present in the secondary lymphoid organs for up to 66 weeks[197,309]. To investigate this, splenocytes from animals vaccinated in this study were inoculated directly into MGIT tubes. There was indeed evidence of residual BCG in these samples; albeit ~2 logs lower than the number of CFU recovered at the end of the 96 hour MGIT culture. Such residual BCG would undoubtedly grow in the culture and MGIT tube in addition to the *in vitro* inoculum of mycobacteria, and the two would be indistinguishable in determining the read-out. Therefore any mycobacterial growth inhibition mediated by the vaccinated animals may be masked by growth of the vaccine itself. To confirm whether this was indeed contributing to the inability to detect a vaccine response in later experiments, it would be useful to conduct an equivalent experiment using the old BCG vaccine strain and determine if the residual BCG was lower or even absent. Human and NHP samples tested for residual BCG were both found to be negative, which is unsurprising as BCG is unlikely to be circulating in the peripheral blood. It should be noted that the problem of residual BCG would only apply to replicating vaccine candidates.

Interestingly, the Fletcher group at LSHTM have recently detected a ~0.7 $\Delta\log_{10}$ CFU between naïve and BCG vaccinated mice, despite seeing similar levels of residual BCG, suggesting that this may not be the cause of the issues described (Helen Fletcher, private communication). One alternative potential explanation for the poor performance of the murine assay is splenocyte viability. Although cell viability was not assessed as part of this project, it has been found by others to be <20% after 96 hours of culture, unlike human PBMC (Kandt and Fletcher, private communications). This may be improved by altering assay conditions, such as gentle rocking rather than 360° rotation as used by Parra *et al*[254].

This work has identified some of the pitfalls associated with the mouse model in this context, and indicates that further optimisation work is required. Unfortunately, the problems encountered precluded the further testing of novel vaccine candidates as planned. It may be that NHPs and humans would be a more appropriate model for this assay in terms of a correlate of vaccine efficacy, although further work is still required to increase the window of difference ($\Delta\log_{10}$ CFU) between pre- and post-vaccination PBMC samples in these species. It has been suggested that this difference should be at least as great as that seen in *in vivo* challenge models to justify the replacement of *M.tb* challenge in preclinical development.

4.6 Conclusions

- The PBMC, and to a lesser extent whole blood, MGIT assay detected a significant response following BCG vaccination but not revaccination in humans; consistent with epidemiological data.

- In keeping with the results of the Phase IIb efficacy trial of MVA85A in South African infants, the PBMC MGIT assay showed no difference between vaccinated and placebo infants or pre- and post-vaccination. There was no difference between mycobacterial growth inhibition in TB cases and controls.

- The whole blood MGIT assay showed a significant effect of BCG vaccination in both Rhesus and Cynomolgus macaques. A modest effect was observed using PBMC from a different study.

- Using mouse splenocytes, a difference was detected between naïve and BCG vaccinated animals in concordance with *in vivo* challenge of experimentally-matched mice.

- A similar pattern of *in vitro* and *in vivo* protection was observed in a preclinical study of a novel TB vaccine candidate.

- Loss of discrimination between naïve and BCG vaccinated mice in later experiments may have been associated with residual BCG arising from a new vaccine strain masking the vaccine effect or with poor splenocyte viability.

5 Blood components influencing mycobacterial growth

5.1 Statement of authorship

Non-human primate samples and haemoglobin levels were provided by Sally Sharpe and Andrew White at Public Health England (PHE). Help with flow cytometry was provided by Iman Satti and help with the BCG-GFP experiments by Paulo Bettencourt.

5.2 Introduction

Whole blood differs from PBMC in several key ways which may be of relevance to mycobacterial growth and inhibition of growth. Whole blood contains neutrophils, erythrocytes and thrombocytes which are not present in the PBMC compartment. Furthermore, the plasma/serum portion contains proteins such as albumin, complement and clotting factors as well as mineral salts, sugars, fats, hormones and vitamins. Any antigen-specific antibodies induced by a vaccine would also be found in the serum. Based on literature in the field and observations from the studies described in previous chapters, I have chosen to concentrate on the effects of haemoglobin, serum factors and neutrophils. The findings may be important in determining the most appropriate compartment for candidate vaccine testing.

5.3 Aims

The aims of the experiments detailed in this chapter were to:

- Investigate the relationship between mycobacterial growth inhibition mediated by whole blood and PBMC
- Investigate the influence of whole blood factors on mycobacterial growth, including haemoglobin, serum (antibodies and complement) and neutrophils

5.4 Results

5.4.1 Whole blood vs. PBMC MGIT

As described in section 3.3.1, a study was conducted of BCG vaccination in 30 healthy UK volunteers. 15 had no history of BCG vaccination and the remaining 15 had been historically vaccinated. Volunteers received a single ID immunisation with BCG-SSI with follow-up bleeds at weeks 4, 8 and 24 post-vaccination (see Figure 4-1). The MGIT assay was performed using whole blood or PBMC from the same 10 volunteers. There was no correlation between the outcome of the two assays at any time-point (Figure 5-1 A-D).

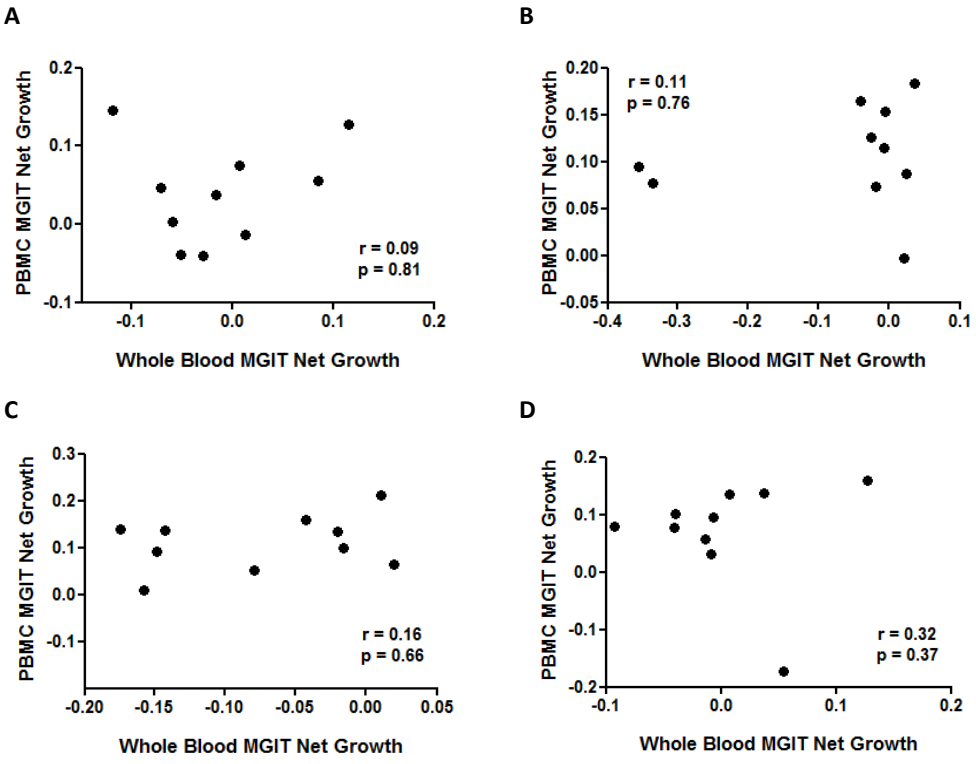

Figure 5-1 No correlation between MGIT mycobacterial growth in whole blood and PBMC. Spearman's correlation between mycobacterial net growth in the whole blood and PBMC MGIT assays at A) week 0, B) week 4, C) week 8 and D) week 24 following BCG vaccination. Net growth = (Log_{10} CFU of sample - Log_{10} CFU of control).

To confirm these findings, a second experiment was performed using matched whole blood and cryopreserved PBMC from 12 healthy volunteers. Again there was no correlation between MGIT outcome for the two compartments (Figure 5-2).

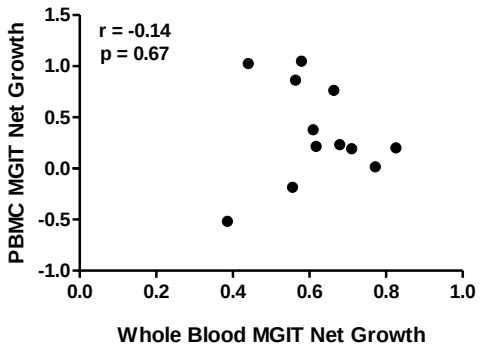

Figure 5-2 No correlation between MGIT mycobacterial growth in whole blood and PBMC II. Spearman's correlation between mycobacterial net growth in the whole blood and PBMC MGIT assays in healthy volunteers at baseline. Net growth = (Log_{10} CFU of sample - Log_{10} CFU of control).

5.4.2 The effect of haemoglobin

The decision to explore the role of haemoglobin was based on observations from some of the studies previously described. In the study of BCG vaccination in Rhesus macaques (see section 4.4.3.1), the haemoglobin level of the animals dropped significantly by week 8 post-BCG ($p<0.05$) (Figure 5-3A). Similarly, in a second study of Rhesus macaques (see section 4.4.3.3), there was a significant reduction in haemoglobin between week 0 and week 8 ($p<0.05$) (Figure 5-3B). Interestingly, haemoglobin was stable during the course of the study of Cynomolgus macaques (section 4.4.3.2). Reduced haemoglobin levels may be caused by repeated bleeds of relatively large volumes, and may influence the outcome of the MGIT assay. Although the positive association between mycobacterial growth and haemoglobin level was not significant, a binary split of the group revealed that the 3 macaques with the

highest haemoglobin concentrations also had the highest mycobacterial growth and vice versa (data not shown).

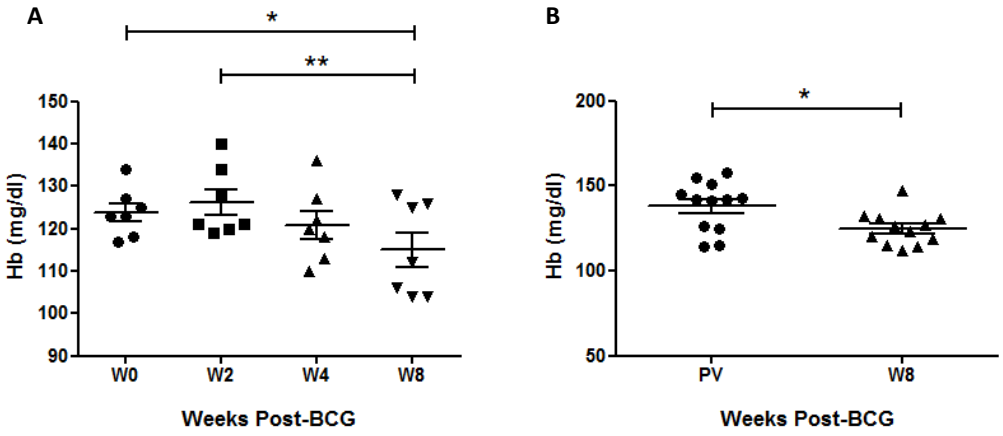

Figure 5-3 Reduction in haemoglobin levels following successive bleeds in Rhesus macaques. Haemoglobin was measured at each time-point during two studies of BCG vaccination in Rhesus macaques. Bars represent the mean values with the SEM. A) Having passed a normality test, a repeated measures ANOVA was performed followed by a Bonferroni post-test where * represents a p-value of <0.05 and ** represents a p value of <0.005. B) Having passed a normality test, a paired t-test was performed where * represents a p-value of <0.05.

Using clinical data from the human and macaque BCG vaccination studies described in the previous chapter, the association between MGIT net growth and haemoglobin was explored. Although there was no significant relationship between mycobacterial growth and haemoglobin (Figure 5-4), a positive correlation was observed between mean corpuscular haemoglobin (MCHGB) at baseline and mycobacterial net growth in the whole blood MGIT at weeks 4 and 8 following vaccination ($p<0.05$ in both cases) in the human study. This association was lost in the PBMC MGIT assay (Figure 5-5).

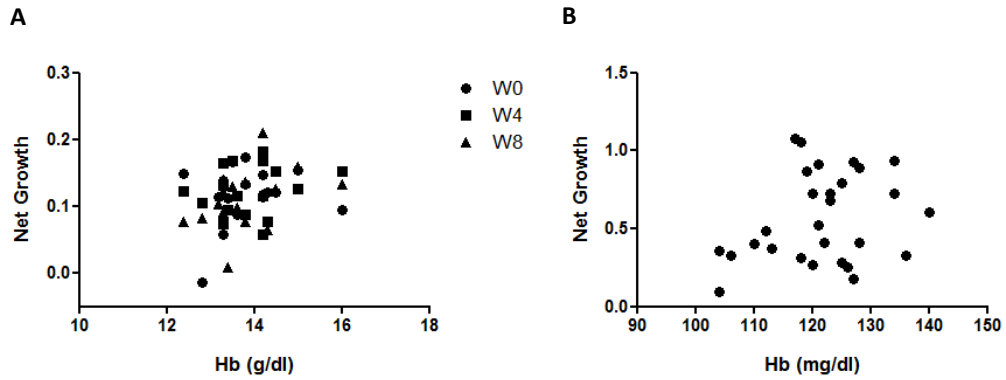

Figure 5-4 Relationship between Hb and MGIT mycobacterial growth. Spearman's correlation between haemoglobin concentration (Hb) and mycobacterial net growth in the whole blood MGIT assays for A) human and B) macaque samples. Net growth = (Log_{10} CFU of sample - Log_{10} CFU of control).

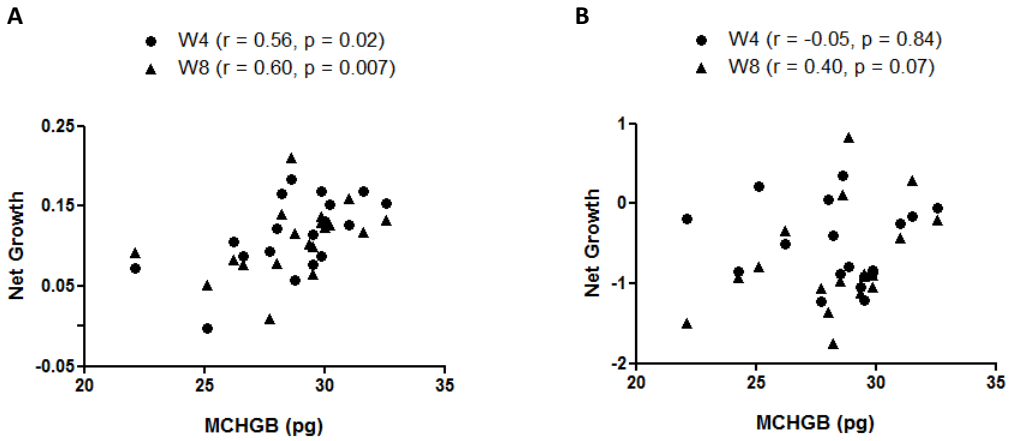

Figure 5-5 Significant correlation between MCHGB and mycobacterial growth in the whole blood, but not PBMC, MGIT assay. Spearman's correlation between mean corpuscular haemoglobin (MCHGB) and mycobacterial net growth in the A) whole blood and B) PBMC MGIT assays. Net growth = (Log_{10} CFU of sample - Log_{10} CFU of control).

5.4.2.1 Adding haemoglobin

To further investigate the effect haemoglobin may have on mycobacterial growth, haemoglobin was added directly to MGIT tubes at increasing concentrations in triplicate. There was a positive association between haemoglobin concentration and mycobacterial growth (Figure 5-6A). In a second experiment, concentrations around the physiological range were investigated and a similar association was observed (Figure 5-6B).

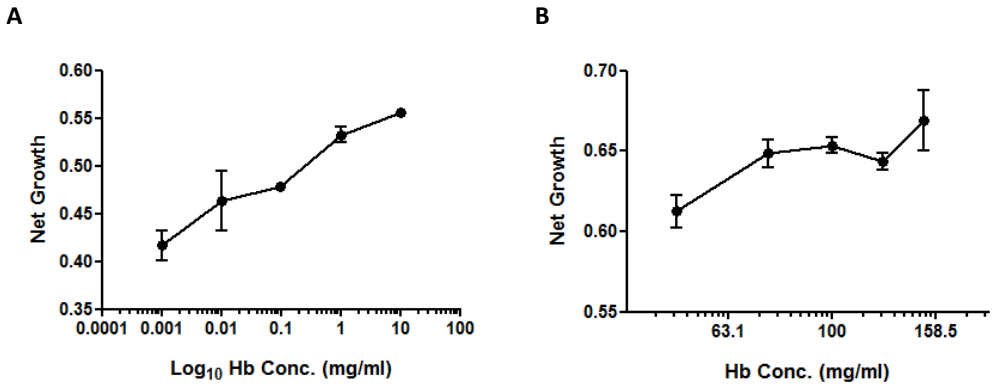

Figure 5-6 Mycobacterial growth increases with increasing Hb concentration. Mycobacterial growth was measured at increasing concentrations of haemoglobin added directly to infected MGIT tubes. Points represent the mean of triplicates with SEM. Net growth = (Log_{10} CFU of sample - Log_{10} CFU of control).

Haemoglobin was then added to 96 hour MGIT cultures of human PBMC, macaque PBMC and mouse splenocytes from two different strains. In all cases, increased haemoglobin concentration resulted in increased mycobacterial growth. This effect appeared to plateau at ~1mg/ml of haemoglobin (Figure 5-7).

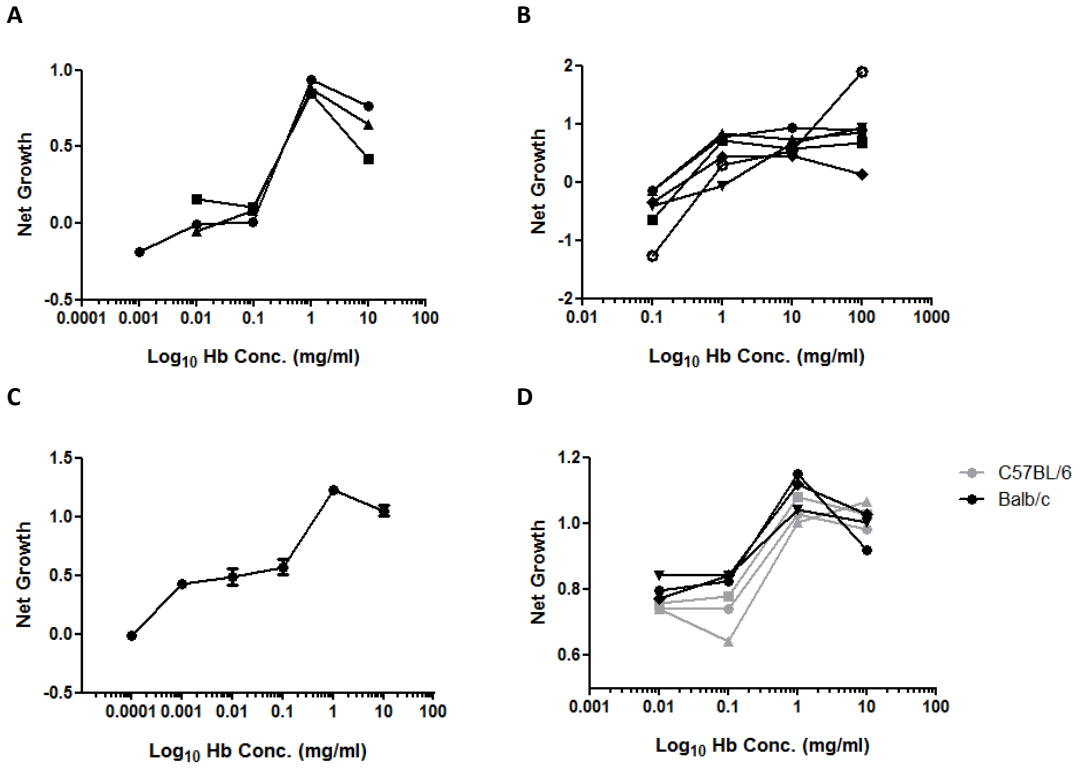

Figure 5-7 MGIT Mycobacterial growth increases with increasing Hb concentration. Mycobacterial net growth was measured at increasing concentrations of haemoglobin added to cultures of A) human PBMC, B) a second experiment of human PBMC, C) macaque PBMC and D) mouse splenocytes. Lines represent individual animals; points represent the mean of triplicates with the SEM. Net growth = (Log_{10} CFU of sample - Log_{10} CFU of control).

5.4.2.2 The effect of iron chelator

To determine whether the observed effect of haemoglobin was due to iron, the iron chelator Deferoxamine (DFO) was added alongside increasing concentrations of haemoglobin. Although DFO did not entirely negate the effect of increasing haemoglobin, there was a reduction in mycobacterial growth in the cultures containing DFO (Area under the curve (AUC) control = 37.7, AUC DFO = 28.1) (Figure 5-8). Addition of 100μM DFO to blood from Cynomolgus macaques resulted in a significant reduction in mycobacterial growth

(control median net growth = 0.008, DFO median net growth = -0.32; $p<0.05$) (Figure 5-9A). A similar pattern was observed using blood from human volunteers (control median net growth = 0.49, DFO median net growth = 0.09; $p<0.05$) (Figure 5-9B).

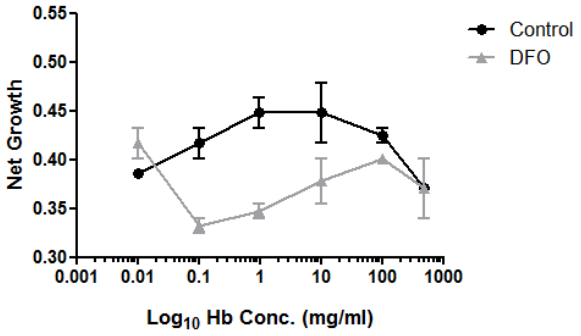

Figure 5-8 Addition of DFO results in decreased MGIT mycobacterial growth. Mycobacterial net growth was measured at increasing concentrations of haemoglobin added to cultures of human whole blood; either with or without the addition of the iron chelator deferoxamine (DFO). Points represent the mean of triplicates with the SEM. Net growth = (Log_{10} CFU of sample - Log_{10} CFU of control).

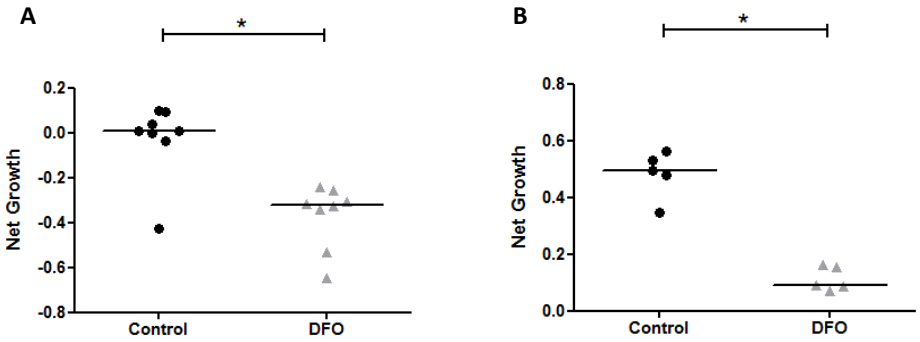

Figure 5-9 Addition of DFO results in decreased MGIT mycobacterial growth. The whole blood MGIT assay was performed on whole blood from A) Cynomolgus macaques and B) human volunteers with and without addition of 100µM of the iron chelator deferoxamine (DFO). Bars represent the median values; a paired t-test was performed where * represents a p value of <0.05. Net growth = (Log_{10} CFU of sample - Log_{10} CFU of control).

A titration of DFO in human whole blood demonstrated a reduction in mycobacterial growth with increasing DFO concentration (Figure 5-10).

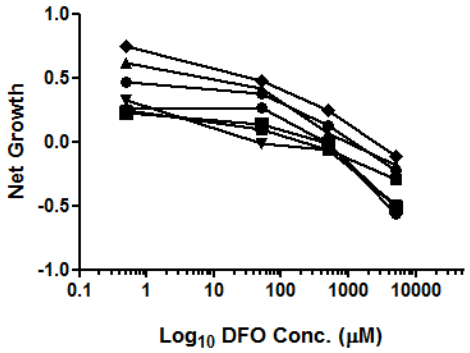

Figure 5-10 Increasing concentration of DFO results in decreased MGIT mycobacterial growth. Mycobacterial net growth was measured at increasing concentrations of the iron chelator deferoxamine (DFO) added to cultures of whole blood from healthy human volunteers. Lines represent individual animals. Net growth = (Log_{10} CFU of sample - Log_{10} CFU of control).

5.4.2.3 The effect of iron

To further investigate the effect of iron on mycobacterial growth in this assay, the concentration of ferrous iron was titrated in whole blood samples from 5 human volunteers. There was an increase in mycobacterial growth with increasing iron concentration, although the large error bars suggest a larger sample size may be required to see a clearer effect (Figure 5-11A). Addition of ferrous iron to blood from Cynomolgus macaques resulted in a significant increase in mycobacterial growth (control median net growth = 0.32, Fe net growth = 0.65; $p<0.05$) (Figure 5-11B).

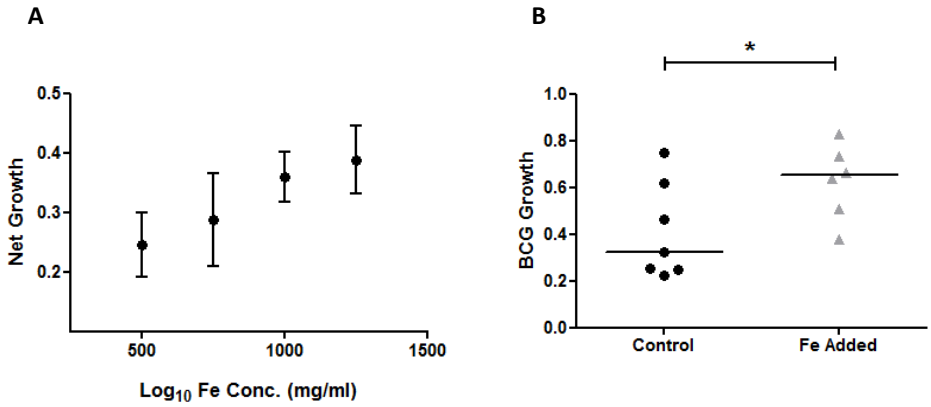

Figure 5-11 Addition of iron results in increased MGIT mycobacterial growth. A) Mycobacterial net growth was measured at increasing concentrations of ferrous iron (Fe) added to cultures of whole blood from human volunteers. Points represent the mean of 5 volunteers with the SEM. B) The whole blood MGIT assay was performed on blood from Cynomolgus macaques with and without addition of 100mg/ml of ferrous iron (Fe). Bars represent the median values; a paired t-test was performed where * represents a p value of <0.05. Net growth = (Log_{10} CFU of sample - Log_{10} CFU of control).

5.4.2.4 NHP haemoglobin study

A study was conducted to further explore the effect of repeated bleeds on haemoglobin levels in Cynomolgus macaques. Sequential bleeds were performed in an attempt to induce a decrease in haemoglobin. It was postulated that such an effect may be removed as a confounder by either 'saturating out' differences by artificially adding in haemoglobin or iron, or chelating iron using DFO. 20ml of blood was taken from each of 7 Cynomologus macaques at three time-points: once at baseline, once two weeks later and once 2 days after that on the day of necropsy (Figure 5-12). The animals were BCG naïve and did not receive any intervention.

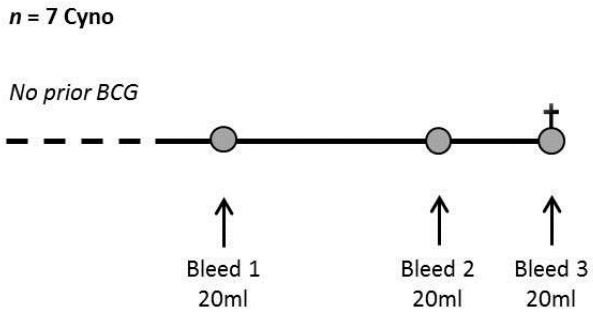

Figure 5-12 Schematic of Cynomolgus macaque haemoglobin study design. 7 Cynomolgus macaques were bled 20ml at baseline, two weeks later and 2 days after that on the day of necropsy.

Unfortunately the repeated bleeds did not have an effect on haemoglobin concentration in this study (Figure 5-13A); therefore it was not possible to determine what effect the other conditions may have had. However, adding iron and haemoglobin both increased mycobacterial growth whereas adding the iron chelator DFO reduced mycobacterial growth (Figure 5-13B). There was a significant reduction in the area under the curve (AUC) for DFO compared with the control; the AUC for each condition can be found in Table 5-1. There were no significant changes in mycobacterial growth over the course of the study, although a slight reduction at bleed 3 was mirrored across all conditions tested.

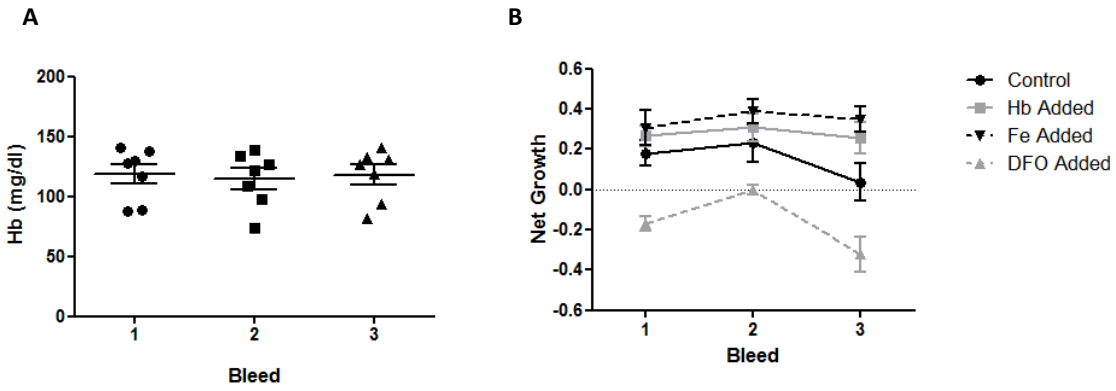

Figure 5-13 The effect of sequential bleeds and addition of Hb, Fe and DFO on MGIT mycobacterial growth in Cynomolgus macaques. Macaques received 3 sequential bleeds of 20ml. A) Haemoglobin concentration over the course of the study; bars represent the mean values with the SEM. B) Mycobacterial net growth during the course of the study with haemoglobin (Hb), iron (Fe) or the iron chelator deferoxamine (DFO) added. Points represent the mean of 7 animals with the SEM. For both sets of data, a repeated measures ANOVA was performed but no significant differences were observed between bleeds. Net growth = (Log_{10} CFU of sample - Log_{10} CFU of control).

Condition	Mean AUC	Corrected p-value (vs. control)
Control	3.28	n/a
Hb Added	4.44	0.31
Fe Added	5.39	0.20
DFO Added	1.61	**0.002

Table 5-1 Area under the curve is increased by addition of Hb and Fe and decreased by addition of DFO. The mean area under the curve (AUC) of mycobacterial net growth during the course of the study for normal blood (control) or blood with haemoglobin (Hb), iron (Fe) or the iron chelator deferoxamine (DFO) added. A paired t-test was performed on the AUC between each condition and the control, with a Bonferroni correction for multiple comparisons.

5.4.3 The effect of serum

5.4.3.1 Induction of IgG antibodies following vaccination

To determine whether BCG vaccination induced antigen-specific IgG antibodies, an ELISA was performed using the serum of 4 human volunteers from the BCG vaccination study described. Serum was taken from pre-vaccination and 4 weeks post-vaccination. Different cell fractions of *M.bovis* (whole cell, cell wall, cell membrane and cytosol) were used as the

antigen. There were no differences in optical density (OD) between pre- and post-BCG vaccination IgG against any of the cell fractions (Figure 5-14).

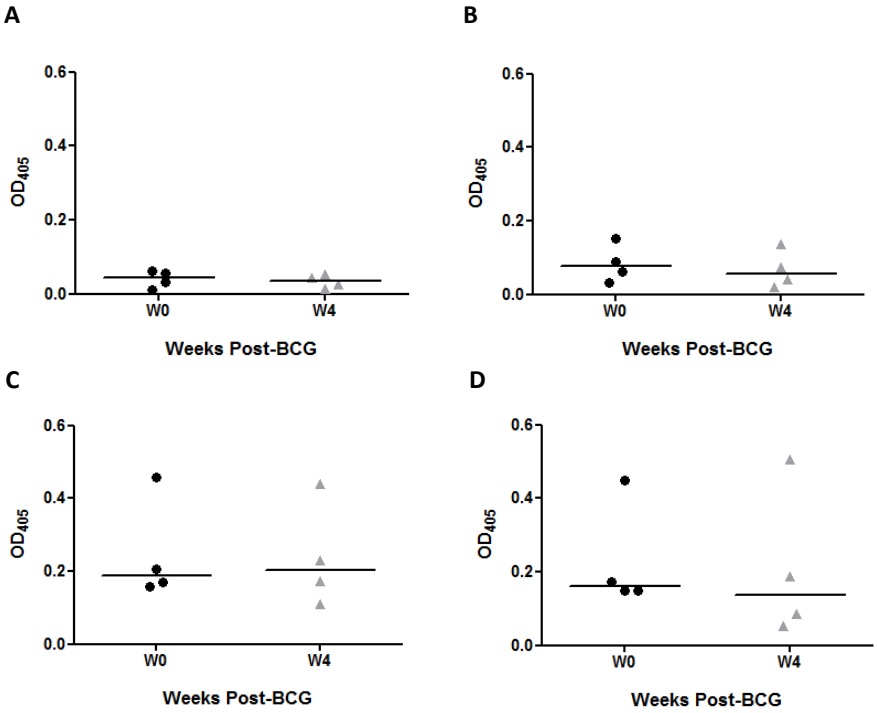

Figure 5-14 Specific IgG responses to *M.bovis* fractions by ELISA are unchanged following BCG vaccination. Pre- and 4 weeks post-BCG vaccination IgG antibody responses against A) whole cell lysate, B) cell wall, C) cell membrane and D) cytosol of *M.bovis*. OD values reported have had the background subtracted. Bars represent the median values. A Wilcoxon matched-pairs signed rank test was performed where there were no differences following vaccination.

To confirm these findings, ELISA assays were performed on all 15 volunteers receiving primary BCG vaccination in the BCG study. Serum from pre-vaccination and 4 and 8 weeks post-vaccination was studied. Again, no effect of BCG vaccination was observed on levels of BCG-specific IgG antibodies (Figure 5-15A). Serum from the NHP study described in the previous chapter (see section 4.4.3.2) was also investigated using an ELISA for BCG-specific IgG. A similar pattern was observed, with no effect of BCG vaccination. However, a modest

increase in antibody was induced by a second, larger dose (or 'challenge') of BCG (Figure 5-15B).

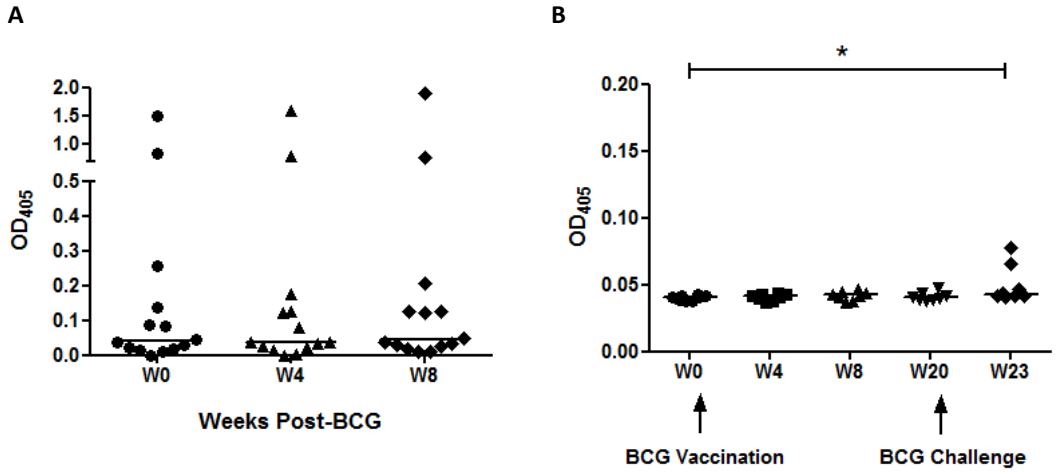

Figure 5-15 Specific IgG responses to whole BCG by ELISA are unchanged following BCG vaccination. Pre- and 4 weeks post-BCG vaccination IgG antibody responses against whole BCG for A) human volunteers and B) Cynomolgus macaques. OD values reported have had the background subtracted. Bars represent the median values. A repeated measures ANOVA was performed followed by a Dunnett's post-test (all groups vs. W0) where * represents a p-value of <0.05.

To determine whether levels of BCG-specific IgG antibodies have a significant effect on mycobacterial growth in the whole blood MGIT assay, the relationship between MGIT net growth and ELISA OD were investigated. No correlation between these variables was observed at any time-point in either the human (Figure 5-16) or macaque (Figure 5-17) BCG vaccination studies. The two volunteers in the human study who showed relatively high BCG-specific IgG levels at baseline and throughout the study did not mediate increased mycobacterial growth inhibition in the whole blood MGIT.

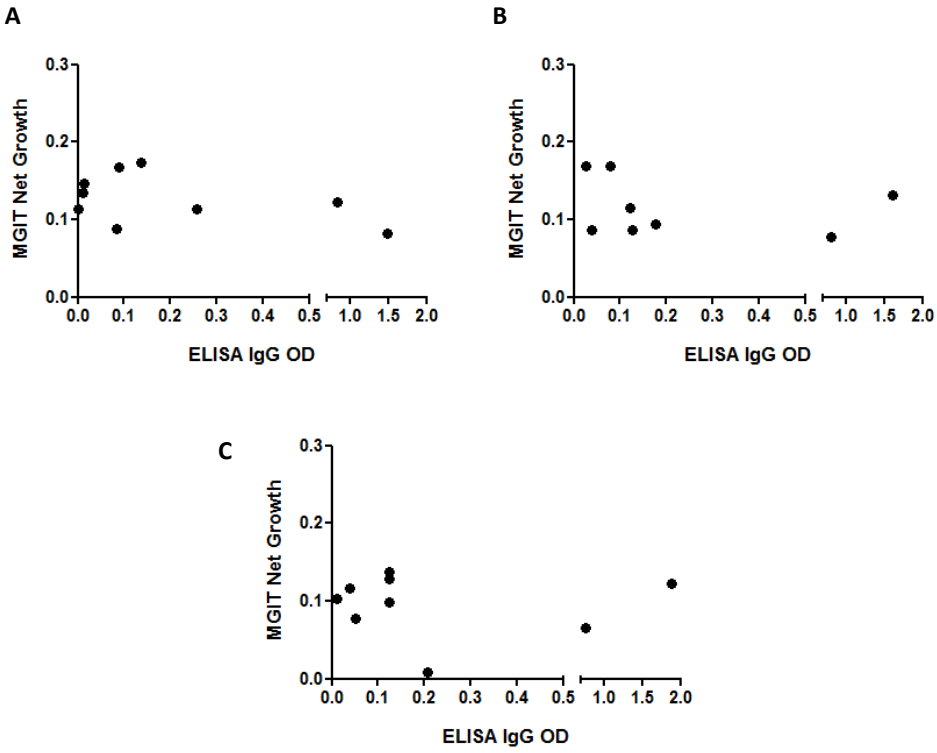

Figure 5-16 Human IgG antibody levels do not correlate with whole blood MGIT mycobacterial growth. Spearman's correlation between BCG-specific IgG antibody OD by ELISA and mycobacterial net growth in the whole blood MGIT assay at A) week 0, B) week 4 and C) week 8 following BCG vaccination in human volunteers. Net growth = (Log_{10} CFU of sample - Log_{10} CFU of control). OD values reported have had the background subtracted.

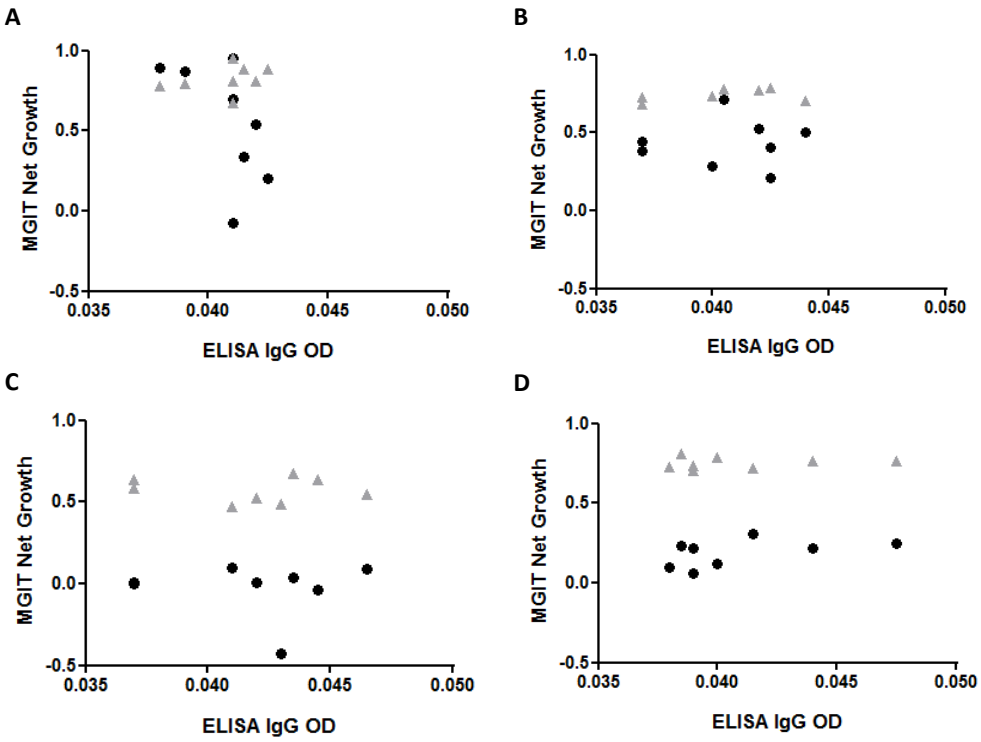

Figure 5-17 Macaque IgG antibody levels do not correlate with whole blood MGIT mycobacterial growth. Spearman's correlation between BCG-specific IgG antibody OD by ELISA and mycobacterial net growth in the whole blood MGIT assay at A) week 0, B) week 4, C) week 8 and D) week 20 following BCG vaccination in Cynomolgus macaques. Black circles indicate MGIT using BCG infection and grey triangles indicate MGIT using *M.tb* infection. Net growth = (Log_{10} CFU of sample - Log_{10} CFU of control). OD values reported have had the background subtracted.

5.4.3.2 The effect of serum on mycobacterial growth

To determine whether any BCG vaccination-induced changes in serum affected mycobacterial growth in the MGIT, the assay was performed using serum from pre- and post-vaccination in human volunteers. When mycobacteria were cultured in media containing pre-/post-BCG serum with no cells present, there was no effect on mycobacterial growth (Figure 5-18A). It was hypothesised that any changes to antigen-specific immunity, such as antibody induction, would require the presence of cells to mediate an effect. Therefore in the

subsequent experiment, pre-/post-BCG serum was added on a background of pooled BCG-naïve cells, allowing any observed differences to be attributed to the serum. There was no effect of BCG vaccination on the ability of serum factors to inhibit mycobacterial growth (Figure 5-18B). To ensure that this was not due to poor interactions with non-autologous cells, a final experiment was performed using pre-/post-BCG serum on a background of matched autologous cells taken at baseline. Consistent with previous findings, no effect of BCG vaccination was observed (Figure 5-18C).

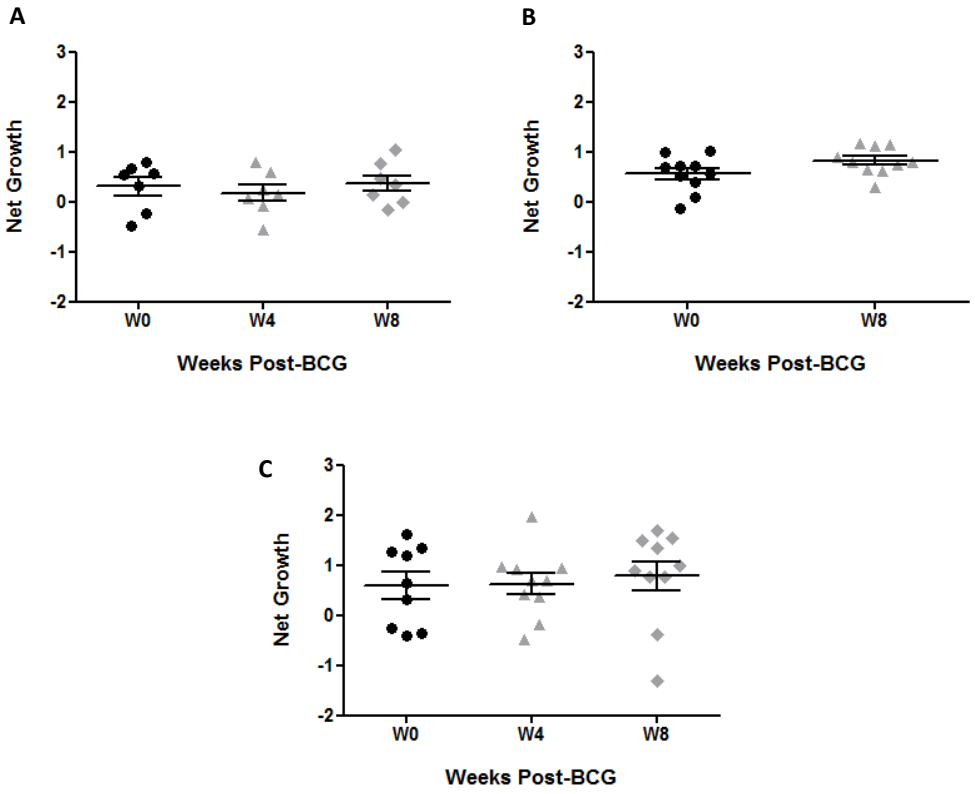

Figure 5-18 MGIT mycobacterial growth is unchanged by pre- or post-BCG vaccination serum. The PBMC MGIT assay was performed using serum from pre- and post-BCG vaccination. Mycobacteria and serum were cultured with A) no cells, B) pooled BCG-naïve PBMC or C) matched autologous BCG-naïve PBMC. Bars represent the mean with the SEM. For all sets of data, a repeated measures ANOVA (or paired t-test in the case of B) was performed but no significant differences were observed between groups. Net growth = (Log_{10} CFU of sample - Log_{10} CFU of control).

5.4.3.3 IgG antibody depletion

Total IgG antibody was depleted from human serum taken from 3 naïve and 3 BCG-vaccinated volunteers (at 8 weeks post-vaccination). Depletions, performed using Protein G, had an efficiency of 83-92% (Figure 5-19A). There was no difference between control and IgG-depleted samples, although higher mycobacterial growth was observed in the naïve compared with BCG vaccinated volunteers under both conditions (Figure 19B). There was no correlation between IgG levels and mycobacterial net growth (data not shown).

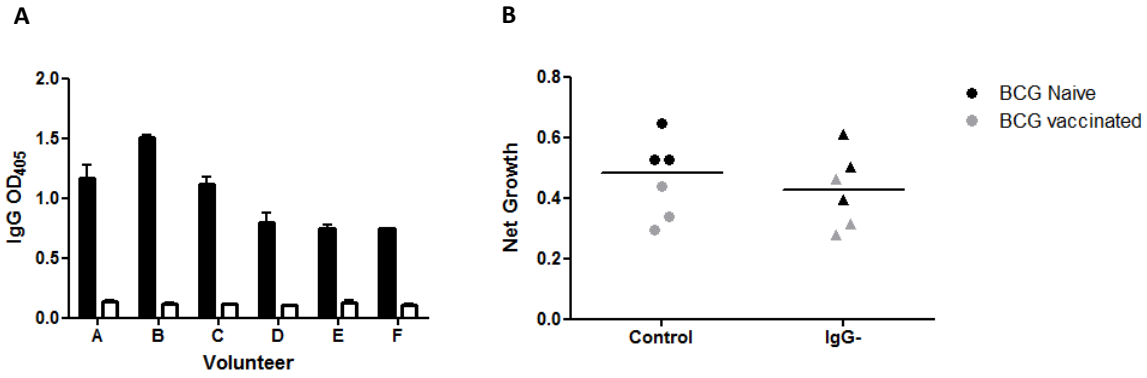

Figure 5-19 IgG antibody depletion was efficient but did not affect MGIT mycobacterial growth. A) Efficiency of IgG depletion measured by ELISA; black bars represent the undepleted sample and white bars the depleted. B) The PBMC MGIT assay performed using serum from BCG naïve and vaccinated human volunteers that was either undepleted or depleted of total IgG. Bars represent the median values. A Wilcoxon matched-pairs test was performed but no difference was observed between groups. Net growth = (Log_{10} CFU of sample - Log_{10} CFU of control).

5.4.3.4 A role for innate serum factors

It was observed previously (see section 3.3.4.2) that mycobacterial growth was significantly lower when using heat-inactivated serum compared with normal serum in the MGIT culture. This finding was confirmed in a second experiment of 6 healthy volunteers (serum median net growth = 0.76, HI serum median net growth = 0.33; $p<0.05$) (Figure 5-20).

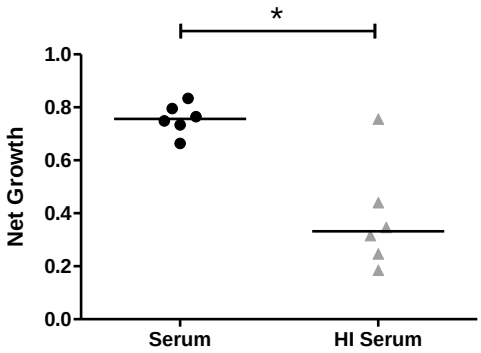

Figure 5-20 Heat inactivation of serum results in reduced MGIT mycobacterial growth. The PBMC MGIT assay performed using either normal of heat inactivated serum. Bars represent the median values. A Wilcoxon matched-pairs test was performed where * represents a p value of <0.05. Net growth = (Log_{10} CFU of sample - Log_{10} CFU of control).

To further investigate this effect, an experiment was performed comparing normal and heat inactivated serum in the absence and presence of PBMC. There was no difference between serum from BCG naïve and vaccinated volunteers, so all serum was grouped together. Interestingly, in the absence of PBMC, there was no difference in mycobacterial growth when serum was heat inactivated or not. However, when PBMC were present the previous finding of lower mycobacterial growth with heat inactivated serum was confirmed. Furthermore, there was a significant increase in mycobacterial growth between normal serum

in the absence and presence of PBMC. However, when serum was heat inactivated, the presence of PBMC did not make a difference (Figure 5-21).

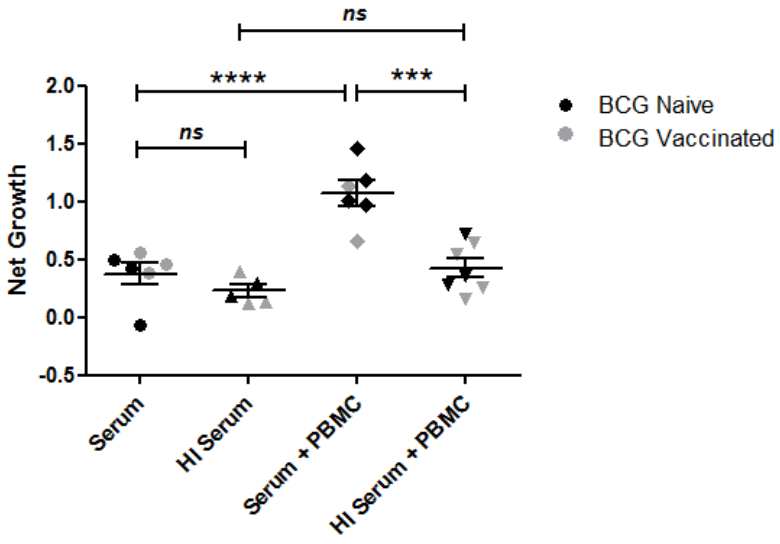

Figure 5-21 Heat inactivation of serum results in reduced MGIT mycobacterial growth in the presence, but not absence, of PBMC. The MGIT assay was performed using normal or heat inactivated serum in the presence or absence of PBMC. Bars represent the mean values with the SEM. Having passed a normality test, a one-way ANOVA was performed followed by Bonferroni post-test (comparing selected groups to exclude the invalid HI serum vs. serum + PBMC and serum vs. HI serum + PBMC comparisons) where *** represents a p-value of <0.0005 and **** represents a p-value of <0.0001. Net growth = (Log_{10} CFU of sample - Log_{10} CFU of control).

It is well-documented that complement plays a role in the uptake of mycobacteria into monocytes, the target cell for mycobacterial survival and replication[274,310]. It was therefore postulated that by destroying complement through heat-inactivation of serum, mycobacterial infection of monocytes was reduced, thus decreasing overall net growth. Such an effect would not be expected in the absence of PBMC as no monocytes would be present for

infection. This would also explain why increased mycobacterial growth is observed between the absence and presence of PBMC using normal serum, but not heat inactivated serum.

To test this hypothesis, PBMC MGIT assays were performed using serum from 6 healthy volunteers. In parallel, cultures of monocyte cell lines were set up containing the same serum, either normal or heat inactivated. Monocyte cultures were infected with BCG-GFP for 1 hour at an MOI of 1:1. The percentage of infected monocytes was determined by flow cytometry (Figure 5-22).

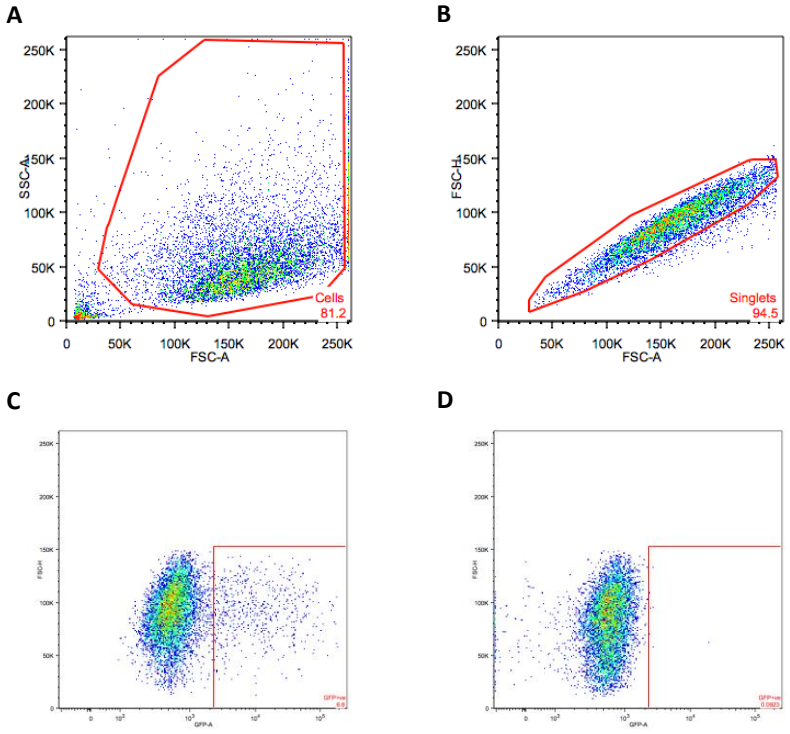

Figure 5-22 BCG-GFP gating strategy. A) Live cells were gated on FSC-A vs. SSC-A then B) singlets on FSC-A vs. FSC-H. C) Gating GFP-positive cells with D) an uninfected sample.

The percentage of infected monocytes was significantly higher using normal compared with heat inactivated serum (median = 5.7% and 1.3% respectively) ($p<0.05$) (Figure 5-23A).

Mycobacterial net growth in the MGIT correlated positively with the percentage of infected monocytes (Figure 5-23B).

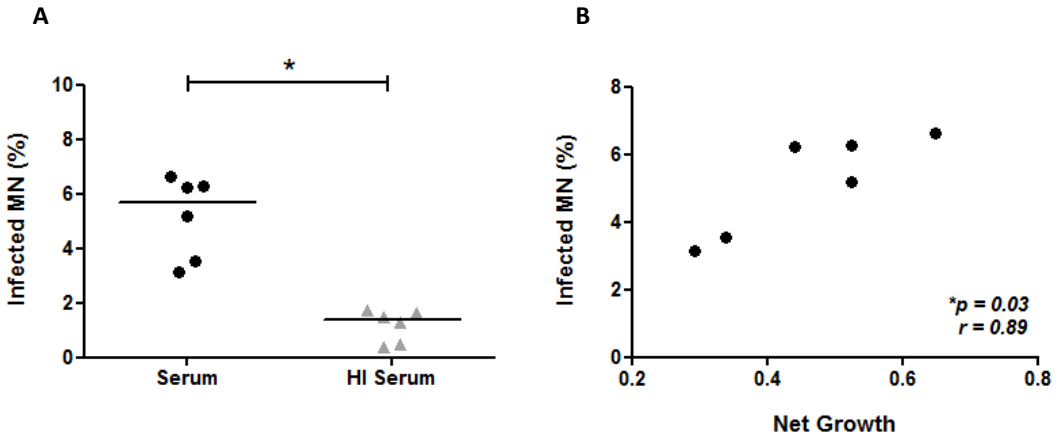

Figure 5-23 Heat inactivation of serum reduces uptake of BCG by monocytes. A) Percentage of infected monocytes after a 1hr culture with BCG-GFP in medium containing normal or HI serum. Bars represent the median values. A Wilcoxon matched-pairs test was performed where * represents a p value of <0.05. B) Spearman's correlation between MGIT mycobacterial growth and percentage of infected monocytes in the BCG-GFP culture. Net growth = (Log_{10} CFU of sample - Log_{10} CFU of control).

A second experiment was performed using the BCG-GFP monocyte infection assay to confirm the association between MGIT mycobacterial growth and proportion of infected monocytes. Again a significant positive correlation was observed ($p<0.05$) (Figure 5-24).

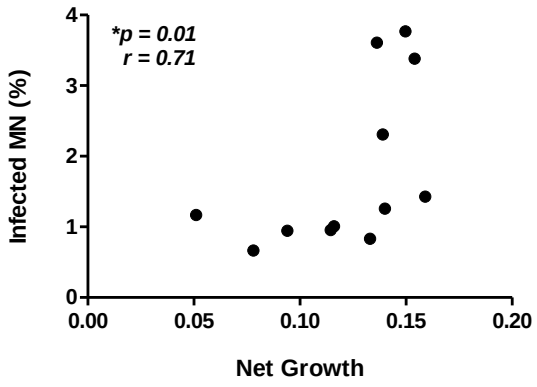

Figure 5-24 MGIT mycobacterial growth correlates with BCG uptake by monocytes. Spearman's correlation between mycobacterial net growth in the MGIT assay and percentage of infected monocytes in the 1 hour BCG-GFP culture. Net growth = (Log_{10} CFU of sample - Log_{10} CFU of control).

5.4.3.5 Pre-opsonisation of mycobacteria

Based on these findings, it was hypothesised that the observed increase in monocyte uptake may be due to one or more opsonising proteins. To investigate this, mycobacteria were incubated for 1 hour with medium containing either normal or heat inactivated serum. Mycobacteria were washed prior to the MGIT culture which contained heat inactivated serum only. Overall mycobacterial growth was significantly higher following pre-opsonisation with normal compared with heat inactivated serum (median net growth = 0.39 and 0.16 respectively; $p<0.05$) (Figure 5-25).

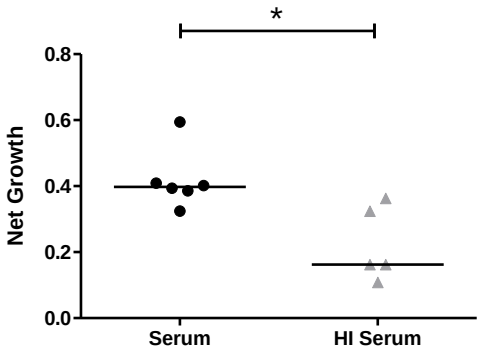

Figure 5-25 Pre-opsonisation of mycobacteria with normal vs. HI serum results in increased MGIT mycobacterial growth. Mycobacteria were pre-opsonised with either normal or heat inactivated serum prior to the MGIT culture. Bars represent the median values. A Wilcoxon matched-pairs test was performed where * represents a p value of <0.05. Net growth = (Log_{10} CFU of sample - Log_{10} CFU of control).

5.4.4 The effect of neutrophils

5.4.4.1 Neutrophil frequency vs. whole blood MGIT

The association between neutrophil count and mycobacterial growth was investigated using data from the human BCG study. No correlations were observed at any time-point (Figure 5-26). Interestingly, volunteers appeared to diverge into two groups of low neutrophil count (<3x10^9/L) and high neutrophil count (>4x10^9/L), though all were within the normal range. The group with high neutrophil counts did not appear to mediate greater mycobacterial growth inhibition or vice versa.

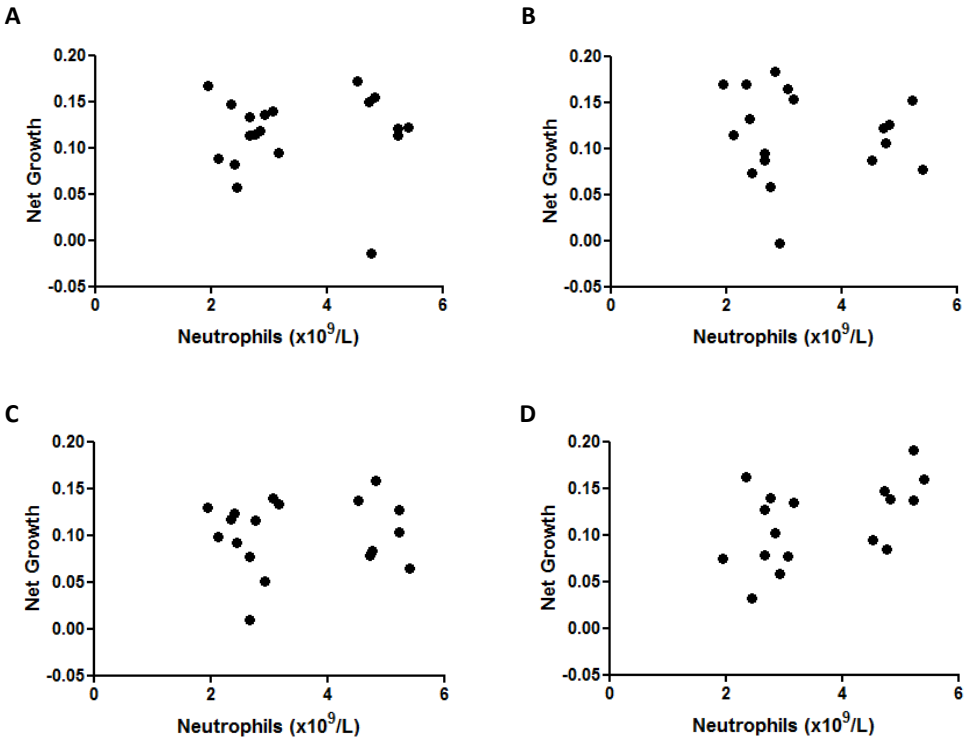

Figure 5-26 Neutrophil count does not correlate with MGIT mycobacterial growth. Spearman's correlation between neutrophil count and mycobacterial net growth in the whole blood MGIT assay at A) week 0, B) week 4, C) week 8 and D) week 24 following primary BCG vaccination or revaccination in human volunteers. Net growth = (Log_{10} CFU of sample - Log_{10} CFU of control).

5.4.4.2 Neutrophil depletions

Using whole blood from 5 healthy PPD-positive volunteers, neutrophils were depleted using magnetic beads. The positive fraction was retained and added back in to an additional set of depleted samples. Depletions were confirmed using flow cytometry gating on the granulocyte marker CD66b (Figure 5-27). All depletions were successful, with an efficiency of 91-94% (Table 5-2). Depletion of neutrophils resulted in a non-significant increase in mycobacterial growth compared with the control (median net growth = 0.73 and 0.67 respectively), and adding neutrophils back resulted in a reduction in mycobacterial growth compared with the depleted samples that was approaching statistical significance (median net growth = 0.65 and 0.73 respectively; p = 0.05) (Figure 5-28).

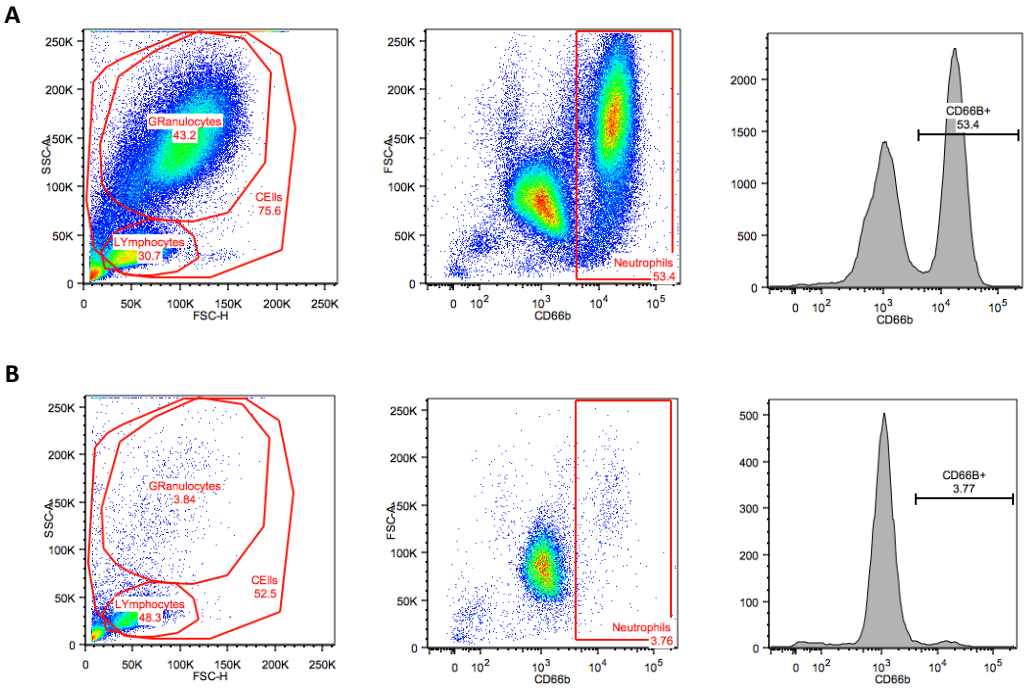

Figure 5-27 Neutrophil depletion gating strategy. Lymphocytes and granulocytes were gated on forward scatter (FSC) vs. side scatter (SSC). Neutrophils were gated as CD66b-positive cells against FSC and a histogram was drawn to evaluate the change in neutrophil frequency following depletion. The figure shows the first volunteer with the A) undepleted and B) depleted fraction.

Volunteer	Neutrophil freq. (undepleted)	Neutrophil freq. (depleted)	Efficiency of depletion (%)
1	53.4	3.70	93
2	59.1	4.88	92
3	58.0	3.14	95
4	68.4	5.89	91
5	63.1	3.88	94

Table 5-2 Efficiency of neutrophil depletions. Frequency of neutrophils are expressed as the number of CD66b expressing cells as a proportion of all live cells.

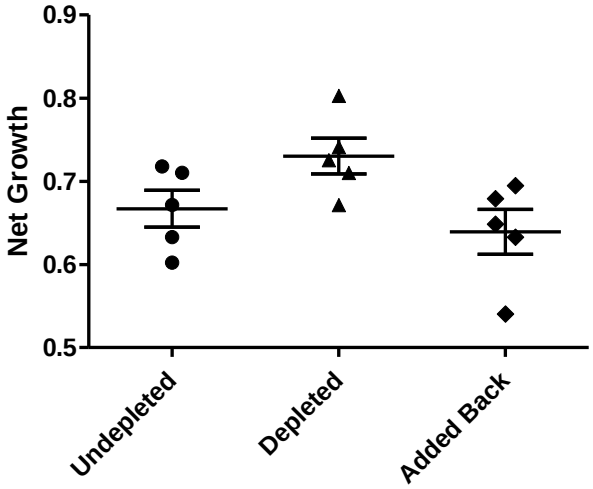

Figure 5-28 Depletion of neutrophils results in a non-significant increase in MGIT mycobacterial growth. The whole blood MGIT assay was performed on undepleted blood, and blood that had been depleted of neutrophils using magnetic beads. In the third group, neutrophils were added back to depleted blood. Bars represent the mean values with SEM. Having passed a normality test, a one-way ANOVA was performed followed by a Bonferroni post-test where no differences were statistically significant. Net growth = (Log_{10} CFU of sample - Log_{10} CFU of control).

5.5 Discussion

The relationship between the whole blood and PBMC MGIT data was explored in two separate studies, and no association was observed. As described, whole blood contains several components in addition to PBMC which may influence mycobacterial growth. These include red blood cells, neutrophils, and serum factors such as antibodies and complement. To begin to understand which blood components may be responsible for the discrepancy in outcome of the two assays, selected factors were investigated. Based on observations of a reduction in haemoglobin over time in the NHP studies, haemoglobin was explored as a potential confounder. The fall in haemoglobin levels in the Rhesus macaques is likely due to 5 repeated bleeds (1 screening and 4 study bleeds) of 20ml over a 10 week period. Adult Rhesus macaques have a blood volume of 280-770ml (NC3Rs blood sample volumes guidelines), meaning that a single bleed represents up to 7% of the total circulating blood. It is important to note that these volumes and bleed schedules are within the NC3Rs guidelines and that the drop in haemoglobin did not represent clinical anaemia (in that the animals were asymptomatic), but was nonetheless a biologically significant reduction. This effect was not observed in the study of Cynomolgus macaques, which may be due to a less intense sample schedule with no screening or week 2 bleed. The Cynomolgus macaques also had a lower mean age and higher mean weight compared with the Rhesus animals, which may have made them more resistant to the effects of repeated bleeds.

When the association between haemoglobin level and mycobacterial growth in the whole blood MGIT was explored, the association was not significant. However, in the human BCG study, additional haematological parameters were available from the clinical data. Although clinical data was collected at baseline only, it is considered that human haemoglobin levels would remain stable over a 24 week period, and be unaffected by repeated bleeds of small volume relative to size. Interestingly, mycobacterial growth at weeks 4 and 8 correlated

significantly with mean corpuscular haemoglobin (MCHGB). MCHGB may represent a more sensitive measure, as it also takes into account the number of red blood cells and is able to detect iron-deficiency anaemia where haemoglobin alone is not[311,312]. The fact that haemoglobin and MCHGB have an almost significant correlation (p=0.07) in this study suggests that mycobacterial growth may also be associated with this measure given a larger sample size. Unsurprisingly, the relationship was lost in the PBMC MGIT, where red blood cells and haemoglobin are absent.

To further investigate the effect of haemoglobin on mycobacterial growth, haemoglobin was artificially added to MGIT tubes or cultures of human/macaque PBMC and mouse splenocytes. In all cases, increased haemoglobin concentration resulted in increased mycobacterial growth. Haemoglobin contains carbon and carries bound oxygen and iron; all of which are used in the metabolism and growth of mycobacteria and may account for this relationship. In the cultures, the effect plateaued at a concentration of approximately 1mg/ml. This may be a biological effect, as mycobacteria are saturated with iron for example, and any further increase is ineffectual. However, it may also be a technical effect of the MGIT system, as high concentrations of haemoglobin result in deep red pigmentation which may interfere with measurements of fluorescence. It would be useful to repeat this experiment with traditional CFU plating rather than Bactec MGIT quantification to delineate these effects.

To determine whether iron is responsible for the effect of haemoglobin, the iron chelator deferoxamine (DFO) was added alongside increasing concentrations of haemoglobin. There was a reduction in mycobacterial growth in the cultures containing DFO, suggesting that iron is indeed playing a role. The fact that DFO did not entirely negate the effect of increasing haemoglobin suggests that other constituents of haemoglobin may also mediate an effect, or that the concentration of DFO was not high enough to chelate all of the iron. Unfortunately, cell viability studies indicated that a higher concentration of DFO would be detrimental to

cell viability so could not be used. Addition of ferrous iron to MGIT cultures resulted in increased mycobacterial growth, confirming the influence of iron. This is consistent with literature on iron and mycobacteria, which demonstrates the importance of iron for the growth and pathogenesis of *M.tb*. Early work by Kochan *et al*. showed that *M.tb* bacilli can only grow in serum with a sufficient concentration of iron[313]. Addition of iron increases both intra- and extra-cellular mycobacterial growth *in vitro*[314,315]; effects that are prevented by exposure to iron chelating agents[315]. *In vivo*, increased iron results in decreased resistance to TB disease and worse clinical outcome[316-318]. Furthermore, it has been suggested that iron overload contributes to TB susceptibility in Africa[319], and that correction of iron overload in mice eliminates this effect[147].

The majority of dietary iron in the host (about 95%) is stored in the form of heme: primarily as haemoglobin[320]. Many bacteria, both Gram-negative and Gram-positive, are known to use heme as a major source of iron[321-323]. Tullius *et al*. proposed that mycobacteria could similarly sequester iron from heme or haemoglobin at both intracellular and extracellular sites of infection; intracellular mycobacteria encountering heme diffused from the macrophage phagolysosome that degrades red blood cells. In 2011, it was demonstrated that *M.tb* can indeed utilise heme from haemoglobin[324], and the pathway by which it does so has since been characterised. To date, four members of the host-derived heme uptake pathway have been described, including Rv0203 and MhuD, the mycobacterium heme degrader which catalyses the final step of heme acquisition and degradation to iron and organic by-products[325-328]. It is therefore biologically plausible that mycobacteria may be sequestering iron from haemoglobin in the whole blood MGIT assay and utilising it for growth.

In an attempt to address the issue of haemoglobin as a potential confounder in the whole blood MGIT assay, a macaque study was designed involving 3 sequential bleeds of 20ml. This is the maximum permissible in a study with no intervention due to ethical regulations. It was hoped that with just 2 days between the second and third bleeds (day of necropsy), a drop

in haemoglobin would be induced. At each bleed, MGIT assays were performed with an excess of iron or haemoglobin, or addition of DFO. By saturating out, or eliminating, any differences in iron concentration between bleeds, any confounding effect of haemoglobin on mycobacterial growth would be removed. Unfortunately the bleeds did not induce a drop in haemoglobin and therefore it was not possible to assess the impact of these interventions. This may be because only 3 bleeds were allowed, whereas in the studies with an observed effect, 5 or more bleeds were taken in total. Furthermore, whilst the initial studies used Rhesus macaques; only Cynomolgus macaques were available for this repeat experiment and in the previous study of BCG vaccination in this species, haemoglobin was stable. The disparity may be due to species differences or other variables that were not controlled for such as size and age of the animals. The study did, however, provide confirmation of the previous findings that addition of haemoglobin or iron increase mycobacterial growth, and addition of iron chelator reduces mycobacterial growth.

The fact that haemoglobin and iron can influence bacterial growth is an important consideration when selecting an appropriate compartment for immunological assays. The reduction in haemoglobin following sequential bleeds in NHPs is a potential confounder in time-course experiments and would apply to all such experiments in small animals. Although humans are more resistant to such perturbations due to their relative size, it would be prudent to take into account variation in iron status when comparing different populations, for example. In most countries of sub-Saharan Africa, anaemia (due to malnutrition, malaria and helminth infections) is considered a widespread and serious public health problem[329]. A trial of whole blood mycobacterial growth inhibition mediated by a vaccine may as such vary depending on the study population. This is another aspect in favour of the PBMC MGIT assay, where red blood cells and haemoglobin are absent from the culture. The confounding effect of haemoglobin may ‘mask’ other effects and may indeed play a role in the reduced

ability of the whole blood MGIT to detect a vaccine response compared with the PBMC assay in the human BCG study.

Another major difference between the whole blood and PBMC MGIT assays is the presence of autologous serum in blood. Although pooled human AB serum (PHS) is added to the PBMC assay medium, this is standardised between each culture, meaning that any effect of vaccination on serum components would not be represented. One such component is antibodies. As described in the introduction, the role of antibodies in TB disease is widely debated, and evidence for an antibody response induced by BCG vaccination is conflicting. In the human and macaque studies described, there was no induction of BCG-specific IgG following primary vaccination. This is consistent with several reports in the literature. Krambovitis *et al*. saw no change in IgG antibody levels at 2 months or 2 years post-BCG vaccination[330], and in a separate study, previous BCG vaccination had no effect on the levels of IgG, IgM or IgA to *M.tb*[331]. Calves vaccinated with 1 or 2 doses of *M.bovis* BCG administered 6 weeks apart also failed to mount a detectable antibody response[332]. However, there are also many reports of antibody induction, though this is generally modest or only detectable after a significant period of time or vaccine boost[333-338]. In the human study, antibodies were measured at 4 and 8 weeks post-BCG. This may not be sufficient time to mount a response; indeed a trial of BCG vaccination in infants showed an agglutinin response only after a considerable period of time[335]. Similarly, in a study of 66 infants in Turkey, levels of IgG were significantly greater than baseline only at 15 months post-BCG[336]. However, in the macaque study, antibodies measured at 20 weeks still showed no increase; rather it took a second high-dose vaccination or 'challenge' with BCG to induce a modest induction. Although little work has been done on the immunology of BCG revaccination, one study found that serum from volunteers who had received 2 BCG vaccinations 6 months apart contained a significantly increased level of LAM-specific IgG[334]. It would be interesting to

perform ELISAs on serum from the BCG revaccinated group in the human study to see if a similar effect is observed.

There was no association between IgG response and mycobacterial growth in either the human or macaque BCG studies. This is unsurprising as mycobacterial growth was inhibited following BCG vaccination, whereas the IgG response did not change. Interestingly, two of the human volunteers showed relatively high levels of BCG-specific IgG at baseline which remained stable throughout the study. All volunteers were screened for latent *M.tb* infection by ELISpot and any history of TB disease was an exclusion criterion at screening. However, it is possible that these volunteers had previous exposure to non-tuberculous environmental mycobacteria (NTM) which had induced an antibody response. A study of Crohn's disease in Birmingham measured serum antibody responses to a range of NTMs including *M.avium*, *M.Kansasii* and *M.vaccae*. They found that 7% of the healthy control population had antibody titres to one or more of the mycobacteria species tested[339]. Given the taxonomic and structural similarities between species, one would expect cross-reactivity between other NTMs and BCG. Cho *et al*. stressed the reactive nature of mycobacterial antigens and the effect of environmental priming[340]. Differential exposure to environmental mycobacteria in the human population likely explains, at least in part, the greater range in human IgG levels at baseline compared with germ-free macaques. Mycobacterial growth inhibition mediated by the two high-reacting human volunteers was not superior compared with the other volunteers.

The overall lack of correlation between IgG level and mycobacterial growth may be due to a number of factors. The confounding effect of haemoglobin in the whole blood assay may mask such associations, which cannot be measured in the PBMC assay due to the lack of autologous serum. Alternatively, antibody level may not be the most relevant measure. Evidence in the literature indicates a disparity between antibody titre and avidity. Perley *et al*. found that while patients with active TB disease had slightly elevated antibody titres compared to uninfected controls, there was a decrease in avidity[341]. It would be interesting to

explore the effect of BCG vaccination on antibody avidity, which may be a more functional measure. Finally, IgG may not be the most appropriate class of antibody; *M.tb*-specific IgA and IgM have also been reported in the literature. However, subsequent experiments did not point toward a functional difference in combined antibody pre- and post-vaccination. There was no difference in mycobacterial growth when pre- and post-BCG serum was used (regardless of the presence of cells), or when total IgG was depleted. This is in contrast to the work of de Vallière *et al*., who showed that mycobacterial growth inhibition was enhanced by BCG-induced antibodies, and that these effects were reversed be preabsorption of IgG with Protein G[334]. Overall, my findings suggest that the vaccine effect observed in the MGIT assay is mediated by alternative components of the immune system in the populations studied. Despite some evidence supporting a role for antibodies against *M.tb*[154], the predominant paradigm in TB has long been that T cells, and not antibodies, are required for host resistance[106]. These findings arguably justify supplementation with PHS rather than autologous serum in the PBMC MGIT, and further support the use of the PBMC assay as an adequate representation of the relevant functional response.

It was noted in the previous chapter that levels of week 4 Antigen 85A-specific IgG in the MVA85A efficacy trial were associated with reduced risk of TB disease (Fletcher *et al*. manuscript submitted). This suggests that antibodies may in fact play a role in protection against TB; at least in this population. MVA85A significantly boosted Ag85A specific IgG, and levels were higher in the MVA85A when compared to the placebo group. However, levels of these antibodies were also rising in the placebo group who received BCG alone. This work suggests that BCG vaccination induces more specific IgG responses, which may have been missed in the studies described where a general response to whole BCG antigen was measured. This may also be due to the later time-point at which antibodies were measured in the efficacy trial, which was 4 weeks post-MVA85A and therefore several months post-BCG. Furthermore, antibodies may be more relevant in infants or SA

populations, which warrants further investigation. Either way, it raises the possibility that TB vaccine candidates other than BCG may induce or boost a detectable antibody response with protective value, in which case the use of time-point matched autologous serum in the MGIT assay would be recommended; or indeed a more suitable antibody-based assay.

A role for innate factors in serum was suggested by previous work showing that heat inactivating serum reduced mycobacterial growth. These findings were confirmed in a second experiment, as well as a larger study comparing normal and heat inactivated serum in the presence and absence of PBMC. It was found that the effect of serum heat inactivation was only mediated in the presence of cells, and that addition of cells increased mycobacterial growth in the presence of normal but not heat inactivated serum. It was hypothesised that this effect was driven by one or more components of serum, destroyed by heat inactivation, which aided uptake into monocytes (the target cell for mycobacterial survival and replication). Using BCG-GFP to visualise monocyte infection rates, this hypothesis was confirmed, and a correlation was observed between monocyte uptake and mycobacterial growth. The BCG-GFP monocyte culture requires further optimisation as the low rates of infection indicate that the MOI and culture period could be increased. Pre-opsonisation of mycobacteria in normal vs. heat inactivated serum for 1 hour indicated that a modest effect could be mediated despite only heat inactivated serum being present for the 96 hour culture.

These findings are consistent with *in vitro* studies of complement from the 1990s. Schlesinger *et al*. demonstrated that complement component C3 fragments (C3b and C3bi) are fixed to *M.tb* by the alternative complement pathway, and act as the major ligand mediating macrophage adherence and ingestion via surface receptors CR1, CR3 and CR4[274]. It was later shown that opsonisation of *M.tb* with complement not only permits interaction with macrophage CRs but also affects phagosome-lysosome fusion, allowing survival of the bacterium inside the macrophage[342]. It is well-known that heat inactivation destroys complement, providing a plausible explanation for the observed effects. It is an important

next step to extend these experiments to add complement proteins (such as C3) back in to heat inactivated serum to see if monocyte uptake and mycobacterial growth is restored. Alternatively, specific components of complement could be depleted from normal serum using antibodies. In recent years, genome-wide association studies (GWASs) have identified polymorphisms in complement genes as determinants of host susceptibility to infectious disease[343]. Importantly, an association has been proposed between complement CR1 polymorphisms and tuberculosis susceptibility in African individuals[344]. Furthermore, variants of mannose binding lectin (MBL) that would ordinarily activate the complement system have been shown to have a protective effect against TB in studies conducted in South Africa[345], India[346] and Denmark[347]. Although innate factors such as complement are unlikely to vary between vaccine conditions, these findings are relevant for decisions in development of the PBMC MGIT assay. Different groups may use normal or heat inactivated serum as standard, and a consistent choice must be clearly specified in the protocol. Furthermore, it may be beneficial to use a single batch of PHS across experiments requiring direct comparison.

Finally, the role of neutrophils was investigated. As discussed previously, such innate components are considered less relevant when considering a vaccine effect. Rather, the induction of longer-term memory responses is desirable. However, neutrophils may be important in explaining some of the differences between the whole blood and PBMC MGIT results. The outcome of the 96 hour whole blood culture will be a complex combination of innate and cellular responses, and neutrophils are one of the first lines of defence against *M.tb*[348]. Interestingly, there was no correlation between neutrophils and mycobacterial growth in the human BCG study. Depletion of neutrophils did mediate a non-significant increase in mycobacterial growth; an effect that was reversed by returning the positive fraction. It is possible that the modest effect was due to the small numbers used, as the technical challenges

associated with this experiment only permitted a sample size of 5. It would be beneficial to repeat the experiment using more volunteers.

The role of neutrophils in TB disease is controversial, with disparity between *in vitro* studies regarding the killing of internalised mycobacteria. Several reports suggest an inability of neutrophils to inhibit mycobacterial growth[65-67,349,350], while as many indicate either restriction or killing[62-64,351,352]. Lowe *et al*. suggest that both killing and failure to kill are potential outcomes *in vivo* just as *in vitro*, dependent on many host- and organism-specific factors[260]. Neutrophils may even be detrimental, directly contributing to disease pathogenesis[57]. In a microarray study, Berry *et al*. described the human whole blood transcriptional signature of TB. This was dominated by a neutrophil-driven IFN-inducible transcript which was associated with active TB disease[353]. Furthermore, Eruslanov *et al*. showed that mice with genetic susceptibility to TB exhibited high and prolonged neutrophil accumulation in the lungs following infection, which at this early stage was deleterious rather than protective[66]. Conversely, it has been reported that risk of TB infection was inversely associated with peripheral blood neutrophil count in UK TB-contacts[56].

It would be interesting to use the whole blood MGIT as a tool for further investigation into the role of neutrophils in the context of TB patients. However, for the purposes of this project it can be concluded that neutrophils may contribute to the differences in mycobacterial growth between the whole blood and PBMC assays; though their effect appears modest compared with, for example, that of haemoglobin or complement. It is important to note that the mycobacterial inoculum required for the PBMC MGIT is 100 to 1000 fold lower than that used in the whole blood assay, as a higher inoculum overwhelms the vaccine response (discussed in previous chapters). It was hypothesised that this superior ability of whole blood to inhibit mycobacterial growth was driven by neutrophils, and it is therefore surprising to see such a negligible effect of depletion. This may be a technical effect as neutrophils are notoriously difficult to work with; or a biological effect if other factors in whole blood are

able to compensate in the absence of neutrophils in a way that PBMC are not. It is clear from the literature that the role of neutrophils in TB may be too complex to model in this single experiment and further work is required.

5.6 Conclusions

- There was no correlation between mycobacterial growth inhibition mediated by whole blood and PBMC MGIT.
- There was an association between haemoglobin and mycobacterial growth, which may contribute to these differences. This was, at least in part, due to the sequestration and utilisation of iron by mycobacteria.
- IgG antibodies were not induced by BCG vaccination, and did not appear to play a role in determining mycobacterial growth.
- Heat inactivation of serum reduced mycobacterial growth, associated with a reduction of uptake into monocytes. This may be due to the destruction of opsonising complement components.
- There was no association between neutrophil frequency and mycobacterial growth, and depletion of neutrophils had a modest effect.
- The PBMC MGIT assay may be preferable for the assessment of vaccine efficacy, as haemoglobin is removed as a potential confounder, autologous serum may not be important, and induction of a durable response is more relevant than innate factors such as neutrophils.

6 PBMC-mediated immune mechanisms

6.1 Statement of authorship

Assistance with Luminex was provided by Steve Smith at the London School of Hygiene and Tropical Medicine. Samples and help for the final ML ratio experiment were provided by Vivek Naranbhai, who also conducted the cell sorting for the experiment. In the MVA85A correlates study, flow cytometry was conducted by Iman Satti. Gene expression microarrays and associated analysis in 'R' were performed by Magali Matsumiya and Julius Muller.

6.2 Introduction

An understanding of the immune mechanisms underlying mycobacterial growth inhibition *in vitro* may aid in defining a correlate of protection from TB. This would be greatly beneficial not only in refining a relevant assay for testing vaccine efficacy, but also in designing a more effective vaccine itself. As described in the preceding chapters, the PBMC-based MGIT assay demonstrates superior ability to detect a vaccine-induced response in humans compared with whole blood. Immune mechanisms at play in PBMC are likely to be similarly relevant in whole blood, as there are no additional components, but relevant responses may be masked in blood by confounders such as haemoglobin. In this chapter I have explored the contribution of a range of immune mechanisms that are present in, but not exclusive to, the PBMC compartment.

6.3 Aims

The aim of the experiments detailed in this chapter was to investigate the immune mechanisms underlying mycobacterial growth inhibition including the role of monocytes, CD4+ and CD8+ T cells, cytokines and gene expression.

6.4 Results

6.4.1 Monocytes and ML ratio

6.4.1.1 Monocyte frequency and ML ratio vs. mycobacterial growth

It was noted in the early stages of this project that mycobacterial growth appeared to be affected by monocyte levels. Indeed, more growth was observed after a pre-culture cell rest of 2 hours compared with overnight, associated with a loss of monocytes in the overnight rest. Using clinical data from the human BCG study (described in section 3.3.1), monocyte count correlated significantly with mycobacterial growth in the whole blood MGIT at baseline ($p<0.05$) (Figure 6-1A). Furthermore, a correlation was observed between the ratio of monocytes to lymphocytes (ML ratio) and mycobacterial growth ($p<0.05$) (Figure 6-1B). These associations were not present using PBMC MGIT data from this study (data not shown). However, comparing the same parameters in the MVA85A correlates of risk study (described in section 4.4.2.3), there was a significant correlation between PBMC MGIT mycobacterial growth and both classical monocyte frequency (CD14+C16- cells) and ML ratio measured by flow cytometry ($p<0.0005$ and $p<0.005$ respectively) (Figure 6-1C-D). There was no association with frequency of inflammatory monocytes (CD14+CD16+ cells).

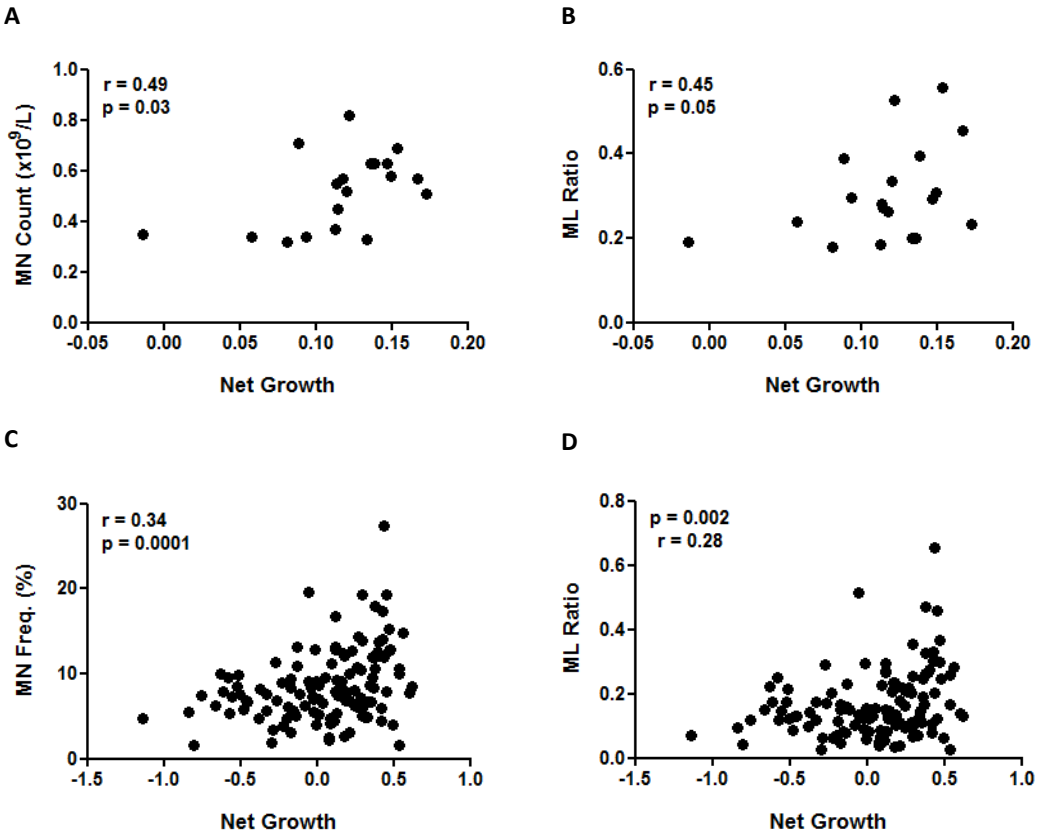

Figure 6-1 Monocyte frequency and ML ratio correlate positively with MGIT mycobacterial growth. Spearman's correlation between mycobacterial net growth in the whole blood MGIT assay and A) monocyte count and B) monocyte to lymphocyte ratio (from clinical data). Spearman's correlation between mycobacterial net growth in the PBMC MGIT assay and C) classical monocyte frequency and D) monocyte to lymphocyte ratio (from flow cytometry data). Net growth = (Log_{10} CFU of sample - Log_{10} CFU of control).

6.4.1.2 Monocyte depletions

Monocytes were depleted using CD14+ specific magnetic beads and MACS columns, and depletions were confirmed by flow cytometry (Figure 6-2).

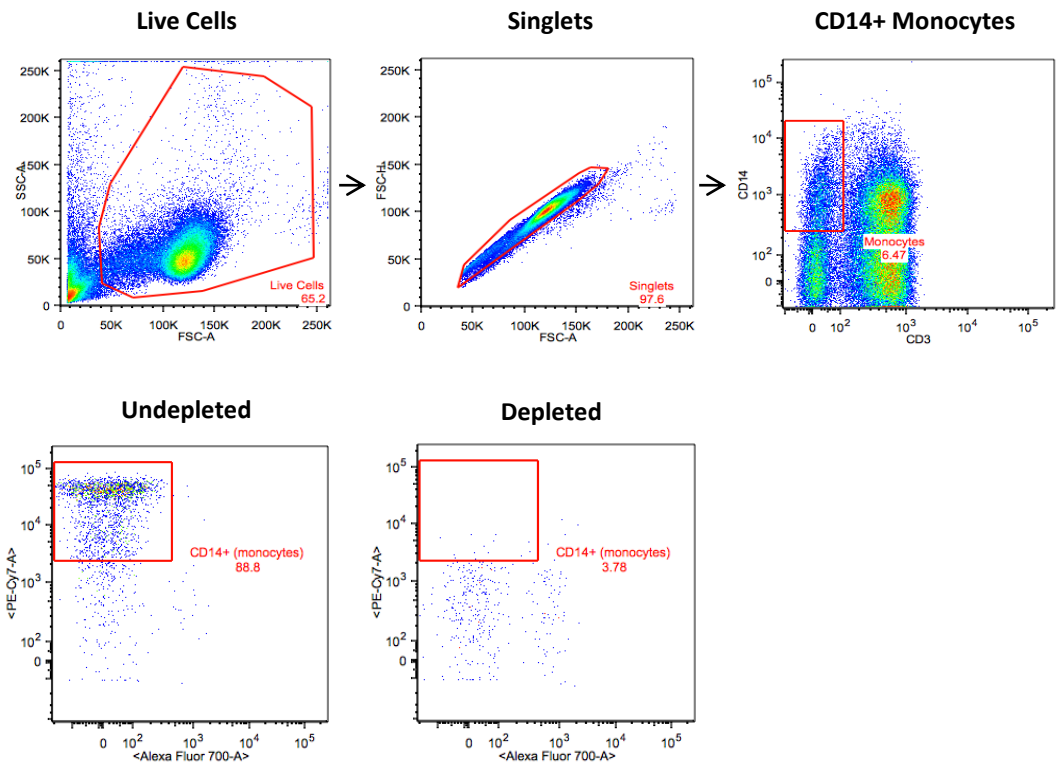

Figure 6-2 Monocyte depletion gating strategy. Live cells were gated on forward scatter (FSC) vs. side scatter (SSC), followed by singlets. Monocytes were gated as CD3-CD14+ cells.

The undepleted or depleted samples were added to PBMC MGIT cultures and mycobacterial growth determined. In the first experiment using human cells, monocyte depletion was not complete (range 63 to 93%). However, a significant reduction in mycobacterial growth was observed in the monocyte-depleted cultures (undepleted median = 0.49, depleted median = -0.21; $p<0.05$) (Figure 6-3A). This experiment was repeated with some optimisation of the depletion protocol, including a longer period of incubation with the beads and mixing on a

rocking platform. Depletion in this experiment was more successful (range 87 to 98%), but no difference was observed between undepleted and monocyte-depleted samples (Figure 6-3B). In all cases, matched cultures were normalised for abundance of remaining cell types, and were subjected to the same processing including running through depletion columns but in the absence of magnetic beads.

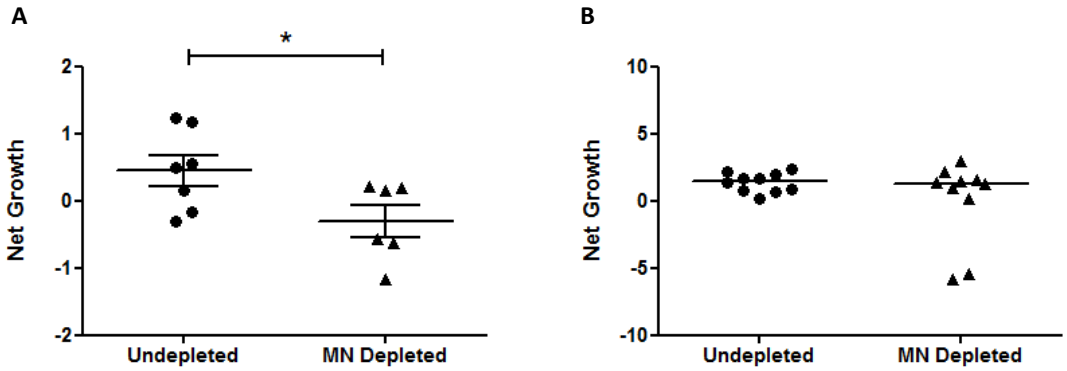

Figure 6-3 Inefficient, but not efficient, depletion of monocytes from human PBMC results in decreased MGIT mycobacterial growth. The MGIT assay was performed using undepleted PBMC, and PBMC that had been depleted of monocytes using magnetic beads. A) Using samples from healthy human volunteers with a less efficient depletion protocol. Bars represent the mean values with the SEM; having passed a normality test, a paired t-test was performed where * represents a p value of <0.05. B) A repeat experiment in human volunteers with an optimised depletion protocol. Bars represent the median values; a Wilcoxon matched-pairs signed-rank test was performed with no statistically significant differences between groups. Net growth = (Log_{10} CFU of sample - Log_{10} CFU of control).

Two similar experiments were performed using mouse splenocytes; the second of which used both naïve and BCG-vaccinated mice. Monocyte depletion was efficient (95-98%) but had no effect in either case (Figure 6-4).

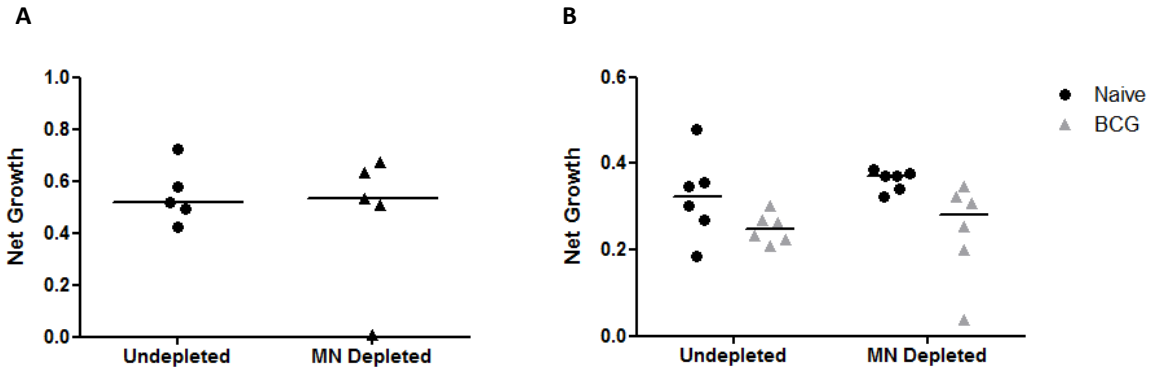

Figure 6-4 Depletion of monocytes from mouse splenocytes does not significantly alter MGIT mycobacterial growth. The MGIT assay was performed using undepleted splenocytes, and splenocytes that had been depleted of monocytes using magnetic beads from A) healthy naïve mice and B) naïve and BCG-vaccinated mice. Bars represent the median values. A) A Wilcoxon matched-pairs signed-rank test was performed and B) A two-way ANOVA with a Bonferroni post-test where there were no statistically significant differences between groups. Net growth = (Log_{10} CFU of sample - Log_{10} CFU of control).

6.4.1.3 Artificially altering ML ratio

To further explore the effect of ML ratio, monocytes and lymphocytes were sorted using plastic adherence. They were then mixed at ratios that represent the 25th (0.04), 50th (0.19) and 75th (0.30) centiles of the background population. Cultures with no monocytes were also included. In a preliminary experiment with 3 healthy volunteers, there was a trend towards a 'Goldilocks' effect whereby too few or too many monocytes relative to lymphocytes were associated with poorer mycobacterial control, whereas mid-range ML ratios were associated with superior inhibition (Figure 6-5A). A similar pattern was observed in a second, larger experiment (Figure 6-5B). A final experiment in 13 volunteers using cell sorting by magnetic beads further confirmed these findings. A significant increase in mycobacterial growth was observed between an ML ratio of 0.04 and 0.3 (median net growth = -0.92 and -0.35 respectively; $p<0.05$) (Figure 6-5C).

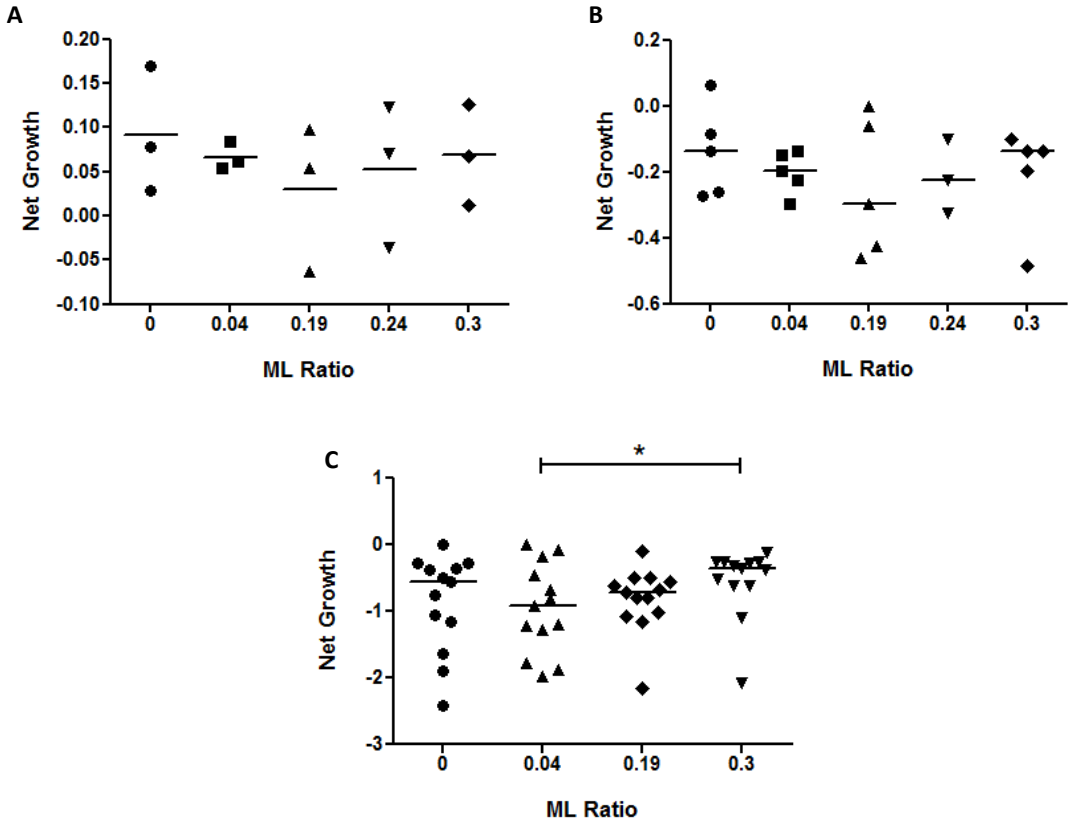

Figure 6-5 Artificially altering ML ratio affects MGIT mycobacterial growth. The MGIT assay was performed using human PBMC. Cells were sorted into monocytes and lymphocytes by A and B) adherence or C) magnetic beads. They were then mixed together at the ratios stated, representing the 25th (0.04), 50th (0.19) and 75th (0.3) centiles of the background population. Bars represent the median values. A Kruskal-Wallis with a Dunn's post-test was performed where * represents a p value of <0.05. Net growth = (Log_{10} CFU of sample - Log_{10} CFU of control).

6.4.2 CD4+ and CD8+ T cells

Where flow cytometry data was available, the association between mycobacterial growth and frequency of CD4+ and CD8+ T cells was tested in the studies described. No correlations were observed (data not shown), which was surprising as the adaptive cellular immune response is considered critical for protective immunity. To explore the impact of these cell

types, CD4+ or CD8+ T cells were depleted using magnetic beads. Depletions were confirmed by flow cytometry, the gating strategy of which is described below (Figure 6-6).

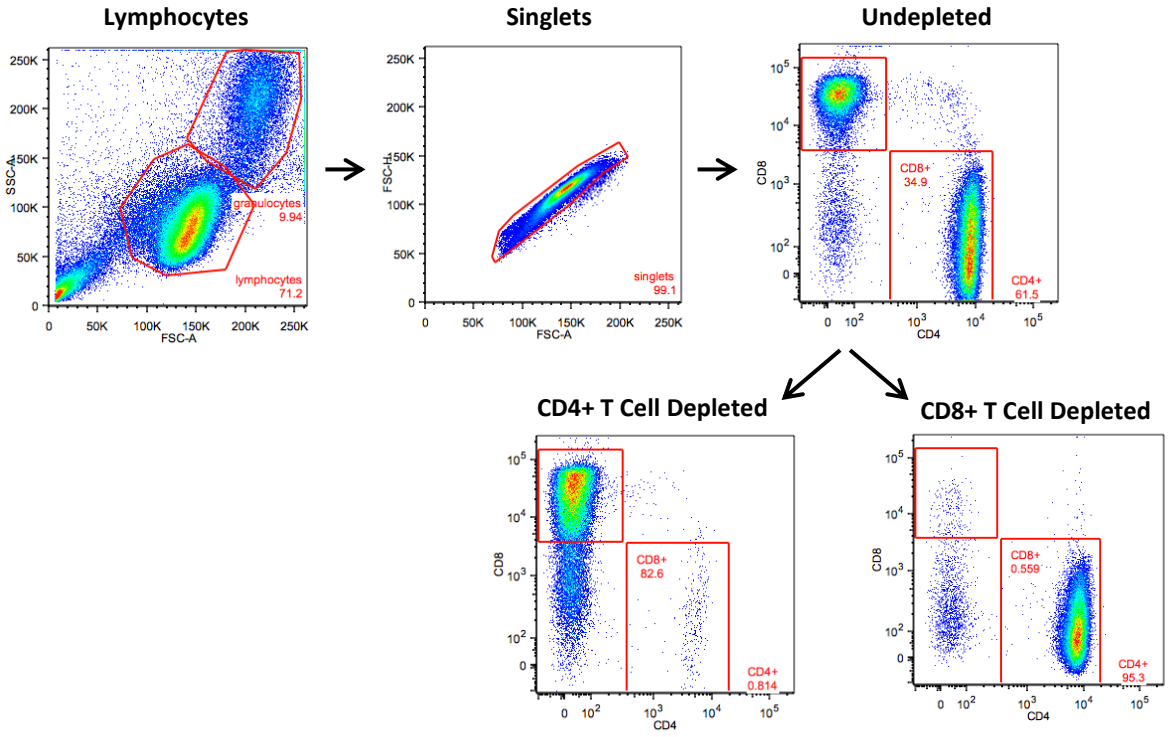

Figure 6-6 CD4+/CD8+ T cell depletion gating strategy. Lymphocytes and granulocytes were gated on forward scatter (FSC) vs. side scatter (SSC), followed by singlets. The figure shows the first volunteer with the undepleted and depleted fractions.

6.4.2.1 CD4+ T cell depletion

CD4+ T cells were depleted (using CD4-specific magnetic beads and MACS columns) from PBMC taken from historically BCG vaccinated healthy humans and splenocytes from BCG vaccinated mice. Depletion had no effect on mycobacterial growth in either experiment (Figure 6-7).

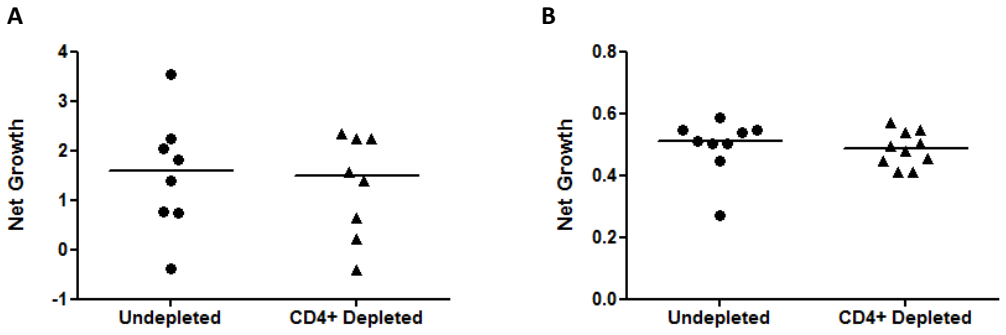

Figure 6-7 Depletion of CD4+ T cells does not affect MGIT mycobacterial growth. The MGIT assay was performed using A) human PBMC and B) mouse splenocytes, which were either undepleted or depleted of CD4+ T cells using magnetic beads. Bars represent the median values. A Wilcoxon matched-pairs signed-rank test was performed where there were no statistically significant differences between groups. Net growth = (Log_{10} CFU of sample - Log_{10} CFU of control).

Two further experiments were performed using mouse splenocytes; the second using naïve mice as a control. In both experiments there was a trend toward increased mycobacterial growth in the CD4+ T cell depleted samples, though this was not statistically significant. Interestingly, this was the case in both naïve and BCG-vaccinated mice (Figure 6-8).

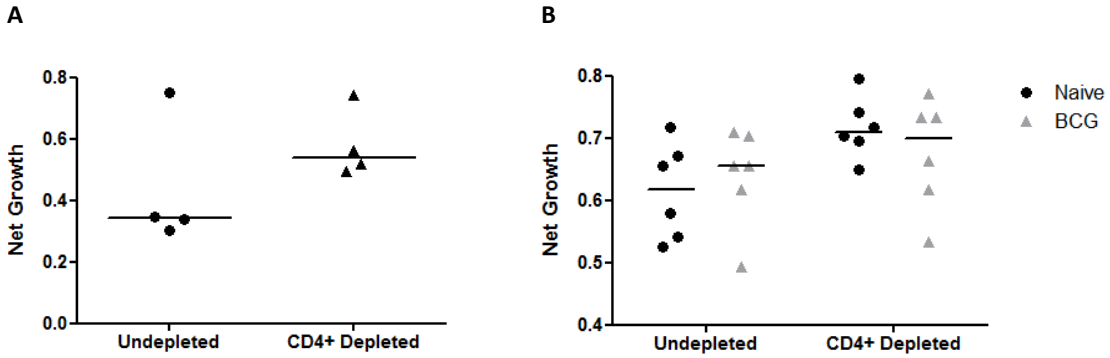

Figure 6-8 Depletion of CD4+ T cells does not significantly alter MGIT mycobacterial growth. The MGIT assay was performed using mouse splenocytes from A) BCG vaccinated mice and B) naïve and BCG-vaccinated mice, which were either undepleted or depleted of CD4+ T cells using magnetic beads. Bars represent the median values. A) A Wilcoxon matched-pairs signed-rank test and B) A two-way ANOVA were performed. Net growth = (Log_{10} CFU of sample - Log_{10} CFU of control).

6.4.2.2 CD8+ T cell depletion

CD8+ T cells were depleted (using CD8-specific magnetic beads and MACS columns) from PBMC taken from historically BCG vaccinated healthy humans and splenocytes from naïve and BCG vaccinated mice. Depletion had no effect on mycobacterial growth in human PBMC (Figure 6-9A). However, when naïve and BCG-vaccinated mice were used, there was a trend towards increased mycobacterial growth in the CD8+ T cell depleted samples for the BCG-vaccinated mice only. This was not statistically significant (Figure 6-9B).

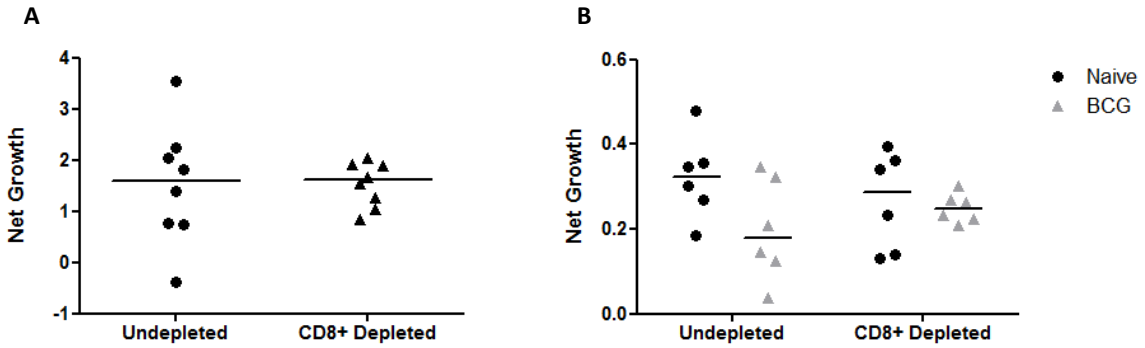

Figure 6-9 Depleting CD8+ T cells does not significantly alter MGIT mycobacterial growth. The MGIT assay was performed using A) human PBMC and B) mouse splenocytes from naïve and BCG-vaccinated mice. Cells were either undepleted or depleted of CD8+ T cells using magnetic beads. Bars represent the median values. A) A Wilcoxon matched-pairs signed-rank test and B) A two-way ANOVA were performed where there were no statistically significant differences between groups. Net growth = (Log_{10} CFU of sample - Log_{10} CFU of control).

6.4.3 Correlates cell frequency analysis

Using samples from the infant MVA85A Phase IIb efficacy trial with MVA85A described in section 4.4.2.3, the relationship between frequencies of different cellular subsets by flow cytometry and MGIT mycobacterial growth were investigated using regression analysis. To increase the power of the model, all data was combined from both time-points (baseline and day 28) and vaccine groups (MVA85A and placebo) using robust variance estimation to adjust for cluster-correlated data. Univariate linear regression indicated that the frequency of total T cells (T.CD3) and classical monocytes (C.MON) made a significant positive contribution to mycobacterial growth ($p<0.05$ and $p<0.0001$ respectively).

Putative CD16-negative NK cells (NK.16NEG) (based on negative gating ie. CD3-negative, CD19-negative, CD14-negative) made a significant negative contribution ($p<0.0001$). Frequencies of B cells (B.CD19), inflammatory monocytes (I.MON) and putative CD16-positive NK cells (NK.16POS) did not affect mycobacterial growth (Figure 6-10). Multiple regression analysis indicated that a model containing the three significant variables explained 23% of MGIT variance. Within this model, total T cells (T.CD3) was not a significant predictor ($p=0.82$). Classical monocyte frequency (C.MON) made a significant positive contribution ($p<0.0001$) and putative CD16-negative NK cells (NK.16NEG) made a significant negative contribution ($p<0.0001$).

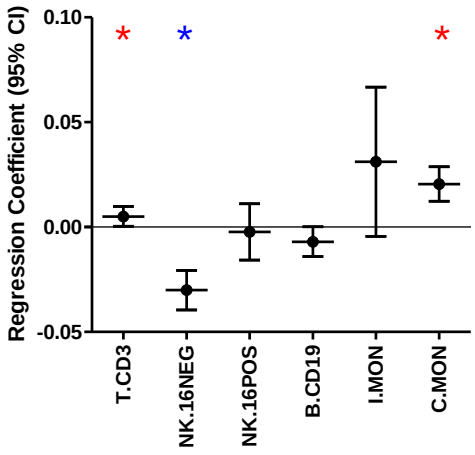

Figure 6-10 Regression coefficients for cell type frequencies. Univariate regression analysis was used to determine the relative contributions of different cell types (measured by flow cytometry) to MGIT mycobacterial growth in BCG vaccinated South African infants. Data was combined from both pre- and post-vaccination time-points; robust variance estimation was used to adjust for cluster-correlated data. * represents a significant p-value; red = positive association, blue = negative association.

6.4.4 Cytokines

6.4.4.1 IFN-γ

As described in section 3.3.1, a study was conducted of BCG vaccination in 30 healthy UK volunteers. 15 had no history of BCG vaccination and the remaining 15 had been historically vaccinated with BCG. All volunteers had 3 pre-vaccination bleeds which were averaged to a single pre-vaccination value. Volunteers received a single intradermal immunisation with BCG-SSI with follow-up bleeds at weeks 4, 8 and 24 post-vaccination (see Figure 4-1). Fresh T cells were stimulated overnight with PPD, and IFN-γ responses were detected using an *ex vivo* ELISpot assay at each visit. There was a significantly greater response from the historically BCG vaccinated compared with naïve individuals at baseline (Figure 6-11). The revaccinated volunteers also had a significantly higher response at weeks 4 and 24 compared with those receiving primary vaccination. There was a significant increase in PPD-specific IFN-γ production at 4 weeks and 8 weeks post-vaccination in both groups receiving primary and secondary BCG, returning to baseline by week 24 (Figure 6-12).

No associations were observed between IFN-γ ELISpot response to PPD and mycobacterial growth in the whole blood assay for volunteers receiving primary BCG vaccination (Figure 6-13) or secondary vaccination (Figure 6-14) at any time-point.

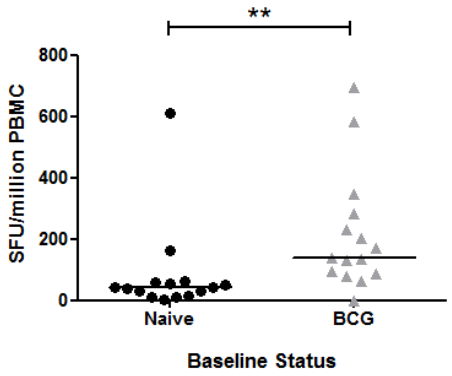

Figure 6-11 IFNγ ELISpot response to PPD at baseline is higher in historically BCG vaccinated compared with naïve individuals. An IFN-γ ELISpot was performed against PPD using fresh PBMC from individuals that were either naïve or had been historically vaccinated with BCG. Bars represent the median values; a Wilcoxon matched-pairs signed-rank test was performed where ** represents a p value of <0.005.

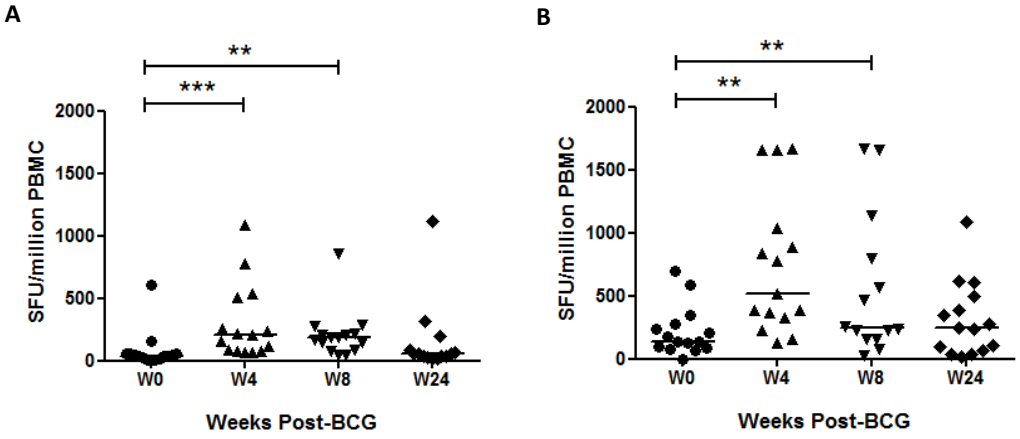

Figure 6-12 IFNγ ELISpot response to PPD increases following BCG vaccination in humans. An IFN-γ ELISpot was performed against PPD using fresh PBMC from individuals receiving A) primary BCG vaccination or B) revaccination. Bars represent the median values; a Kruskal-Wallis with a Dunn's post-test was performed where ** represents a p value of <0.005 and *** represents a p value of <0.0005.

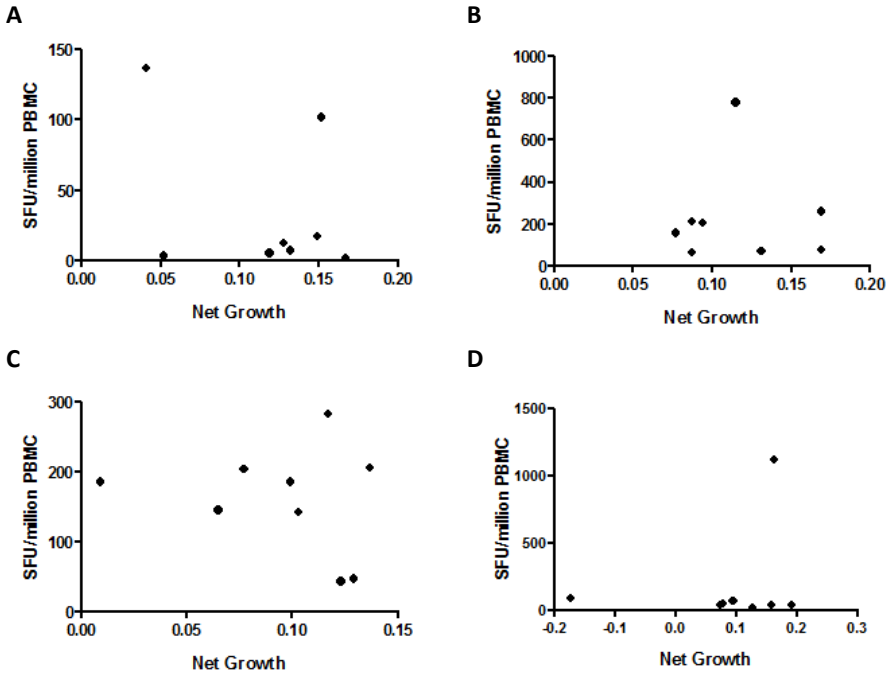

Figure 6-13 IFN-γ ELISpot to PPD does not correlate with whole blood MGIT mycobacterial growth in humans. Spearman's correlation between PPD IFN-γ ELISpot and mycobacterial growth in the whole blood MGIT assay in volunteers receiving primary BCG vaccination at A) 0 weeks, B) 4 weeks, C) 8 weeks and D) 24 weeks post-vaccination. Net growth = (Log_{10} CFU of sample - Log_{10} CFU of control).

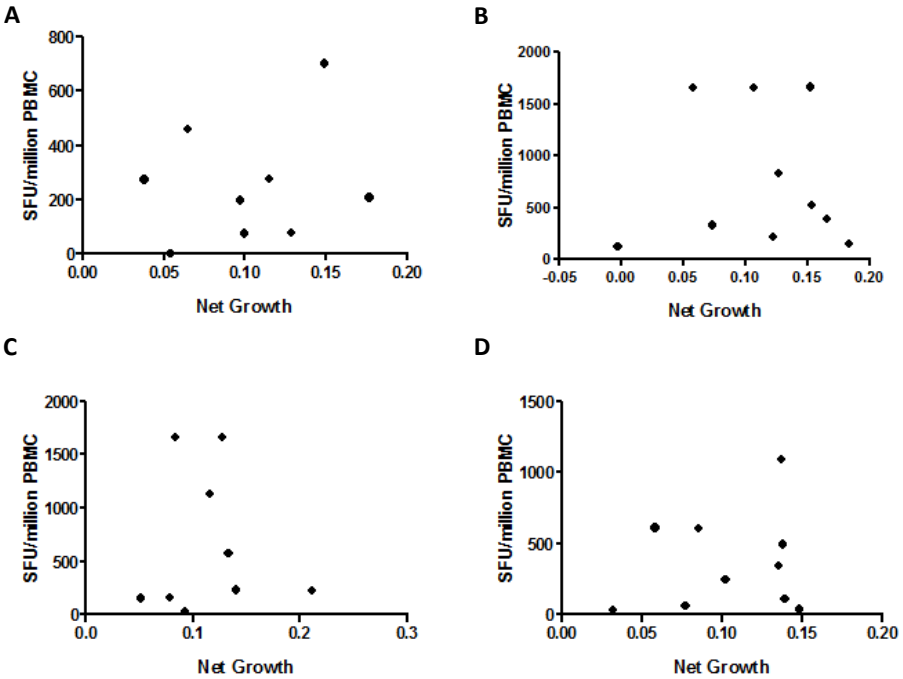

Figure 6-14 IFN-γ ELISpot to PPD does not correlate with whole blood MGIT mycobacterial growth in humans. Spearman's correlation between PPD IFN-γ ELISpot and mycobacterial growth in the whole blood MGIT assay in volunteers receiving BCG revaccination at A) 0 weeks, B) 4 weeks, C) 8 weeks and D) 24 weeks post-vaccination. Net growth = (Log_{10} CFU of sample - Log_{10} CFU of control).

When associations were explored between IFN-γ ELISpot response and mycobacterial growth in the PBMC MGIT, there were no significant associations at most time-points (data not shown). However, in the group receiving BCG revaccination, there was a negative correlation with mycobacterial growth at 4 weeks, which represents the peak of the IFN-γ ELISpot response ($p<0.005$) (Figure 6-15A). Also in this group, a strong IFN-γ ELISpot response at baseline, prior to revaccination with BCG, correlated with increased mycobacterial growth at 24 weeks following revaccination ($p<0.05$) (Figure 6-15B).

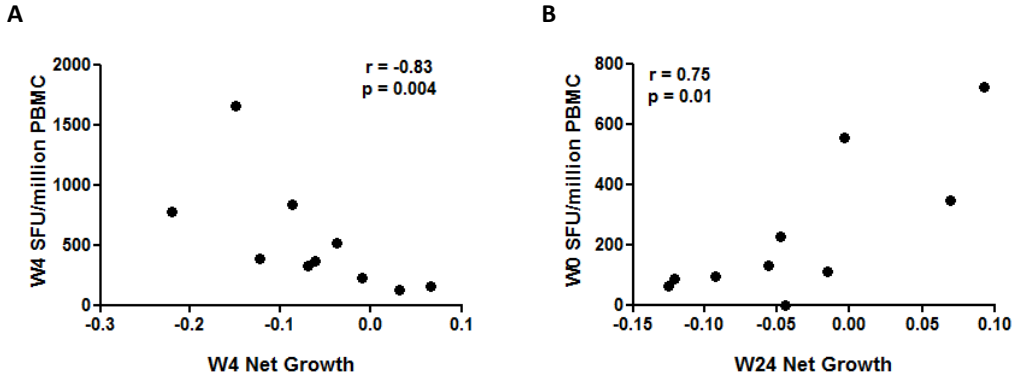

Figure 6-15 IFN-γ ELISpot to PPD correlates with PBMC MGIT mycobacterial growth at weeks 4 and 24 post-revaccination. Spearman's correlation between PPD IFN-γ ELISpot and mycobacterial net growth in the PBMC MGIT assay in volunteers receiving BCG revaccination at A) 4 weeks following revaccination and B) ELISpot at baseline with mycobacterial growth at week 24 post-revaccination. Net growth = (Log_{10} CFU of sample - Log_{10} CFU of control).

In the study of BCG vaccination in Cynomolgus macaques, there was a similar pattern in IFN-γ ELISpot response to PPD to that seen in the human volunteers. Though not statistically significant, the response peaked at week 4 and returned to baseline by week 20 (Figure 6-16). Again this did not correlate with mycobacterial growth in the BCG whole blood MGIT assay (Figure 6-17A-D), or the *M.tb* MGIT assay (data not shown).

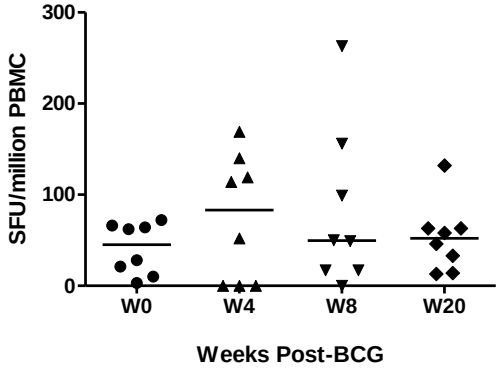

Figure 6-16 IFNγ ELISpot response to PPD following BCG in NHPs. An IFN-γ ELISpot was performed against PPD using fresh PBMC from Cynomolgus macaques receiving primary BCG vaccination. Bars represent the median values; a Kruskal-Wallis test was performed where there were no statistically significant differences.

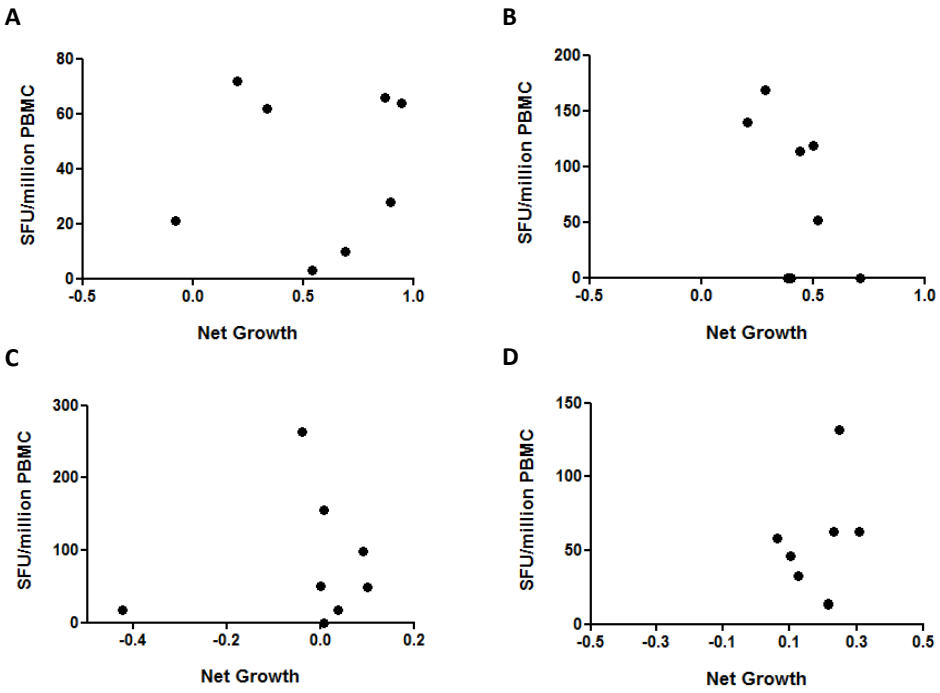

Figure 6-17 IFN-γ ELISpot to PPD does not correlate with whole blood MGIT mycobacterial growth in NHPs. Spearman's correlation between PPD IFN-γ ELISpot and mycobacterial net growth in the whole blood MGIT assay in Cynomolgus macaques receiving BCG revaccination at A) 0 weeks, B) 4 weeks, C) 8 weeks and D) 20 weeks post-vaccination. Net growth = (Log_{10} CFU of sample - Log_{10} CFU of control).

To further explore the role of IFN-γ, recombinant IFN-γ (rIFN-γ) was added to healthy naïve mouse splenocytes. There was a significant reduction in mycobacterial growth in cultures supplemented with rIFN-γ compared with controls (median net growth = 0.96 and 0.46 respectively; $p<0.05$) (Figure 6-18).

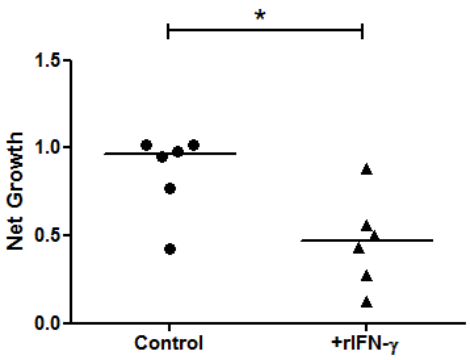

Figure 6-18 Addition of rIFN-γ results in reduced MGIT mycobacterial growth in mouse splenocytes. The MGIT assay was performed using splenocytes from healthy naïve mice with or without the addition of rIFN-γ. Bars represent the median values; a Wilcoxon matched-pairs signed-rank test was performed where * represents a p value of <0.05.

6.4.4.2 Cytokine production following MVA85A

In the MVA85A Pilot correlates study described in section 4.4.2.1, cytokine production was measured from 96 hour MGIT culture supernatants using a 30-plex Luminex panel. There was a significant increase in the concentration of 11 out of 30 (37%) cytokines tested at 12 weeks post-MVA85A vaccination (Figure 6-19). This time-point also represented the peak of response in the MGIT assay (see Figure 4-9).

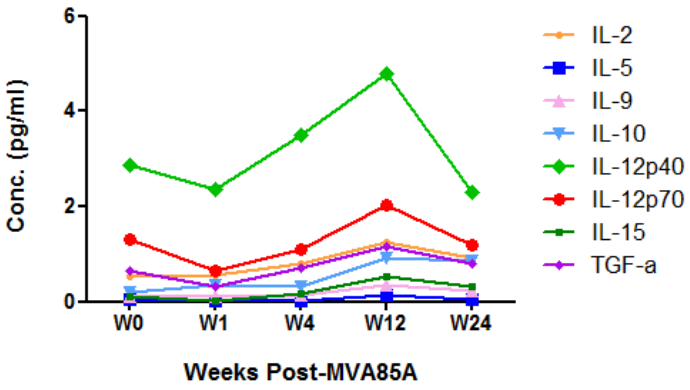

Figure 6-19 Cytokine production following MVA85A vaccination. Cytokine levels of the 8 out of 30 cytokines that increased in concentration following MVA85A vaccination in BCG-vaccinated South African infants. A Kruskal-Wallis test was performed followed by a Mann-Whitney matched-pairs test with $p<0.05$.

As week 12 represented the peak of both the cytokine and MGIT response, correlations between cytokine concentration and mycobacterial growth were assessed at this time-point. A positive correlation was observed for 9 (30%) of the cytokines measured, and a negative correlation for 1 cytokine (IL-8), as detailed in Table 6-1. However, none of these were significant after a Bonferroni correction for multiple comparisons. Representative correlations for IL-7, IL-1Ra, Eotaxin and IFN-γ are shown in Figure 6-20.

	Cytokine	r	p
Th1	IFN-γ	0.778	0.023
	IL-12p40	0.792	0.019
	IL-12p70	0.073	0.846
	TNF-α	0.810	0.015
	TNF-β	-0.820	0.846
	IL-2	0.110	0.795
Th2	IL-10	0.122	0.774
	IL-13	-0.114	0.788
	IL-9	-0.321	0.438
	IL-5	0.091	0.830
Th17	IL-15	-0.130	0.976
	IL-1Ra	0.980	0.000
	IL-1a	0.595	0.120
	IL-1β	0.735	0.038
	IL-6	0.571	0.139
	IL-7	0.929	0.002
	IL-17	0.530	0.177
Growth Factors	G-CSF	0.690	0.058
	GM-CSF	0.762	0.028
	FGF-2	-0.300	0.470
	VEGF	0.548	0.160
	TGF-α	0.421	0.298
	IL-3	0.056	0.895
Chemokines/ Inflammatory response	MDC	0.833	0.010
	Eotaxin	0.850	0.007
	IFN-a2	0.690	0.058
	MIP-1α	0.738	0.037
	MIP-1β	0.595	0.120
	IP-10	0.144	0.734
	IL-8	-0.764	0.027

Table 6-1 Correlations between cytokine concentration and MGIT mycobacterial growth at 12 weeks post-MVA85A vaccination. Spearman's correlations between cytokine concentration by Luminex and mycobacterial growth by PBMC MGIT at week 12 following MVA85A vaccination in BCG-vaccinated South African infants. Grey represents significant correlations not corrected for multiple comparisons. No correlations were significant following a Bonferroni correction.

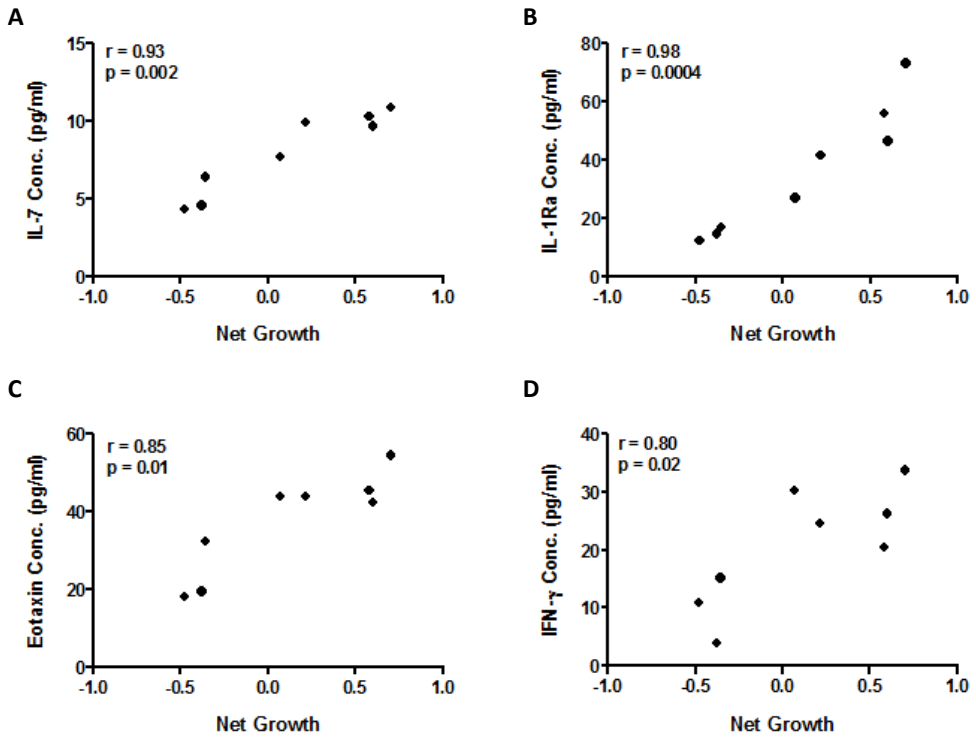

Figure 6-20 Correlations between cytokine concentration and MGIT mycobacterial growth at 12 weeks post-MVA85A vaccination. Spearman's correlation between mycobacterial net growth in the PBMC MGIT assay and concentration of A) IL-7, B) IL-1Ra, C) Eotaxin and D) IFN-γ at 12 weeks post-MVA85A vaccination in South African infants. Net growth = (Log_{10} CFU of sample - Log_{10} CFU of control).

Luminex analysis was also performed on MGIT supernatants from a subset of 20 infants from the MVA85A correlates study (see section 4.4.2.3). As there was no difference in mycobacterial growth or protection from TB between baseline and week 4 following vaccination, cytokines were measured at baseline only. Of 40 measurable cytokines on the panel, 30 (75%) were significantly correlated with mycobacterial growth at this time-point. After a Bonferroni correction for multiple comparisons, 12 cytokines (30%) were significantly correlated. Correlations are detailed in Table 6-2 and representative correlations are shown in Figure 6-21.

	Cytokine	r	p
Th1	IFN-γ	0.691	0.001
	IL-12p40	0.638	0.002
	IL-12p70	0.305	0.192
	sCD40L	0.375	0.103
	Flt3L	0.469	0.037
	TNF-α	0.291	0.213
	TNF-β	0.734	0.000
	IL-2	0.529	0.017
Th2	IL-10	0.171	0.001
	IL-13	0.482	0.043
	IFN-α	0.648	0.002
	IL-4	0.789	0.000
	IL-9	0.371	0.107
	IL-5	0.447	0.048
Th17	IL-15	0.508	0.031
	IL-1Ra	0.554	0.017
	IL-1a	0.579	0.012
	IL-1β	0.585	0.007
	IL-6	0.463	0.040
	IL-7	0.828	0.000
	IL-17	0.739	0.000
Growth Factors	TGF-α	0.735	0.001
	G-CSF	0.656	0.003
	GM-CSF	0.812	0.000
	GRO	0.690	0.002
	FGF-2	0.679	0.002
	EGF	0.278	0.264
	VEGF	0.522	0.018
	PDGF-AA	0.418	0.084
	PDGF-BB	0.150	0.553
Chemokines/ Inflammatory response	MCP-3	0.734	0.001
	MDC	0.523	0.026
	Eotaxin	0.676	0.002
	Fraktalkine	0.691	0.001
	IFN-a2	0.717	0.001
	MCP-1	0.809	0.000
	MIP-1α	0.228	0.334
	MIP-1β	0.448	0.048
	IP-10	0.383	0.095
	RANTES	-0.242	0.304

Table 6-2 Correlations between cytokine concentration and MGIT mycobacterial growth at baseline. Spearman's correlations between cytokine concentration by Luminex and mycobacterial growth by PBMC MGIT at baseline in BCG-vaccinated South African infants. Grey represents significant correlations; darker grey represents correlations still significant after a Bonferroni correction for multiple comparisons.

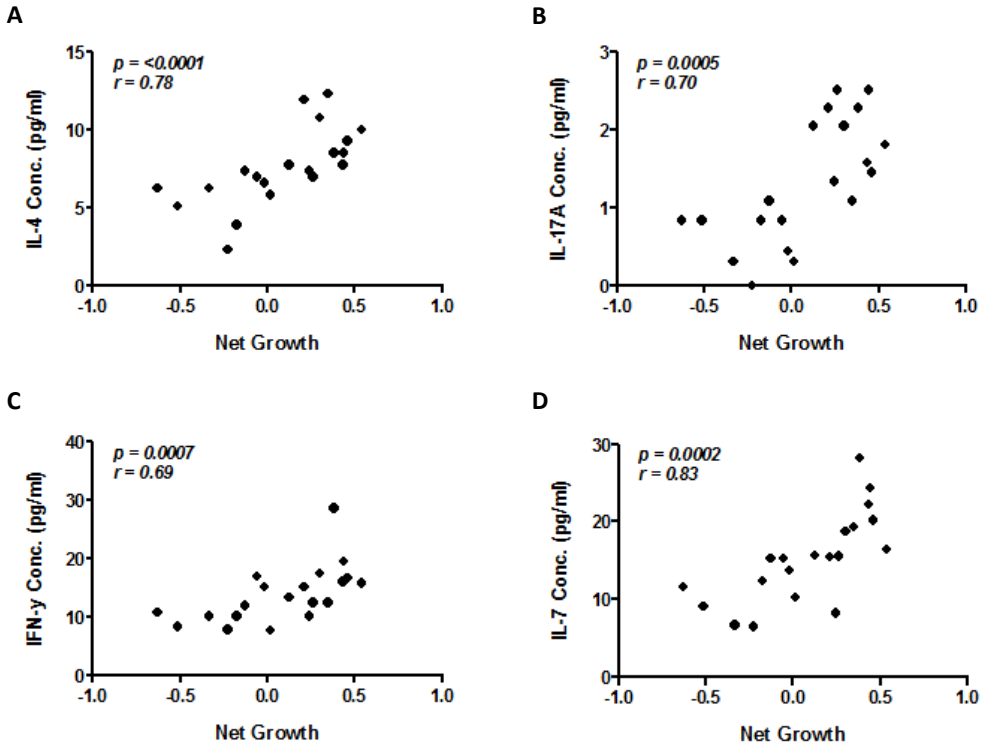

Figure 6-21 Correlations between cytokine concentration and MGIT mycobacterial growth at baseline. Spearman's correlation between mycobacterial net growth in the PBMC MGIT assay and concentration of A) IL-4, B) IL-17A, C) IFN-γ and D) IL-7 at baseline in South African BCG-vaccinated infants. Net growth = (Log_{10} CFU of sample - Log_{10} CFU of control).

A heat-map of this data was constructed using a binary split of MGIT mycobacterial growth into low (below the median) and high (above the median). A pattern is observed of low cytokine expression across most cytokines for those with low mycobacterial growth, and high

cytokine expression for those with high mycobacterial growth. A mixed group is also present (Figure 6-22).

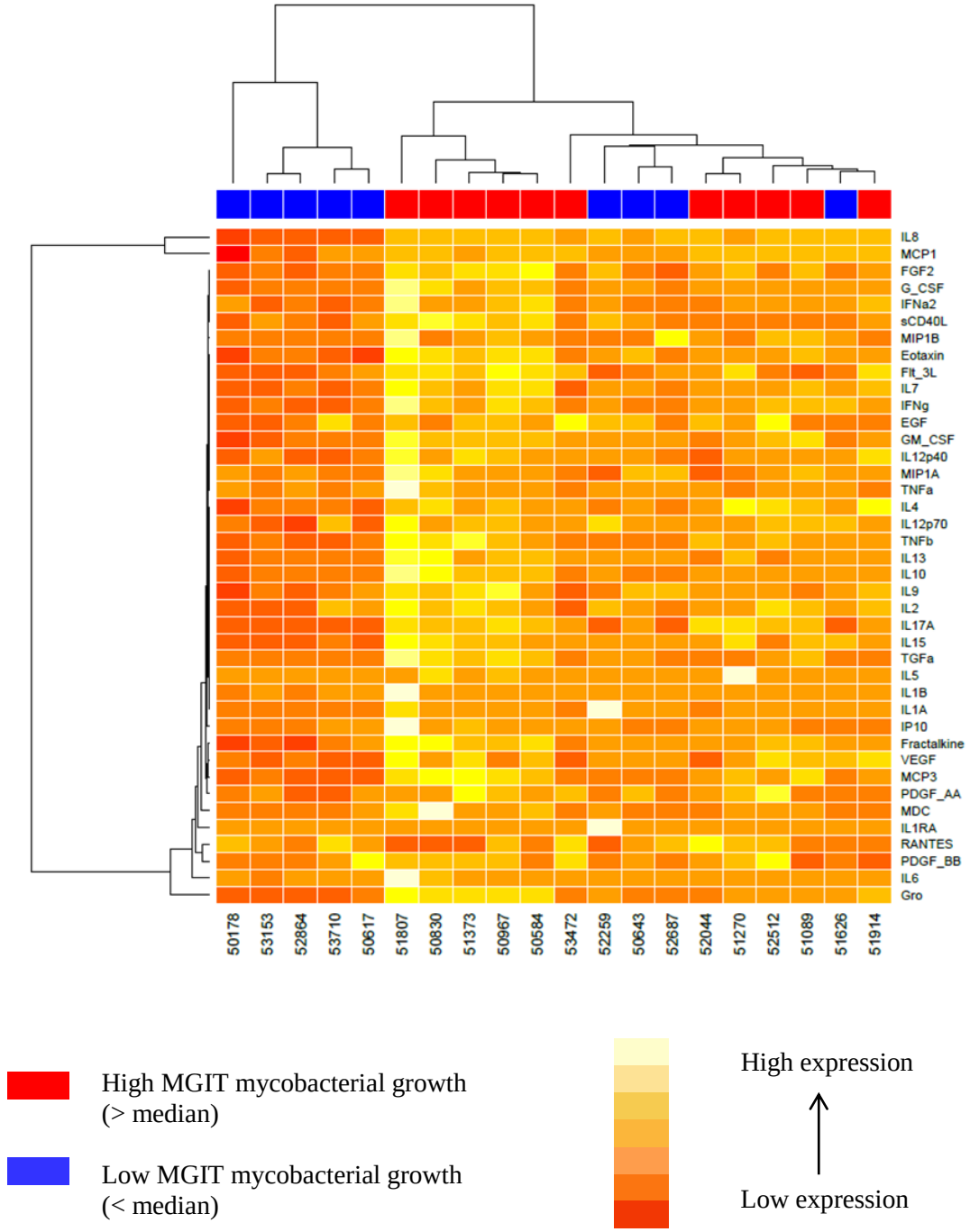

Figure 6-22 Cytokine concentration vs. mycobacterial growth. Heat map showing the relationship between mycobacterial growth in the PBMC MGIT assay and cytokine concentration at baseline in BCG-vaccinated SA infants. Constructed in 'R' using Euclidean distance and average clustering methods.

Correlations between cytokines that showed an association with mycobacterial growth were examined by Spearman's rank correlation. All cytokines correlated significantly with the production of multiple other cytokines. IFN-γ correlated with other pro-inflammatory cytokines including IL-2 ($r = 0.7$, $p<0.005$) and IL-6 ($r = 0.8$, $p<0.0001$); and also with Th2 cytokines such as IL-10 ($r = 0.9$, $p<0.0001$) and IL-13 ($r = 0.8$, $p<0.0001$). IFN-γ also correlated with chemokines such as IL-8 ($r = 0.8$, $p<0.0001$) and growth factors such as GM-CSF ($r = 0.8$, $p<0.0001$). IL-10 accounted for 39% of variability in MGIT mycobacterial growth in a stepwise linear regression model ($F(1, 18) = 11.3$, $p<0.005$, $R^2 = 0.39$, $R^2_{adjusted} = 0.35$), and significantly predicted mycobacterial growth ($\beta = 0.62$, $t = 3.36$, $p<0.005$), and correlated significantly with all other cytokines.

6.4.4.3 IL-10

Given this result in addition to extensive literature indicating an important immunoregulatory role for IL-10 in TB, it was decided to further explore the effect of IL-10 on mycobacterial growth. Initially, recombinant IL-10 (rIL-10) was added to healthy naïve human PBMC. There was a significant increase in mycobacterial growth in cultures supplemented with rIL-10 compared with controls (median net growth = 0.71 and 1.05 respectively; $p<0.05$) (Figure 6-23A). It was also shown that an increased concentration of rIL-10 was associated with increased mycobacterial growth in human PBMC (Figure 6-23B).

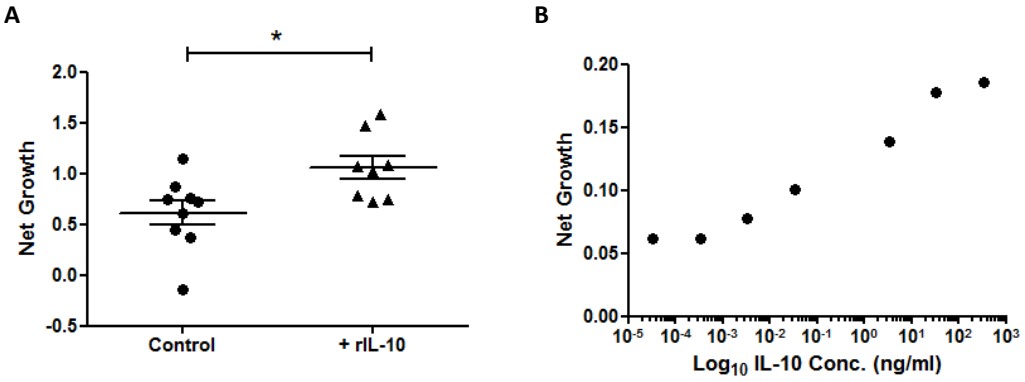

Figure 6-23 Addition of rIL-10 results in increased MGIT mycobacterial growth in human PBMC. The MGIT assay was performed using PBMC from healthy naïve human volunteers A) with or without the addition of rIL-10 (bars represent the mean values with the SEM; a paired t-test was performed where * represents a p value of <0.05) or B) with supplementation with an increasing concentration of rIL-10; points represent the mean of duplicate cultures. Net growth = (Log_{10} CFU of sample - Log_{10} CFU of control).

As IL-10 is thought to play an immunoregulatory role in TB, the effect of increased IL-10 on the production of other cytokines was analysed by Luminex. The MGIT assay was performed using healthy human PBMC cultured with or without the addition of rIL-10. Supernatants taken from these cultures at 96 hours were assessed for production of other cytokines. Of the 12 cytokines that were measurable, 3 were significantly down-regulated in cultures supplemented with rIL-10 compared with control cultures (MDC, MIP-1α and TNF-α; $p<0.05$) (Figure 6-24A-C). A further 3 cytokines had reduced expression but the difference between conditions was not significant (IL-8, IP-10 and Eotaxin) (Figure 6-24D-F). MCP-1 was the only cytokine to show increased expression in the rIL-10 supplemented cultures ($p<0.005$) (Figure 6-24G). 5 cytokines did not differ between conditions (EGF, PDGF-AA, PDGF-BB, IL-3 and TGF-α) (Figure 6-24H-L).

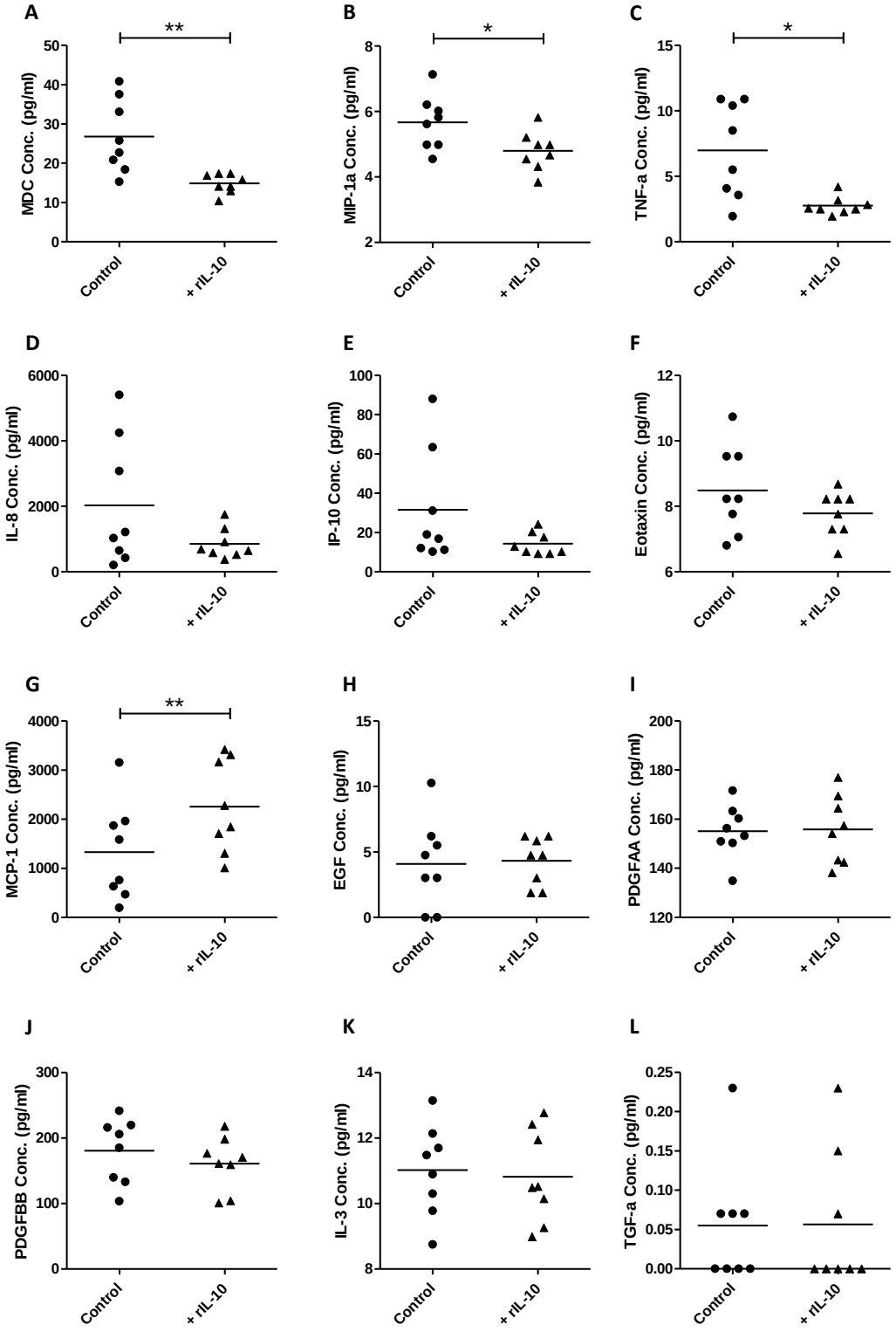

Figure 6-24 Addition of rIL-10 affects production of other cytokines. The PBMC MGIT assay was performed with or without the addition of rIL-10. Cytokine concentration was measured in the supernatants taken from 96hr MGIT cultures. Bars represent the median values; a Wilcoxon matched-pairs signed-rank test was performed where * represents a p value of <0.05 and ** represents a p value of <0.005.

6.4.4.3 The kinetics of the cytokine response

It was expected that some cytokines would correlate positively with mycobacterial growth and some negatively, depending on their function. It was therefore surprising to find that almost all correlations were positive. As cytokines were only measured in supernatants taken at 96 hours, it was hypothesised that by this stage increasing mycobacterial growth was driving increased production of cytokines rather than the cytokine response driving immune control of growth. Therefore a time-course experiment was conducted to compare cytokine production at 24-hour intervals throughout the MGIT culture. Interestingly, cytokines appeared to follow one of two patterns: gradually increasing in concentration during the course of the culture (Figure 6-25), or peaking at 48 hours and returning to baseline by 72 hours (Figure 6-26). When the association between cytokine concentration and mycobacterial growth was assessed, there were many positive correlations at 96 hours in accordance with the previous experiments. However, at 24 and 48 hours correlations were predominantly negative. All correlations are shown in Table 6-3 (correlations were not corrected for multiple comparisons as this was a hypothesis-generating exercise).

HOURS	EGF	Eotaxin	TGF-a	GM-CSF	IFN-γ	Gro	IL-10	MCP-3	MDC	PDGF-AA	PDGF-BB	IL-1Ra	IL-1a	IL-1b	IL-3	IL-6	IL-8	IP-10	MCP-1	MIP-1a	MIP-1b	TNF-a	IL12-p70	sCD40L	IL-5
24	-.294	-.273	-.570	-.653	-.680*	-.357	-.765*	-.533	-.343	.017	-.669*	-.653	-.487	-.513	-.071	-.393	-.643	-.042	-.611	-.552	-.293	-.444	.255	.299	.320
48	-.815**	-.669*	-.668*	-.806**	-.658	-.685	-.916**	-.728*	-.904**	-.636	-.921**	-.711*	-.962**	-.962**	-.377	-.921**	-.214	-.301	-.527	-.971**	-.762*	-.921**	-.833**	-.022	-.442
72	-.026	.152	-.556	-.444	-.128	0.000	.203	.200	.050	.033	-.051	.050	-.126	-.085	.267	-.233	.433	.167	.067	-.025	.033	-.383	-.075	.139	.168
96	.048	-.258	.323	.323	.723*	.476	.282	.214	.500	.310	.619	.119	.238	.419	-.571	.214	.464	.452	.500	.275	.095	.476	.072	-.109	-.173

Table 6-3 Correlations between cytokine concentration and MGIT mycobacterial growth at different culture periods. Spearman's r values for correlations between cytokine concentration by Luminex and mycobacterial growth by PBMC MGIT in healthy human volunteers. Blue = negative correlations and red = positive correlations. Darker colours represent stronger correlations; * represent a p value of <0.05, ** represents a p value of <0.005.

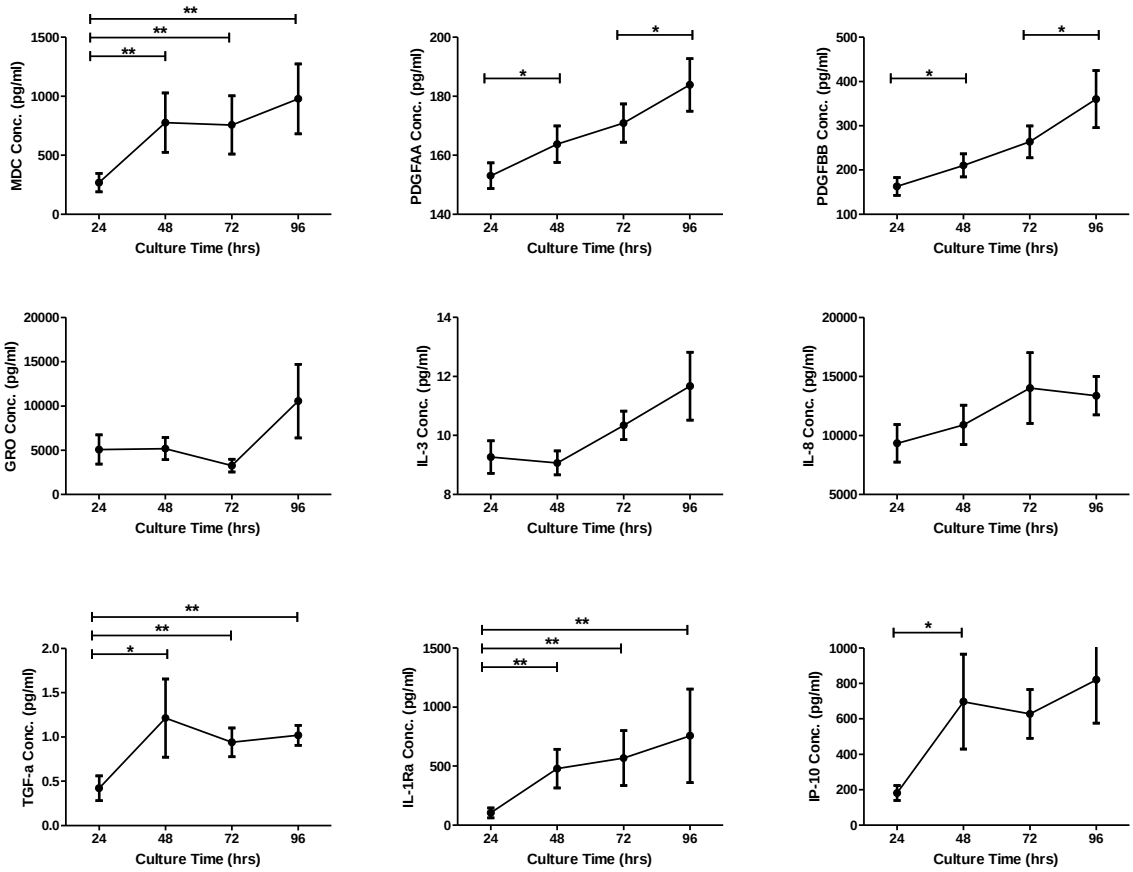

Figure 6-25 Kinetic of cytokine production during the 96 hour culture period. The MGIT assay was performed using PBMC from healthy naïve human volunteers. Cytokine expression was measured in the supernatants taken from MGIT cultures at 24 hour intervals during the culture. Cytokines were selected that followed a similar kinetic over the course of the culture. Points represent the mean of 9 volunteers with the SEM; a Wilcoxon matched-pairs signed-rank test was performed where * represents a p value of <0.05 and ** represents a p value of <0.005.

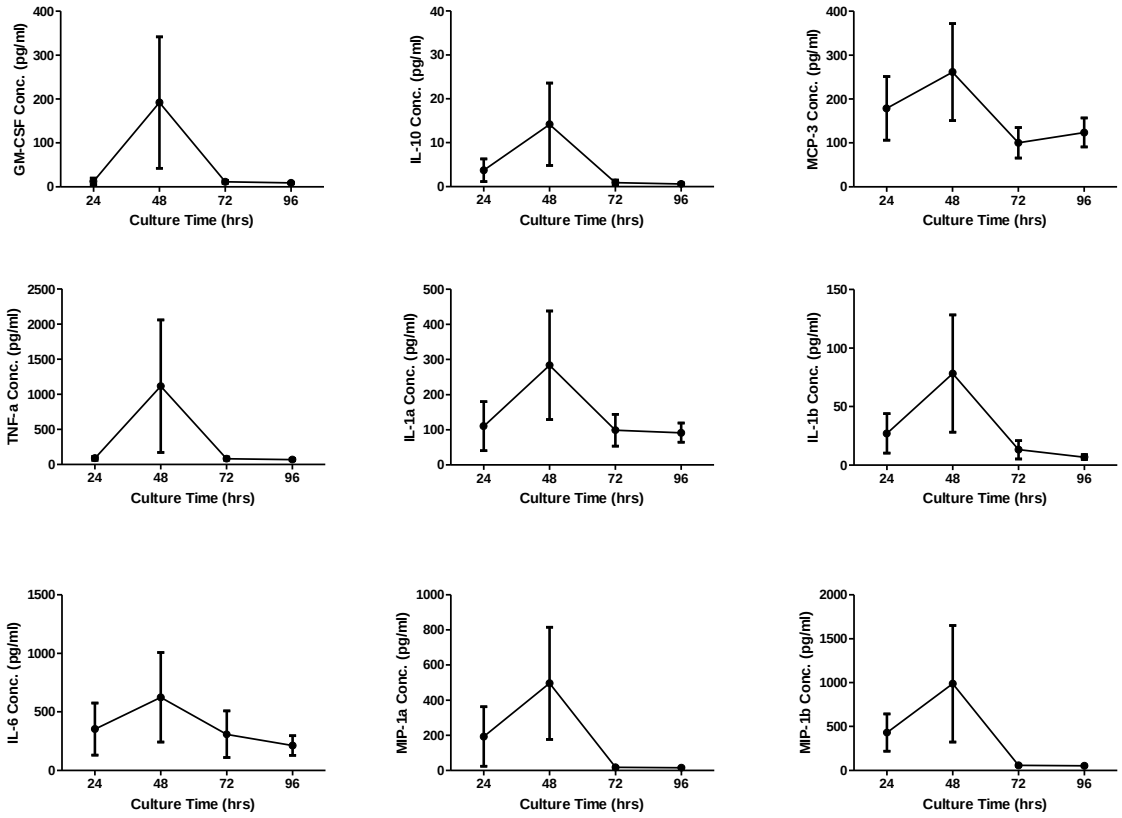

Figure 6-26 Kinetic of cytokine production during the 96 hour culture period II. The MGIT assay was performed using PBMC from healthy naïve human volunteers. Cytokine expression was measured in the supernatants taken from MGIT cultures at 24 hour intervals during the culture. Cytokines were selected that followed a similar kinetic over the course of the culture. Points represent the mean of 9 volunteers with the SEM; a Wilcoxon matched-pairs signed-rank test was performed where no differences were significant.

To identify cytokines of importance, both the kinetic of the response and the correlation with mycobacterial growth were examined. Those cytokines that both increased in expression significantly at 48 hours and inversely correlated with mycobacterial growth at this time-point were MDC, PDGF-BB, TGF-α and IL-1Ra (Figure 6-27).

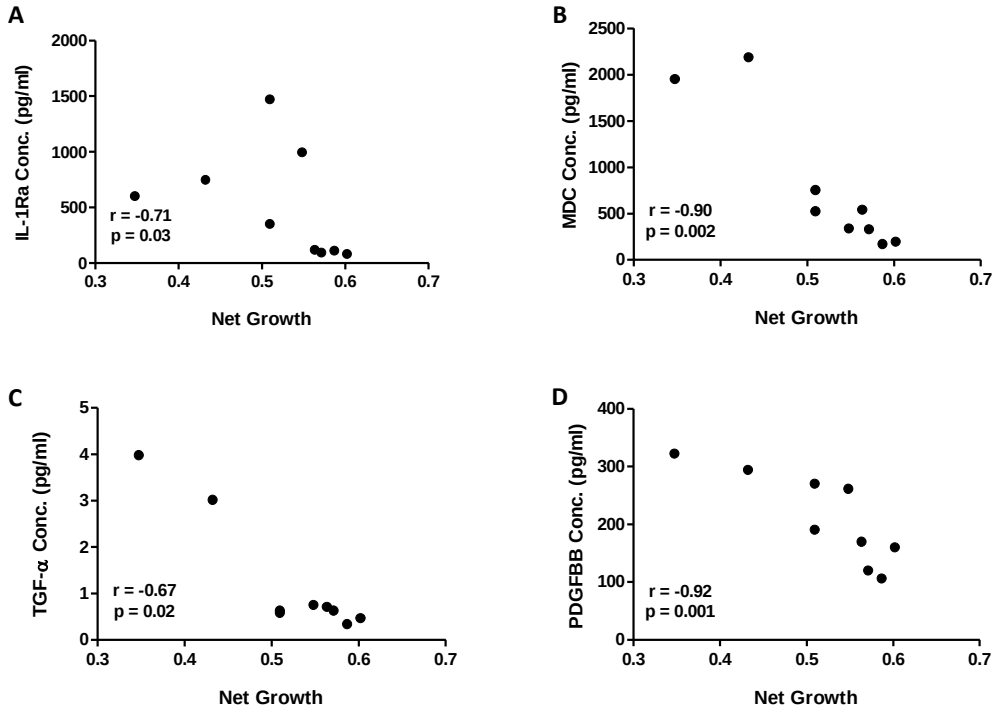

Figure 6-27 Inverse correlations between cytokine concentration and MGIT mycobacterial growth after a 48 hour culture period. Spearman's correlation between mycobacterial net growth at 48 hours in the PBMC MGIT assay and concentration of A) IL-1Ra, B) MDC, C) TGF-α and D) PDGF-BB in healthy human volunteers. Net growth = (Log_{10} CFU of sample - Log_{10} CFU of control).

6.4.5 Gene expression

Using gene expression microarray data from the infant MVA85A correlates study (section 4.4.2.3), the relationship between mycobacterial growth and gene expression was explored. As MVA85A vaccination did not enhance growth inhibition or protection from TB disease, data was used from baseline only. With the help of Julius Muller, the R package Significance Analysis of Microarrays (SAMR) was used to identify genes whose expression correlated with mycobacterial growth following a Benjamini-Hochberg false discovery rate multiple testing correction. Cells were either unstimulated or stimulated overnight with BCG at an MOI of 1:1. There were no significant correlations with the unstimulated samples following correction for multiple comparisons. However, of the 23,036 genes on the array, expression of 2,002 genes correlated significantly with mycobacterial growth (adj. $p<0.05$) in the stimulated samples. Interestingly, these included the haemoglobin-related genes HBB, HBA1 and HBA2 which had a high $\log_2$ fold change. A volcano plot of all correlated genes is shown in Figure 6-28. Genes that had an absolute $\log_2$ fold change of greater than 1 (ie. per one unit increase in MGIT mycobacterial growth, there was at least one unit increase in gene expression) are mapped in Figure 6-29 (unstimulated) and Figure 6-30 (stimulated).

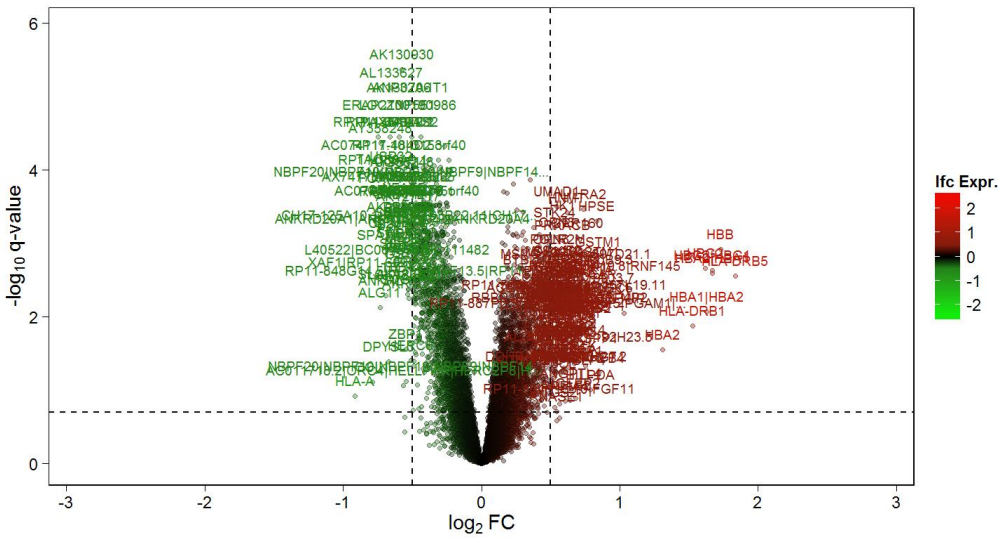

Figure 6-28 Relationship between microarray gene expression and MGIT mycobacterial growth. Volcano plot showing the relationship between mycobacterial growth in the PBMC MGIT assay and gene expression at baseline in South African BCG-vaccinated infants. Red indicates positive correlations and green indicates negative correlations; log_2FC indicates the strength of the correlation.

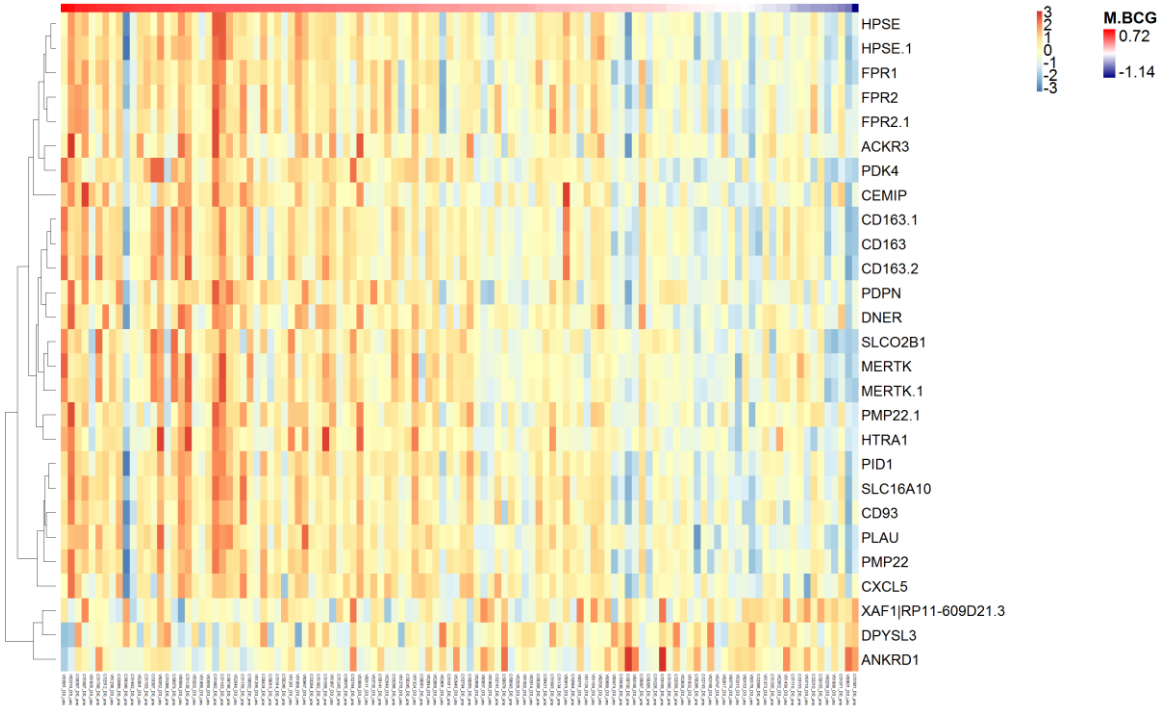

Figure 6-29 Heat map of gene expression vs. MGIT mycobacterial growth (unstim). Heat map showing the relationship between mycobacterial growth in the PBMC MGIT assay and gene expression at baseline in South African BCG-vaccinated infants. Genes were selected that had an absolute log_2 fold change of greater than 1 (ie. per one unit increase in MGIT mycobacterial growth, there was at least one unit increase in gene expression).

Many genes which correlated positively with mycobacterial growth in the unstimulated samples have been associated with TB including FPR, CD163 and CXCL5. It is also possible

to discern some negative correlations to the bottom of the heat map. In the stimulated samples, there were many more correlations including CD14, FCAR, IL-24 and TREM1.

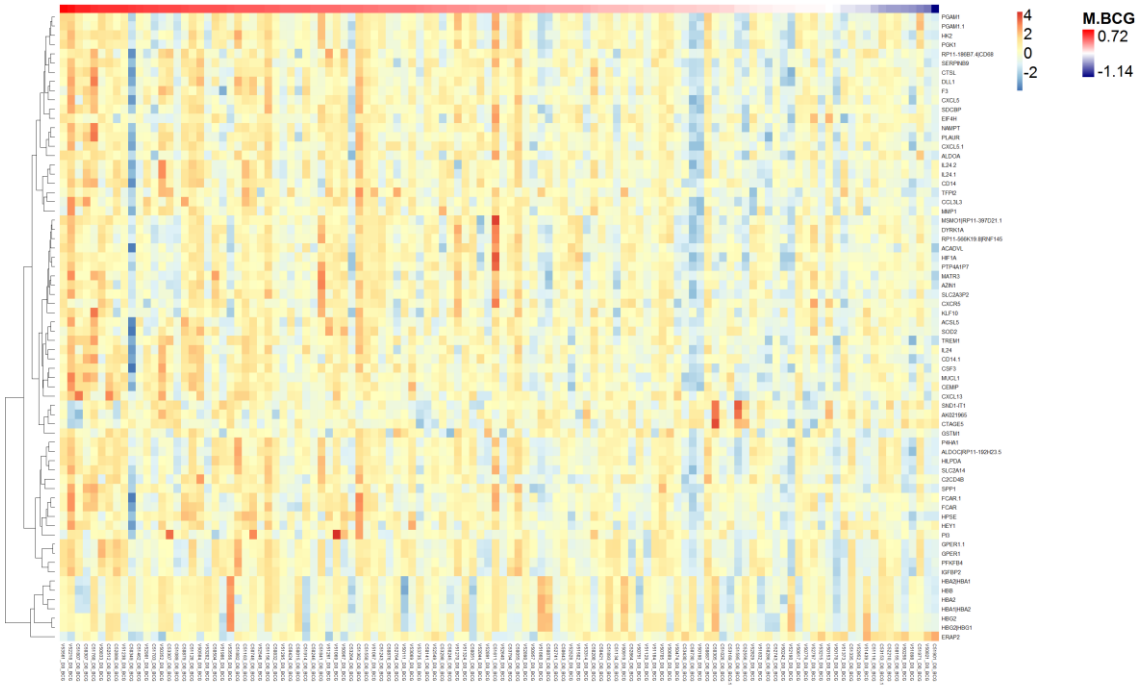

Figure 6-30 Heat map of gene expression vs. MGIT mycobacterial growth (BCG stim). Heat map showing the relationship between mycobacterial growth in the PBMC MGIT assay and gene expression at baseline in South African BCG-vaccinated infants following overnight stimulation with BCG. Genes were selected that had an absolute $\log_2$ fold change of greater than 1 (ie. per one unit increase in MGIT mycobacterial growth, there was at least one unit increase in gene expression).

As the BCG stimulated samples are more representative of the conditions in the MGIT assay (as cultures are infected with BCG), the top 200 gene correlations from this group were entered into the Database for Annotation, Visualisation and Integrated Discovery (DAVID) for pathway analysis. The top pathway hit was 'Immune Response', defined as "any immune system process that functions in the calibrated response of an organism to a potential internal

or invasive threat" (adj. p = $6x10^{-6}$) (Table 6-4). This pathway contained 24 genes including CD14, HAMP, IL-1Ra and CXCL5 (Table 6-5). The correlations between MGIT mycobacterial growth and expression of CD14 and HAMP are shown in Figure 6-31.

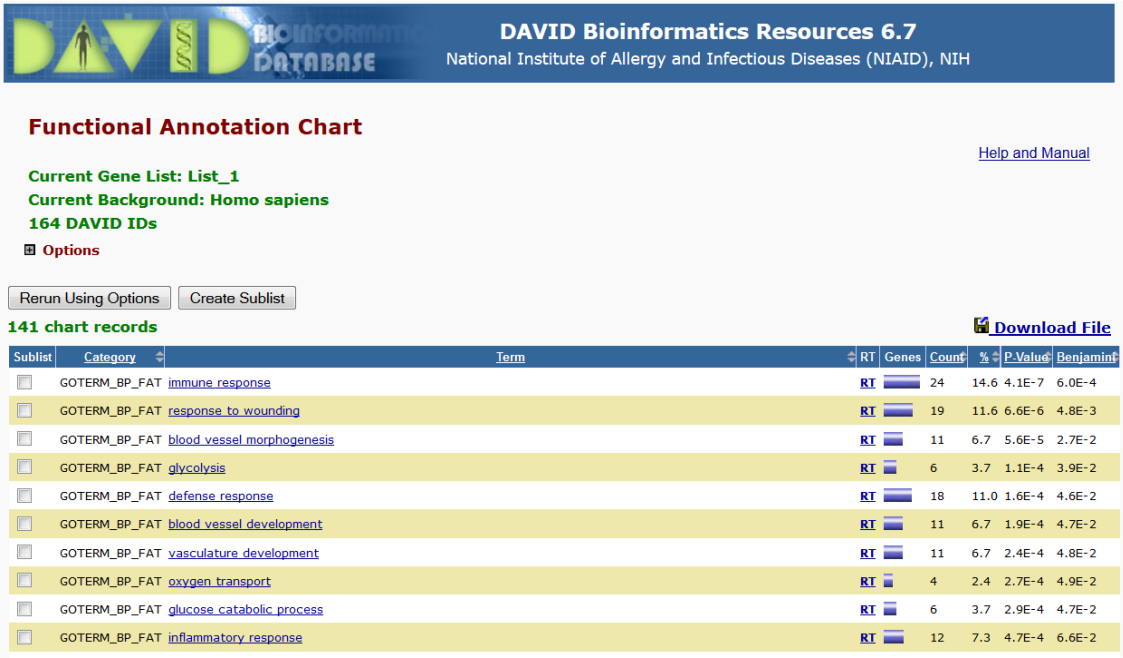

DAVID Bioinformatics Resources 6.7
National Institute of Allergy and Infectious Diseases (NIAID), NIH

Functional Annotation Chart

Help and Manual

Current Gene List: List_1
Current Background: Homo sapiens
164 DAVID IDs

Options

Rerun Using Options | Create Sublist

141 chart records

Download File

Sublist	Category	Term	RT	Genes	Count	%	P-Value	Benjamini
	GOTERM_BP_FAT	immune response	RT		24	14.6	4.1E-7	6.0E-4
	GOTERM_BP_FAT	response to wounding	RT		19	11.6	6.6E-6	4.8E-3
	GOTERM_BP_FAT	blood vessel morphogenesis	RT		11	6.7	5.6E-5	2.7E-2
	GOTERM_BP_FAT	glycolysis	RT		6	3.7	1.1E-4	3.9E-2
	GOTERM_BP_FAT	defense response	RT		18	11.0	1.6E-4	4.6E-2
	GOTERM_BP_FAT	blood vessel development	RT		11	6.7	1.9E-4	4.7E-2
	GOTERM_BP_FAT	vasculature development	RT		11	6.7	2.4E-4	4.8E-2
	GOTERM_BP_FAT	oxygen transport	RT		4	2.4	2.7E-4	4.9E-2
	GOTERM_BP_FAT	glucose catabolic process	RT		6	3.7	2.9E-4	4.7E-2
	GOTERM_BP_FAT	inflammatory response	RT		12	7.3	4.7E-4	6.6E-2

Table 6-4 Results of DAVID Pathway analysis. The top 200 genes that correlated significantly with MGIT mycobacterial growth were entered into DAVID for pathway analysis. The top hit was immune response followed by response to wounding, blood vessel morphogenesis, glycolysis and defence response.

Gene symbol	Gene name	Reported association with *M.tb*
BCL10	B-cell CCL/lymphoma 10	-
CD14	CD14 molecule	May be involved in uptake of *M.tb* into macrophages[354]
CD274	CD274 molecule	Expression increased in blood from active TB patients[355]
FCAR	Fc fragment of IgA, receptor for	A human IgA monoclonal antibody protects mice[356]
GEM	GTP binding protein	-
GCH1	GTP cyclohydrolase 1	KO mice more resistant to *M.tb* (Stylianou *et al*. unpublished)
NLRP3	NLR family, pyrin domain containing 3	Plays a critical role in necrotic death triggered by *M.tb*[357]
ST6GAL1	ST6 beta-galactosamide alpha-2,6-sialytransferase 1	-
CXCL13	Chemokine (C-X-C motif) ligand 13	Controls T-cell placement and the optimal activation of macrophages for *M.tb* control[358]
CXCL5	Chemokine (C-X-C motif) ligand 15	KO mice resistant to infection[359]
CSF3	Colony stimulating factor 3 (granulocyte)	Suppression compromises antimycobacterial immunity[360]
HAMP	Hepcidin antimicrobial peptide	Encodes hepcidin (upregulated in response to mycobacteria)[361]
IL1RN	Interleukin 1 receptor antagonist	Strongly induced by *M.tb*; polymorphisms affect disease[362]
LILRA6	Leukocyte immunoglobulin-like receptor, subfamily A, member 6	Downregulated in culture of monocytes with mycobacteria (Hogan *et al*. unpublished)
LILRA3	Leukocyte immunoglobulin-like receptor, subfamily A, member 3	Downregulated in culture of monocytes with mycobacteria (Hogan *et al*. unpublished)
HLA-DRB5	Major histocompatibility complex, Class II, DR beta 5	Involved in antigen presentation by APCs[363]
OSM	Oncostatin M	*M.tb* increases monocyte secretion *in vitro*[364]
OLR1	Oxidised low density lipoprotein receptor 1	-
PTPRC	Protein tyrosine phosphatase, receptor type, C	-
SLC11A1	Solute carrier family 11, member 1	Polymorphisms associated with *M.tb* risk[365]
TLR8	Toll-like receptor 8	Polymorphisms associated with *M.tb* susceptibility[366]
TREM1	Triggering receptor expressed on myeloid cells 1	Serum levels associated with prognosis in pulmonary TB[367]
YWHAZ	Tyrosine 3-monooxygenase/tryptophan 5-monooxygenase activation protein	-
VEGFA	Vascular endothelial growth factor	Higher level in active disease[368]

Table 6-5 Immune response pathway genes. The 24 genes belonging to the immune response pathway defined by DAVID pathway analysis that correlated significantly with MGIT mycobacterial growth.

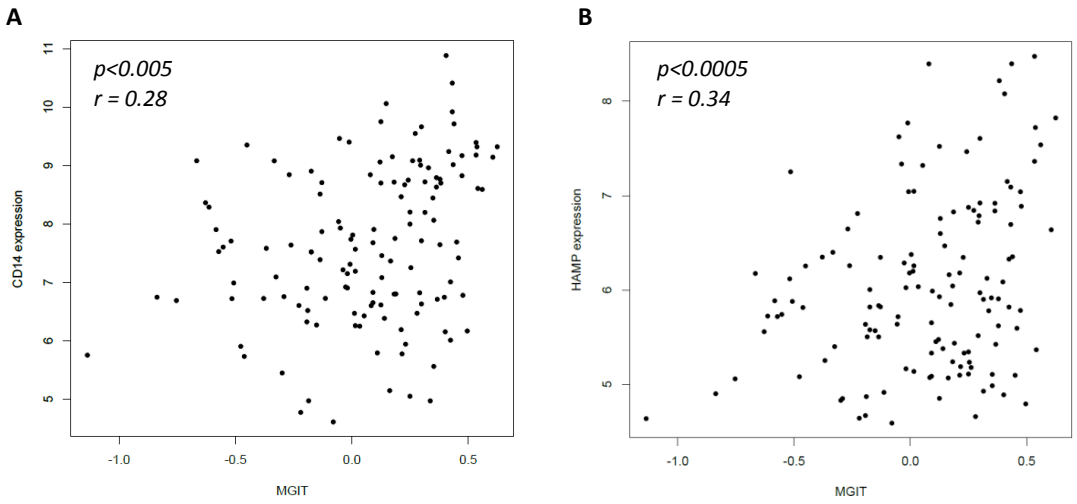

Figure 6-31 Correlation between gene expression and MGIT mycobacterial growth. Spearman's correlation between mycobacterial net growth in the PBMC MGIT assay and expression of A) CD14 and B) HAMP in BCG-vaccinated South African infants at baseline. Net growth = (Log_{10} CFU of sample - Log_{10} CFU of control).

10 genes of interest from this analysis (CD14, HAMP, CD274, CXCL5, FCAR, VEGFA, NLRP3, SLC11A1, TLR8 and TREM1) were selected for further testing in a validation cohort of 20 South African infants using qPCR. Unfortunately RNA yields were very low, and although expression of the housekeeping gene GAPDH was detectable, expression of the target genes was too low for analysis in all but 2 samples. Thus it was not possible to confirm correlations with the MGIT outcome in this experiment.

6.5 Discussion

It has become clear over the course of this project that monocyte number is a critical determining factor in the outcome of both the whole blood and PBMC MGIT assays. Two very different measures of monocyte number (clinical monocyte count and monocyte frequency by flow cytometry) were shown to correlate positively with mycobacterial growth in two different populations. This is biologically plausible, as monocytes represent the main host cell for mycobacterial survival, growth and replication[369]. The more monocytes present, the more 'targets' for mycobacterial infection and the greater the overall number of bacilli. In a whole-transcriptome microarray study of correlates of protection from TB, it was found that, in infants who responded strongly to BCG vaccination, there was a higher percentage of monocytes in those who went on to develop TB disease compared with those who did not (Fletcher *et al*. manuscript submitted). It is likely that the association with classical monocytes (rather than activated) observed in the correlates study is due to this subtype making up 90-95% of the monocyte population[370]. The importance of classical monocytes in the MGIT assay was further supported by univariate and multiple linear regression analysis of the correlates of risk study data. This indicated that total T cells, classical monocytes and CD16-negative putative NK cells were important determinants in MGIT mycobacterial growth. A model containing these three components explained 23% of MGIT variance; to which classical monocyte frequency made a significant positive contribution.

As cell-mediated immunity is known to play a critical role in the recognition and elimination of intracellular pathogens, it follows that the outcome is also dependent on the number of lymphocytes; hence the importance of monocyte to lymphocyte (or ML) ratio. ML ratio correlated with whole blood MGIT mycobacterial growth in the human BCG study, though not with PBMC MGIT. This may be due to small numbers, as a significant correlation was observed in the larger infant correlates study which also used PBMC. Furthermore, the ML

ratio in the BCG study was taken from clinical data at baseline, while in the infant correlates study, it was measured using flow cytometry on matched thawed samples and was as such more representative of the cells in the assay (particularly given the effect of freeze-thawing on monocyte viability). This association is consistent with evidence in the literature. The impact of ML ratio on mycobacterial infection was first described in the 1920s by Sabin *et al*., who found that the ML ratio in peripheral blood correlated with extent of mycobacterial disease in both rabbits and humans[371-373]. Largely since neglected, there has been a recent resurgence of interest in the ML ratio. Naranbhai *et al*. demonstrated that ML ratio was associated with risk of TB disease in a series of recent cohort studies of adults, infants and pregnant women in sub-Saharan Africa[374-376]. Furthermore, the aforementioned study by Fletcher *et al*. found that the relative abundance of myeloid-specific and lymphoid-specific gene transcripts was associated with risk of TB (Fletcher *et al*. manuscript submitted). In cattle, the ML ratio has been shown to correlate with inhibition of mycobacterial growth *in vitro*[377,378]. ML ratio has also been associated with outcome in a range of cancers[379-382], and risk of influenza[383] and clinical malaria[384]. In a recent efficacy trial of the malaria vaccine RTS,S, ML ratio accounted for differences in vaccine efficacy among volunteers[385].

Interestingly, this is not a straightforward linear relationship. Although a direct correlation was observed within the physiological range of ML ratio, removing monocytes had an effect on MGIT mycobacterial growth only when depletions were inefficient. Following optimisation of the depletion protocol, more effective elimination of monocytes did not reduce mycobacterial growth. In keeping with these observations, when the ML ratio was altered artificially, there was a reduction in mycobacterial growth with reduced ML ratio but only up to a point. An ML ratio of 0 (or close to 0) was associated with increased mycobacterial growth again. In three separate experiments, there was a trend towards this 'Goldilocks' effect whereby too few or too many monocytes relative to lymphocytes were associated with poorer mycobacterial control, whereas mid-range ML ratios were associated

with superior inhibition. This is consistent with the work of Naranbhai *et al*, which found that risk of TB disease was significantly higher for patients with ML ratios lower than the 5th percentile or greater than the 95th percentile[374]. In her rabbit experiments, Sabin altered the number of monocytes *in vivo* using A-3 phosphatide or monocyte anti-serum and observed that an artificially low or high ML ratio was associated with lethality of mycobacterial challenge[372]. Finally, in the transcriptomics study of Fletcher *et al*., infants who responded strongly to BCG had a relative abundance of myeloid cells in the peripheral blood. Presence of high numbers, or activation, of these cells was associated with risk of TB disease. In the weaker responders, there were lower numbers of myeloid cells, and activation of these cells (and inflammation) was associated with lack of TB disease (Fletcher *et al*. manuscript submitted). This relationship between extreme ML ratios and mycobacterial growth supports recent evidence that extremes of immunity are associated with TB disease[386,387].

Rather than simply the result of relative abundance, the ontogeny of monocytes and lymphocytes, reflected in their ratio, may affect their ability to respond to mycobacterial infection. Haematopoietic stem cells (HSCs) have distinct lineage biases and may be classified as myeloid-biased, balanced or lymphoid-biased depending on their relative proportions of progeny[388,389]. The frequencies of these cell types likely determines peripheral ML ratio; indeed, myeloid-biased HSCs accumulate with age and explain the relative increase in myeloid cells in blood. A recent study suggests that the ML ratio is affected by inflammatory signals (particularly interferons) through lineage-bias during haematopoiesis, and that this has a lasting effect on the transcriptional and anti-mycobacterial profile of the monocyte progeny (Naranbhai, Fletcher, Tanner *et al*. manuscript submitted). The PBMC MGIT was performed as part of this work, and qualitative differences in monocyte function were found to partially explain the ML ratio association with mycobacterial growth. It would be interesting to explore the functional profile of monocytes in the studies described in this chapter through flow cytometry or gene expression analysis.

Depleting CD4+ or CD8+ T cells did not significantly affect mycobacterial growth in human PBMC or mouse splenocytes, and there was no correlation between the frequency of either cell type and mycobacterial growth in the studies assessed. This was surprising, as Th1 cell mediated immunity is known to be important in protection against TB[106]. There is evidence in the literature that TB disease is worsened in mice depleted of CD4+ T cells *in vivo*[390], and that adoptive transfer of CD4+ T cells from immunised mice protects non-immune mice against *M.tb* challenge[391]. Furthermore, AIDS patients with lowered CD4+ T cell counts have dramatically increased susceptibility to TB disease[88,89]. Evidence for the role of CD8+ T cells is more controversial; as *M.tb* resides in the phagosome of macrophages, it was generally believed that antigens would be preferentially presented by the MHC Class II pathway[392]. However, recent evidence has indicated the presence of CD8+ T cells in TB patients[393-395], which are an integral component of granulomas and could be specific for *M.tb* antigens[396,397]. Flynn *et al*. and others demonstrated the need for an intact MHC Class I pathway in protection of mice against TB disease[143,145,398]. It is also now apparent that CD8+ T cells are potent producers of IFN-γ and actively kill infected cells via the granule-exocytosis pathway[399].

The experiments described used PBMC from healthy human volunteers who had been historically vaccinated with BCG. However, time of vaccination may have been up to 30 years ago, and it is possible that these individuals do not have an effective memory response. Orme has suggested that a possible explanation for the poor efficacy of the BCG vaccine may be a failure to induce T_{CM} cells and thus a long-term cellular response[196]. Indeed, with the exception of a 60-year follow-up study in Alaska[186], no trials of BCG have demonstrated a meaningful reduction in TB incidence maintained for more than 15 years[400-402]. A previous study using the whole blood MGIT assay suggests that CD4+ and CD8+ T cell depletion has an effect in tuberculin-positive donors only[252]. Indeed in the experiment of naïve and BCG vaccinated mice, there was a trend toward increased mycobacterial growth following CD8+ T

cell depletion in the vaccinated mice only. However, CD4+ T cell depletion resulted in a trend toward increased growth in both groups, suggesting a potential role for non-antigen-specific cells. There is evidence in the literature that mycobacteria non-specific CD4+ T cells migrate vigorously through the granuloma following TB infection in mice[403]. It is unclear to what extent the findings in mice may be usefully interpreted, given the small numbers and the problems encountered with the splenocyte MGIT assay.

However, the observed lack of effect of T cell depletions is consistent with similar MGIA studies. Cheon *et al*. found that depletion of either CD4+ T cells or CD8+ T cells alone in the whole blood MGIT assay did not affect *M.tb* growth[252], and Marsay also failed to see an effect of depletions in the splenocyte MGIT (Marsay, unpublished data). In a study by Worku *et al*., enriching PBMC for CD4+ or CD8+ T cells did not reduce mycobacterial growth using the Hoft cultured MGIA[248]. It is possible that the individual effect mediated by each cell type is not strong enough to observe, or that one can compensate for the loss of another (redundancy) - it would be interesting to extend this work to the depletion of multiple cell types in tandem. Indeed in the Cheon study, *M.tb* growth increased significantly when both CD4+ and CD8+ T cells were removed simultaneously[252]. Alternatively, the relationship may be more complex, as with monocytes; depleting different proportions of T cells may help to further understand their contribution. Finally, it is possible that antigen-specific T cells play a lesser role when cultures are challenged with avirulent mycobacteria such as BCG, as in the experiments described. Deletion of several regions occurred during and after the process of BCG attenuation[404], and the lack of immunogenic proteins such as ESAT-6 and HspX may fail to activate an effective specific response. Conducting these experiments with a more virulent strain of *M.tb* such as HN878 (W-Beijing), which is known to induce a potent Th1 response[31], would help to address this possibility. As discussed in section 1.3.2, mice may not be a relevant model for investigating the role of CD8+ T cells as they lack features relating to CD8+ T cell function and specificity such as the cytotoxic protein granulysin[141].

Interestingly, CD16- putative NK cells made a strongly significant negative contribution in the multiple regression analysis of the correlates of risk study. NK cells belong to a newly-described family of immune cells known as innate lymphoid cells (ILCs). ILCs mirror the phenotypes and functions of T cells but do not express acquired antigen receptors or undergo clonal selection and expansion[405]. CD16 is the FcγRIII molecule through which NK cells mediate antibody-dependent cellular cytotoxicity against target cells coated with immunoglobulin G[406]. CD16- NK cells are a relatively small population (~10% of NK cells) about which little is known, although freshly isolated CD16- human NK cells have been shown to be the primary source of NK-cell derived cytokines such as IFN-γ, TNF-α, TNF-β and GM-CSF[70]. It follows that a greater frequency of such cells would be associated with reduced mycobacterial growth, as these cytokines play a role in inducing macrophage activation, cell recruitment and other proinflammatory activities. Concordantly, in a study of NK cell subsets, putative resistant subjects displaying a positive tuberculin skin test (TST+) demonstrated increased levels of CD16- NK cells compared with active TB patients[407]. Unfortunately this data was not available until the latter stages of this project, and it was not possible to further explore the important role of these cells. In future it would be interesting to perform some CD16- NK cell specific depletions or use splenocytes from NK-deficient mice in the MGIT assay.

In the study of BCG vaccination in human volunteers, there was a significant increase in the IFN-γ ELISpot response to PPD following both primary vaccination and revaccination with BCG. The response peaked at 4 weeks post-BCG and returned to baseline by week 24. ELISpot responses were higher in revaccinated volunteers at baseline, week 4 and week 24 post-BCG compared with volunteers receiving primary vaccination. These observations were in keeping with the literature on IFN-γ responses to BCG vaccination and revaccination[408]. Interestingly, the gross patterns of response were similar to those seen in the MGIT assay; peaking at weeks 4 to 8 and returning to baseline by week 24. Furthermore, greater

mycobacterial growth in the naïve vs. historically vaccinated volunteers at baseline was mirrored by a smaller PPD-specific IFN-γ response.

Two correlations were picked up in the human BCG study using the PBMC MGIT assay, but none using the whole blood assay. In the revaccinated group, there was an inverse correlation between mycobacterial growth and PPD-specific IFN-γ ELISpot response at 4 weeks post-BCG, which represented the peak of the ELISpot response. However, given that revaccination did not mediate a reduction in mycobacterial growth, this apparent contribution of the T cell response to control of mycobacterial growth is likely to be modest or partial. In the same group, a direct correlation was seen between IFN-γ response at week 0 and MGIT mycobacterial growth at week 24. Interestingly, a significant increase in mycobacterial growth was observed at week 24 compared with baseline in the revaccinated volunteers using the PBMC MGIT. This suggests that a higher baseline immune response to PPD is associated with a longer term lack of control of mycobacterial growth following BCG revaccination; consistent with *in vivo* reports indicating that a prior immune response to PPD can interfere with the establishment of protective immunity otherwise conferred by BCG vaccination[409]. Such a response may arise from previous BCG vaccination, exposure to environmental mycobacteria, or exposure to *M.tb*. In a study of BCG revaccination in Brazil, efficacy was reduced in older children who were more likely to have a PPD response at time of vaccination, and in cities where there was higher exposure to environmental mycobacteria and *M.tb*[410].

However, overall IFN-γ ELISpot response at most time-points did not correlate with MGIT mycobacterial growth. While revaccination induced a greater number of PPD-specific T cells than primary vaccination, this did not translate into an improved capacity to control mycobacterial growth in the MGIT assay. Similarly, there was no correlation between mycobacterial growth and ELISpot response in the Cynomolgus macaque study. This is consistent with reports of other MGIAs. In 2002, Hoft *et al*. compared the outcomes of three

different growth inhibition assays following BCG vaccination and revaccination in human volunteers. Although IFN-γ levels increased, none of the MGIAs correlated with this response[247]. Similarly, in a study of BCG vaccination in 50 neonates in South Africa, vaccination induced significantly higher IFN-γ production in response to both BCG and PPD but this did not correlate with mycobacterial growth in the *lux* assay[250]. Although BCG vaccination clearly induces a Th1 response, and IFN-γ is known to be essential for immunity against TB[411-413], several reports indicate that it does not correlate with protection and may not be a good measure of vaccine efficacy[225,235,414]. Therefore a lack of association between this measure and the MGIT assay suggests that the assay is providing more information about the complex host-pathogen interactions and could potentially represent a more accurate surrogate of protective immunity.

When recombinant IFN-γ (rIFN-γ) was added to the mouse splenocyte MGIT culture, there was a significant reduction in mycobacterial growth. This supports the idea that IFN-γ is necessary, if not sufficient, for bacterial control following mycobacterial infection. Interestingly, a similar experiment was conducted by Rook *et al*. in the 1980s, culturing human monocytes or murine peritoneal macrophages with *M.tb*. They showed that rIFN-γ increased inhibition of *M.tb* by the murine but not human cells[415]. In some instances, IFN-γ actually enhanced mycobacterial growth in the human cells; a phenomenon also reported by Douvas *et al*. following pre-treatment of human macrophages with rIFN-γ[416]. The importance of IFN-γ in mice has been demonstrated in terms of its ability to induce nitric oxide synthase (NOS2)[417,418], but a non-redundant role in defending humans against *M.tb* is less clear. Although NOS2 is expressed in human TB[419,420], there is no genetic or pharmacological evidence suggesting its contribution to *M.tb* control. It would be interesting to conduct the same rIFN-γ experiment with human PBMC to confirm this species difference, and indeed to explore correlations between mycobacterial growth and IFN-γ responses in the murine model.

Unfortunately the problems encountered with the mouse splenocyte assay have thus far precluded such analysis.

A range of different cytokines were measured following MVA85A vaccination using Luminex analysis of MGIT supernatants. Several cytokines increased in expression at 12 weeks following vaccination, which were a mixture of Th1 (IL-2, IL-12), Th2 (IL-5, IL-9, IL-10), Th17 (IL-15) cytokines and growth factors (TGF-α). This is similar to reports of complex cytokine profiles induced by BCG vaccination[421,422]. As week 12 also represented the peak of the MGIT response, associations between mycobacterial growth and cytokine expression were assessed at this time-point. Mycobacterial growth correlated positively with IFN-γ, TNF-α, IL-12p40, IL-7, IL-1β, GM-CSF, MIP-1α, MDC and Eotaxin; and negatively with IL-8. Proinflammatory cytokines are known to activate infected macrophages and promote stimulation of Th1 cells and CD8+ T cells, so it is perhaps surprising to see a positive correlation with mycobacterial growth. However, this may be the result of increased growth inducing increased cytokine production rather than the inverse - particularly given the late stage in the culture at which cytokines were sampled. It is well-documented that active *M.tb* infection results in increased production of both Th1 and Th2 cytokines *in vivo*[116,423], and a similar effect is proposed *in vitro*. It has been shown that levels of IFN-γ and other cytokines correlate better with bacterial burden than with disease control, and overexpression of proinflammatory cytokines in TB disease has been well-documented[232-234,424].

The negative correlation observed with IL-8 expression is consistent with reports of this chemokine contributing to mycobacterial killing[425]. Increased production of IL-8 by *M.bovis* infected cells has been associated with the recruitment of NK cell subpopulations[426,427], which fits in with the apparent role for NK cells in this assay. Interestingly, sphingosine-1-phosphate (S1P) in serum has been shown to suppress TLR-induced IL-8 secretion from human T cells[428], which may explain some of the serum effects observed in Chapter 1.

When Luminex analysis was repeated on supernatants from the correlates study at baseline, there were significant positive correlations between mycobacterial growth and 75% of the cytokines. This may be due to a larger sample size increasing ability to detect associations, and samples were taken from a different time-point. Where measurable, correlations observed in the previous study were confirmed; again the cytokines represented a complex combination of different arms of the immune response. There were many correlations between different cytokines, with proinflammatory cytokines correlating with Th2, Th17 cytokines and chemokines as well as other Th1 cytokines. This, in addition to the large number of cytokines contributing to each component of the PCA, suggests that different arms of the immune response are highly interlinked. Using stepwise multiple linear regression, a fitted model consisting of IL-10 alone explained 35% of the variance in MGIT outcome. As well as correlating strongly with the MGIT in this study, IL-10 showed significant correlations with all other cytokines measured, highlighting its importance in determining mycobacterial growth. Experimental addition of recombinant IL-10 (rIL-10) to the PBMC MGIT culture also increased growth. These findings are consistent with evidence in the literature that IL-10 has immunosuppressive activity and may contribute to mycobacterial disease. IL-10 has been shown to inhibit T cell proliferation and IFN-γ production, resulting in the down-regulation of macrophage activity[429]. It further compromises macrophage microbicidal mechanisms through inhibition of TNF and NO secretion[136,430], and reduces antigen presentation by down-regulation of costimulatory molecules and MHC class II[431]. There is evidence *in vivo* of IL-10 production in TB patients[432], and gene-disrupted mice have increased resistance to infection[433]. Mice overexpressing IL-10 show increased susceptibility to reactivation of disease, with substantial levels of the cytokine present in the lung lesions[434]. IL-10 is known to be produced by macrophages, DCs, neutrophils, NK cells, T_{regs}, CD4+ T cells and to a lesser extent CD8+ T cells following stimulation[435]. It would be interesting to

determine which cells are important producers of IL-10 in the MGIT assay using flow cytometry.

To further explore the immunoregulatory effects of IL-10, the MGIT assay was performed using human PBMC cultured with or without the addition of rIL-10. Supernatants taken from these cultures at 96 hours were assessed for production of other cytokines. Addition of IL-10 resulted in a significant decrease in expression of TNF-α, MDC and MIP-1α. IL-10 has previously been shown to inhibit the production of TNF-α by macrophage cell lines[436-438], and TNF-α plays an important role in controlling TB disease. TNF induces phagocytosis and killing of mycobacteria by macrophages, and is required for the formation of granulomas which sequester mycobacteria and prevent dissemination[110]. Cases of reactivated latent *M.tb* infection were widely reported following the introduction of anti-TNF-α therapeutic agents for chronic inflammatory conditions such as inflammatory bowel disease[439]. MDC (macrophage-derived chemokine, or CCL22) has previously been shown to be inhibited by IL-10[440]. It plays a crucial role in innate immune recruitment of leukocytes at an infectious focus, and enhances the phagocytic and killing activities of infected macrophages[441]. Also a chemokine, MIP-1α is one of the three major beta-chemokines produced in response to *M.tb* infection and has been shown to suppress intracellular growth of *M.tb* 2 to 3-fold[442]. Thus it is biologically plausible that the down-regulation of these cytokines by rIL-10 would contribute to the increase in mycobacterial growth observed in these cultures. There were also non-statistically significant reductions in other cytokines including IL-8 and IP-10, which likely contribute in a similar manner. MCP-1 was the only measurably cytokine to be increased by addition of IL-10, consistent with reports that this cytokine is strongly secreted by macrophages and up-regulated by IL-10[443,444]. MCP-1 stimulates Th2 polarisation and overexpression of this cytokine results in increased susceptibility to *M.tb* infection in mice[445] and humans[446].

The Luminex analysis for the first two studies indicated correlations between cytokine expression and MGIT mycobacterial growth that were almost exclusively positive. This was surprising, as one might expect to see opposing effects of cytokines with proinflammatory and immunosuppressive roles. It was hypothesised that this was due to the late time-point at which the cytokines were sampled (after 96 hours of culture), by which time the balance may have tipped and increased mycobacterial growth is inducing increased cytokine production rather than increased cytokine production controlling mycobacterial growth. Thus the cytokine profile was assessed at 24-hour intervals throughout the culture. Plausibly, correlations at 24 and 48 hours were predominantly negative, changing to positive by 72 and 96 hours. This follows for proinflammatory cytokines such as IFN-γ, which was significantly associated with reduced mycobacterial growth at 24 hours, and increased mycobacterial growth at 96 hours. A Th1 response induced by mycobacterial infection may initially act to control it, but mycobacterial growth may have overwhelmed the immune response by 96 hours. This does pose the question of whether 96 hours is indeed the optimum period for this assay; experiments comparing the effect of BCG vaccination in cultures of different lengths are warranted. Interestingly, IL-5 and sCD40L, which are both immunoregulatory cytokines, show the inverse pattern with a positive correlation (albeit weak) at 24 hours turning negative by 96 hours.

Four key cytokines were identified which both increased in expression significantly at 48 hours and also inversely correlated with mycobacterial growth at this time-point. These were MDC, PDGF-BB, TGF-α and IL-1Ra. As described, MDC plays an important role in innate immune recruitment of leukocytes at an infectious focus, and enhances the phagocytic and killing activities of infected macrophages[441]. TGF-α and PDGF-BB are both growth factors which may be important in mycobacterial infection. PDGF-BB is significantly elevated in the pleural effusions of TB patients compared with those of healthy controls[447], and has been shown to be upregulated in alveolar macrophages by IFN-γ from PPD-stimulated

lymphocytes[448]. IL-1Ra is a competitive inhibitor of proinflammatory IL-1 bioactivity as it binds to the same receptor, and as such regulates inflammation to prevent cell damage[362]. Both IL-1β and IL-1Ra are strongly induced by *M.tb*, and there is evidence that IL-1Ra polymorphism influences the outcome of infection[449].

The expression of over 2,000 genes from BCG-stimulated PBMC correlated significantly with MGIT mycobacterial growth in the stimulated samples. This large number of genes indicates that mycobacterial growth inhibition is a complex product of many different mechanisms and interactions within the immune system. Many of these genes are known to be important in immunity against *M.tb*, including CD14, HAMP and TREM1. CD14 is expressed predominantly by macrophages and monocytes[450], and this association is in keeping with the previously observed strong relationship between monocyte frequency and mycobacterial growth. Interestingly, the HAMP gene encodes the peptide hormone hepcidin, which is the principal regulator of systemic iron homeostasis and plays a key role in regulating iron storage in macrophages[451]. Hepcidin mediates the destruction of the iron transporter protein ferroportin, resulting in increased iron levels within the macrophage[452]. It is unclear whether the observed relationship is due to increased levels of hepcidin leading to increased iron in the macrophage and therefore enhanced mycobacterial growth; or whether increased mycobacterial growth stimulates hepcidin production as an (in this case seemingly misdirected) immune mechanism. Indeed, it has been shown that hepcidin is upregulated in macrophages in response to mycobacteria and IFN-γ in both mice and humans[361,453]. Either way, this was an interesting finding given the role of iron identified in the previous chapter. Furthermore, significant positive correlations were observed with the haemoglobin-related genes HBB, HBA1 and HBA2 which supports the findings of chapter 5. It is not clear why this effect is still present in the PBMC MGIT, but PBMC may retain some residual effect of haemoglobin expression that occurred in whole blood. TREM1 (triggering receptor expressed on myeloid cells-1) is a glycoprotein specifically expressed on the surface of macrophages

and neutrophils. Increased expression of TREM1 was associated with increased mycobacterial growth, consistent with *in vivo* data indicating that higher serum levels of soluble TREM1 lead to poorer prognosis in pulmonary TB[367].

Pathway analysis was applied in an attempt to break down this data in a functional sense. Encouragingly, genes which correlated with mycobacterial growth were found to be significantly enriched for the 'immune response' pathway. This pathway comprised many genes known to be important in immunity against *M.tb*, including CD14 and HAMP. HLADRB5 was the only gene in the immune response pathway to show an inverse correlation with mycobacterial growth. This gene encodes the HLA class II histocompatibility antigen (HLA), DRB5 beta chain which makes up part of the class II molecule, anchored to the cell membrane. HLA class II plays a central role in the immune system, presenting peptides from extracellular proteins on the surface of APCs such as macrophages; and mycobacterial antigens/peptides have been shown to be presented in association with HLA-DR in particular[454]. Increased expression of this gene may thus be associated with increased antigen presentation and Th1 cell activation and a consequent reduction in mycobacterial growth.

Unfortunately it was not possible to validate these genes in a second cohort of 20 infants from the same population. The low yields of RNA observed may have been due to poor sample handling in South Africa, as although use of stored samples for exploratory immunological analysis was ethically approved, these samples were not originally collected, processed or stored with gene expression analysis in mind. The use of a stabilising reagent such as TRIzol, RNAlater or PrepProtect may have improved RNA yield and quality[455]. Furthermore, cell viability following thawing was particularly low in these samples, which may have preferentially affected functionality of specific cell types. A correlation has been reported between the expression of defined genes in RNA isolates and the representation of cell types in the corresponding sample[456]. That expression of GAPDH was detectable indicates that

cDNA was present following RNA extraction and conversion, but expression of the target genes would be lower than this constitutively highly expressed housekeeper and were thus not measurable. This experiment will be repeated using an alternative sample set. It would also be interesting to explore gene associations with mycobacterial growth in other populations with different HLA types, as these studies were conducted in South African infants only.

Despite the complex nature of the immune response to mycobacteria and the many components constituting the functional response observed in the MGIT assay, some key mechanisms have been identified in this chapter. Importantly, the number of monocytes and ML ratio are critical determinants of how well mycobacterial growth is controlled, together with the production of cytokines such as IL-10 and IFN-γ. It is likely that different mechanisms mediate mycobacterial growth inhibition in different species. Although the human and NHP responses to mycobacteria bear a high degree of similarity, recent genome-wide studies have identified species-specific immune differences, and relative cell frequencies and marker expression have been shown to differ[457,458]. In mice, nitric oxide (NO) plays a pivotal role in mycobacterial killing by monocytes, whereas its contribution in humans is controversial[459]. Furthermore, IFN-γ appears to affect mycobacterial growth differently in humans and mice in the studies of Crowle described above[243]. It will be necessary to consider immune mechanisms across species as well as further exploring those already identified.

6.6 Conclusions

- Monocyte frequency is a critical determinant of mycobacterial growth inhibition as measured by the MGIT assay.
- ML ratio is also a correlate of *in vitro* growth, demonstrating a 'Goldilocks' effect whereby too few or too many monocytes relative to lymphocytes is associated with poorer mycobacterial control, whereas mid-range ML ratios are associated with superior inhibition (in keeping with *in vivo* findings in the literature).
- Depleting CD4+ or CD8+ T cells alone did not impact MGIT mycobacterial growth, although conclusions cannot be drawn regarding their importance in this assay given the limited data obtained.
- Mycobacterial growth inhibition does not correlate with IFN-γ ELISpot response. Given that IFN-γ does not correlate with protection, the MGIT assay may be providing more information about the complex host-pathogen interactions involved and could potentially represent a more accurate surrogate of protective immunity.
- Cytokines correlating with mycobacterial growth represent a complex mixture of Th1, Th2, Th17 cytokines, growth factors and chemokines, with the immunosuppressive cytokine IL-10 appearing to play a central role.
- The expression of many genes correlated with mycobacterial growth, and these were significantly enriched for the 'immune response' pathway. This pathway included a number of genes known to be important in immunity against *M.tb*, including CD14 and HAMP; further supporting the influence of monocytes and iron.

Conclusions and Future Directions

7 Conclusions and future directions

7.1 Summary

With the emergence of drug-resistant strains, the spread of HIV and increased immigration, infection with *M.tb* continues to pose a major global health and socioeconomic threat. Although the BCG vaccine confers reliable protection against disseminated TB during childhood, protection against adult pulmonary disease varies dramatically, with the lowest efficacies found in the tropics where TB incidence is greatest. Development of an improved vaccine is paramount. Candidate vaccines are currently tested using preclinical animal models such as mice, guinea pigs and non-human primates. However, such early testing requires the use of large numbers of animals, long costly experiments and highly specialised facilities. Furthermore, animal models can be extremely variable and it remains unclear whether successful outcomes are predictive of efficacy or even safety in humans. Arguably the greatest challenge in developing an *in vitro* alternative to animal models in the TB vaccine field, or indeed in developing a vaccine itself, is the lack of a single parameter which robustly correlates with protection. Although IFN-γ is known to be essential for immunity against TB, and is widely used as the primary immunological readout in vaccine studies, it fails to correlate with protection. Furthermore, it has recently been shown that the frequency and extended cytokine profile of *M.tb* specific T cells does not allow differentiation between protected and non-protected infants.

There is much interest in emerging 'functional assays' which take into account a whole range of immune mechanisms, such as mycobacterial growth inhibition assays (MGIAs). The output from such an assay, or an underlying immune mechanism that is identified, may represent a biomarker of protective efficacy. The use of a validated, strong surrogate of protection in place of animal models for the down-selection of new TB vaccine candidates at

an early preclinical stage would significantly reduce the numbers of animals used in TB challenge experiments and accelerate vaccine development by shortening clinical trials. Although several groups have demonstrated the potential use of MGIAs, they have not been adopted by vaccine developers, in part due to concerns regarding reproducibility and transferability. Having attempted to transfer some of these assays in the host group, the whole blood MGIT assay developed by Wallis *et al*. was selected for its superior reproducibility, relative simplicity and highly sensitive quantitative output. It was decided to develop a PBMC-based adaptation to enable retrospective study of cryopreserved trial samples, for the logistical advantages of batching samples, and the relevance of the cellular compartment to vaccine efficacy.

Though problems were initially encountered with intra-assay variability, this was improved by various optimisation steps. The PBMC MGIT assay had reduced inter-assay variability and was better able to detect a BCG-induced vaccine effect in humans compared with the whole blood assay. Both assays successfully detected a response to BCG in non-human primates, and a correlation was observed between *in vitro* MGIT outcome and *in vivo* protection from BCG challenge. The mouse splenocyte MGIT produced varying results, with issues encountered in the latter stages of the project. A range of experiments were performed to elucidate the whole blood mechanisms influencing mycobacterial growth and the immune mechanisms underlying growth inhibition in the PBMC MGIT assay. Haemoglobin was found to be an important confounder in whole blood, and monocytes and CD16- putative NK cells were the major cellular subsets influencing mycobacterial growth in PBMC.

7.2 Main Findings

A novel PBMC based adaptation of the Wallis MGIT assay was developed and performed alongside the original whole blood protocol using samples from healthy volunteers. Variability was assessed by repeated baseline sampling. Inter-assay variability was greater in the whole blood compared with the PBMC assay; likely due to the need for real-time sampling with whole blood while PBMC may be cryopreserved and run in a single batch. However, the PBMC assay had greater intra-assay variability, and different assay conditions were tested in an attempt to reduce this. By optimising pre-culture conditions, mycobacterial inoculum and stock preparation, culture conditions and 96-hour processing steps, intra-assay variability was considerably improved and this protocol was taken forward for testing in different species.

In a clinical trial of primary BCG vaccination and revaccination in healthy UK adults, the whole blood MGIT assay detected a modest reduction in mycobacterial growth at 8 weeks post-primary BCG in the naïve volunteers. However, the PBMC assay detected a greater response at both 4 and 8 weeks post-primary BCG in the same group. There was no effect of revaccination using either assay. This suggests that the PBMC assay has greater sensitivity to detect a vaccine response; PBMC may represent a 'cleaner' compartment without the potentially confounding factors present in whole blood. When the PBMC MGIT assay was applied to samples from the MVA85A phase IIb efficacy trial in South African infants, no differences in mycobacterial growth were observed between placebo and MVA85A vaccinated infants, or between pre- and 4 weeks post-vaccination for either group. This was consistent with the *in vivo* outcome of the trial, in which MVA85A did not confer greater protection over BCG. There was also no difference in MGIT outcome between infants who went on to develop TB disease and those who did not, suggesting that the assay may not represent a correlate of protection. This may be due to the small sample size (as few infants

developed disease by the stringent end-point definition) or the sensitivity of the assay not being great enough with more optimisation work required. Indeed the window of difference between mycobacterial growth in samples pre- and post-BCG was relatively small, and conditions such as the MOI may need to be further explored to maximise this sensitivity. Alternatively, the PBMC compartment may lack an immune component important in mediating protection such as antibodies - indeed antigen-85A specific IgG at week 4 was one of the few correlates of risk of TB disease identified in this study (Fletcher *et al*. manuscript submitted).

The whole blood MGIT assay performed well in non-human primates, where a large effect of BCG vaccination was detected in both Rhesus and Cynomolgus macaques. Importantly, there was a significant correlation between *M.tb* MGIT at peak of response and *in vivo* protection from BCG challenge, as measured by lymph node CFU. Furthermore, this was at an individual level, which is a far more rigorous measure of association than correlation at the between-group level. This suggests that the assay may in fact have promise as a correlate of protection; differences between this and the infant efficacy study include the use of whole blood and *in vitro* infection with *M.tb* rather than BCG (though there was a trend toward a correlation using BCG, and outcomes using BCG and *M.tb* were shown to correlate in chapter 1).

Results of the murine splenocyte assay were disappointing, as it was initially able to pick up an effect of BCG vaccination, but this was lost in later experiments. This may be due to a change in BCG strain used and the effect of residual BCG recovered from the spleens of vaccinated mice. Alternatively, there may have been an issue with splenocyte viability or performance of the Bactec MGIT machine. These possibilities are currently being investigated. However, prior to these issues, the assay was applied to the pre-clinical testing of a novel TB vaccine candidate. Although a correlation between group medians was not statistically significant, there was a clear trend and distinct similarities between the *in vitro*

MGIT and *in vivo* challenge results. Although the MGIT appeared less sensitive than *in vivo* challenge, the observation of similar patterns between groups is promising; particularly given the limitation of small group size in this study.

Due to the observed discrepancy between whole blood and PBMC MGIT outcome, the next stage of the project concentrated on identifying blood components that influence mycobacterial growth. Neutrophils did not appear to be an important determinant, which was surprising as one might consider this cell type the major difference between the compartments. Furthermore, antibodies did not seem to play a role; there was no induction of specific IgG observed following BCG vaccination, no correlation with mycobacterial growth and no effect of total IgG depletion. This was not consistent with the findings of the correlates study where IgG was found to be a determinant of risk. However, as discussed there were some important differences including the time-point, antibody specificity and population studied. Heat inactivation of serum reduced mycobacterial growth, and this was associated with a reduction in uptake into monocytes. This may be due to the destruction of opsonising complement components. A surprising discovery was the large effect of haemoglobin level, which may alter mycobacterial growth by determining iron availability. A correlation was observed between mean corpuscular haemoglobin and MGIT outcome in the human BCG study, and artificially supplementing cultures with haemoglobin increased mycobacterial growth across species. These findings suggest that haemoglobin is a potential confounder to whole blood assays of bacterial killing and this should be taken into account when interpreting results. Overall, this work indicates that the PBMC compartment may be preferable for the assessment of vaccine efficacy, as haemoglobin is removed as a confounder, autologous serum may not be important (though this may be specific to the assessment of BCG in healthy UK adults), and induction of a durable memory response is more relevant than innate factors such as neutrophils.

The final portion of this project aimed to gain a further understanding of the immune mechanisms underlying mycobacterial growth inhibition *in vitro*, concentrating on the PBMC MGIT assay. The major finding was a critical role for monocytes in determining the outcome of the assay: monocyte frequency correlated with mycobacterial growth across different populations, and multiple regression analysis of the correlates of risk study data revealed monocytes as a major contributing factor. A complex association between mycobacterial growth and ML ratio was observed, with few or too many monocytes relative to lymphocytes associated with poorer mycobacterial control, and mid-range ML ratios associated with superior inhibition. This is consistent with recent literature on the ML ratio both in TB and other diseases.

Depleting CD4+ or CD8+ T cells alone did not impact mycobacterial growth, suggesting that these cell types are not important determinants of control in this assay, or follow a more complex pattern. CD16- NK cells were found to be a major contributor to MGIT variance, which is interesting as they are a little-studied cell subset of modest proportions. Mycobacterial growth inhibition did not correlate with the IFN-γ ELISpot response, in keeping with other MGIAs in the literature. This suggests that the MGIT assay is providing more information about the functional response as a whole and could potentially represent a more accurate surrogate of protective immunity. Using Luminex analysis, many cytokines were found to correlate with mycobacterial growth, and these represented a complex mix of Th1, Th2 and Th17 cytokines, growth factors and chemokines. The immunoregulatory cytokine IL-10 was found to play a central role, and influenced the levels of other cytokines in the culture. The genes correlating with mycobacterial growth also represented a complex mixture, but were shown by pathways analysis to be significantly enriched for the 'immune response' pathway. This pathway included a number of genes known to be important for immunity against *M.tb*, including HAMP and CD14, further supporting the influence of iron and monocytes in this assay.

7.3 Future directions

7.3.1 Optimisation of the MGIT assay

It has been suggested that the window of difference between mycobacterial growth in naïve and vaccinated samples should be at least as great as that seen in *in vivo* challenge models to justify the replacement of *M.tb* challenge in preclinical development. Although the assay was able to detect a response in most of the experiments in this project, the window of difference was approximately 0.2 $\Delta\log_{10}$ CFU, while *in vivo* challenge in the mouse sees differences of around 1 $\log_{10}$ CFU in the spleen and lung. The Fletcher group at LSHTM and the Morris group at the FDA have observed differences of up to 0.7 $\Delta\log_{10}$ CFU using the splenocyte MGIT assay (private communication), indicating that there is potential to improve on the Oxford findings. Further optimisation of the assay, for example through fine-tuning of the MOI and culture period, may increase this difference and provide a more sensitive measure. Clearly more work needs to be done to understand and rectify the issues that arose with the murine splenocyte assay. Potential problems with cell viability must be addressed, and the introduction of gas exchange may be necessary (for example by using plates rather than sealed tubes). A gentler rotation method may be more suitable for this cell type, as used by the FDA group. Ensuring that there is no residual BCG present in the splenocytes of vaccinated mice may also improve the outcome of the assay. This could be achieved through different vaccination routes, the use of different BCG stocks or number of CFU per vaccination.

7.3.2 Biological validation by correlation with *in vivo* protection

The utility of the MGIT assay in vaccine testing may only be determined through biological validation to demonstrate that the assay is measuring something meaningful in terms of protection from TB. A degree of biological validation was achieved in this project, as a correlation was observed between the *in vitro* MGIT response and *in vivo* protection from

BCG challenge in NHPs. Using mouse splenocytes, a difference was detected between naïve and BCG vaccinated animals in accordance with *in vivo* challenge of experimentally-matched mice. Furthermore, there was a similar pattern between groups in a preclinical mouse study of a novel TB vaccine candidate. In humans, an effect of primary BCG vaccination but not revaccination was consistent with epidemiological data in this population. The lack of an effect in the MGIT assay following MVA85A in BCG-vaccinated South African infants was in concordance with the *in vivo* findings of the efficacy trial. However, further validation is required, particularly with respect to *M.tb* rather than BCG challenge in animal models. Unfortunately, this was planned for the testing of vaccines with varying efficacies in the mouse model, but due to the problems encountered this was not possible. If these issues can be resolved, validation should remain a priority.

7.3.3 Testing novel TB vaccine candidates

The vaccine candidates MVA85A and the NIBSC candidate were tested using the MGIT assay as part of this project. Again, issues with the murine splenocyte assay precluded the testing of other preclinical vaccine candidates as planned. Ongoing studies in the host group of novel candidates comprising ChAdOx with various antigens in mice alongside *in vivo* challenge would provide an excellent sample base for this work. PBMC are also available from Public Health England from a study of 16 Rhesus macaques comparing different vaccine regimens which mediated different levels of protection *in vivo*. The NHP PBMC MGIT assay requires further optimisation before these samples are applied.

7.3.4 Elucidating the immune mechanisms underlying growth inhibition

Several important immune mechanisms were identified in this project, but further work is required to complete the story. Crucially, CD16- NK cells were identified as a major contributor to MGIT variance in the correlates of risk study in SA infants, but there was not time to further investigate their role. It would be interesting to do some cell depletion studies

to confirm their function. Furthermore, as these cells are prolific cytokine-producers, Luminex analysis could be performed in their presence and absence to define their cytokine output alongside flow cytometry to determine the influence this has on the frequency and phenotype of other cellular subsets. Recent work by Riley *et al*. has suggested that NK cells may have a CD4+ T cell-dependent activity following vaccination (unpublished data); thus the pre-BCG CD4+ T cell subset could be sorted and added to post-BCG CD4+ T cell depleted samples to determine whether NK cell IFN-γ secretion is dependent on this vaccine response. Although antibodies did not appear to affect mycobacterial growth in the population studied (healthy UK adults), it is important to determine whether this is true for other populations such as SA infants, where antibody titre represented a correlate of risk in the study described.

It was found that IL-10 played an important role in determining mycobacterial growth, and it is necessary to determine which cells are major producers of this cytokine in the MGIT culture. This could be achieved through flow cytometry. Further studies could be conducted using the splenocytes from IL-10 KO and wildtype mice looking at their relative ability to control mycobacterial growth. Another interesting finding was that the heat inactivation of serum reduces mycobacterial growth by a mechanism that appears to involve decreased uptake by monocytes. The BCG-GFP model used in these experiments requires further optimisation, such as determining culture time. Although a culture of just 1 hour was sufficient to detect a modest effect, this could be increased to maximise the differences observed. Furthermore, although complement is likely to be mediating this response, this was not demonstrated by these experiments. Adding different complement proteins back in to heat inactivated serum would allow confirmation of this hypothesis and also the relevant proteins to be defined. Alternatively, specific components of complement could be depleted from normal serum using antibodies.

One crucial future direction is to consider immune mechanisms in the context of vaccination. For example, while monocytes or NK cells are clearly an important determinant in mycobacterial growth, how does their frequency and phenotype alter pre- and post-vaccination, and does this drive the vaccine-induced difference in MGIT outcome? The same applies to the cytokines and genes identified in chapter 6.

7.4 Concluding words

Functional assays are notoriously difficult to work with, as they represent a complex sum of the parts and all their interactions rather than a straightforward read-out of one response such as IFN-γ. Growth inhibition assays in both malaria and HIV disease models have involved a protracted and laborious process of development, optimisation and validation. Given the slow-growing, fastidious nature of mycobacteria and the complexity of challenge models, developing a mycobacterial growth inhibition assay is an ambitious task. However, with the lack of an immune correlate of protection from TB severely hampering development of an effective vaccine, such an assay could be game-changing in the field.

The utility of an MGIA is two-fold: evaluating vaccine efficacy *in vitro* and determining the immune mechanisms involved in mycobacterial growth inhibition. The latter would aid in a better understanding of the immune response to TB as a whole, directing future design of more effective vaccines. This project reports some preliminary findings regarding immune mechanisms which warrant further investigation and validation across species.

As with all functional assays, problems with variability are the main barrier to effective discriminant validity. Although optimisation work was performed to improve reproducibility, the complexity of the biological response limits the extent to which this may be achieved. It then becomes a question of power, whereby larger sample sizes may be required to see a vaccine effect. However, even with the small numbers employed in this project, it has been

demonstrated that the MGIT assay has the ability to detect a vaccine-induced response and represents a potential surrogate of protection from TB.

A BCG-induced reduction in mycobacterial growth was detected in humans, NHPs and mice. A correlation was observed between the *in vitro* MGIT response and *in vivo* protection from challenge in the mouse and NHP models. There was also concordance between the *in vitro* MGIT response and epidemiological data or *in vivo* outcome of the efficacy trial in humans. Although further work is needed, this assay has the potential to be applied in preclinical vaccine testing, reducing the number of animals used in TB challenge experiments and accelerating the development of an effective vaccine.

8 Appendix

8.1 MGIT standard curve

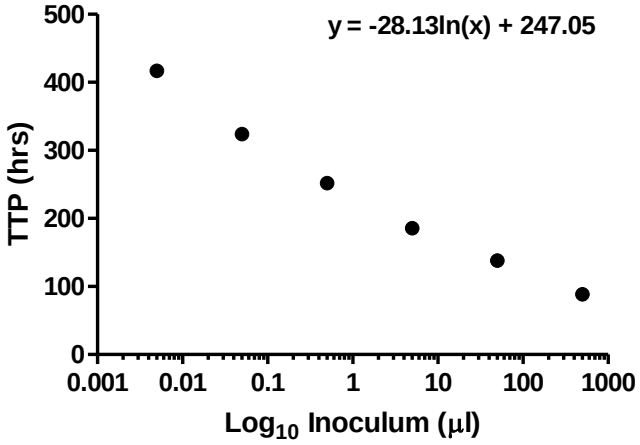

Figure 8-1 MGIT Standard curve. A standard curve was created using the inoculum volume against time to positivity (TTP) values and an equation calculated in the form of y = m (ln x) + c where y = TTP, m = slope and c = the y-intercept (logarithmic straight line).

Example calculation of 'Net Growth' value (given the above stock of $3.5x10^4$ CFU/ml):

1) TTP (control) = 9 days 23 hours, 9 days 21 hours. Mean TTP = 238 hrs

   TTP (sample) = 8 days 12 hours, 8 days 14 hours. Mean TTP = 205 hrs

2) Apparent inoculum volume (control) = EXP((238-247.05)/(-28.13)) = 1.38µl

   Apparent inoculum volume (sample) = EXP((205-247.05)/(-28.13)) = 4.46µl

3) Apparent CFU input (control) = 1.38 x 35 = 48.3

   Apparent CFU input (sample) = 4.46 x 35 = 156.1

4) Log_{10} CFU (control) = 1.68

   Log_{10} CFU (sample) = 2.19

5) Log_{10} CFU (sample) - Log_{10} CFU (control) = 2.19 - 1.68 = **0.51**

8.2 Flow cytometry panels

A

Marker	Colour	Vol/test (µl)
CD3	AF-700	0.5
CD4	APC	2
CD8	EF-NC605	2
CD14	PE/Cy7	2

B

Marker	Colour	Vol/test (µl)
CD3	PB	0.4
CD4	EF-NC650	0.13
CD8	APC EF-780	0.4
CD11b	APC	0.4

Table 8-1 Flow cytometry panels used in this project. $1x10^6$ cells/well were resuspended in 50µl/well of surface staining mix containing the stated antibody cocktail suspended in PBS/BSA for A) humans and B) mice.

8.3 Definition of primary endpoint (1) of TB disease in the MVA85A efficacy trial

Any of the following criteria:

- Isolation of Mycobacterium tuberculosis from any site
- Identification of M tuberculosis by an approved molecular diagnostic technique from any site
- Histopathology diagnostic for tuberculosis disease (eg, caseating granulomas)
- Choroidal tubercle diagnosed by an ophthalmologist
- Miliary pattern on chest radiograph in an HIV-negative infant
- Clinical diagnosis of tuberculous meningitis (cerebrospinal fluid protein concentrations >0·6 g/L and pleocytosis of >50 cells per µL with >50% mononuclear cells) with features of basal meningeal enhancement and hydrocephalus on head CT
- Vertebral spondylosis
- One smear or histology specimen positive for auramine-positive bacilli from a normally sterile body site

- One of each of the following:
- Evidence of mycobacterial infection defined as two acid-fast positive smears (each from a separate collection) that were morphologically consistent with mycobacteria from either sputum or gastric aspirate that were not found to be non-tuberculous mycobacteria bacteria on culture; QuantiFERON-TB Gold In-tube test conversion from negative to positive; or tuberculin skin test ≥15 mm

and

- Radiographic findings compatible with tuberculosis defined as ≥1 of the following factors identified independently by at least two of three paediatric radiologists serving on a masked review panel: calcified Ghon focus, pulmonary cavity, hilar or mediastinal adenopathy, pleural effusion, or airspace opacification

and

- Clinical manifestations compatible with tuberculosis defined as cough without improvement for >2 weeks; weight loss of >10% of bodyweight for >2 months; or failure to thrive, defined as crossing >1 complete major centile band (<97th–90th, <90th–75th, <75th–50th, <50th–25th, <25th–10th, and <10th–3rd weight-for-age centiles) downward for >2 months.

(Adapted from Tameris *et al*. 2013[219])

References

1 Daniel, T. M. The history of tuberculosis. *Respir Med* **100**, 1862-1870, doi:10.1016/j.rmed.2006.08.006 (2006).

2 Fogel, N. Tuberculosis: A disease without boundaries. *Tuberculosis (Edinb)* **95**, 527-531, doi:10.1016/j.tube.2015.05.017 (2015).

3 Keshavjee, S. & Farmer, P. E. Tuberculosis, drug resistance, and the history of modern medicine. *N Engl J Med* **367**, 931-936, doi:10.1056/NEJMra1205429 (2012).

4 WHO. (World Health Organisation (WHO) Tuberculosis Fact Sheet, Reviewed March 2014).

5 Munro, S. A. *et al.* Patient adherence to tuberculosis treatment: a systematic review of qualitative research. *PLoS Med* **4**, e238, doi:10.1371/journal.pmed.0040238 (2007).

6 WHO. (World Health Organisation (WHO) Global Tuberculosis Report, 2014).

7 Connolly, M. & Nunn, P. Women and tuberculosis. *World Health Stat Q* **49**, 115-119 (1996).

8 Molina, R. L., Diouf, K. & Nour, N. M. Tuberculosis and the obstetrician-gynecologist: a global perspective. *Rev Obstet Gynecol* **6**, 174-181 (2013).

9 Alcaïs, A., Fieschi, C., Abel, L. & Casanova, J. L. Tuberculosis in children and adults: two distinct genetic diseases. *J Exp Med* **202**, 1617-1621, doi:10.1084/jem.20052302 (2005).

10 Zumla, A., Malon, P., Henderson, J. & Grange, J. M. Impact of HIV infection on tuberculosis. *Postgrad Med J* **76**, 259-268 (2000).

11 Bates, M., Marais, B. J. & Zumla, A. Tuberculosis Comorbidity with Communicable and Noncommunicable Diseases. *Cold Spring Harb Perspect Med*, doi:10.1101/cshperspect.a017889 (2015).

12 Kwan, C. K. & Ernst, J. D. HIV and tuberculosis: a deadly human syndemic. *Clin Microbiol Rev* **24**, 351-376, doi:10.1128/CMR.00042-10 (2011).

13 Whalen, C. *et al.* Accelerated course of human immunodeficiency virus infection after tuberculosis. *Am J Respir Crit Care Med* **151**, 129-135, doi:10.1164/ajrccm.151.1.7812542 (1995).

14 WHO. (World Health Organisation Collaborative Framework for Care and Control of Tuberculosis and Diabetes, 2014).

15 Dye, C., Lönnroth, K., Jaramillo, E., Williams, B. G. & Raviglione, M. Trends in tuberculosis incidence and their determinants in 134 countries. *Bull World Health Organ* **87**, 683-691 (2009).

16 Faustini, A., Hall, A. J. & Perucci, C. A. Risk factors for multidrug resistant tuberculosis in Europe: a systematic review. *Thorax* **61**, 158-163, doi:10.1136/thx.2005.045963 (2006).

17 Lucas, S. B. *The biology of the mycobacteria*. (1989).

18 Niederweis, M., Danilchanka, O., Huff, J., Hoffmann, C. & Engelhardt, H. Mycobacterial outer membranes: in search of proteins. *Trends Microbiol* **18**, 109-116, doi:10.1016/j.tim.2009.12.005 (2010).

19 Parish, T. & Stoker, N. G. Mycobacteria: bugs and bugbears (two steps forward and one step back). *Mol Biotechnol* **13**, 191-200, doi:10.1385/MB:13:3:191 (1999).

20 Gopinath, K. & Singh, S. Non-tuberculous mycobacteria in TB-endemic countries: are we neglecting the danger? *PLoS Negl Trop Dis* **4**, e615, doi:10.1371/journal.pntd.0000615 (2010).

21 Johnson, M. M. & Odell, J. A. Nontuberculous mycobacterial pulmonary infections. *J Thorac Dis* **6**, 210-220, doi:10.3978/j.issn.2072-1439.2013.12.24 (2014).

22 Sexton, P. & Harrison, A. C. Susceptibility to nontuberculous mycobacterial lung disease. *Eur Respir J* **31**, 1322-1333, doi:10.1183/09031936.00140007 (2008).

23 Wirth, T. *et al.* Origin, spread and demography of the Mycobacterium tuberculosis complex. *PLoS Pathog* **4**, e1000160, doi:10.1371/journal.ppat.1000160 (2008).

24 Allix-Béguec, C. *et al.* Importance of identifying Mycobacterium bovis as a causative agent of human tuberculosis. *Eur Respir J* **35**, 692-694, doi:10.1183/09031936.00137309 (2010).
25 Park, D. *et al.* Tuberculosis due to Mycobacterium bovis in patients coinfected with human immunodeficiency virus. *Clin Infect Dis* **51**, 1343-1346, doi:10.1086/657118 (2010).
26 Cole, S. T. *et al.* Deciphering the biology of Mycobacterium tuberculosis from the complete genome sequence. *Nature* **393**, 537-544, doi:10.1038/31159 (1998).
27 Kolattukudy, P. E., Fernandes, N. D., Azad, A. K., Fitzmaurice, A. M. & Sirakova, T. D. Biochemistry and molecular genetics of cell-wall lipid biosynthesis in mycobacteria. *Mol Microbiol* **24**, 263-270 (1997).
28 Gagneux, S. Host-pathogen coevolution in human tuberculosis. *Philos Trans R Soc Lond B Biol Sci* **367**, 850-859, doi:10.1098/rstb.2011.0316 (2012).
29 Manabe, Y. C. *et al.* Different strains of Mycobacterium tuberculosis cause various spectrums of disease in the rabbit model of tuberculosis. *Infect Immun* **71**, 6004-6011 (2003).
30 Gopal, R. *et al.* Unexpected role for IL-17 in protective immunity against hypervirulent Mycobacterium tuberculosis HN878 infection. *PLoS Pathog* **10**, e1004099, doi:10.1371/journal.ppat.1004099 (2014).
31 Ordway, D. *et al.* The hypervirulent Mycobacterium tuberculosis strain HN878 induces a potent TH1 response followed by rapid down-regulation. *J Immunol* **179**, 522-531 (2007).
32 Kieser, K. J. & Rubin, E. J. How sisters grow apart: mycobacterial growth and division. *Nat Rev Microbiol* **12**, 550-562, doi:10.1038/nrmicro3299 (2014).
33 Orme, I. M. A new unifying theory of the pathogenesis of tuberculosis. *Tuberculosis (Edinb)* **94**, 8-14, doi:10.1016/j.tube.2013.07.004 (2014).
34 Ernst, J. D. The immunological life cycle of tuberculosis. *Nat Rev Immunol* **12**, 581-591, doi:10.1038/nri3259 (2012).
35 Lin, P. L. & Flynn, J. L. Understanding latent tuberculosis: a moving target. *J Immunol* **185**, 15-22, doi:10.4049/jimmunol.0903856 (2010).
36 Tiemersma, E. W., van der Werf, M. J., Borgdorff, M. W., Williams, B. G. & Nagelkerke, N. J. Natural history of tuberculosis: duration and fatality of untreated pulmonary tuberculosis in HIV negative patients: a systematic review. *PLoS One* **6**, e17601, doi:10.1371/journal.pone.0017601 (2011).
37 Golden, M. P. & Vikram, H. R. Extrapulmonary tuberculosis: an overview. *Am Fam Physician* **72**, 1761-1768 (2005).
38 Lee, J. Y. Diagnosis and treatment of extrapulmonary tuberculosis. *Tuberc Respir Dis (Seoul)* **78**, 47-55, doi:10.4046/trd.2015.78.2.47 (2015).
39 Sharma, S. K., Mohan, A. & Sharma, A. Challenges in the diagnosis & treatment of miliary tuberculosis. *Indian J Med Res* **135**, 703-730 (2012).
40 Kimbrell, D. A. & Beutler, B. The evolution and genetics of innate immunity. *Nat Rev Genet* **2**, 256-267, doi:10.1038/35066006 (2001).
41 van Crevel, R., Ottenhoff, T. H. & van der Meer, J. W. Innate immunity to Mycobacterium tuberculosis. *Clin Microbiol Rev* **15**, 294-309 (2002).
42 de Chastellier, C. The many niches and strategies used by pathogenic mycobacteria for survival within host macrophages. *Immunobiology* **214**, 526-542, doi:10.1016/j.imbio.2008.12.005 (2009).
43 Sia, J. K., Georgieva, M. & Rengarajan, J. Innate Immune Defenses in Human Tuberculosis: An Overview of the Interactions between Mycobacterium tuberculosis and Innate Immune Cells. *J Immunol Res* **2015**, 747543, doi:10.1155/2015/747543 (2015).
44 Ernst, J. D. Macrophage receptors for Mycobacterium tuberculosis. *Infect Immun* **66**, 1277-1281 (1998).
45 Luzio, J. P., Pryor, P. R. & Bright, N. A. Lysosomes: fusion and function. *Nat Rev Mol Cell Biol* **8**, 622-632, doi:10.1038/nrm2217 (2007).

46 van der Wel, N. *et al.* M. tuberculosis and M. leprae translocate from the phagolysosome to the cytosol in myeloid cells. *Cell* **129**, 1287-1298, doi:10.1016/j.cell.2007.05.059 (2007).
47 Crowle, A. J., Dahl, R., Ross, E. & May, M. H. Evidence that vesicles containing living, virulent Mycobacterium tuberculosis or Mycobacterium avium in cultured human macrophages are not acidic. *Infect Immun* **59**, 1823-1831 (1991).
48 Clemens, D. L. & Horwitz, M. A. Characterization of the Mycobacterium tuberculosis phagosome and evidence that phagosomal maturation is inhibited. *J Exp Med* **181**, 257-270 (1995).
49 Ferrari, G., Langen, H., Naito, M. & Pieters, J. A coat protein on phagosomes involved in the intracellular survival of mycobacteria. *Cell* **97**, 435-447 (1999).
50 Armstrong, J. A. & Hart, P. D. Phagosome-lysosome interactions in cultured macrophages infected with virulent tubercle bacilli. Reversal of the usual nonfusion pattern and observations on bacterial survival. *J Exp Med* **142**, 1-16 (1975).
51 Lee, B. Y., Clemens, D. L. & Horwitz, M. A. The metabolic activity of Mycobacterium tuberculosis, assessed by use of a novel inducible GFP expression system, correlates with its capacity to inhibit phagosomal maturation and acidification in human macrophages. *Mol Microbiol* **68**, 1047-1060, doi:10.1111/j.1365-2958.2008.06214.x (2008).
52 Geijtenbeek, T. B. *et al.* Mycobacteria target DC-SIGN to suppress dendritic cell function. *J Exp Med* **197**, 7-17 (2003).
53 Tailleux, L. *et al.* Constrained intracellular survival of Mycobacterium tuberculosis in human dendritic cells. *J Immunol* **170**, 1939-1948 (2003).
54 Lozza, L. *et al.* Communication between Human Dendritic Cell Subsets in Tuberculosis: Requirements for Naive CD4(+) T Cell Stimulation. *Front Immunol* **5**, 324, doi:10.3389/fimmu.2014.00324 (2014).
55 Hanekom, W. A. *et al.* Mycobacterium tuberculosis inhibits maturation of human monocyte-derived dendritic cells in vitro. *J Infect Dis* **188**, 257-266, doi:10.1086/376451 (2003).
56 Martineau, A. R. *et al.* Neutrophil-mediated innate immune resistance to mycobacteria. *J Clin Invest* **117**, 1988-1994, doi:10.1172/JCI31097 (2007).
57 Martineau, A. R. *et al.* High-dose vitamin D(3) during intensive-phase antimicrobial treatment of pulmonary tuberculosis: a double-blind randomised controlled trial. *Lancet* **377**, 242-250, doi:10.1016/S0140-6736(10)61889-2 (2011).
58 Barrios-Payán, J., Aguilar-León, D., Lascurain-Ledezma, R. & Hernández-Pando, R. [Neutrophil participation in early control and immune activation during experimental pulmonary tuberculosis]. *Gac Med Mex* **142**, 273-281 (2006).
59 Fulton, S. A., Reba, S. M., Martin, T. D. & Boom, W. H. Neutrophil-mediated mycobacteriocidal immunity in the lung during Mycobacterium bovis BCG infection in C57BL/6 mice. *Infect Immun* **70**, 5322-5327 (2002).
60 Seiler, P. *et al.* Rapid neutrophil response controls fast-replicating intracellular bacteria but not slow-replicating Mycobacterium tuberculosis. *J Infect Dis* **181**, 671-680, doi:10.1086/315278 (2000).
61 Barnes, P. F. *et al.* Predictors of short-term prognosis in patients with pulmonary tuberculosis. *J Infect Dis* **158**, 366-371 (1988).
62 Bermudez, L. E., Petrofsky, M. & Stevens, P. Treatment with recombinant granulocyte colony-stimulating factor (Filgrastin) stimulates neutrophils and tissue macrophages and induces an effective non-specific response against Mycobacterium avium in mice. *Immunology* **94**, 297-303 (1998).
63 Sugawara, I., Udagawa, T. & Yamada, H. Rat neutrophils prevent the development of tuberculosis. *Infect Immun* **72**, 1804-1806 (2004).
64 Hartmann, P. *et al.* Phagocytosis and killing of Mycobacterium avium complex by human neutrophils. *J Leukoc Biol* **69**, 397-404 (2001).
65 Smith, C. C., Barr, R. M. & Alexander, J. Studies on the interaction of Mycobacterium microti and Mycobacterium lepraemurium with mouse polymorphonuclear leucocytes. *J Gen Microbiol* **112**, 185-189 (1979).

66 Eruslanov, E. B. *et al.* Neutrophil responses to Mycobacterium tuberculosis infection in genetically susceptible and resistant mice. *Infect Immun* **73**, 1744-1753, doi:10.1128/IAI.73.3.1744-1753.2005 (2005).
67 Denis, M. Human neutrophils, activated with cytokines or not, do not kill virulent Mycobacterium tuberculosis. *J Infect Dis* **163**, 919-920 (1991).
68 Petrofsky, M. & Bermudez, L. E. Neutrophils from Mycobacterium avium-infected mice produce TNF-alpha, IL-12, and IL-1 beta and have a putative role in early host response. *Clin Immunol* **91**, 354-358, doi:10.1006/clim.1999.4709 (1999).
69 Mantovani, A., Cassatella, M. A., Costantini, C. & Jaillon, S. Neutrophils in the activation and regulation of innate and adaptive immunity. *Nat Rev Immunol* **11**, 519-531, doi:10.1038/nri3024 (2011).
70 Cooper, M. A., Fehniger, T. A. & Caligiuri, M. A. The biology of human natural killer-cell subsets. *Trends Immunol* **22**, 633-640 (2001).
71 Junqueira-Kipnis, A. P. *et al.* NK cells respond to pulmonary infection with Mycobacterium tuberculosis, but play a minimal role in protection. *J Immunol* **171**, 6039-6045 (2003).
72 Vankayalapati, R. *et al.* The NKp46 receptor contributes to NK cell lysis of mononuclear phagocytes infected with an intracellular bacterium. *J Immunol* **168**, 3451-3457 (2002).
73 Vankayalapati, R. *et al.* Role of NK cell-activating receptors and their ligands in the lysis of mononuclear phagocytes infected with an intracellular bacterium. *J Immunol* **175**, 4611-4617 (2005).
74 Brill, K. J. *et al.* Human natural killer cells mediate killing of intracellular Mycobacterium tuberculosis H37Rv via granule-independent mechanisms. *Infect Immun* **69**, 1755-1765, doi:10.1128/IAI.69.3.1755-1765.2001 (2001).
75 Vankayalapati, R. *et al.* NK cells regulate CD8+ T cell effector function in response to an intracellular pathogen. *J Immunol* **172**, 130-137 (2004).
76 Zhang, R., Zheng, X., Li, B., Wei, H. & Tian, Z. Human NK cells positively regulate gammadelta T cells in response to Mycobacterium tuberculosis. *J Immunol* **176**, 2610-2616 (2006).
77 Feng, C. G. *et al.* NK cell-derived IFN-gamma differentially regulates innate resistance and neutrophil response in T cell-deficient hosts infected with Mycobacterium tuberculosis. *J Immunol* **177**, 7086-7093 (2006).
78 Wolf, A. J. *et al.* Initiation of the adaptive immune response to Mycobacterium tuberculosis depends on antigen production in the local lymph node, not the lungs. *J Exp Med* **205**, 105-115, doi:10.1084/jem.20071367 (2008).
79 Chackerian, A. A., Alt, J. M., Perera, T. V., Dascher, C. C. & Behar, S. M. Dissemination of Mycobacterium tuberculosis is influenced by host factors and precedes the initiation of T-cell immunity. *Infect Immun* **70**, 4501-4509 (2002).
80 Khader, S. A. *et al.* Interleukin 12p40 is required for dendritic cell migration and T cell priming after Mycobacterium tuberculosis infection. *J Exp Med* **203**, 1805-1815, doi:10.1084/jem.20052545 (2006).
81 Srivastava, S. & Ernst, J. D. Cell-to-cell transfer of M. tuberculosis antigens optimizes CD4 T cell priming. *Cell Host Microbe* **15**, 741-752, doi:10.1016/j.chom.2014.05.007 (2014).
82 Tian, T., Woodworth, J., Skold, M. & Behar, S. M. In vivo depletion of CD11c+ cells delays the CD4+ T cell response to Mycobacterium tuberculosis and exacerbates the outcome of infection. *J Immunol* **175**, 3268-3272 (2005).
83 Caruso, A. M. *et al.* Mice deficient in CD4 T cells have only transiently diminished levels of IFN-gamma, yet succumb to tuberculosis. *J Immunol* **162**, 5407-5416 (1999).
84 Mogues, T., Goodrich, M. E., Ryan, L., LaCourse, R. & North, R. J. The relative importance of T cell subsets in immunity and immunopathology of airborne Mycobacterium tuberculosis infection in mice. *J Exp Med* **193**, 271-280 (2001).
85 Scanga, C. A. *et al.* Depletion of CD4(+) T cells causes reactivation of murine persistent tuberculosis despite continued expression of interferon gamma and nitric oxide synthase 2. *J Exp Med* **192**, 347-358 (2000).

86 Lin, P. L. *et al.* CD4 T cell depletion exacerbates acute Mycobacterium tuberculosis while reactivation of latent infection is dependent on severity of tissue depletion in cynomolgus macaques. *AIDS Res Hum Retroviruses* **28**, 1693-1702, doi:10.1089/aid.2012.0028 (2012).
87 Diedrich, C. R. *et al.* Reactivation of latent tuberculosis in cynomolgus macaques infected with SIV is associated with early peripheral T cell depletion and not virus load. *PLoS One* **5**, e9611, doi:10.1371/journal.pone.0009611 (2010).
88 Geldmacher, C., Zumla, A. & Hoelscher, M. Interaction between HIV and Mycobacterium tuberculosis: HIV-1-induced CD4 T-cell depletion and the development of active tuberculosis. *Curr Opin HIV AIDS* **7**, 268-275, doi:10.1097/COH.0b013e3283524e32 (2012).
89 Jones, B. E. *et al.* Relationship of the manifestations of tuberculosis to CD4 cell counts in patients with human immunodeficiency virus infection. *Am Rev Respir Dis* **148**, 1292-1297, doi:10.1164/ajrccm/148.5.1292 (1993).
90 Zhu, J., Yamane, H. & Paul, W. E. Differentiation of effector CD4 T cell populations (*). *Annu Rev Immunol* **28**, 445-489, doi:10.1146/annurev-immunol-030409-101212 (2010).
91 Wan, Y. Y. & Flavell, R. A. How diverse--CD4 effector T cells and their functions. *J Mol Cell Biol* **1**, 20-36, doi:10.1093/jmcb/mjp001 (2009).
92 Kidd, P. Th1/Th2 balance: the hypothesis, its limitations, and implications for health and disease. *Altern Med Rev* **8**, 223-246 (2003).
93 Jung, Y. J., Ryan, L., LaCourse, R. & North, R. J. Properties and protective value of the secondary versus primary T helper type 1 response to airborne Mycobacterium tuberculosis infection in mice. *J Exp Med* **201**, 1915-1924, doi:10.1084/jem.20050265 (2005).
94 Yamamura, M. *et al.* Defining protective responses to pathogens: cytokine profiles in leprosy lesions. *Science* **254**, 277-279 (1991).
95 Nathan, C. F. *et al.* Local and systemic effects of intradermal recombinant interferon-gamma in patients with lepromatous leprosy. *N Engl J Med* **315**, 6-15, doi:10.1056/NEJM198607033150102 (1986).
96 Kaplan, G. *et al.* Cellular responses to the intradermal injection of recombinant human gamma-interferon in lepromatous leprosy patients. *Am J Pathol* **128**, 345-353 (1987).
97 Orme, I. M. *et al.* T lymphocytes mediating protection and cellular cytolysis during the course of Mycobacterium tuberculosis infection. Evidence for different kinetics and recognition of a wide spectrum of protein antigens. *J Immunol* **148**, 189-196 (1992).
98 Flynn, J. L. *et al.* An essential role for interferon gamma in resistance to Mycobacterium tuberculosis infection. *J Exp Med* **178**, 2249-2254 (1993).
99 Cooper, A. M. *et al.* Disseminated tuberculosis in interferon gamma gene-disrupted mice. *J Exp Med* **178**, 2243-2247 (1993).
100 Bustamante, J., Boisson-Dupuis, S., Abel, L. & Casanova, J. L. Mendelian susceptibility to mycobacterial disease: genetic, immunological, and clinical features of inborn errors of IFN-γ immunity. *Semin Immunol* **26**, 454-470, doi:10.1016/j.smim.2014.09.008 (2014).
101 Chan, J., Xing, Y., Magliozzo, R. S. & Bloom, B. R. Killing of virulent Mycobacterium tuberculosis by reactive nitrogen intermediates produced by activated murine macrophages. *J Exp Med* **175**, 1111-1122 (1992).
102 MacMicking, J. D. *et al.* Identification of nitric oxide synthase as a protective locus against tuberculosis. *Proc Natl Acad Sci U S A* **94**, 5243-5248 (1997).
103 MacMicking, J. D., Taylor, G. A. & McKinney, J. D. Immune control of tuberculosis by IFN-gamma-inducible LRG-47. *Science* **302**, 654-659, doi:10.1126/science.1088063 (2003).
104 Gutierrez, M. G. *et al.* Autophagy is a defense mechanism inhibiting BCG and Mycobacterium tuberculosis survival in infected macrophages. *Cell* **119**, 753-766, doi:10.1016/j.cell.2004.11.038 (2004).
105 Fabri, M. *et al.* Vitamin D is required for IFN-gamma-mediated antimicrobial activity of human macrophages. *Sci Transl Med* **3**, 104ra102, doi:10.1126/scitranslmed.3003045 (2011).

106 North, R. J. Importance of thymus-derived lymphocytes in cell-mediated immunity to infection. *Cell Immunol* **7**, 166-176 (1973).
107 Caccamo, N. *et al.* Multifunctional CD4(+) T cells correlate with active Mycobacterium tuberculosis infection. *Eur J Immunol* **40**, 2211-2220, doi:10.1002/eji.201040455 (2010).
108 Harris, J. & Keane, J. How tumour necrosis factor blockers interfere with tuberculosis immunity. *Clin Exp Immunol* **161**, 1-9, doi:10.1111/j.1365-2249.2010.04146.x (2010).
109 Mohan, V. P. *et al.* Effects of tumor necrosis factor alpha on host immune response in chronic persistent tuberculosis: possible role for limiting pathology. *Infect Immun* **69**, 1847-1855, doi:10.1128/iai.69.3.1847-1855.2001 (2001).
110 Lin, P. L., Plessner, H. L., Voitenok, N. N. & Flynn, J. L. Tumor necrosis factor and tuberculosis. *J Investig Dermatol Symp Proc* **12**, 22-25, doi:10.1038/sj.jidsymp.5650027 (2007).
111 Nambiar, J. K., Ryan, A. A., Kong, C. U., Britton, W. J. & Triccas, J. A. Modulation of pulmonary DC function by vaccine-encoded GM-CSF enhances protective immunity against Mycobacterium tuberculosis infection. *Eur J Immunol* **40**, 153-161, doi:10.1002/eji.200939665 (2010).
112 Darrah, P. A. *et al.* Multifunctional TH1 cells define a correlate of vaccine-mediated protection against Leishmania major. *Nat Med* **13**, 843-850, doi:10.1038/nm1592 (2007).
113 Boaz, M. J., Waters, A., Murad, S., Easterbrook, P. J. & Vyakarnam, A. Presence of HIV-1 Gag-specific IFN-gamma+IL-2+ and CD28+IL-2+ CD4 T cell responses is associated with nonprogression in HIV-1 infection. *J Immunol* **169**, 6376-6385 (2002).
114 Jeong, Y. H. *et al.* Differentiation of antigen-specific T cells with limited functional capacity during Mycobacterium tuberculosis infection. *Infect Immun* **82**, 132-139, doi:10.1128/IAI.00480-13 (2014).
115 Day, C. L. *et al.* Functional capacity of Mycobacterium tuberculosis-specific T cell responses in humans is associated with mycobacterial load. *J Immunol* **187**, 2222-2232, doi:10.4049/jimmunol.1101122 (2011).
116 Sutherland, J. S., Adetifa, I. M., Hill, P. C., Adegbola, R. A. & Ota, M. O. Pattern and diversity of cytokine production differentiates between Mycobacterium tuberculosis infection and disease. *Eur J Immunol* **39**, 723-729, doi:10.1002/eji.200838693 (2009).
117 Qiu, Z. *et al.* Multifunctional CD4 T cell responses in patients with active tuberculosis. *Sci Rep* **2**, 216, doi:10.1038/srep00216 (2012).
118 Rook, G. A. Th2 cytokines in susceptibility to tuberculosis. *Curr Mol Med* **7**, 327-337 (2007).
119 Howard, A. D. & Zwilling, B. S. Reactivation of tuberculosis is associated with a shift from type 1 to type 2 cytokines. *Clin Exp Immunol* **115**, 428-434 (1999).
120 Lienhardt, C. *et al.* Active tuberculosis in Africa is associated with reduced Th1 and increased Th2 activity in vivo. *Eur J Immunol* **32**, 1605-1613, doi:10.1002/1521-4141(200206)32:6<1605::aid-immu1605>3.0.co;2-6 (2002).
121 Mazzarella, G. *et al.* T lymphocyte phenotypic profile in lung segments affected by cavitary and non-cavitary tuberculosis. *Clin Exp Immunol* **132**, 283-288 (2003).
122 Resende Co, T., Hirsch, C. S., Toossi, Z., Dietze, R. & Ribeiro-Rodrigues, R. Intestinal helminth co-infection has a negative impact on both anti-Mycobacterium tuberculosis immunity and clinical response to tuberculosis therapy. *Clin Exp Immunol* **147**, 45-52, doi:10.1111/j.1365-2249.2006.03247.x (2007).
123 Potian, J. A. *et al.* Preexisting helminth infection induces inhibition of innate pulmonary anti-tuberculosis defense by engaging the IL-4 receptor pathway. *J Exp Med* **208**, 1863-1874, doi:10.1084/jem.20091473 (2011).
124 Hübner, M. P. *et al.* Chronic helminth infection does not exacerbate Mycobacterium tuberculosis infection. *PLoS Negl Trop Dis* **6**, e1970, doi:10.1371/journal.pntd.0001970 (2012).
125 Elias, D. *et al.* Effect of deworming on human T cell responses to mycobacterial antigens in helminth-exposed individuals before and after bacille Calmette-Guerin (BCG) vaccination. *Clin Exp Immunol* **123**, 219-225 (2001).

126 Elias, D. *et al.* Schistosoma mansoni infection reduces the protective efficacy of BCG vaccination against virulent Mycobacterium tuberculosis. *Vaccine* **23**, 1326-1334, doi:10.1016/j.vaccine.2004.09.038 (2005).
127 Elias, D., Britton, S., Aseffa, A., Engers, H. & Akuffo, H. Poor immunogenicity of BCG in helminth infected population is associated with increased in vitro TGF-beta production. *Vaccine* **26**, 3897-3902, doi:10.1016/j.vaccine.2008.04.083 (2008).
128 Torrado, E. & Cooper, A. M. IL-17 and Th17 cells in tuberculosis. *Cytokine Growth Factor Rev* **21**, 455-462, doi:10.1016/j.cytogfr.2010.10.004 (2010).
129 Lockhart, E., Green, A. M. & Flynn, J. L. IL-17 production is dominated by gammadelta T cells rather than CD4 T cells during Mycobacterium tuberculosis infection. *J Immunol* **177**, 4662-4669 (2006).
130 Umemura, M. *et al.* IL-17-mediated regulation of innate and acquired immune response against pulmonary Mycobacterium bovis bacille Calmette-Guerin infection. *J Immunol* **178**, 3786-3796 (2007).
131 Ye, P. *et al.* Interleukin-17 and lung host defense against Klebsiella pneumoniae infection. *Am J Respir Cell Mol Biol* **25**, 335-340, doi:10.1165/ajrcmb.25.3.4424 (2001).
132 Okamoto Yoshida, Y. *et al.* Essential role of IL-17A in the formation of a mycobacterial infection-induced granuloma in the lung. *J Immunol* **184**, 4414-4422, doi:10.4049/jimmunol.0903332 (2010).
133 Kursar, M. *et al.* Cutting Edge: Regulatory T cells prevent efficient clearance of Mycobacterium tuberculosis. *J Immunol* **178**, 2661-2665 (2007).
134 Guyot-Revol, V., Innes, J. A., Hackforth, S., Hinks, T. & Lalvani, A. Regulatory T cells are expanded in blood and disease sites in patients with tuberculosis. *Am J Respir Crit Care Med* **173**, 803-810, doi:10.1164/rccm.200508-1294OC (2006).
135 Fehervari, Z. & Sakaguchi, S. Development and function of CD25+CD4+ regulatory T cells. *Curr Opin Immunol* **16**, 203-208, doi:10.1016/j.coi.2004.01.004 (2004).
136 Redford, P. S., Murray, P. J. & O'Garra, A. The role of IL-10 in immune regulation during M. tuberculosis infection. *Mucosal Immunol* **4**, 261-270, doi:10.1038/mi.2011.7 (2011).
137 Einarsdottir, T., Lockhart, E. & Flynn, J. L. Cytotoxicity and secretion of gamma interferon are carried out by distinct CD8 T cells during Mycobacterium tuberculosis infection. *Infect Immun* **77**, 4621-4630, doi:10.1128/iai.00415-09 (2009).
138 Lin, P. L. & Flynn, J. L. CD8 T cells and Mycobacterium tuberculosis infection. *Semin Immunopathol* **37**, 239-249, doi:10.1007/s00281-015-0490-8 (2015).
139 Serbina, N. V., Liu, C. C., Scanga, C. A. & Flynn, J. L. CD8+ CTL from lungs of Mycobacterium tuberculosis-infected mice express perforin in vivo and lyse infected macrophages. *J Immunol* **165**, 353-363 (2000).
140 Cho, S. *et al.* Antimicrobial activity of MHC class I-restricted CD8+ T cells in human tuberculosis. *Proc Natl Acad Sci U S A* **97**, 12210-12215, doi:10.1073/pnas.210391497 (2000).
141 Stenger, S., Rosat, J. P., Bloom, B. R., Krensky, A. M. & Modlin, R. L. Granulysin: a lethal weapon of cytolytic T cells. *Immunol Today* **20**, 390-394 (1999).
142 Kamath, A. B. *et al.* Cytolytic CD8+ T cells recognizing CFP10 are recruited to the lung after Mycobacterium tuberculosis infection. *J Exp Med* **200**, 1479-1489, doi:10.1084/jem.20041690 (2004).
143 Flynn, J. L., Goldstein, M. M., Triebold, K. J., Koller, B. & Bloom, B. R. Major histocompatibility complex class I-restricted T cells are required for resistance to Mycobacterium tuberculosis infection. *Proc Natl Acad Sci U S A* **89**, 12013-12017 (1992).
144 Muller, I., Cobbold, S. P., Waldmann, H. & Kaufmann, S. H. Impaired resistance to Mycobacterium tuberculosis infection after selective in vivo depletion of L3T4+ and Lyt-2+ T cells. *Infect Immun* **55**, 2037-2041 (1987).
145 Sousa, A. O. *et al.* Relative contributions of distinct MHC class I-dependent cell populations in protection to tuberculosis infection in mice. *Proc Natl Acad Sci U S A* **97**, 4204-4208 (2000).

146 Urdahl, K. B., Liggitt, D. & Bevan, M. J. CD8+ T cells accumulate in the lungs of Mycobacterium tuberculosis-infected Kb-/-Db-/- mice, but provide minimal protection. *J Immunol* **170**, 1987-1994 (2003).
147 Schaible, U. E., Collins, H. L., Priem, F. & Kaufmann, S. H. Correction of the iron overload defect in beta-2-microglobulin knockout mice by lactoferrin abolishes their increased susceptibility to tuberculosis. *J Exp Med* **196**, 1507-1513 (2002).
148 van Pinxteren, L. A., Cassidy, J. P., Smedegaard, B. H., Agger, E. M. & Andersen, P. Control of latent Mycobacterium tuberculosis infection is dependent on CD8 T cells. *Eur J Immunol* **30**, 3689-3698, doi:10.1002/1521-4141(200012)30:12<3689::aid-immu3689>3.0.co;2-4 (2000).
149 Porcelli, S. A. The CD1 family: a third lineage of antigen-presenting molecules. *Adv Immunol* **59**, 1-98 (1995).
150 Chen, C. Y. *et al.* A critical role for CD8 T cells in a nonhuman primate model of tuberculosis. *PLoS Pathog* **5**, e1000392, doi:10.1371/journal.ppat.1000392 (2009).
151 Cooper, A. M. Cell-mediated immune responses in tuberculosis. *Annu Rev Immunol* **27**, 393-422, doi:10.1146/annurev.immunol.021908.132703 (2009).
152 Lund, F. E. & Randall, T. D. Effector and regulatory B cells: modulators of CD4+ T cell immunity. *Nat Rev Immunol* **10**, 236-247, doi:10.1038/nri2729 (2010).
153 Kurt-Jones, E. A. *et al.* The role of antigen-presenting B cells in T cell priming in vivo. Studies of B cell-deficient mice. *J Immunol* **140**, 3773-3778 (1988).
154 Chan, J. *et al.* The role of B cells and humoral immunity in Mycobacterium tuberculosis infection. *Semin Immunol* **26**, 588-600, doi:10.1016/j.smim.2014.10.005 (2014).
155 Glatman-Freedman, A. & Casadevall, A. Serum therapy for tuberculosis revisited: reappraisal of the role of antibody-mediated immunity against Mycobacterium tuberculosis. *Clin Microbiol Rev* **11**, 514-532 (1998).
156 Hamasur, B. *et al.* A mycobacterial lipoarabinomannan specific monoclonal antibody and its F(ab') fragment prolong survival of mice infected with Mycobacterium tuberculosis. *Clin Exp Immunol* **138**, 30-38, doi:10.1111/j.1365-2249.2004.02593.x (2004).
157 Reljic, R. *et al.* Intranasal IFNgamma extends passive IgA antibody protection of mice against Mycobacterium tuberculosis lung infection. *Clin Exp Immunol* **143**, 467-473, doi:10.1111/j.1365-2249.2006.03012.x (2006).
158 Teitelbaum, R. *et al.* A mAb recognizing a surface antigen of Mycobacterium tuberculosis enhances host survival. *Proc Natl Acad Sci U S A* **95**, 15688-15693 (1998).
159 Costello, A. M. *et al.* Does antibody to mycobacterial antigens, including lipoarabinomannan, limit dissemination in childhood tuberculosis? *Trans R Soc Trop Med Hyg* **86**, 686-692 (1992).
160 Sanchez-Rodriguez, C. *et al.* An IgG antibody response to the antigen 85 complex is associated with good outcome in Mexican Totonaca Indians with pulmonary tuberculosis. *Int J Tuberc Lung Dis* **6**, 706-712 (2002).
161 Hamasur, B. *et al.* Mycobacterium tuberculosis arabinomannan-protein conjugates protect against tuberculosis. *Vaccine* **21**, 4081-4093 (2003).
162 Algood, H. M., Lin, P. L. & Flynn, J. L. Tumor necrosis factor and chemokine interactions in the formation and maintenance of granulomas in tuberculosis. *Clin Infect Dis* **41 Suppl 3**, S189-193, doi:10.1086/429994 (2005).
163 Ramakrishnan, L. Revisiting the role of the granuloma in tuberculosis. *Nat Rev Immunol* **12**, 352-366, doi:10.1038/nri3211 (2012).
164 Guirado, E. & Schlesinger, L. S. Modeling the Mycobacterium tuberculosis Granuloma - the Critical Battlefield in Host Immunity and Disease. *Front Immunol* **4**, 98, doi:10.3389/fimmu.2013.00098 (2013).
165 Pepper, M. & Jenkins, M. K. Origins of CD4(+) effector and central memory T cells. *Nat Immunol* **12**, 467-471 (2011).
166 Reinhardt, R. L., Khoruts, A., Merica, R., Zell, T. & Jenkins, M. K. Visualizing the generation of memory CD4 T cells in the whole body. *Nature* **410**, 101-105, doi:10.1038/35065111 (2001).

167 Cyster, J. G. Chemokines, sphingosine-1-phosphate, and cell migration in secondary lymphoid organs. *Annu Rev Immunol* **23**, 127-159, doi:10.1146/annurev.immunol.23.021704.115628 (2005).
168 Orme, I. M. Characteristics and specificity of acquired immunologic memory to Mycobacterium tuberculosis infection. *J Immunol* **140**, 3589-3593 (1988).
169 Andersen, P. & Heron, I. Specificity of a protective memory immune response against Mycobacterium tuberculosis. *Infect Immun* **61**, 844-851 (1993).
170 Henao-Tamayo, M. I. *et al.* Phenotypic definition of effector and memory T-lymphocyte subsets in mice chronically infected with Mycobacterium tuberculosis. *Clin Vaccine Immunol* **17**, 618-625, doi:10.1128/CVI.00368-09 (2010).
171 Rodrigues, L. C., Diwan, V. K. & Wheeler, J. G. Protective effect of BCG against tuberculous meningitis and miliary tuberculosis: a meta-analysis. *Int J Epidemiol* **22**, 1154-1158 (1993).
172 Trunz, B. B., Fine, P. & Dye, C. Effect of BCG vaccination on childhood tuberculous meningitis and miliary tuberculosis worldwide: a meta-analysis and assessment of cost-effectiveness. *Lancet* **367**, 1173-1180, doi:10.1016/s0140-6736(06)68507-3 (2006).
173 Romanus, V. *et al.* Atypical mycobacteria in extrapulmonary disease among children. Incidence in Sweden from 1969 to 1990, related to changing BCG-vaccination coverage. *Tuber Lung Dis* **76**, 300-310 (1995).
174 Trnka, L., Dankova, D. & Svandova, E. Six years' experience with the discontinuation of BCG vaccination. 4. Protective effect of BCG vaccination against the Mycobacterium avium intracellulare complex. *Tuber Lung Dis* **75**, 348-352, doi:10.1016/0962-8479(94)90080-9 (1994).
175 Romanus, V., Svensson, A. & Hallander, H. O. The impact of changing BCG coverage on tuberculosis incidence in Swedish-born children between 1969 and 1989. *Tuber Lung Dis* **73**, 150-161, doi:10.1016/0962-8479(92)90149-e (1992).
176 Rodrigues, L. C., Kerr-Pontes, L. R., Frietas, M. V. & Barreto, M. L. Long lasting BCG protection against leprosy. *Vaccine* **25**, 6842-6844, doi:10.1016/j.vaccine.2007.07.032 (2007).
177 Ponnighaus, J. M. *et al.* Efficacy of BCG vaccine against leprosy and tuberculosis in northern Malawi. *Lancet* **339**, 636-639 (1992).
178 de Castro, M. J., Pardo-Seco, J. & Martinon-Torres, F. Nonspecific (Heterologous) Protection of Neonatal BCG Vaccination Against Hospitalization Due to Respiratory Infection and Sepsis. *Clin Infect Dis* **60**, 1611-1619, doi:10.1093/cid/civ144 (2015).
179 Shann, F. in *J Infect Dis* Vol. 204 182-184 (2011).
180 Basu Roy, R. *et al.* Identifying predictors of interferon-γ release assay results in pediatric latent tuberculosis: a protective role of bacillus Calmette-Guerin?: a pTB-NET collaborative study. *Am J Respir Crit Care Med* **186**, 378-384, doi:10.1164/rccm.201201-0026OC (2012).
181 Sutherland, I. & Lindgren, I. The protective effect of BCG vaccination as indicated by autopsy studies. *Tubercle* **60**, 225-231 (1979).
182 Mahomed, H. *et al.* The impact of a change in bacille Calmette-Guérin vaccine policy on tuberculosis incidence in children in Cape Town, South Africa. *Pediatr Infect Dis J* **25**, 1167-1172, doi:10.1097/01.inf.0000243765.33880.54 (2006).
183 Moyo, S. *et al.* Age-related tuberculosis incidence and severity in children under 5 years of age in Cape Town, South Africa. *Int J Tuberc Lung Dis* **14**, 149-154 (2010).
184 Hesseling, A. C. *et al.* Bacille Calmette-Guerin vaccine-induced disease in HIV-infected and HIV-uninfected children. *Clin Infect Dis* **42**, 548-558, doi:10.1086/499953 (2006).
185 Colditz, G. A. *et al.* Efficacy of BCG vaccine in the prevention of tuberculosis. Meta-analysis of the published literature. *Jama* **271**, 698-702 (1994).
186 Aronson, N. E. *et al.* Long-term efficacy of BCG vaccine in American Indians and Alaska Natives: A 60-year follow-up study. *JAMA* **291**, 2086-2091, doi:10.1001/jama.291.17.2086 (2004).

187 Narayanan, P. R. Influence of sex, age & nontuberculous infection at intake on the efficacy of BCG: re-analysis of 15-year data from a double-blind randomized control trial in South India. *Indian J Med Res* **123**, 119-124 (2006).
188 Palmer, C. E. & Long, M. W. Effects of infection with atypical mycobacteria on BCG vaccination and tuberculosis. *Am Rev Respir Dis* **94**, 553-568 (1966).
189 Edwards, L. B., Acquaviva, F. A., Livesay, V. T., Cross, F. W. & Palmer, C. E. An atlas of sensitivity to tuberculin, PPD-B, and histoplasmin in the United States. *Am Rev Respir Dis* **99**, Suppl:1-132 (1969).
190 Fine, P. E. Variation in protection by BCG: implications of and for heterologous immunity. *Lancet* **346**, 1339-1345 (1995).
191 Black, G. F. *et al.* Patterns and implications of naturally acquired immune responses to environmental and tuberculous mycobacterial antigens in northern Malawi. *J Infect Dis* **184**, 322-329, doi:10.1086/322042 (2001).
192 Brandt, L. *et al.* Failure of the Mycobacterium bovis BCG vaccine: some species of environmental mycobacteria block multiplication of BCG and induction of protective immunity to tuberculosis. *Infect Immun* **70**, 672-678 (2002).
193 Andersen, P. & Doherty, T. M. The success and failure of BCG - implications for a novel tuberculosis vaccine. *Nat Rev Microbiol* **3**, 656-662, doi:10.1038/nrmicro1211 (2005).
194 Orme, I. M. Evidence for a biphasic memory T-cell response to high dose BCG vaccination in mice. *Tubercle* **69**, 125-131 (1988).
195 Kipnis, A., Irwin, S., Izzo, A. A., Basaraba, R. J. & Orme, I. M. Memory T lymphocytes generated by Mycobacterium bovis BCG vaccination reside within a CD4 CD44lo CD62 ligand(hi) population. *Infect Immun* **73**, 7759-7764, doi:10.1128/IAI.73.11.7759-7764.2005 (2005).
196 Orme, I. M. The Achilles heel of BCG. *Tuberculosis (Edinb)* **90**, 329-332, doi:10.1016/j.tube.2010.06.002 (2010).
197 Kaveh, D. A., Carmen Garcia-Pelayo, M. & Hogarth, P. J. Persistent BCG bacilli perpetuate CD4 T effector memory and optimal protection against tuberculosis. *Vaccine* **32**, 6911-6918, doi:10.1016/j.vaccine.2014.10.041 (2014).
198 Kamath, A., Woodworth, J. S. & Behar, S. M. Antigen-specific CD8+ T cells and the development of central memory during Mycobacterium tuberculosis infection. *J Immunol* **177**, 6361-6369 (2006).
199 Hoft, D. F. *et al.* A new recombinant bacille Calmette-Guérin vaccine safely induces significantly enhanced tuberculosis-specific immunity in human volunteers. *J Infect Dis* **198**, 1491-1501, doi:10.1086/592450 (2008).
200 Farinacci, M., Weber, S. & Kaufmann, S. H. The recombinant tuberculosis vaccine rBCG ΔureC::hly(+) induces apoptotic vesicles for improved priming of CD4(+) and CD8(+) T cells. *Vaccine* **30**, 7608-7614, doi:10.1016/j.vaccine.2012.10.031 (2012).
201 Sun, R. *et al.* Novel recombinant BCG expressing perfringolysin O and the over-expression of key immunodominant antigens; pre-clinical characterization, safety and protection against challenge with Mycobacterium tuberculosis. *Vaccine* **27**, 4412-4423, doi:10.1016/j.vaccine.2009.05.048 (2009).
202 Kupferschmidt, K. Infectious disease. Taking a new shot at a TB vaccine. *Science* **334**, 1488-1490, doi:10.1126/science.334.6062.1488 (2011).
203 Martin, C. *et al.* The live Mycobacterium tuberculosis phoP mutant strain is more attenuated than BCG and confers protective immunity against tuberculosis in mice and guinea pigs. *Vaccine* **24**, 3408-3419, doi:10.1016/j.vaccine.2006.03.017 (2006).
204 Larsen, M. H. *et al.* Efficacy and safety of live attenuated persistent and rapidly cleared Mycobacterium tuberculosis vaccine candidates in non-human primates. *Vaccine* **27**, 4709-4717, doi:10.1016/j.vaccine.2009.05.050 (2009).
205 von Reyn, C. F. *et al.* Prevention of tuberculosis in Bacille Calmette-Guérin-primed, HIV-infected adults boosted with an inactivated whole-cell mycobacterial vaccine. *AIDS* **24**, 675-685, doi:10.1097/QAD.0b013e3283350f1b (2010).

206 Thacher, E. G. *et al.* Safety and immunogenicity of the M72/AS01 candidate tuberculosis vaccine in HIV-infected adults on combination antiretroviral therapy: a phase I/II, randomized trial. *AIDS* **28**, 1769-1781, doi:10.1097/QAD.0000000000000343 (2014).
207 van Dissel, J. T. *et al.* Ag85B-ESAT-6 adjuvanted with IC31® promotes strong and long-lived Mycobacterium tuberculosis specific T cell responses in volunteers with previous BCG vaccination or tuberculosis infection. *Vaccine* **29**, 2100-2109, doi:10.1016/j.vaccine.2010.12.135 (2011).
208 Abel, B. *et al.* The novel tuberculosis vaccine, AERAS-402, induces robust and polyfunctional CD4+ and CD8+ T cells in adults. *Am J Respir Crit Care Med* **181**, 1407-1417, doi:10.1164/rccm.200910-1484OC (2010).
209 Goonetilleke, N. P. *et al.* Enhanced immunogenicity and protective efficacy against Mycobacterium tuberculosis of bacille Calmette-Guérin vaccine using mucosal administration and boosting with a recombinant modified vaccinia virus Ankara. *J Immunol* **171**, 1602-1609 (2003).
210 Williams, A. *et al.* Boosting with poxviruses enhances Mycobacterium bovis BCG efficacy against tuberculosis in guinea pigs. *Infect Immun* **73**, 3814-3816, doi:10.1128/IAI.73.6.3814-3816.2005 (2005).
211 Verreck, F. A. *et al.* MVA.85A boosting of BCG and an attenuated, phoP deficient M. tuberculosis vaccine both show protective efficacy against tuberculosis in rhesus macaques. *PLoS One* **4**, e5264, doi:10.1371/journal.pone.0005264 (2009).
212 Vordermeier, H. M. *et al.* Viral booster vaccines improve Mycobacterium bovis BCG-induced protection against bovine tuberculosis. *Infect Immun* **77**, 3364-3373, doi:10.1128/IAI.00287-09 (2009).
213 McShane, H. *et al.* Recombinant modified vaccinia virus Ankara expressing antigen 85A boosts BCG-primed and naturally acquired antimycobacterial immunity in humans. *Nat Med* **10**, 1240-1244, doi:10.1038/nm1128 (2004).
214 Ndiaye, B. P. *et al.* Safety, immunogenicity, and efficacy of the candidate tuberculosis vaccine MVA85A in healthy adults infected with HIV-1: a randomised, placebo-controlled, phase 2 trial. *Lancet Respir Med* **3**, 190-200, doi:10.1016/S2213-2600(15)00037-5 (2015).
215 Scriba, T. J. *et al.* A phase IIa trial of the new tuberculosis vaccine, MVA85A, in HIV- and/or Mycobacterium tuberculosis-infected adults. *Am J Respir Crit Care Med* **185**, 769-778, doi:10.1164/rccm.201108-1548OC (2012).
216 Scriba, T. J. *et al.* Dose-finding study of the novel tuberculosis vaccine, MVA85A, in healthy BCG-vaccinated infants. *J Infect Dis* **203**, 1832-1843, doi:10.1093/infdis/jir195 (2011).
217 Scriba, T. J. *et al.* Modified vaccinia Ankara-expressing Ag85A, a novel tuberculosis vaccine, is safe in adolescents and children, and induces polyfunctional CD4+ T cells. *Eur J Immunol* **40**, 279-290, doi:10.1002/eji.200939754 (2010).
218 Beveridge, N. E. *et al.* Immunisation with BCG and recombinant MVA85A induces long-lasting, polyfunctional Mycobacterium tuberculosis-specific CD4+ memory T lymphocyte populations. *Eur J Immunol* **37**, 3089-3100, doi:10.1002/eji.200737504 (2007).
219 Tameris, M. D. *et al.* Safety and efficacy of MVA85A, a new tuberculosis vaccine, in infants previously vaccinated with BCG: a randomised, placebo-controlled phase 2b trial. *Lancet* **381**, 1021-1028, doi:10.1016/S0140-6736(13)60177-4 (2013).
220 Tanner, R. *et al.* Serum indoleamine 2,3-dioxygenase activity is associated with reduced immunogenicity following vaccination with MVA85A. *BMC Infect Dis* **14**, 660, doi:10.1186/s12879-014-0660-7 (2014).
221 Walrath, J. R. & Silver, R. F. The α4β1 integrin in localization of Mycobacterium tuberculosis-specific T helper type 1 cells to the human lung. *Am J Respir Cell Mol Biol* **45**, 24-30, doi:10.1165/rcmb.2010-0241OC (2011).
222 Barclay, W. R. *et al.* Protection of monkeys against airborne tuberculosis by aerosol vaccination with bacillus Calmette-Guerin. *Am Rev Respir Dis* **107**, 351-358 (1973).

223 White, A. D. *et al.* Evaluation of the safety and immunogenicity of a candidate tuberculosis vaccine, MVA85A, delivered by aerosol to the lungs of macaques. *Clin Vaccine Immunol* **20**, 663-672, doi:10.1128/CVI.00690-12 (2013).
224 Satti, I. *et al.* Safety and immunogenicity of a candidate tuberculosis vaccine MVA85A delivered by aerosol in BCG-vaccinated healthy adults: a phase 1, double-blind, randomised controlled trial. *Lancet Infect Dis* **14**, 939-946, doi:10.1016/S1473-3099(14)70845-X (2014).
225 Elias, D., Akuffo, H. & Britton, S. PPD induced in vitro interferon gamma production is not a reliable correlate of protection against Mycobacterium tuberculosis. *Trans R Soc Trop Med Hyg* **99**, 363-368, doi:10.1016/j.trstmh.2004.08.006 (2005).
226 McShane, H. & Williams, A. A review of preclinical animal models utilised for TB vaccine evaluation in the context of recent human efficacy data. *Tuberculosis (Edinb)* **94**, 105-110, doi:10.1016/j.tube.2013.11.003 (2014).
227 Niemann, S. & Supply, P. Diversity and evolution of Mycobacterium tuberculosis: moving to whole-genome-based approaches. *Cold Spring Harb Perspect Med* **4**, a021188, doi:10.1101/cshperspect.a021188 (2014).
228 Orme, I. M. & Basaraba, R. J. The formation of the granuloma in tuberculosis infection. *Semin Immunol* **26**, 601-609, doi:10.1016/j.smim.2014.09.009 (2014).
229 McShane, H. *et al.* Boosting BCG with MVA85A: the first candidate subunit vaccine for tuberculosis in clinical trials. *Tuberculosis (Edinb)* **85**, 47-52, doi:10.1016/j.tube.2004.09.015 (2005).
230 Suntharalingam, G. *et al.* Cytokine storm in a phase 1 trial of the anti-CD28 monoclonal antibody TGN1412. *N Engl J Med* **355**, 1018-1028, doi:10.1056/NEJMoa063842 (2006).
231 McKenzie, R. *et al.* Hepatic failure and lactic acidosis due to fialuridine (FIAU), an investigational nucleoside analogue for chronic hepatitis B. *N Engl J Med* **333**, 1099-1105, doi:10.1056/NEJM199510263331702 (1995).
232 Diel, R., Loddenkemper, R., Niemann, S., Meywald-Walter, K. & Nienhaus, A. Negative and positive predictive value of a whole-blood interferon-γ release assay for developing active tuberculosis: an update. *Am J Respir Crit Care Med* **183**, 88-95, doi:10.1164/rccm.201006-0974OC (2011).
233 Mattila, J. T., Diedrich, C. R., Lin, P. L., Phuah, J. & Flynn, J. L. Simian immunodeficiency virus-induced changes in T cell cytokine responses in cynomolgus macaques with latent Mycobacterium tuberculosis infection are associated with timing of reactivation. *J Immunol* **186**, 3527-3537, doi:10.4049/jimmunol.1003773 (2011).
234 Lazarevic, V., Nolt, D. & Flynn, J. L. Long-term control of Mycobacterium tuberculosis infection is mediated by dynamic immune responses. *J Immunol* **175**, 1107-1117 (2005).
235 Mittrücker, H. W. *et al.* Poor correlation between BCG vaccination-induced T cell responses and protection against tuberculosis. *Proc Natl Acad Sci U S A* **104**, 12434-12439, doi:10.1073/pnas.0703510104 (2007).
236 Hawkridge, T. *et al.* Safety and immunogenicity of a new tuberculosis vaccine, MVA85A, in healthy adults in South Africa. *J Infect Dis* **198**, 544-552, doi:10.1086/590185 (2008).
237 Lindenstrøm, T. *et al.* Tuberculosis subunit vaccination provides long-term protective immunity characterized by multifunctional CD4 memory T cells. *J Immunol* **182**, 8047-8055, doi:10.4049/jimmunol.0801592 (2009).
238 Derrick, S. C., Yabe, I. M., Yang, A. & Morris, S. L. Vaccine-induced anti-tuberculosis protective immunity in mice correlates with the magnitude and quality of multifunctional CD4 T cells. *Vaccine* **29**, 2902-2909, doi:10.1016/j.vaccine.2011.02.010 (2011).
239 Kagina, B. M. *et al.* Specific T cell frequency and cytokine expression profile do not correlate with protection against tuberculosis after bacillus Calmette-Guérin vaccination of newborns. *Am J Respir Crit Care Med* **182**, 1073-1079, doi:10.1164/rccm.201003-0334OC (2010).
240 Bhatt, K., Verma, S., Ellner, J. J. & Salgame, P. Quest for correlates of protection against tuberculosis. *Clin Vaccine Immunol* **22**, 258-266, doi:10.1128/CVI.00721-14 (2015).

241 Tanca, A., Deligios, M., Addis, M. F. & Uzzau, S. High throughput genomic and proteomic technologies in the fight against infectious diseases. *J Infect Dev Ctries* **7**, 182-190 (2013).
242 Crowle, A. J. & May, M. Preliminary demonstration of human tuberculoimmunity in vitro. *Infect Immun* **31**, 453-464 (1981).
243 Steele, J. *et al.* Inhibition of virulent Mycobacterium tuberculosis by murine peritoneal macrophages and human alveolar lavage cells: the effects of lymphokines and recombinant gamma interferon. *Tubercle* **67**, 289-294 (1986).
244 Cheng, S. H. *et al.* Demonstration of increased anti-mycobacterial activity in peripheral blood monocytes after BCG vaccination in British school children. *Clin Exp Immunol* **74**, 20-25 (1988).
245 Cheng, S. H. *et al.* Monocyte antimycobacterial activity before and after Mycobacterium bovis BCG vaccination in Chingleput, India, and London, United Kingdom. *Infect Immun* **61**, 4501-4503 (1993).
246 Silver, R. F., Li, Q., Boom, W. H. & Ellner, J. J. Lymphocyte-dependent inhibition of growth of virulent Mycobacterium tuberculosis H37Rv within human monocytes: requirement for CD4+ T cells in purified protein derivative-positive, but not in purified protein derivative-negative subjects. *J Immunol* **160**, 2408-2417 (1998).
247 Hoft, D. F. *et al.* Investigation of the relationships between immune-mediated inhibition of mycobacterial growth and other potential surrogate markers of protective Mycobacterium tuberculosis immunity. *J Infect Dis* **186**, 1448-1457, doi:10.1086/344359 (2002).
248 Worku, S. & Hoft, D. F. In vitro measurement of protective mycobacterial immunity: antigen-specific expansion of T cells capable of inhibiting intracellular growth of bacille Calmette-Guérin. *Clin Infect Dis* **30 Suppl 3**, S257-261, doi:10.1086/313887 (2000).
249 Kampmann, B. *et al.* Evaluation of human antimycobacterial immunity using recombinant reporter mycobacteria. *J Infect Dis* **182**, 895-901, doi:10.1086/315766 (2000).
250 Kampmann, B. *et al.* Novel human in vitro system for evaluating antimycobacterial vaccines. *Infect Immun* **72**, 6401-6407, doi:10.1128/IAI.72.11.6401-6407.2004 (2004).
251 Wallis, R. S. *et al.* A whole blood bactericidal assay for tuberculosis. *J Infect Dis* **183**, 1300-1303, doi:10.1086/319679 (2001).
252 Cheon, S. H. *et al.* Bactericidal activity in whole blood as a potential surrogate marker of immunity after vaccination against tuberculosis. *Clin Diagn Lab Immunol* **9**, 901-907 (2002).
253 Cowley, S. C. & Elkins, K. L. CD4+ T cells mediate IFN-gamma-independent control of Mycobacterium tuberculosis infection both in vitro and in vivo. *J Immunol* **171**, 4689-4699 (2003).
254 Parra, M. *et al.* Development of a murine mycobacterial growth inhibition assay for evaluating vaccines against Mycobacterium tuberculosis. *Clin Vaccine Immunol* **16**, 1025-1032, doi:10.1128/CVI.00067-09 (2009).
255 Marsay, L. *et al.* Mycobacterial growth inhibition in murine splenocytes as a surrogate for protection against Mycobacterium tuberculosis (M. tb). *Tuberculosis (Edinb)* **93**, 551-557, doi:10.1016/j.tube.2013.04.007 (2013).
256 Fletcher, H. A. *et al.* Inhibition of mycobacterial growth in vitro following primary but not secondary vaccination with Mycobacterium bovis BCG. *Clin Vaccine Immunol* **20**, 1683-1689, doi:10.1128/CVI.00427-13 (2013).
257 Sutton, S. Vol. 16 74-80 (Journal of GXP Compliance, 2012).
258 Orme, I. M., Andersen, P. & Boom, W. H. T cell response to Mycobacterium tuberculosis. *J Infect Dis* **167**, 1481-1497 (1993).
259 Manca, C. *et al.* Virulence of a Mycobacterium tuberculosis clinical isolate in mice is determined by failure to induce Th1 type immunity and is associated with induction of IFN-alpha /beta. *Proc Natl Acad Sci U S A* **98**, 5752-5757, doi:10.1073/pnas.091096998 (2001).

260 Lowe, D. M., Redford, P. S., Wilkinson, R. J., O'Garra, A. & Martineau, A. R. Neutrophils in tuberculosis: friend or foe? *Trends Immunol* **33**, 14-25, doi:10.1016/j.it.2011.10.003 (2012).
261 Tuomela, M., Stanescu, I. & Krohn, K. Validation overview of bio-analytical methods. *Gene Ther* **12 Suppl 1**, S131-138, doi:10.1038/sj.gt.3302627 (2005).
262 Cicchetti, D. V. & Sparrow, S. A. Developing criteria for establishing interrater reliability of specific items: applications to assessment of adaptive behavior. *Am J Ment Defic* **86**, 127-137 (1981).
263 Cicchetti, D. V. The precision of reliability and validity estimates re-visited: distinguishing between clinical and statistical significance of sample size requirements. *J Clin Exp Neuropsychol* **23**, 695-700, doi:10.1076/jcen.23.5.695.1249 (2001).
264 Banerjee, S., Farhana, A., Ehtesham, N. Z. & Hasnain, S. E. Iron acquisition, assimilation and regulation in mycobacteria. *Infect Genet Evol* **11**, 825-838, doi:10.1016/j.meegid.2011.02.016 (2011).
265 Marrero, J., Trujillo, C., Rhee, K. Y. & Ehrt, S. Glucose phosphorylation is required for Mycobacterium tuberculosis persistence in mice. *PLoS Pathog* **9**, e1003116, doi:10.1371/journal.ppat.1003116 (2013).
266 BOGEN, E. Streptomycin treatment for tuberculosis. *J Natl Med Assoc* **40**, 32 (1948).
267 Menzies, D. *et al.* Standardized treatment of active tuberculosis in patients with previous treatment and/or with mono-resistance to isoniazid: a systematic review and meta-analysis. *PLoS Med* **6**, e1000150 (2009).
268 Springer, B. *et al.* Mechanisms of streptomycin resistance: selection of mutations in the 16S rRNA gene conferring resistance. *Antimicrob Agents Chemother* **45**, 2877-2884, doi:10.1128/AAC.45.10.2877-2884.2001 (2001).
269 Karasawa, T., Wang, Q., Fu, Y., Cohen, D. M. & Steyger, P. S. TRPV4 enhances the cellular uptake of aminoglycoside antibiotics. *J Cell Sci* **121**, 2871-2879, doi:10.1242/jcs.023705 (2008).
270 Bonventre, P. F. & Imhoff, J. G. Uptake of h-dihydrostreptomycin by macrophages in culture. *Infect Immun* **2**, 89-95 (1970).
271 Harris, S. A. *et al.* Process of assay selection and optimization for the study of case and control samples from a phase IIb efficacy trial of a candidate tuberculosis vaccine, MVA85A. *Clin Vaccine Immunol* **21**, 1005-1011, doi:10.1128/CVI.00128-14 (2014).
272 Kuerten, S. *et al.* Resting of Cryopreserved PBMC Does Not Generally Benefit the Performance of Antigen-Specific T Cell ELISPOT Assays. *Cells* **1**, 409-427, doi:10.3390/cells1030409 (2012).
273 Ochang, E. A. Vol. 3 (eds Dami Collier, Ibidunni Bode-Sojobi, Rita Oladele, & Oyinlola Oduyebo) 46-49 (International Journal of Mycobacteriology, 2014).
274 Schlesinger, L. S., Bellinger-Kawahara, C. G., Payne, N. R. & Horwitz, M. A. Phagocytosis of Mycobacterium tuberculosis is mediated by human monocyte complement receptors and complement component C3. *J Immunol* **144**, 2771-2780 (1990).
275 Jackson, K., Sievers, A. & Dwyer, B. Effect of agitation of BACTEC 13A blood cultures on recovery of Mycobacterium avium complex. *J Clin Microbiol* **29**, 1801-1803 (1991).
276 WEISS, D. W. The effects of mechanical agitation on the growth of the H37Ra strain of M. tuberculosis. *Am Rev Tuberc* **79**, 813-815 (1959).
277 Schuck, S., Honsho, M., Ekroos, K., Shevchenko, A. & Simons, K. Resistance of cell membranes to different detergents. *Proc Natl Acad Sci U S A* **100**, 5795-5800, doi:10.1073/pnas.0631579100 (2003).
278 Kolibab, K. *et al.* A practical in vitro growth inhibition assay for the evaluation of TB vaccines. *Vaccine* **28**, 317-322, doi:10.1016/j.vaccine.2009.10.047 (2009).
279 Minassian, A. M. *et al.* A human challenge model for Mycobacterium tuberculosis using Mycobacterium bovis bacille Calmette-Guerin. *J Infect Dis* **205**, 1035-1042, doi:10.1093/infdis/jis012 (2012).
280 Garnier, T. *et al.* The complete genome sequence of Mycobacterium bovis. *Proc Natl Acad Sci U S A* **100**, 7877-7882, doi:10.1073/pnas.1130426100 (2003).

281 Hart, P. D. & Sutherland, I. BCG and vole bacillus vaccines in the prevention of tuberculosis in adolescence and early adult life. *Br Med J* **2**, 293-295 (1977).
282 Springett, V. H. B.C.G. vaccination in Birmingham: an assessment of its contribution to tuberculosis control in 1956-67. *Tubercle* **50**, 159-170 (1969).
283 Sutherland, I. & Springett, V. H. Effectiveness of BCG vaccination in England and Wales in 1983. *Tubercle* **68**, 81-92 (1987).
284 Lin, P. L. *et al.* The multistage vaccine H56 boosts the effects of BCG to protect cynomolgus macaques against active tuberculosis and reactivation of latent Mycobacterium tuberculosis infection. *J Clin Invest* **122**, 303-314, doi:10.1172/JCI46252 (2012).
285 Janicki, B. W., Good, R. C., Minden, P., Affronti, L. F. & Hymes, W. F. Immune responses in rhesus monkeys after bacillus Calmette-Guerin vaccination and aerosol challenge with Mycobacterium tuberculosis. *Am Rev Respir Dis* **107**, 359-366 (1973).
286 Langermans, J. A. *et al.* Divergent effect of bacillus Calmette-Guérin (BCG) vaccination on Mycobacterium tuberculosis infection in highly related macaque species: implications for primate models in tuberculosis vaccine research. *Proc Natl Acad Sci U S A* **98**, 11497-11502, doi:10.1073/pnas.201404898 (2001).
287 Gormus, B. J. *et al.* Protective immunization of monkeys with BCG or BCG plus heat-killed Mycobacterium leprae: clinical results. *Lepr Rev* **69**, 6-23 (1998).
288 Derrick, S. C., Kolibab, K., Yang, A. & Morris, S. L. Intranasal administration of Mycobacterium bovis BCG induces superior protection against aerosol infection with Mycobacterium tuberculosis in mice. *Clin Vaccine Immunol* **21**, 1443-1451, doi:10.1128/CVI.00394-14 (2014).
289 Giri, P. K., Verma, I. & Khuller, G. K. Protective efficacy of intranasal vaccination with Mycobacterium bovis BCG against airway Mycobacterium tuberculosis challenge in mice. *J Infect* **53**, 350-356, doi:10.1016/j.jinf.2005.12.017 (2006).
290 Tala-Heikkila, M., Nurmela, T., Tala, E. & Tuominen, J. Evaluation of the BCG revaccination programme of schoolchildren in Finland. *Bull Int Union Tuberc Lung Dis* **66**, 57-59 (1991).
291 Leung, C. C. *et al.* Efficacy of the BCG revaccination programme in a cohort given BCG vaccination at birth in Hong Kong. *Int J Tuberc Lung Dis* **5**, 717-723 (2001).
292 Sepulveda, R. L., Parcha, C. & Sorensen, R. U. Case-control study of the efficacy of BCG immunization against pulmonary tuberculosis in young adults in Santiago, Chile. *Tuber Lung Dis* **73**, 372-377, doi:10.1016/0962-8479(92)90043-J (1992).
293 Rodrigues, L. C. *et al.* Effect of BCG revaccination on incidence of tuberculosis in school-aged children in Brazil: the BCG-REVAC cluster-randomised trial. *Lancet* **366**, 1290-1295, doi:10.1016/S0140-6736(05)67145-0 (2005).
294 Erkeller-Yuksel, F. M. *et al.* Age-related changes in human blood lymphocyte subpopulations. *J Pediatr* **120**, 216-222 (1992).
295 Hicks, M. J. *et al.* Age-related changes in T- and B-lymphocyte subpopulations in the peripheral blood. *Arch Pathol Lab Med* **107**, 518-523 (1983).
296 Heyns, L. *et al.* Nosocomial transmission of Mycobacterium tuberculosis in kangaroo mother care units: a risk in tuberculosis-endemic areas. *Acta Paediatr* **95**, 535-539, doi:10.1080/08035250600636560 (2006).
297 LINCOLN, E. M. Course and prognosis of tuberculosis in children. *Am J Med* **9**, 623-632 (1950).
298 Seddon, J. A. *et al.* Impact of drug resistance on clinical outcome in children with tuberculous meningitis. *Pediatr Infect Dis J* **31**, 711-716, doi:10.1097/INF.0b013e318253acf8 (2012).
299 Vanden Driessche, K., Persson, A., Marais, B. J., Fink, P. J. & Urdahl, K. B. Immune vulnerability of infants to tuberculosis. *Clin Dev Immunol* **2013**, 781320, doi:10.1155/2013/781320 (2013).
300 Seder, R. A. & Hill, A. V. Vaccines against intracellular infections requiring cellular immunity. *Nature* **406**, 793-798, doi:10.1038/35021239 (2000).

301 O'Connor, S. L. *et al.* Comprehensive characterization of MHC class II haplotypes in Mauritian cynomolgus macaques. *Immunogenetics* **59**, 449-462, doi:10.1007/s00251-007-0209-7 (2007).
302 Wiseman, R. W. *et al.* Simian immunodeficiency virus SIVmac239 infection of major histocompatibility complex-identical cynomolgus macaques from Mauritius. *J Virol* **81**, 349-361, doi:10.1128/JVI.01841-06 (2007).
303 Mee, E. T. *et al.* MHC haplotype frequencies in a UK breeding colony of Mauritian cynomolgus macaques mirror those found in a distinct population from the same geographic origin. *J Med Primatol* **38**, 1-14, doi:10.1111/j.1600-0684.2008.00299.x (2009).
304 Aspinall, R., Del Giudice, G., Effros, R. B., Grubeck-Loebenstein, B. & Sambhara, S. Challenges for vaccination in the elderly. *Immun Ageing* **4**, 9, doi:10.1186/1742-4933-4-9 (2007).
305 Dunachie, S., Hill, A. V. & Fletcher, H. A. Profiling the host response to malaria vaccination and malaria challenge. *Vaccine*, doi:10.1016/j.vaccine.2015.07.107 (2015).
306 McArthur, M. A. *et al.* Activation of Salmonella Typhi-specific regulatory T cells in typhoid disease in a wild-type S. Typhi challenge model. *PLoS Pathog* **11**, e1004914, doi:10.1371/journal.ppat.1004914 (2015).
307 Shirley, D. A. & McArthur, M. A. The utility of human challenge studies in vaccine development: lessons learned from cholera. *Vaccine (Auckl)* **2011**, 3-13, doi:10.2147/VDT.S23634 (2011).
308 Harris, S. A. *et al.* Evaluation of a human BCG challenge model to assess antimycobacterial immunity induced by BCG and a candidate tuberculosis vaccine, MVA85A, alone and in combination. *J Infect Dis* **209**, 1259-1268, doi:10.1093/infdis/jit647 (2014).
309 Olsen, A. W., Brandt, L., Agger, E. M., van Pinxteren, L. A. & Andersen, P. The influence of remaining live BCG organisms in vaccinated mice on the maintenance of immunity to tuberculosis. *Scand J Immunol* **60**, 273-277, doi:10.1111/j.0300-9475.2004.01471.x (2004).
310 Hirsch, C. S., Ellner, J. J., Russell, D. G. & Rich, E. A. Complement receptor-mediated uptake and tumor necrosis factor-alpha-mediated growth inhibition of Mycobacterium tuberculosis by human alveolar macrophages. *J Immunol* **152**, 743-753 (1994).
311 KASPER, C. K., WHISSELL, D. Y. & WALLERSTEIN, R. O. CLINICAL ASPECTS OF IRON DEFICIENCY. *JAMA* **191**, 359-363 (1965).
312 O Broin, S. D., Kelleher, B. P., McCann, S. R., Ryder, R. J. & Scott, J. M. The value of the erythrocyte indices as a screening procedure in predicting nutritional deficiencies. *Clin Lab Haematol* **12**, 247-255 (1990).
313 Kochan, I., Golden, C. A. & Bukovic, J. A. Mechanism of tuberculostasis in mammalian serum. II. Induction of serum tuberculostasis in guinea pigs. *J Bacteriol* **100**, 64-70 (1969).
314 Raghu, B., Sarma, G. R. & Venkatesan, P. Effect of iron on the growth and siderophore production of mycobacteria. *Biochem Mol Biol Int* **31**, 341-348 (1993).
315 Serafín-López, J. *et al.* The effect of iron on the expression of cytokines in macrophages infected with Mycobacterium tuberculosis. *Scand J Immunol* **60**, 329-337, doi:10.1111/j.0300-9475.2004.01482.x (2004).
316 Lounis, N., Truffot-Pernot, C., Grosset, J., Gordeuk, V. R. & Boelaert, J. R. Iron and Mycobacterium tuberculosis infection. *J Clin Virol* **20**, 123-126 (2001).
317 Gordeuk, V. R., McLaren, C. E., MacPhail, A. P., Deichsel, G. & Bothwell, T. H. Associations of iron overload in Africa with hepatocellular carcinoma and tuberculosis: Strachan's 1929 thesis revisited. *Blood* **87**, 3470-3476 (1996).
318 Gangaidzo, I. T. *et al.* Association of pulmonary tuberculosis with increased dietary iron. *J Infect Dis* **184**, 936-939, doi:10.1086/323203 (2001).
319 Moyo, V. M., Gangaidzo, I. T., Gordeuk, V. R., Kiire, C. F. & Macphail, A. P. Tuberculosis and iron overload in Africa: a review. *Cent Afr J Med* **43**, 334-339 (1997).

320 Runyen-Janecky, L. J. Role and regulation of heme iron acquisition in gram-negative pathogens. *Front Cell Infect Microbiol* **3**, 55, doi:10.3389/fcimb.2013.00055 (2013).
321 Cescau, S. *et al.* Heme acquisition by hemophores. *Biometals* **20**, 603-613, doi:10.1007/s10534-006-9050-y (2007).
322 Wilks, A. & Burkhard, K. A. Heme and virulence: how bacterial pathogens regulate, transport and utilize heme. *Nat Prod Rep* **24**, 511-522, doi:10.1039/b604193k (2007).
323 Wandersman, C. & Stojiljkovic, I. Bacterial heme sources: the role of heme, hemoprotein receptors and hemophores. *Curr Opin Microbiol* **3**, 215-220 (2000).
324 Tullius, M. V. *et al.* Discovery and characterization of a unique mycobacterial heme acquisition system. *Proc Natl Acad Sci U S A* **108**, 5051-5056, doi:10.1073/pnas.1009516108 (2011).
325 Owens, C. P., Du, J., Dawson, J. H. & Goulding, C. W. Characterization of heme ligation properties of Rv0203, a secreted heme binding protein involved in Mycobacterium tuberculosis heme uptake. *Biochemistry* **51**, 1518-1531, doi:10.1021/bi2018305 (2012).
326 Owens, C. P. *et al.* The Mycobacterium tuberculosis secreted protein Rv0203 transfers heme to membrane proteins MmpL3 and MmpL11. *J Biol Chem* **288**, 21714-21728, doi:10.1074/jbc.M113.453076 (2013).
327 Chim, N., Iniguez, A., Nguyen, T. Q. & Goulding, C. W. Unusual diheme conformation of the heme-degrading protein from Mycobacterium tuberculosis. *J Mol Biol* **395**, 595-608, doi:10.1016/j.jmb.2009.11.025 (2010).
328 Nambu, S., Matsui, T., Goulding, C. W., Takahashi, S. & Ikeda-Saito, M. A new way to degrade heme: the Mycobacterium tuberculosis enzyme MhuD catalyzes heme degradation without generating CO. *J Biol Chem* **288**, 10101-10109, doi:10.1074/jbc.M112.448399 (2013).
329 McCuskee, S., Brickley, E. B., Wood, A. & Mossialos, E. Malaria and macronutrient deficiency as correlates of anemia in young children: a systematic review of observational studies. *Ann Glob Health* **80**, 458-465, doi:10.1016/j.aogh.2015.01.003 (2014).
330 Krambovitis, E. Detection of antibodies to Mycobacterium tuberculosis plasma membrane antigen by enzyme-linked immunosorbent assay. *J Med Microbiol* **21**, 257-264 (1986).
331 Kardjito, T., Handoyo, I. & Grange, J. M. Diagnosis of active tuberculosis by immunological methods. 1. The effect of tuberculin reactivity and previous BCG vaccination on the antibody levels determined by ELISA. *Tubercle* **63**, 269-274 (1982).
332 Nonnecke, B. J. *et al.* Development of an adult-like cell-mediated immune response in calves after early vaccination with Mycobacterium bovis bacillus Calmette-Guérin. *J Dairy Sci* **88**, 195-210, doi:10.3168/jds.S0022-0302(05)72678-3 (2005).
333 Turneer, M. *et al.* The humoral immune response after BCG vaccination in humans: consequences for the serodiagnosis of tuberculosis. *Eur Respir J* **1**, 589-593 (1988).
334 de Vallière, S., Abate, G., Blazevic, A., Heuertz, R. M. & Hoft, D. F. Enhancement of innate and cell-mediated immunity by antimycobacterial antibodies. *Infect Immun* **73**, 6711-6720, doi:10.1128/IAI.73.10.6711-6720.2005 (2005).
335 LAGERCRANTZ, R. & ENELL, H. Tuberculin-sensitivity and antibodies (agglutinins) after BCG-vaccination. *Acta Paediatr* **42**, 316-322 (1953).
336 Beyazova, U., Rota, S., Cevheroğlu, C. & Karsligil, T. Humoral immune response in infants after BCG vaccination. *Tuber Lung Dis* **76**, 248-253 (1995).
337 Sturgill, T. L., Giguère, S., Berghaus, L. J., Hurley, D. J. & Hondalus, M. K. Comparison of antibody and cell-mediated immune responses of foals and adult horses after vaccination with live Mycobacterium bovis BCG. *Vaccine* **32**, 1362-1367, doi:10.1016/j.vaccine.2014.01.032 (2014).
338 Hoft, D. F. *et al.* A double-blind, placebo-controlled study of Mycobacterium-specific human immune responses induced by intradermal bacille Calmette-Guérin vaccination. *J Lab Clin Med* **134**, 244-252 (1999).
339 Stainsby, K. J., Lowes, J. R., Allan, R. N. & Ibbotson, J. P. Antibodies to Mycobacterium paratuberculosis and nine species of environmental mycobacteria in Crohn's disease and control subjects. *Gut* **34**, 371-374 (1993).

340 Cho, S. N., Brennan, P. J., Yoshimura, H. H., Korelitz, B. I. & Graham, D. Y. Mycobacterial aetiology of Crohn's disease: serologic study using common mycobacterial antigens and a species-specific glycolipid antigen from Mycobacterium paratuberculosis. *Gut* **27**, 1353-1356 (1986).
341 Perley, C. C. *et al.* The human antibody response to the surface of Mycobacterium tuberculosis. *PLoS One* **9**, e98938, doi:10.1371/journal.pone.0098938 (2014).
342 Velasco-Velázquez, M. A., Barrera, D., González-Arenas, A., Rosales, C. & Agramonte-Hevia, J. Macrophage--Mycobacterium tuberculosis interactions: role of complement receptor 3. *Microb Pathog* **35**, 125-131 (2003).
343 Chapman, S. J. & Hill, A. V. Human genetic susceptibility to infectious disease. *Nat Rev Genet* **13**, 175-188, doi:10.1038/nrg3114 (2012).
344 Fitness, J. *et al.* Large-scale candidate gene study of tuberculosis susceptibility in the Karonga district of northern Malawi. *Am J Trop Med Hyg* **71**, 341-349 (2004).
345 Hoal-Van Helden, E. G. *et al.* Mannose-binding protein B allele confers protection against tuberculous meningitis. *Pediatr Res* **45**, 459-464, doi:10.1203/00006450-199904010-00002 (1999).
346 Selvaraj, P., Narayanan, P. R. & Reetha, A. M. Association of functional mutant homozygotes of the mannose binding protein gene with susceptibility to pulmonary tuberculosis in India. *Tuber Lung Dis* **79**, 221-227, doi:10.1054/tuld.1999.0204 (1999).
347 Søborg, C. *et al.* Mannose-binding lectin polymorphisms in clinical tuberculosis. *J Infect Dis* **188**, 777-782, doi:10.1086/377183 (2003).
348 Alemán, M. Neutrophil apoptosis in the context of tuberculosis infection. *Tuberculosis (Edinb)* **95**, 359-363, doi:10.1016/j.tube.2015.03.010 (2015).
349 Aston, C., Rom, W. N., Talbot, A. T. & Reibman, J. Early inhibition of mycobacterial growth by human alveolar macrophages is not due to nitric oxide. *Am J Respir Crit Care Med* **157**, 1943-1950, doi:10.1164/ajrccm.157.6.9705028 (1998).
350 Reyes-Ruvalcaba, D., González-Cortés, C. & Rivero-Lezcano, O. M. Human phagocytes lack the ability to kill Mycobacterium gordonae, a non-pathogenic mycobacteria. *Immunol Lett* **116**, 72-78, doi:10.1016/j.imlet.2007.11.010 (2008).
351 Jones, G. S., Amirault, H. J. & Andersen, B. R. Killing of Mycobacterium tuberculosis by neutrophils: a nonoxidative process. *J Infect Dis* **162**, 700-704 (1990).
352 Kisich, K. O., Higgins, M., Diamond, G. & Heifets, L. Tumor necrosis factor alpha stimulates killing of Mycobacterium tuberculosis by human neutrophils. *Infect Immun* **70**, 4591-4599 (2002).
353 Berry, M. P. *et al.* An interferon-inducible neutrophil-driven blood transcriptional signature in human tuberculosis. *Nature* **466**, 973-977, doi:10.1038/nature09247 (2010).
354 Peterson, P. K. *et al.* CD14 receptor-mediated uptake of nonopsonized Mycobacterium tuberculosis by human microglia. *Infect Immun* **63**, 1598-1602 (1995).
355 McNab, F. W. *et al.* Programmed death ligand 1 is over-expressed by neutrophils in the blood of patients with active tuberculosis. *Eur J Immunol* **41**, 1941-1947, doi:10.1002/eji.201141421 (2011).
356 Balu, S. *et al.* A novel human IgA monoclonal antibody protects against tuberculosis. *J Immunol* **186**, 3113-3119, doi:10.4049/jimmunol.1003189 (2011).
357 Wong, K. W. & Jacobs, W. R. Critical role for NLRP3 in necrotic death triggered by Mycobacterium tuberculosis. *Cell Microbiol* **13**, 1371-1384, doi:10.1111/j.1462-5822.2011.01625.x (2011).
358 Khader, S. A. *et al.* In a murine tuberculosis model, the absence of homeostatic chemokines delays granuloma formation and protective immunity. *J Immunol* **183**, 8004-8014, doi:10.4049/jimmunol.0901937 (2009).
359 Nouailles, G. *et al.* CXCL5-secreting pulmonary epithelial cells drive destructive neutrophilic inflammation in tuberculosis. *J Clin Invest* **124**, 1268-1282, doi:10.1172/JCI72030 (2014).
360 Sarkar, S. *et al.* Suppression of the NF-κB pathway by diesel exhaust particles impairs human antimycobacterial immunity. *J Immunol* **188**, 2778-2793, doi:10.4049/jimmunol.1101380 (2012).

361 Sow, F. B. *et al.* Mycobacterium tuberculosis components stimulate production of the antimicrobial peptide hepcidin. *Tuberculosis (Edinb)* **91**, 314-321, doi:10.1016/j.tube.2011.03.003 (2011).
362 Witkin, S. S., Gerber, S. & Ledger, W. J. Influence of interleukin-1 receptor antagonist gene polymorphism on disease. *Clin Infect Dis* **34**, 204-209, doi:10.1086/338261 (2002).
363 Handunnetthi, L., Ramagopalan, S. V., Ebers, G. C. & Knight, J. C. Regulation of major histocompatibility complex class II gene expression, genetic variation and disease. *Genes Immun* **11**, 99-112, doi:10.1038/gene.2009.83 (2010).
364 O'Kane, C. M., Elkington, P. T. & Friedland, J. S. Monocyte-dependent oncostatin M and TNF-alpha synergize to stimulate unopposed matrix metalloproteinase-1/3 secretion from human lung fibroblasts in tuberculosis. *Eur J Immunol* **38**, 1321-1330, doi:10.1002/eji.200737855 (2008).
365 Meilang, Q. *et al.* Polymorphisms in the SLC11A1 gene and tuberculosis risk: a meta-analysis update. *Int J Tuberc Lung Dis* **16**, 437-446, doi:10.5588/ijtld.10.0743 (2012).
366 Dalgic, N. *et al.* Relationship between toll-like receptor 8 gene polymorphisms and pediatric pulmonary tuberculosis. *Dis Markers* **31**, 33-38, doi:10.3233/DMA-2011-0800 (2011).
367 Huang, C. T. *et al.* High serum levels of procalcitonin and soluble TREM-1 correlated with poor prognosis in pulmonary tuberculosis. *J Infect* **68**, 440-447, doi:10.1016/j.jinf.2013.12.012 (2014).
368 Alatas, F. *et al.* Vascular endothelial growth factor levels in active pulmonary tuberculosis. *Chest* **125**, 2156-2159 (2004).
369 Srivastava, S., Ernst, J. D. & Desvignes, L. Beyond macrophages: the diversity of mononuclear cells in tuberculosis. *Immunol Rev* **262**, 179-192, doi:10.1111/imr.12217 (2014).
370 Strauss-Ayali, D., Conrad, S. M. & Mosser, D. M. Monocyte subpopulations and their differentiation patterns during infection. *J Leukoc Biol* **82**, 244-252, doi:10.1189/jlb.0307191 (2007).
371 CA, D. & FR, S. The relation of the tubercle and the monocyte:lymphocyte ratio to resistance and susceptibility in tuberculosis. *J Exp Med.*, 113–152, doi:10.1084/jem.52.90063.113. (1930).
372 FR, S., CA, D. & RS, C. Studies of the blood in experimental tuberculosis: the monocyte-lymphocyte ratio; the anemia-leucopenia phase. *Transactions of the 22nd Annual Meeting of the National Tuberculosis Association*, 252–256 (1926).
373 RS, C., FR, S., S, S. & JA, K. The role of the monocyte in tuberculosis. *Bull Johns Hopkins Hosp.* **XXXVII**, 231–280 (1925).
374 Naranbhai, V. *et al.* Ratio of monocytes to lymphocytes in peripheral blood identifies adults at risk of incident tuberculosis among HIV-infected adults initiating antiretroviral therapy. *J Infect Dis* **209**, 500-509, doi:10.1093/infdis/jit494 (2014).
375 Naranbhai, V. *et al.* The association between the ratio of monocytes:lymphocytes at age 3 months and risk of tuberculosis (TB) in the first two years of life. *BMC Med* **12**, 120, doi:10.1186/s12916-014-0120-7 (2014).
376 Naranbhai, V. *et al.* The association between the ratio of monocytes: lymphocytes and risk of tuberculosis among HIV-infected postpartum women. *J Acquir Immune Defic Syndr* **67**, 573-575, doi:10.1097/QAI.0000000000000353 (2014).
377 Carpenter, E., Fray, L. & Gormley, E. Cellular responses and Mycobacterium bovis BCG growth inhibition by bovine lymphocytes. *Immunol Cell Biol* **75**, 554-560, doi:10.1038/icb.1997.86 (1997).
378 Denis, M., Wedlock, D. N. & Buddle, B. M. Ability of T cell subsets and their soluble mediators to modulate the replication of Mycobacterium bovis in bovine macrophages. *Cell Immunol* **232**, 1-8, doi:10.1016/j.cellimm.2005.01.003 (2004).
379 Lin, G. N. *et al.* Increased lymphocyte to monocyte ratio is associated with better prognosis in patients with newly diagnosed metastatic nasopharyngeal carcinoma receiving chemotherapy. *Tumour Biol* **35**, 10849-10854, doi:10.1007/s13277-014-2362-6 (2014).

380 Li, Z. M. *et al.* Blood lymphocyte-to-monocyte ratio identifies high-risk patients in diffuse large B-cell lymphoma treated with R-CHOP. *PLoS One* **7**, e41658, doi:10.1371/journal.pone.0041658 (2012).
381 Porrata, L. F. *et al.* Peripheral blood lymphocyte/monocyte ratio at diagnosis and survival in nodular lymphocyte-predominant Hodgkin lymphoma. *Br J Haematol* **157**, 321-330, doi:10.1111/j.1365-2141.2012.09067.x (2012).
382 Shin, S. J. *et al.* Prognostic significance of absolute lymphocyte count/absolute monocyte count ratio at diagnosis in patients with multiple myeloma. *Korean J Pathol* **47**, 526-533, doi:10.4132/KoreanJPathol.2013.47.6.526 (2013).
383 Merekoulias, G., Alexopoulos, E. C., Belezos, T., Panagiotopoulou, E. & Jelastopulu, D. M. Lymphocyte to monocyte ratio as a screening tool for influenza. *PLoS Curr* **2**, RRN1154 (2010).
384 Warimwe, G. M. *et al.* The ratio of monocytes to lymphocytes in peripheral blood correlates with increased susceptibility to clinical malaria in Kenyan children. *PLoS One* **8**, e57320, doi:10.1371/journal.pone.0057320 (2013).
385 Warimwe, G. M. *et al.* Peripheral blood monocyte-to-lymphocyte ratio at study enrollment predicts efficacy of the RTS,S malaria vaccine: analysis of pooled phase II clinical trial data. *BMC Med* **11**, 184, doi:10.1186/1741-7015-11-184 (2013).
386 Tobin, D. M. *et al.* Host genotype-specific therapies can optimize the inflammatory response to mycobacterial infections. *Cell* **148**, 434-446, doi:10.1016/j.cell.2011.12.023 (2012).
387 Casadevall, A. & Pirofski, L. A. The damage-response framework of microbial pathogenesis. *Nat Rev Microbiol* **1**, 17-24, doi:10.1038/nrmicro732 (2003).
388 Schroeder, T. Hematopoietic stem cell heterogeneity: subtypes, not unpredictable behavior. *Cell Stem Cell* **6**, 203-207, doi:10.1016/j.stem.2010.02.006 (2010).
389 Muller-Sieburg, C. E., Sieburg, H. B., Bernitz, J. M. & Cattarossi, G. Stem cell heterogeneity: implications for aging and regenerative medicine. *Blood* **119**, 3900-3907, doi:10.1182/blood-2011-12-376749 (2012).
390 Pedrazzini, T., Hug, K. & Louis, J. A. Importance of L3T4+ and Lyt-2+ cells in the immunologic control of infection with Mycobacterium bovis strain bacillus Calmette-Guérin in mice. Assessment by elimination of T cell subsets in vivo. *J Immunol* **139**, 2032-2037 (1987).
391 Orme, I. M. The kinetics of emergence and loss of mediator T lymphocytes acquired in response to infection with Mycobacterium tuberculosis. *J Immunol* **138**, 293-298 (1987).
392 Woodworth, J. S. & Behar, S. M. Mycobacterium tuberculosis-specific CD8+ T cells and their role in immunity. *Crit Rev Immunol* **26**, 317-352 (2006).
393 Randhawa, P. S. Lymphocyte subsets in granulomas of human tuberculosis: an in situ immunofluorescence study using monoclonal antibodies. *Pathology* **22**, 153-155 (1990).
394 Guzman, J., Bross, K. J., Würtemberger, G., Freudenberg, N. & Costabel, U. Tuberculous pleural effusions: lymphocyte phenotypes in comparison with other lymphocyte-rich effusions. *Diagn Cytopathol* **5**, 139-144 (1989).
395 Manca, F. *et al.* Limited clonal heterogeneity of antigen-specific T cells localizing in the pleural space during mycobacterial infection. *Infect Immun* **59**, 503-513 (1991).
396 Rees, A., Scoging, A., Mehlert, A., Young, D. B. & Ivanyi, J. Specificity of proliferative response of human CD8 clones to mycobacterial antigens. *Eur J Immunol* **18**, 1881-1887, doi:10.1002/eji.1830181203 (1988).
397 Lalvani, A. *et al.* Human cytolytic and interferon gamma-secreting CD8+ T lymphocytes specific for Mycobacterium tuberculosis. *Proc Natl Acad Sci U S A* **95**, 270-275 (1998).
398 Behar, S. M., Dascher, C. C., Grusby, M. J., Wang, C. R. & Brenner, M. B. Susceptibility of mice deficient in CD1D or TAP1 to infection with Mycobacterium tuberculosis. *J Exp Med* **189**, 1973-1980 (1999).
399 Stenger, S. *et al.* Differential effects of cytolytic T cell subsets on intracellular infection. *Science* **276**, 1684-1687 (1997).
400 (ICMR), T. R. C. Fifteen year follow up of trial of BCG vaccines in south India for tuberculosis prevention. 1999. *Indian J Med Res* **137**, 14 p following p571 (2013).

401 ROSENTHAL, S. R. *et al.* BCG vaccination against tuberculosis in Chicago. A twenty-year study statistically analyzed. *Pediatrics* **28**, 622-641 (1961).
402 Comstock, G. W., Woolpert, S. F. & Livesay, V. T. Tuberculosis studies in Muscogee County, Georgia. Twenty-year evaluation of a community trial of BCG vaccination. *Public Health Rep* **91**, 276-280 (1976).
403 Egen, J. G. *et al.* Intravital imaging reveals limited antigen presentation and T cell effector function in mycobacterial granulomas. *Immunity* **34**, 807-819, doi:10.1016/j.immuni.2011.03.022 (2011).
404 Liu, J., Tran, V., Leung, A. S., Alexander, D. C. & Zhu, B. BCG vaccines: their mechanisms of attenuation and impact on safety and protective efficacy. *Hum Vaccin* **5**, 70-78 (2009).
405 Eberl, G., Colonna, M., Di Santo, J. P. & McKenzie, A. N. Innate lymphoid cells. Innate lymphoid cells: a new paradigm in immunology. *Science* **348**, aaa6566, doi:10.1126/science.aaa6566 (2015).
406 Moretta, L. *et al.* Human natural killer cells: origin, receptors, function, and clinical applications. *Int Arch Allergy Immunol* **164**, 253-264, doi:10.1159/000365632 (2014).
407 Barcelos, W. *et al.* Natural killer cell subpopulations in putative resistant individuals and patients with active Mycobacterium tuberculosis infection. *Scand J Immunol* **68**, 92-102, doi:10.1111/j.1365-3083.2008.02116.x (2008).
408 Whelan, K. T. *et al.* Safety and immunogenicity of boosting BCG vaccinated subjects with BCG: comparison with boosting with a new TB vaccine, MVA85A. *PLoS One* **4**, e5934, doi:10.1371/journal.pone.0005934 (2009).
409 Black, G. F. *et al.* BCG-induced increase in interferon-gamma response to mycobacterial antigens and efficacy of BCG vaccination in Malawi and the UK: two randomised controlled studies. *Lancet* **359**, 1393-1401, doi:10.1016/S0140-6736(02)08353-8 (2002).
410 Barreto, M. L. *et al.* Evidence of an effect of BCG revaccination on incidence of tuberculosis in school-aged children in Brazil: second report of the BCG-REVAC cluster-randomised trial. *Vaccine* **29**, 4875-4877, doi:10.1016/j.vaccine.2011.05.023 (2011).
411 Kaufmann, S. H. & Andersen, P. Immunity to mycobacteria with emphasis on tuberculosis: implications for rational design of an effective tuberculosis vaccine. *Chem Immunol* **70**, 21-59 (1998).
412 Stenger, S. & Modlin, R. L. T cell mediated immunity to Mycobacterium tuberculosis. *Curr Opin Microbiol* **2**, 89-93 (1999).
413 Newport, M. J. *et al.* A mutation in the interferon-gamma-receptor gene and susceptibility to mycobacterial infection. *N Engl J Med* **335**, 1941-1949, doi:10.1056/NEJM199612263352602 (1996).
414 Majlessi, L. *et al.* An increase in antimycobacterial Th1-cell responses by prime-boost protocols of immunization does not enhance protection against tuberculosis. *Infect Immun* **74**, 2128-2137, doi:10.1128/IAI.74.4.2128-2137.2006 (2006).
415 Rook, G. A., Steele, J., Ainsworth, M. & Champion, B. R. Activation of macrophages to inhibit proliferation of Mycobacterium tuberculosis: comparison of the effects of recombinant gamma-interferon on human monocytes and murine peritoneal macrophages. *Immunology* **59**, 333-338 (1986).
416 Douvas, G. S., Looker, D. L., Vatter, A. E. & Crowle, A. J. Gamma interferon activates human macrophages to become tumoricidal and leishmanicidal but enhances replication of macrophage-associated mycobacteria. *Infect Immun* **50**, 1-8 (1985).
417 Rojas, M., Barrera, L. F., Puzo, G. & Garcia, L. F. Differential induction of apoptosis by virulent Mycobacterium tuberculosis in resistant and susceptible murine macrophages: role of nitric oxide and mycobacterial products. *J Immunol* **159**, 1352-1361 (1997).
418 Chan, E. D., Chan, J. & Schluger, N. W. What is the role of nitric oxide in murine and human host defense against tuberculosis?Current knowledge. *Am J Respir Cell Mol Biol* **25**, 606-612, doi:10.1165/ajrcmb.25.5.4487 (2001).
419 Choi, H. S., Rai, P. R., Chu, H. W., Cool, C. & Chan, E. D. Analysis of nitric oxide synthase and nitrotyrosine expression in human pulmonary tuberculosis. *Am J Respir Crit Care Med* **166**, 178-186 (2002).

420 Schön, T. *et al.* Local production of nitric oxide in patients with tuberculosis. *Int J Tuberc Lung Dis* **8**, 1134-1137 (2004).
421 Lalor, M. K. *et al.* Complex cytokine profiles induced by BCG vaccination in UK infants. *Vaccine* **28**, 1635-1641, doi:10.1016/j.vaccine.2009.11.004 (2010).
422 Soares, A. P. *et al.* Bacillus Calmette-Guérin vaccination of human newborns induces T cells with complex cytokine and phenotypic profiles. *J Immunol* **180**, 3569-3577 (2008).
423 Handzel, Z. T. *et al.* Increased Th1 and Th2 type cytokine production in patients with active tuberculosis. *Isr Med Assoc J* **9**, 479-483 (2007).
424 Abebe, F., Mustafa, T., Nerland, A. H. & Bjune, G. A. Cytokine profile during latent and slowly progressive primary tuberculosis: a possible role for interleukin-15 in mediating clinical disease. *Clin Exp Immunol* **143**, 180-192, doi:10.1111/j.1365-2249.2005.02976.x (2006).
425 O'Kane, C. M., Boyle, J. J., Horncastle, D. E., Elkington, P. T. & Friedland, J. S. Monocyte-dependent fibroblast CXCL8 secretion occurs in tuberculosis and limits survival of mycobacteria within macrophages. *J Immunol* **178**, 3767-3776 (2007).
426 Siddiqui, N. & Hope, J. Differential recruitment and activation of natural killer cell sub-populations by Mycobacterium bovis-infected dendritic cells. *Eur J Immunol* **43**, 159-169, doi:10.1002/eji.201242736 (2013).
427 Vujanovic, L., Ballard, W., Thorne, S. H., Vujanovic, N. L. & Butterfield, L. H. Adenovirus-engineered human dendritic cells induce natural killer cell chemotaxis via CXCL8/IL-8 and CXCL10/IP-10. *Oncoimmunology* **1**, 448-457 (2012).
428 Sharma, N., Akhade, A. S. & Qadri, A. Sphingosine-1-phosphate suppresses TLR-induced CXCL8 secretion from human T cells. *J Leukoc Biol* **93**, 521-528, doi:10.1189/jlb.0712328 (2013).
429 Gong, J. H. *et al.* Interleukin-10 downregulates Mycobacterium tuberculosis-induced Th1 responses and CTLA-4 expression. *Infect Immun* **64**, 913-918 (1996).
430 Gazzinelli, R. T., Oswald, I. P., James, S. L. & Sher, A. IL-10 inhibits parasite killing and nitrogen oxide production by IFN-gamma-activated macrophages. *J Immunol* **148**, 1792-1796 (1992).
431 Moore, K. W., de Waal Malefyt, R., Coffman, R. L. & O'Garra, A. Interleukin-10 and the interleukin-10 receptor. *Annu Rev Immunol* **19**, 683-765, doi:10.1146/annurev.immunol.19.1.683 (2001).
432 Verbon, A. *et al.* Serum concentrations of cytokines in patients with active tuberculosis (TB) and after treatment. *Clin Exp Immunol* **115**, 110-113 (1999).
433 Redford, P. S. *et al.* Enhanced protection to Mycobacterium tuberculosis infection in IL-10-deficient mice is accompanied by early and enhanced Th1 responses in the lung. *Eur J Immunol* **40**, 2200-2210, doi:10.1002/eji.201040433 (2010).
434 Turner, J. *et al.* In vivo IL-10 production reactivates chronic pulmonary tuberculosis in C57BL/6 mice. *J Immunol* **169**, 6343-6351 (2002).
435 Saraiva, M. & O'Garra, A. The regulation of IL-10 production by immune cells. *Nat Rev Immunol* **10**, 170-181, doi:10.1038/nri2711 (2010).
436 Dagvadorj, J. *et al.* Interleukin-10 inhibits tumor necrosis factor-alpha production in lipopolysaccharide-stimulated RAW 264.7 cells through reduced MyD88 expression. *Innate Immun* **14**, 109-115, doi:10.1177/1753425908089618 (2008).
437 Fiorentino, D. F., Zlotnik, A., Mosmann, T. R., Howard, M. & O'Garra, A. IL-10 inhibits cytokine production by activated macrophages. *J Immunol* **147**, 3815-3822 (1991).
438 de Waal Malefyt, R., Abrams, J., Bennett, B., Figdor, C. G. & de Vries, J. E. Interleukin 10(IL-10) inhibits cytokine synthesis by human monocytes: an autoregulatory role of IL-10 produced by monocytes. *J Exp Med* **174**, 1209-1220 (1991).
439 Borekci, S. *et al.* Factors Affecting the Tuberculosis Risk in Patients Receiving Anti-Tumor Necrosis Factor-α Treatment. *Respiration*, doi:10.1159/000434684 (2015).
440 Andrew, D. P. *et al.* STCP-1 (MDC) CC chemokine acts specifically on chronically activated Th2 lymphocytes and is produced by monocytes on stimulation with Th2 cytokines IL-4 and IL-13. *J Immunol* **161**, 5027-5038 (1998).

441 Matsukawa, A. *et al.* Pivotal role of the CC chemokine, macrophage-derived chemokine, in the innate immune response. *J Immunol* **164**, 5362-5368 (2000).
442 Saukkonen, J. J. *et al.* Beta-chemokines are induced by Mycobacterium tuberculosis and inhibit its growth. *Infect Immun* **70**, 1684-1693 (2002).
443 Ikeda, T. *et al.* Interleukin-10 differently regulates monocyte chemoattractant protein-1 gene expression depending on the environment in a human monoblastic cell line, UG3. *J Leukoc Biol* **72**, 1198-1205 (2002).
444 Yano, S. *et al.* T helper 2 cytokines differently regulate monocyte chemoattractant protein-1 production by human peripheral blood monocytes and alveolar macrophages. *J Immunol* **157**, 2660-2665 (1996).
445 Rutledge, B. J. *et al.* High level monocyte chemoattractant protein-1 expression in transgenic mice increases their susceptibility to intracellular pathogens. *J Immunol* **155**, 4838-4843 (1995).
446 Flores-Villanueva, P. O. *et al.* A functional promoter polymorphism in monocyte chemoattractant protein-1 is associated with increased susceptibility to pulmonary tuberculosis. *J Exp Med* **202**, 1649-1658, doi:10.1084/jem.20050126 (2005).
447 Liu, H. *et al.* Induction of CCL8/MCP-2 by mycobacteria through the activation of TLR2/PI3K/Akt signaling pathway. *PLoS One* **8**, e56815, doi:10.1371/journal.pone.0056815 (2013).
448 Wangoo, A., Taylor, I. K., Haynes, A. R. & Shaw, R. J. Up-regulation of alveolar macrophage platelet-derived growth factor-B (PDGF-B) mRNA by interferon-gamma from Mycobacterium tuberculosis antigen (PPD)-stimulated lymphocytes. *Clin Exp Immunol* **94**, 43-50 (1993).
449 Wilkinson, R. J. *et al.* Influence of polymorphism in the genes for the interleukin (IL)-1 receptor antagonist and IL-1beta on tuberculosis. *J Exp Med* **189**, 1863-1874 (1999).
450 Ziegler-Heitbrock, H. W. & Ulevitch, R. J. CD14: cell surface receptor and differentiation marker. *Immunol Today* **14**, 121-125, doi:10.1016/0167-5699(93)90212-4 (1993).
451 Nemeth, E. & Ganz, T. Regulation of iron metabolism by hepcidin. *Annu Rev Nutr* **26**, 323-342, doi:10.1146/annurev.nutr.26.061505.111303 (2006).
452 Johnson, E. E., Sandgren, A., Cherayil, B. J., Murray, M. & Wessling-Resnick, M. Role of ferroportin in macrophage-mediated immunity. *Infect Immun* **78**, 5099-5106, doi:10.1128/IAI.00498-10 (2010).
453 Sow, F. B. *et al.* Expression and localization of hepcidin in macrophages: a role in host defense against tuberculosis. *J Leukoc Biol* **82**, 934-945, doi:10.1189/jlb.0407216 (2007).
454 Mustafa, A. S. Characterization of a cross-reactive, immunodominant and HLA-promiscuous epitope of Mycobacterium tuberculosis-specific major antigenic protein PPE68. *PLoS One* **9**, e103679, doi:10.1371/journal.pone.0103679 (2014).
455 Kang, J. E., Hwang, S. H., Lee, J. H., Park, d. Y. & Kim, H. H. Effects of RBC removal and TRIzol of peripheral blood samples on RNA stability. *Clin Chim Acta* **412**, 1883-1885, doi:10.1016/j.cca.2011.06.016 (2011).
456 Whitney, A. R. *et al.* Individuality and variation in gene expression patterns in human blood. *Proc Natl Acad Sci U S A* **100**, 1896-1901, doi:10.1073/pnas.252784499 (2003).
457 Messaoudi, I., Estep, R., Robinson, B. & Wong, S. W. Nonhuman primate models of human immunology. *Antioxid Redox Signal* **14**, 261-273, doi:10.1089/ars.2010.3241 (2011).
458 Magalhaes, I. *et al.* High content cellular immune profiling reveals differences between rhesus monkeys and men. *Immunology* **131**, 128-140, doi:10.1111/j.1365-2567.2010.03284.x (2010).
459 Yang, C. S., Yuk, J. M. & Jo, E. K. The role of nitric oxide in mycobacterial infections. *Immune Netw* **9**, 46-52, doi:10.4110/in.2009.9.2.46 (2009).